The role of IRE1α in the regulation of cytokine production

A thesis submitted to the National University of Ireland Galway in fulfilment of the requirement for the degree of

Doctor of Philosophy

By

Aaron Talty

Discipline of Biochemistry, School of Natural Sciences,

National University of Ireland, Galway

Thesis Supervisor: Professor Afshin Samali

Thesis Co-supervisor: Dr. Susan Logue

Head of School: Professor Ciaran Morrison

December 2019

Table of contents

Declaration

This thesis is a presentation of my own original research work. Wherever contributions of others are involved, every effort has been made to indicate this clearly at the outset of each chapter.

This work was done under the guidance of Professor Afshin Samali and Dr. Susan Logue, at the National University of Ireland, Galway.

Acknowledgements

There are so many people that have made the past five years memorable and a great learning experience, inside and outside of the lab.

Afshin. Thinking back, I am pretty sure it was the summer of 2012 when I first sent you an email trying to get some summer lab work. The past 8 years have been one hell of a journey and I would like to thank you for giving me a shot all those years ago. I have learned a lot from you and am thankful now for the few kicks up the arse you gave me along the way when I was slacking. Thanks for the opportunity and support.

Susan. I am pretty sure you are one of the main reasons I have a thesis at all. You turned me from a terrible western blotter to a mediocre one, something we can all be proud of. Your support in the lab and for any ideas I had about the project were always appreciated. I will always miss the Friday lab meetings. Best of luck in your lab and I am sure we will be hearing about some ER stress breakthroughs emerging from Canada in the years to come.

Thanks to the rest of the AS/AG crew over the years. Getting through the up's and down's of a PhD is always made easier when you're surrounded by a good bunch of people. Kasia, Shane, Mila, Adrienne, Alaa, Stephanie and Mark. Will miss you all.

Special shout out to the lads. All the messin, seshin and AOE2 rushin was some of the standout stuff from the last few years. Couldn't have gotten through it without the support and slagging of you lot. Aitor, Brian, Chetan, Stuart and John, the future of UPR research is in good hands. Maybe. Thanks also to the rest of my friends from ARC and beyond. Sangeetha, Emma, Mari, Eimear, Higgo, Antonio (Top). It's been a pleasure.

Cześć! Izabela, your constant wheezing and making fun of my physical appearance was something to look forward to everyday. Lab hasn't been the same without you since you left. Thanks so much for your constant encouragement and support over the years. We are so close!

OUGH. Hello like. I think it's a good sign you're good friends with someone when you constantly speak in a made up, stupid language that nobody else understands. In all honesty, Eoghan and myself being in the same lab was probably detrimental to our progress and prospects, but I think we managed. Your help in the lab and outside of it won't be forgotten. All the stupid, drunken stories definitely won't be forgotten. Thanks for everything. That's us gone like. P.S. Give me a job later like.

To my parents, Eileen and Mike. Words can't express how thankful I am for your unending support and motivation. I couldn't have gotten to where I am today without your guidance and hope I made you proud. To my brother and sister, Luke and Ellen, good luck topping this one (hehe).

Finally, Alicja. We met in my second year of the PhD and I don't know if I would have made it to the final one without you. Thank you for your love, support, friendship, advice and above all, patience. It took much longer than we both planned but I am almost ready to leave Galway behind. Things were always made easier by the knowledge you were waiting on the other end. Kocham cię.

Abstract

Inositol-requiring enzyme 1 (IRE1), a key mediator of the unfolded protein response (UPR), has emerging roles within innate immunity and cancer progression. Here we examine how IRE1 signalling influences the production of cytokines and chemokines in health and disease. Specifically, we ask how IRE1 dependent signalling (i) contributes to cytokine and chemokine production in monocytic cells following toll-like receptor (TLR) stimulation and (ii) the influence of IRE1 dependent signalling on cytokine/chemokine production in pancreatic ductal adenocarcinoma (PDAC).

The NLRP3 inflammasome is a central control point within innate immunity. Assembly of the NACHT, LRR and PYD domains-containing protein 3 (NLRP3) inflammasome facilitates caspase-1 activation inducing the processing of the key cytokine pro-IL1β, which is required to mount an effective innate immune response. Following stimulation of TLR4 we observed selective activation of IRE1 RNase signalling in monocytic cells which when inhibited reduced NLRP3 inflammasome assembly and levels of bioactive IL-1β. By carefully dissecting the various steps required for formation of the NLRP3 inflammasome we found that IRE1 RNase activity specifically aided structural assembly of the inflammasome. This work highlights a new and important role for IRE1 within innate immunity and suggests that IRE1 activity contributes to the maintenance of cellular health.

In addition to examining the influence of IRE1 in cellular health, we have also investigated how IRE1 dependent signalling can contribute to disease progression and in particular its role in pancreatic cancer. PDAC is a tumour type known to exhibit a highly inflammatory phenotype with conditions that stimulate basal ER stress levels. We demonstrate that inhibition of IRE1 RNase activity reduces cytokine release and proliferation in PDAC cells. Pancreatic Stellate Cells (PSC) are a key component of the PDAC tumour microenvironment (TME). These cells encapsulate the PDAC tumour and through the production of secreted factors help to create an environment conducive for PDAC growth. We observed that ablating IRE1 RNase activity increased production of secreted factors associated with enhanced natural killer cell activation and decreased factors linked with PDAC tumorigenesis. These

findings suggest a multifaceted role for IRE1 controlled cytokine networks in PDAC progression.

Publications

Aaron Talty, Shane Deegan, Mila Ljujic, Katarzyna Mnich, Serika D. Naicker, Dagmar Quandt , Qingping Zeng, John B. Patterson ,Adrienne M. Gorman, Matthew D. Griffin, Afshin Samali and Susan E. Logue. (2019) Inhibition of IRE1alpha RNase activity reduces NLRP3 inflammasome assembly and processing of pro-IL1beta. Cell Death Dis **10**(9): 622.

Stuart Creedican, **Aaron Talty**, Stephen P. Fitzgerald, Afshin Samali, Ciarán Richardson, Adrienne M. Gorman and Kenneth Martin. (2019) Application of a New Multiplexed Array for Rapid, Sensitive, Simultaneous and Quantitative Assessment of Spliced and Unspliced XBP1. Biological Procedures Online. 21 (1), 1-11.

Abbreviations

ACC	Acinar cell carcinoma
AIM	Absent in melanoma
ALR	AIM2 like receptors
ASC	Apoptosis-associated speck-like protein containing a CARD
ASK1	Apoptosis-kinase 1
ASMA	Alpha Smooth muscle actin
ATF4	Activating transcription factor 4
ATF6	Activating transcription factor 6
ATP	Adenosine triphosphate
BAK	Bcl-2 homologous antagonist/killer
BAX	Bcl associated X protein
BCL2	B-cell lymphoma 2
BH3	Bcl-2 homology domain 3
BIM	Bcl-2-like protein 11
CAF	Cancer associated fibroblast
CAPS	Cryopyrin-associated periodic syndrome
CARD	C-terminal caspase-recruitment domain
CHOP	C/EBP homologous protein
CLR	C-type lectin receptors
CP	Chronic pancreatitis
CSC	Cancer stem cell
CTL	Cytotoxic T lymphocyte
CTLA-4	Cytotoxic T-lymphocyte associated protein 4
CXCL1	C-X-C motif Chemokine Ligand 1
CXCR4	C-X-C chemokine receptor type 4
DAG	Diacylglycerol
DAMPS	Damage associated molecular patterns
DED	Death effector domain
DEPC	Diethyl Pyrocarbonate

DNA	Deoxyribonucleic acid
DTT	Dithiothreitol
ECM	Extracellular matrix
EDEM	ER degradation enhancing α-mannosidase-like protein
EIF2α	Eukaryotic Translation Initiation Factor 2 Alpha
EMT	Epithelial mesenchymal transition
ER	Endoplasmic reticulum
ERAD	ER-associated degradation
ERSE	ER stress response element
FAP-α	Fibroblast activation protein-α
FLNA	Filamin A
GADD34	Growth arrest and DNA damage-inducible protein
GCN2	General control nonderepressible 2
GDP	Guanosine diphosphate
GRP78	78-kDa glucose regulated protein
GSDMA	Gasdermin A
GSDMB	Gasdermin B
GSDMC	Gasdermin C
GSDMD	Gasdermin D
GTP	Guanosine-5'-triphosphate
HIF1α	Hypoxia-inducible factor 1-alpha
HRI	Haem-regulated inhibitor
HSC	Hepatic stellate cells
HSP	Heat shock protein
IFN	Interferon
IKK	IκB kinase
IL	Interleukin
iNOS	Inducible nitric oxide synthase
IP3R	Inositol 1,4,5-triphosphate
IRE1	Inositiol requiring enzyme 1

ISR	Integrated stress response
JNK	c-Jun N-terminal kinase
LeTx	Lethal toxin
LPS	Lipopolysaccharide
LRR	Leucine-rich repeat
MEF	Mouse Embryonic Fibroblasts
miRNA	Micro RNA
MPT	Mitochondiral permeable transition
mRNA	Messenger RNA
MRSA	Methicillin-resistant Staphylococcus aureus
NEK7	NIMA-related kinase 7
NET	Neuroendocrine tumours
NF-κB	Nuclear factor kappa-light-chain-enhancer of activated B cells
NK	Natural killer
NKR	Natural killer cell receptors
NLR	NOD like receptors
NLRC4	NLR family CARD domain-containing protein 4
NLRP3	NACHT, LRR and PYD domains-containing protein 3
NO	Nitric oxide
NOD	Nucleotide-binding oligomerization domain-like receptors
NOS	Nitric oxide synthase
NRF2	Nuclear Factor Erythroid 2, Related Factor 2
ORF	Open reading frames
PAMP	Pathogen associated molecular pattern
PBMC	Peripheral blood mononuclear cell
PCR	Polymerase chain reaction
PDAC	Pancreatic ductal adenocarcinoma
PDI	Protein disulfide isomerase
PD-L1	Programmed cell death-ligand 1
PEK	Pancreatic eIF-2α kinase

PERK	Protein kinase RNA-like endoplasmic reticulum kinase
PIP2	Phosphatidylinositol 4,5-biphosphate
PKR	Protein kinase R
PLC	Phospholipase C
PNETS	Pancreatic neuroendocrine tumours
PRR	Pattern recognition receptors
PSC	Pancreatic stellate cells
PUMA	p53 upregulated modulator of apoptosis
PYCARD	PYD And CARD Domain Containing
PYD	Pyrin domain
QPCR	Quantitative PCR
RER	Rough endoplasmic reticulum
RIDD	Regulated IRE1 dependent decay
RIG	Retinoic inducible gene-1
RIPK	Receptor-interacting serine/threonine-protein kinase 1
RLR	RIG-1-like receptors
RNA	Ribonucleic acid
RNase	Endoribonuclease
ROS	Reactive oxygen species
RTCB	RNA 2',3'-cyclic phosphate and 5'-OH ligase
RT-PCR	Reverse Transcription Polymerase Chain Reaction
SDF-1α	Stromal derived factor-1α
SER	Smooth endoplasmic reticulum
siRNA	Small interfering RNA
SREBP	Sterol regulatory element-binding protein cleavage-activating protein
SRP	Signal Recognition Particle
TAM	Tumour associated macrophages
TERS	Transmissible ER stress
TG	Thapsigargin
TGF	Transforming growth factor

TLR4	Toll like receptor 4
TM	Tunicamycin
TME	Tumour microenvironment
TNBC	Triple negative breast cancer
TNF	Tumour necrosis factor
TRAF	TNF receptor-associated factor 1
TRAPS	Tumour necrosis factor receptor associated periodic syndrome
TRX	Thioredoxin
TWIK2	Two-pore domain weak inwardly rectifying K^+ channel 2
TXNIP	Thioredoxin-interacting protein
UPR	Unfolded protein response
VEGF	Vascular endothelial growth factor
XBP1	X-box binding protein 1
XBP1s	Spliced x-box binding protein 1
XBP1u	Unspliced x-box binding protein 1

Chapter 1: Introduction

1.1 The endoplasmic reticulum

The endoplasmic reticulum (ER) is the term given by Keith R. Porter to describe what was originally defined as a "lace-like reticulum" in chick embryo fibroblast cells via electron microscopy[1]. Today, the ER is known to be a large membrane-bound organelle with a wide diversity of important functions. The ER would also later be defined as having two forms; rough and smooth ER[2]. The rough ER (RER) is home to ribosomes that dot along its surface, hence the name. These ER-associated ribosomes facilitate the co-translational translocation of nascent polypeptides encoding membrane or secretory proteins into the ER itself[3]. This occurs via a complex termed the translocon (SEC61) and once inside the ER, the polypeptides initiate folding and post-translational modifications to reach their active motifs[4]. The smooth ER (SER) appears as a flatter, sheet-like structure when compared to RER and has important roles in calcium regulation, lipid synthesis and hormone production. The RER/SER ratio varies between cell types and is often indicative of the function of that cell[5]. Efficient and accurate protein folding and/or maturation is an essential requirement for correct cellular function and is termed proteostasis, from the term protein homeostasis. Incorrect proteostatic regulation is the cause of a huge range of human diseases and its perturbation can often be lethal. The ER contains an internal region that is separated from the cytosol by a membrane system termed the ER lumen. The ER lumen is the site of folding for newly synthesized proteins and its internal homeostasis is tightly maintained to facilitate efficient folding[6]. Another important aspect of ER proteostasis is a group of proteins called chaperones. Chaperones are a diverse group of multidomain proteins that assist nascent protein maturation by shielding them from harsh environments during folding, stopping protein aggregation and targeting proteins for degradation when necessary. There are numerous chaperone families and they include Heat shock protein (HSP)60, HSP70, HSP90 and HSP100. HSP70 and HSP90 are highly abundant in the ER lumen and one HSP7O family member called Glucose-regulated protein 78 (GRP78) (Also called binding immunoglobulin protein (Bip)) plays a particularly important role in ER biology [7]. Proteostasis, even under ideal ER luminal conditions, can fail and lead to proteins that are not correctly folded. It is of upmost importance that these misfolded proteins are destroyed as they can lead to a myriad of deleterious effects

detrimental to the cell as a whole. The ER carries out protein degradation via two distinct pathways; (1) ER-associated degradation (ERAD) and (2) autophagy. ERAD involves the retrotranslocation of unfolded or misfolded proteins to the cytosol where they are targeted for degradation by the proteasome[8]. Autophagy is a very complex system that involves the recycling of cellular components via targeted degradation of cell organelles or protein aggregates, often under low nutrient conditions[9, 10]. Aside from the ER's role in protein biosynthesis coordination and release via the secretory pathway, it also plays vital roles in lipid biosynthesis, calcium signalling and drug detoxification[11-13].

1.2 ER stress

Perturbation of ER homeostasis results in a cellular response termed "ER stress" that is characterized by a build-up of unfolded proteins[14]. ER stress leads to malfunctions in the protein folding machinery in the ER and to a build-up of unfolded and misfolded proteins. The insults that result in ER stress can be both intrinsic and extrinsic, with the intensity and duration governing the adaptive response issued by the cell. In cancer, a high protein production can put pressure on the ER and lead to ER stress. Neurodegenerative diseases have also been associated with ER stress modalities, contributing to neuron cell death as a result of a build-up of misfolded protein aggregates[15]. It is also important to mention that there are certain cell types that exhibit high basal levels of ER stress and the associated responses due to their physiological function, insulin producing pancreatic β cells being a great example[16]. While intrinsic ER stressors generally arise from genetic perturbations, most extrinsic sources work by disturbing the unique protein folding milieu of the ER[17]. Disruption of the local microenvironment's oxygen, nutrients and glucose in tumours all give rise to ER stress. Another aspect essential to ER homeostasis is the maintenance of temperature. The mammalian physiological temperature is between 36-37˚C and if changed can disrupt cellular homeostasis on a general scale. Acute temperature increases called heat shock can cause ER and Golgi fragmentation[18]. There are also several drug inducers of ER stress that are used in a laboratory environment to mimic ER stress artificially. These include Thapsigargin (Tg), Tunicamycin (Tm) and Dithiothreitol (DTT)[19].

1.3 The unfolded protein response

ER stress activates a proteostasis maintenance network called the unfolded protein response (UPR). This system works in a variety of different ways that ultimately leads to the restoration of ER homeostasis or cell death. This can occur through expansion of the endoplasmic reticulum, a stalling of protein translation or the targeted degradation of misfolded proteins via the ERAD system [20]. This process of maintaining a balance in ER homeostasis is a very dynamic process. It allows the cell to respond effectively but also if the cell stress progresses to a state that is considered beyond repair, an emergency shutdown in the form of apoptotic cell death can be triggered. The precise nature of this altered response to ER stress and what exactly triggers ER stress-associated apoptosis remains an active area of research[21].

1.4 The history of the UPR

Glucose deprivation experiments were the original identifiers of the existence of the UPR when it was shown that the chaperones, GRP78 and GRP94, were induced in cells cultured in glucose-deprived culture medium[22]. Around ten years later, the mechanism behind this induction was identified when misfolded hemagglutinin, a glycoprotein responsible or red blood cell agglutination, induced GRP94 and GRP78[23]. This link between unfolded proteins and chaperone induction was then further elucidated by two labs in the UPR field. Both Kazutoshi Mori and Peter Walter, using *saccharomyces cerevisiae* as a model, made the discovery that a transmembrane kinase known as Inositol-requiring enzyme 1 (IRE1) was responsible for UPR induction[24, 25]. IRE1 was also shown shortly afterwards to cleave the transcription factor HAC1 in yeast and that it was responsible for UPR induction[26, 27]. This series of discoveries marks the beginning of the UPR field itself.

1.5 UPR sensors and activation

The UPR has three primary effectors that function as sensors of misfolded proteins. They are the aforementioned IRE1[28], protein kinase RNA-like ER kinase (PERK)[29] and activating transcription factor 6 (ATF6)[30]. All three proteins are bound to the ER membrane and held in an inactive state by the interaction with an ER chaperone protein called GRP78 (also known as Bip)[31]. GRP78 remains bound to the luminal

domain of the sensors during un-stressed conditions but upon a build-up of misfolded proteins in the ER lumen, GRP78 dissociates as a result of higher affinity for misfolded proteins, stimulating activation of IRE1, PERK and ATF6 and signifying the beginning of the UPR (Figure 1.1). The activation kinetics of all three sensors differs in the duration of their activation and subsequent deactivation. IRE1 is the first sensor to respond to ER stress and also the first to become deactivated, ATF6 displays slightly more longevity in terms of activation time and PERK is the final sensor to become active but also persists longer than IRE1 or ATF6 [32]. However, any data regarding UPR activity kinetics needs to be taken with "a grain of salt" as the intensity of stress, length of the stress, cell type and source of the stress can all attribute to the final UPR response issued.

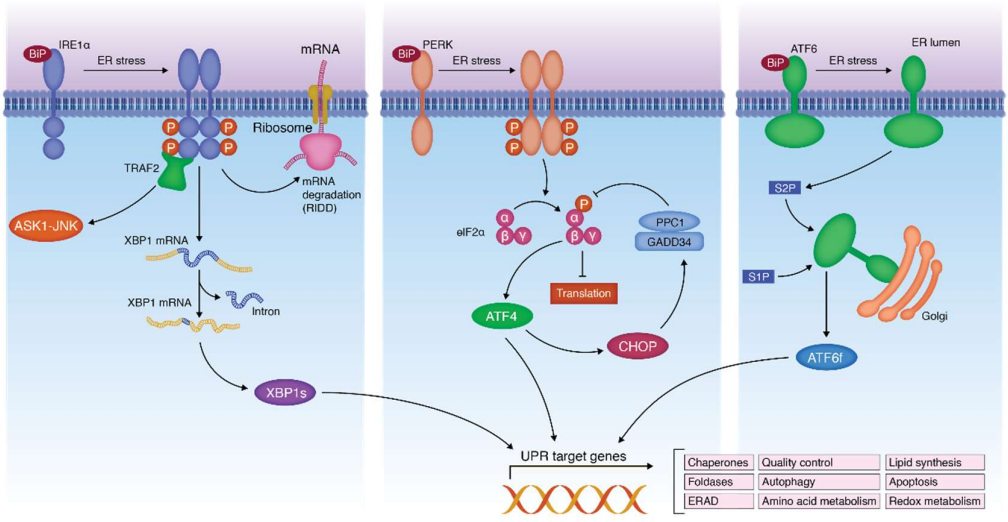

Figure 1.1: The unfolded protein response. Accumulation of unfolded proteins within the ER lumen leads to activation of the three ER stress sensors IRE1, PERK and ATF6 by sequestering GRP78. This leads to activation of primary downstream transcription factors including ATF4, ATF6f, and XBP1s. This promotes expression of chaperones, protein degradation pathway activation, increased ER capacity and reduced protein translation to reduce ER stress.

1.6 PERK

PERK (protein kinase RNA-like endoplasmic reticulum kinase) was originally identified as a kinase (termed pancreatic eIF2α kinase or PEK) capable of phosphorylating the translation regulating protein, eukaryotic initiation factor 2(eIF2α)[33]. It was later shown to be a kinase that was activated and hyper phosphorylated in response to ER

stress[29]. Other proteins also phosphorylate the alpha subunit of eIF2α on S51 and this leads to a stall in translation. These kinases are protein kinase R (PKR), General control nonderepressible 2 (GCN2) and haem regulated inhibitor (HRI) and are collectively termed the integrated stress response (ISR)[34]. Each of the known eIF2α kinases becomes active in response to a specific stress or stimulus. PKR, GCN2 and HRI are activated upon viral infection, amino acid deprivation and heme-deficiency, respectively[35]. PERK is a type I transmembrane serine/threonine kinase comprised of an ER luminal N-terminal domain and a cytosolic C-terminal domain. The N-terminal domain is the site responsible for the binding of GRP78 whilst the C-terminal domain contains the kinase domain responsible for the downstream activation of eIF2α. Upon ER stress, PERK undergoes transautophosphorylation of its cytosolic domain. The activated PERK then phosphorylates eIF2α and leads to an attenuation of cap dependent protein translation, allowing the cell to reduce the load of nascent proteins entering the ER[36]. In unstressed conditions PERK is bound to GRP78 which holds it in an inactive state. Upon ER stress or conditions that perturb correct protein folding, GRP78 dissociates from PERK and allows its activation[31]. The exact mechanism that allows for this dissociation is not fully understood but it is believed that unfolded proteins compete for binding with the PERK N-terminal domain and cause the removal of GRP78. In contrast to the general stall of protein translation that is observed under ER stress in response to PERK activation, select genes are paradoxically upregulated. Activating transcription factor 4 (ATF4) remains translated due to enhanced ribosomal recognition of a vital upstream reading frame (uORF) that allows translation of ATF4 to occur during ER stressed conditions upon eIF2α phosphorylation[37, 38]. This allows for ATF4 protein to be translocated to the nucleus where it acts as a transcription factor. ATF4 activates a variety of genes with a diverse range of molecular outputs. These include the phosphatase Growth arrest and DNA-damage inducing protein (GADD34) which promotes the dephosphorylation of eIF2α and restores protein translation, thus creating a feedback-loop mechanism[39] and C/EBP homologous protein (CHOP) which is a pro-apoptotic transcription factor that can influence cell fate through multiple pathways including the regulation of BCL-2 family members[40].

1.7 ATF6

ATF6 is a 90 KDa type II transmembrane protein that was identified as a UPR sensory protein by Haze et al[30]. ATF6 exists in two similar isoforms, ATF6α and ATF6β. Both isoforms are structurally and functionally similar. ATF6 is located in the ER membrane like its counterparts, IRE1 and PERK. Upon ER stress, ATF6 is translocated to the Golgi apparatus by two Golgi localisation signals (Gls) that are revealed upon GRP78 dissociation. It is then cleaved into its active 50 KDa form by S1 and S2 proteases[41]. S1 and S2 proteases were originally found to be Golgi apparatus-localized enzymes that interact with sterol regulatory element binding proteins (SREBP) involved in cholesterol regulation. The process of how the full length ATF6 protein is removed from the membrane of the ER and transported to the Golgi for processing is still not fully understood. However, it has been suggested that the transport is facilitated by the COPII complex of proteins that detach proteins from the ER membrane to form transport vesicles which travel to the Golgi apparatus, but the precise mechanism remains to be elucidated[42, 43]. Cleaved ATF6 then translocates to the nucleus where it binds the ER- stress response element (ERSE) and regulates genes involved in ER stress[44]. ATF6 has been shown to play an important role in Chaperone upregulation in response to ER stress, this includes GRP78 and GRP94[45]. ATF6 has also been linked to the IRE1 pathway through the induction of XBP1, highlighting cross-activity between the UPR sensor pathways that is likely to become increasingly more evident in the years to come[46].

1.8 IRE1

IRE1 was originally identified as a protein involved in the UPR by Cox et al in 1993[25]. It is the most conserved of the three mammalian UPR sensors and exists in two isoforms, IRE1α[28] and IRE1β[47]. IRE1α has been found to be present in all cell types whereas IRE1β is only found in the intestines[48] and lungs[49]. Analysis of the amino acid sequences from both isoforms determined the percentage similarity between both of their sensor, kinase and RNase domains to be 48, 80 and 61%, respectively. It has also been shown that the RNase domain present in each isoform determines its function[50]. This thesis will focus on IRE1α (Herein referred to as IRE1). IRE1 is a type I transmembrane receptor localised in the ER membrane[51]. It

contains a cytoplasmic C- terminal domain and an ER luminal N-terminal domain. The luminal domain acts as a sensor of ER stress where it becomes activated in the presence of misfolded proteins. The N-terminal is maintained in an inactive state during unstressed conditions by binding to GRP78. Upon conditions of ER stress, the interaction between GRP78 and IRE1 is interrupted. However, there has since been alternative models suggested which indicate that unfolded proteins directly bind to the luminal domain of IRE1 and stimulate its activation[52, 53]. Upon activation of IRE1 as a result of ER stress there is an assembly of IRE1 monomers. The oligomeric state facilitates close proximity between monomers and allows for transautophosphorylation of the kinase domains and the subsequent proximity-based, phosphorylation dependent activation of the RNAse domains[54]. The kinase domain of IRE1 is the less understood of the two active domains but has been linked to cell death[55]. IRE1 has been shown to bind the adaptor protein TNF-receptor-associated factor 2 (TRAF2) which leads to the activation of the downstream kinase c-Jun N-terminal kinase (JNK), a regulator of apoptosis through the BCL-2 family members (Fig. 1.2).

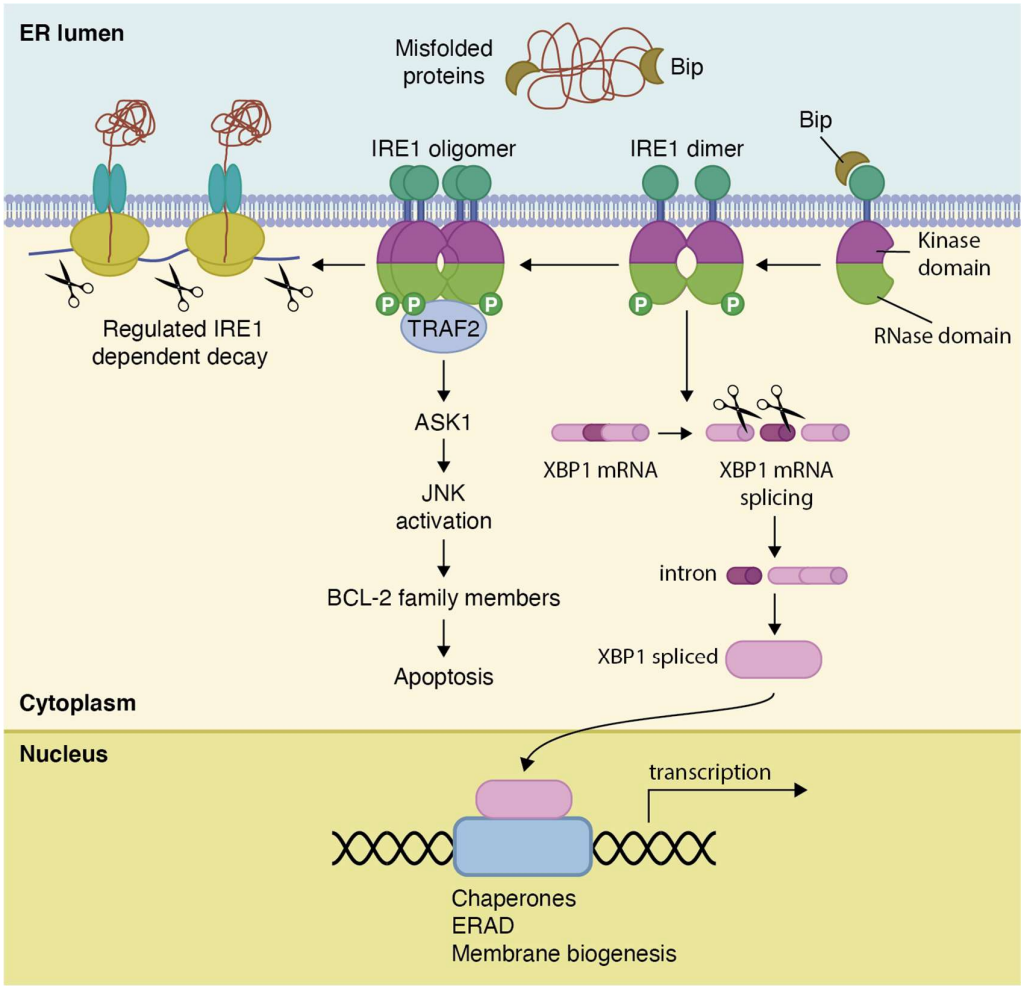

Fig. 1.2 IRE1 structure and function. IRE1 activation begins with dispersal of Bip (also called GRP78) in the luminal domain upon detection of misfolded proteins and enhanced affinity for said proteins. IRE1 undergoes dimerization and subsequent transautophosphorylation via its kinase domain (purple) upon activation. It is believed the degree of oligomerization increases as IRE1 activity is sustained, leading to distinct downstream outputs. IRE1 dimerization at onset of ER stress leads to IRE1 RNase domain mediated "splicing" of the XBP1 mRNA into its active and potent form (XBP1s). XBP1s is a potent transcription factor that relieves ER stress. Upon prolonged or intense ER stress, IRE1 oligomerizes and initiates RIDD activity. RIDD is less understood but causes IRE1 RNase domain associated degradation of ER-associated mRNA or miRNA. Additionally, IRE1 activates a downstream protein cascade that can lead to ER-stress associated apoptosis via a TRAF2-mediated protein scaffold that binds to the kinase domain. This apoptosis is believed to occur due to an ASK1/JNK mediated regulation of BCL-2 apoptotic regulating protein family members.

1.9 IRE1 RNase domain

The IRE1 RNase domain has been shown to exhibit two key functions to date, the unconventional splicing of the transcription factor X Box Binding protein 1 (XBP1)[56] and the targeted degradation of specific mRNAs via a process called regulated IRE1 dependent decay or RIDD[57]. Mechanisms that govern whether IRE1 RNase activity initiates an XBP1 splicing or RIDD response to ER stress is another hot area of research in the field[58]. Certain reports suggest that the oligomerization of IRE1 upon ER stress broadens its substrate range beyond that of XBP1 to a multitude of RIDD substrates[59]. To the contrary, another paper suggests that oligomeric IRE1 favours XBP1s signalling, whereas dimeric IRE1 gives preference to RIDD[60].

1.9.1 XBP1 transcription factor

Unspliced XBP1 is cleaved by the activated IRE1 RNase domain in a manner that results in the removal of a 26 nucleotide basepair intron in a spliceosome-independent manner. The targeting of the unspliced XBP1 sequence by IRE1 RNase activity is dependent on a conserved consensus sequence in the mRNA. This causes the formation of a new stop codon due to a frame-shift in the coding sequence. The spliced mRNA is then re-ligated via a recently identified ligase called RNA 2',3'-Cyclic phosphate and 5'-OH ligase (RTCB) in mammals[61]. Spliced XBP1 (XBP1s) is then transported to the nucleus where it acts as a pro-survival transcription factor via upregulation of genes involved in relieving ER stress and prolonging cell survival[46]. Important examples of these targets are GRP78, PDI, ER quality-control protein heat shock factor protein 40 KDa (DnaJ), p58 and ER degradation enhancing α-mannosidase-like protein (EDEM)[62]. XBP1s also alleviates ER stress via ER membrane expansion[63, 64]. The XBP1 mRNA in its unspliced form (XBP1u) is translated and contributes to IRE1/XBP1 signalling by promoting the splicing of XBP1 via IRE1 by enhancing its association with the ER membrane and also preventing XBP1s translocation to the nucleus[65-67].

1.9.2 RIDD

RIDD signalling involves the cleavage of a subset of RNAs by the IRE1 RNase domain. In comparison to XBP1 signalling, RIDD is relatively new to the field and remains largely ambiguous. However, it is known that target mRNAs are recognised by an

XBP1-like consensus sequence identified by *Oikawa et al[68]*. As of now, 37 potential RIDD targets have been reported across the literature with great variation between cell type and species[69]. While the XBP1-IRE1 axis is generally considered to be pro-survival, RIDD-IRE1 has been suggested to be a pro-apoptotic process but also a pro-survival one. This pro-apoptotic theory arises from a reported mechanism in which IRE1 is shown to regulate caspase-2 and promote apoptosis[70]. There are also counterarguments to this pro-apoptotic RIDD functionality in that it is also believed that RIDD works by cleaving mRNAs within close proximity to reduce nascent protein translation and subsequently reduce the strain on ER homeostasis[71]. Physiological functions for RIDD have been identified in inflammation and glucose metabolism[72, 73]. Like XBP1, it is highly likely that the role of RIDD in a cell is hugely context dependent and varies between cell type. RIDD has also been shown to become hyperactive under conditions where XBP1 is deficient[74], highlighting a particularly important fact to consider when targeting the XBP1 axis.

1.10 IRE1 Kinase Domain

Kinase activity in the IRE1 kinase domain is responsible for the transautophosphorylation and subsequent activation of IRE1 RNase domains. However, there is also evidences for its role as a platform for a complex known as the UPRosome, a proposed bridge between the UPR and apoptosis[32]. This platform consists of multiple protein adaptor molecules that interact with IRE1. This starts with TNF receptor-associated factor 2 (TRAF2), which when bound to IRE1, also binds to apoptosis-kinase 1 (ASK1)[75]. ASK1 activates JNK, a promoter of apoptosis. Phosphorylation of JNK leads to Bcl-2 regulation, key mediators in the cytochrome c associated intrinsic apoptosis pathway. This IRE1α/TRAF2 platform is also capable of inducing pro-apoptotic signalling via caspase-12 signalling and by association with receptor-interacting serine/threonine protein kinase-1 (RIPK1)[76, 77]. IRE1 is also a platform for NF-κB signalling where it, through TRAF2, maintains basal IκB kinase (IKK) levels and as a result basal nuclear factor kappa-light-chain-enhancer of activated B cells (NF-κB) downstream functions[78].

1.11 IRE1: Roles in disease

Often, the UPR plays a physiological role in the cell that, when perturbed, causes disease onset. Examples of these are PERK signalling in proinsulin synthesis in pancreatic β cells[79], XBP1 in fatty acid synthesis[80] and IRE1α in B-cell differentiation[81]. The aforementioned processes are just a few of the known pathological implications of a malfunctioning UPR but in recent years, there has also been a steady focus of the UPR's role in inflammatory signalling and cancer, which are often present together[82]. The role of IRE1α in particular seems to be highly implicated in this field and its role in inflammatory cytokine regulation features centrally in this. This thesis will discuss IRE1α and its role(s) in NLRP3 inflammasome activation and in pancreatic cancer cell-cell signalling, PERK signalling is examined in pancreatic cancer also.

1.11.1 IRE1 in inflammation: What we know

IRE1α plays roles in the maturation, function and survival of many immune cell types[83]. This is actually quite logical when one considers the secretory output of an immune cell and how expansive its ER must be in order to sustain itself. This gives rise to basal IRE1α activity which helps maintain normal cell functionality. A primary output of IRE1α activity in immune cells is the secretion of inflammatory cytokines via the activation of transcription factors downstream of the IRE1α kinase domain such as JNK, NFκB and pathogen recognition receptors such as nucleotide-binding oligomerization domain-containing protein 1/2 (NOD1/2). XBP1 has similarly been associated with cytokine production in splenic cells, macrophages, breast cancer and multiple myeloma cells[84-86]. It is also worth noting that the inverse, cytokine-mediated UPR upregulation has also been shown in liver cells with IL-1β and IL-6 triggering UPR activation via CREBH signalling[87]. Additionally, multiple reports indicate cytokines mediate ER stress in pancreatic β cells[88, 89]. This presents a potential autocrine feedback loop system where cytokines are the cause and product of IRE1α activity in immune disease contexts. The XBP1 axis becomes upregulated during TLR2, TLR4 and TLR7 signalling leading to type 1 interferon induction (IFN), IFN-α and IFN-β, both associated with inflammatory and autoimmune disease progression[90]. In addition to this, XBP1 ablation in dendritic cells leads to reduced

IFN-α and ER-associated apoptosis, highlighting the importance of this[91]. Ablation of IRE1α and XBP1 also was shown to reduce levels of key inflammatory cytokine, IL-1β, in epithelial cells and macrophages. IL-1β and its counterpart IL-18, will be discussed later in much greater detail later along with their associated secretion pathway, the NLRP3 inflammasome. The RIDD arm of IRE1α has also been implicated in IFN signalling through activation of retinoic inducible gene-1 (RIG-1) via cleaved mRNA fragments produced[92]. RIDD has also been associated with the aforementioned NLRP3 inflammasome via thioredoxin Interacting Protein (TXNIP) stabilization upon cleavage of the TXNIP destabilizing miRNA, miR-17[73]. This process increases TXNIP abundance and enhances IL-1β secretion due to TXNIP mediated activation of the NLRP3 inflammasome.

1.12 Inflammation

Immunity can be broadly divided into two key systems: Innate and adaptive immunity. Innate immunity, often considered the more simplistic of the two, relies on germ-line encoded receptors that respond to conserved pathogenic ligands for its activation. In contrast to this, adaptive immunity can be characterized by its ability to generate antibodies in response to an invasion. These antibodies are then used in host defence against future invasions. Comprised of an array of detector and effector molecules, they ultimately coalesce in an efficient and context dependent inflammatory response.

The inflammatory detectors, which initiate the innate immune response, respond to a plethora of stimuli that range from bacterial components to viral DNA, while the effectors initiate the response intracellularly and translate this into an inflammatory response. Immune responses occur across a broad range of cell types and include macrophages, monocytes, mast cells, eosinophils and lymphocytes. Immune cell interactions, both autocrine and paracrine, are largely governed by cytokines. Cytokines allow intracellular communication, protein-protein interaction and ultimately govern all immunogenic processes. Inflammation functions through four key steps; (1) Detection of the inflammatory stimulus via a Pathogen associated receptor (PRR), (2) Destruction and removal of the invading pathogen, (3) restoration of damaged tissue and (4) formation of immunogenic memories to prevent

reoccurrence[93]. Inflammation can be both chronic and acute, the duration and intensity of the response being the important differential between the two. The cause of inflammation varies greatly, with different stimuli eliciting different responses. The type of stimulus that presents itself to a healthy cell determines the intracellular response that will be called upon to react to it. Pathogenic stimuli are detected by specialized pattern recognition receptors (PRRs) which interpret specific stimuli and elicit an appropriate response via stringent signal transduction pathways to control the spread of an infection[94].

1.13 Adaptive immunity

While innate immunity is the initial line of defence against invading pathogens, it lacks a broad range of PAMPS to which it can react. This limitation coupled with the huge variance of pathogens capable of invading and their ability to mutate and avoid detection has led to the development of a second wave of immune activities call the adaptive immune response[95]. Adaptive immunity is made up of a more complex, tightly-regulated interplay between multiple immune cell types. These can broadly be described as antigen presenting cells and B or T lymphocytes. Together, these cells facilitate antigen-specific immune responses and generate immunogenic memory. B and T lymphocytes function by acquiring an enormous repertoire of antigen receptors via a process, called somatic recombination, that are capable of recognising a similarly enormous number of pathogens[96]. Immunogenic memory arises from specialised T and B cells, called memory T and B cells, that upon their first encounter with pathogenic antigens are retained for future encounters in which they can elicit a more robust and rapid immune response to pathogens[97].

1.13.1 T-cells

T cells or T lymphocytes originate in the bone marrow from bone marrow progenitor cells. These progenitor cells migrate to the thymus where they mature, undergo selection and are then released to the periphery. There are many T cell subsets with distinct functions but they can largely be defined as one of three types. (1) Naïve T cells that can recognise and respond to pathogenic antigens (2) memory T cells that have already interacted with an antigen and can induce subsequent, rapid responses to invasion (3) regulatory T cells (Treg) which help

regulate the adaptive immune response. Naïve T cells begin the T- cell mediated response by encountering antigens presented on antigen presenting cells such as dendritic cells (DC's)[98]. This leads to interleukin production, enhanced proliferation and differentiation of T cells which can then travel to site of infection and elicit cytotoxic responses. While in the thymus undergoing maturation, T cells are also differentiated into distinct subpopulations. This is often dependent on their expression of the cell surface receptors CD4 and CD8. In the blood and lymphoid organs, it is believed that 60-70% of T cells are $CD4^+$ and 30-40% are $CD8^+$ positive[93]. CD4+ cells are often called "helper" T cells due to their ability to activate the humoral immune response in B cells[99]. Conversely, CD8+ T cells are designated "killer" T cells and primarily enact the cytotoxic role of T cell populations[100]. A certain component of the circulating CD4+ T cells also differentiated further to make up the aforementioned Treg cells that down modulate immune responses via anti-inflammatory cytokine secretion, such as IL-10 and TGFβ[101]. Additionally, CD4+ T cells also differentiate into multiple other subpopulations designated T- helper 1 (Th1), T- helper 2 (Th2) and T-helper 17 (Th17). While Th1 and Th2 cells are well established in the immune biology literature, Th17 are a relatively recent addition and their differentiation, functions and roles in diseases are still being uncovered. What is known is that they secrete high levels of the cytokine, Il-17 (Hence the name)[102]. Th17 has also been heavily implicated in multiple autoimmune and inflammatory disorders[102].

1.14 Pattern recognition receptors

Originally proposed as part of the model of microbial pattern recognition by Charles Janeway Jr[103], the majority of PRR's are classified into one of five receptor families. These are the Toll-like receptors (TLRs), C-type lectin receptors (CLRs), nucleotide binding domain, leucine-rich repeat (LRR)-containing (also called NOD-like) receptors (NLRs), RIG-1-like receptors (RLRs) and AIM2-like receptors (ALRs). These families and their members can also be further defined by their location as either membrane-bound or membrane-unbound receptors. The membrane bound TLRs and CLRs are found on the cell surface and respond to extracellular, microbial ligands. The membrane unbound families are cytoplasmic and detect a wide variety of

intracellular stimuli. Often the receptors themselves, however, are not enough to induce an immune response. They recruit and bind to specific adaptor molecules which help orchestrate a diverse signal transduction in response to a pathogenic ligand and in some cases, help funnel different receptors into a single lane of traffic, so to speak. The effects of PRR stimulation ultimately leads to transcriptional upregulation of cytokines and interferons, effectors of both innate and adaptive immunity, amongst other things.

1.14.1 Toll-like receptors

The toll-like receptors (TLRs) were the first family of PRR to be identified and are subsequently also the most understood and characterized. To date, there are ten TLR family members in humans and 12 in mice. TLR are receptors that primarily localise to the cell surface but several members are also found intracellularly in the ER, lysosomes or endosomes where they recognise a broad spectrum of PAMPS/DAMPS. TLRs are comprised of a leucine-rich repeat (LRR) domain that recognises PAMPS/DAMPS[104]. TLR's interact with their respective ligands as dimers (either homo- or hetero-) with the help of co-receptors and accessory molecules (described later). TLR's also contain a cytoplasmic toll/IL-1 receptor (TIR) domain that initiates signalling downstream of the receptor itself. This TIR domain allows recruitment of TIR domain-containing adaptor proteins that facilitate this cascade such as MyD88 or TRIF[104]. This signalling cascade culminates in activation of key transcription factor pathways, such as NF-κB, which leads to enhanced cytokine, chemokine and interferon signalling. TLRs can be found expressed on a myriad of cell types ranging from innate immune cell types such as dendritic cells and macrophages but also in fibroblast cells and epithelial cell types. As briefly mentioned above, TLRs can localise both intracellularly and on the cell surface. This distinction is what is used to classify the 10-12 different known TLR family members[105]. The cell surface TLRs include TLR1, TLR2, TLR4, TLR5, TLR6 and TLR10 whereas the endosomal localised TLRs include TLR3, TLR7, TLR8, TLR9, TLR11, TLR12 and TLR13 (Fig. 1.3). The cell surface TLRs primarily recognise microbial membrane components such as lipids, proteins and lipoproteins. TLR4 (discussed more later in Fig. 1.4) recognises bacterial lipopolysaccharide (LPS), TLR2 in combination with either TLR2 or TLR6 recognises a

plethora of triacyl and diacyl lipoproteins that include zymosan, mannan and tGP1-mucin. TLR5 responds to bacterial flagellin alone. The intracellular TLRs primarily recognise bacterial and viral nucleic acids and also self-nucleic acids under autoimmune conditions. TLR3 recognises viral double stranded RNA (dsRNA), TLR7 recognises single stranded viral RNA (ssRNA) and TLR8 responds to bacterial and viral RNA. TLR9 recognises bacterial and viral DNA that contains high levels of unmethylated CpG-DNA motif[106].

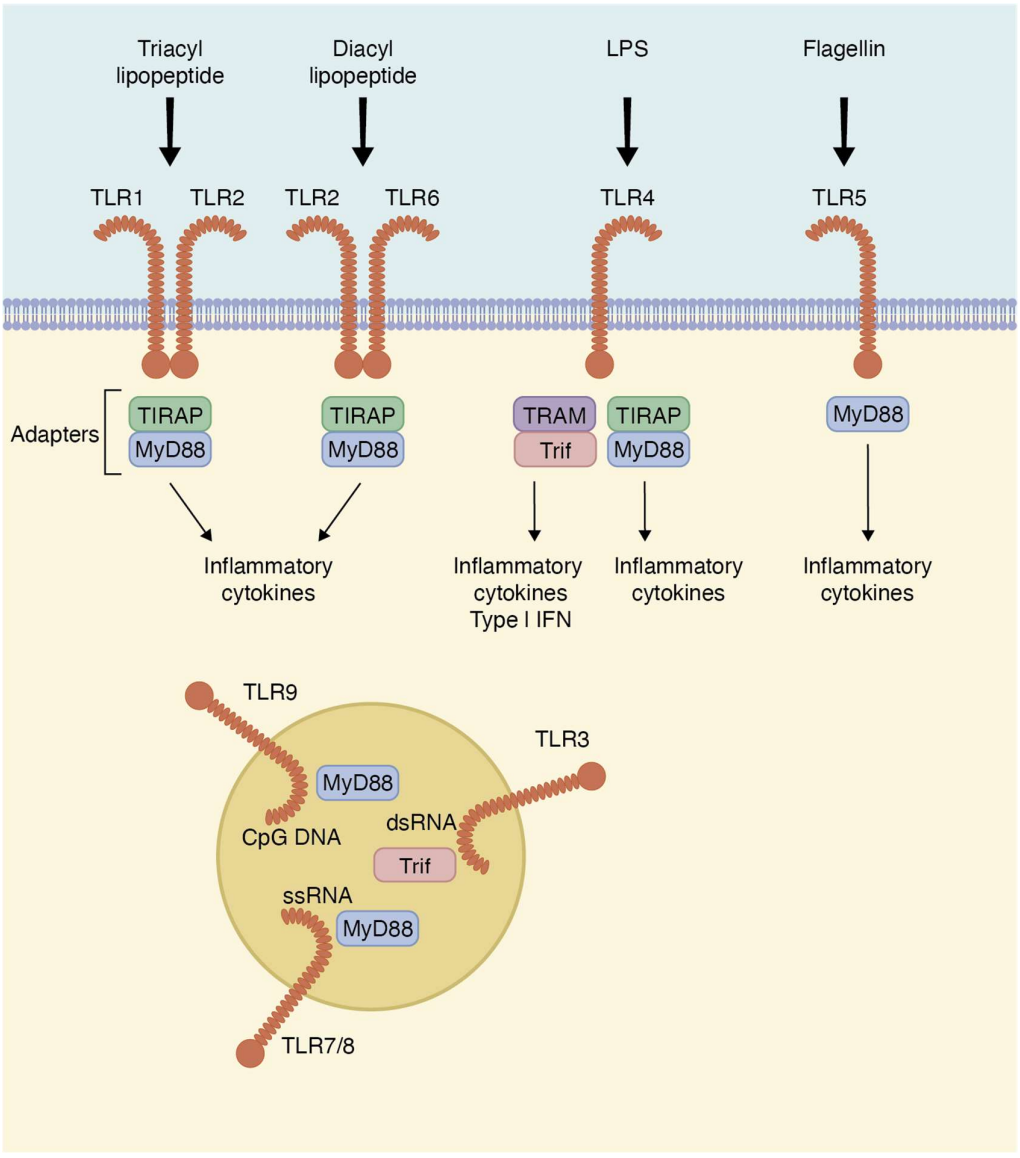

Fig. 1.3 Toll-like receptor (TLR) activation. There are 9 toll-like receptors found in humans. They differ in their localisation and ligand recognition. Across all nine

members, cells can recognise a broad range of endogenous and exogenous PAMPS and DAMPS. TLR9, TLR3 and TLR7/8 are located in endosomes and detect bacterial or viral nucleic acids. The remainder of human TLRs are found on cell surface and detect exogenous PAMPS/DAMPS. Each TLR contains specific downstream adaptor proteins that initiate a signal cascade that leads to activation of various immunomodulatory proteins. TIR domain-containing adaptor protein (TIRAP), TIR-domain containing adaptor inducing IFN-β (TRIF), myeloid differentiation primary response gene 88 (MyD88) and TRIF-related adaptor molecule (TRAM).

1.14.2 TLR4-mediated NLRP3 inflammasome priming

TLR4 was the first TLR family member characterized and is known to be activated by lipopolysaccharide (LPS), a bacterial cell membrane component. TLR4 is also considered to be part of the LPS-multireceptor complex, a complex consisting of multiple proteins essential for LPS induced PRR stimulation (Fig. 1.4). The complex consists of LPS-binding protein (LBP), CD14 and MD-2[107]. The complex operates by binding to large LPS aggregates found on bacterial membranes, transferring it to CD14 which can then transfer it to MD-2, a TLR4 bound protein[108]. This process triggers TLR4 dimerization and initiates a downstream signalling cascade. TLR4's cytoplasmic domain is comprised of a Toll-interleukin 1 receptor (IL-1R) homology domain (TIR domain) that acts as a scaffold for downstream signalling via TIR-domain containing adaptors[109]. These are TIR domain-containing adaptor protein (TIRAP), TIR-domain containing adaptor inducing IFN-β (TRIF), myeloid differentiation primary response gene 88 (MyD88) and TRIF-related adaptor molecule (TRAM)[110] (Fig. 1.3, 1.4). Ultimately, they lead to the activation of three transcription factors, Nuclear factor kappa-light-chain-enhancer of activated B cells (NF-KB)[111], Adaptor protein-1 (AP-1)[112] and IFN regulatory factor 3 (IRF3)[113].

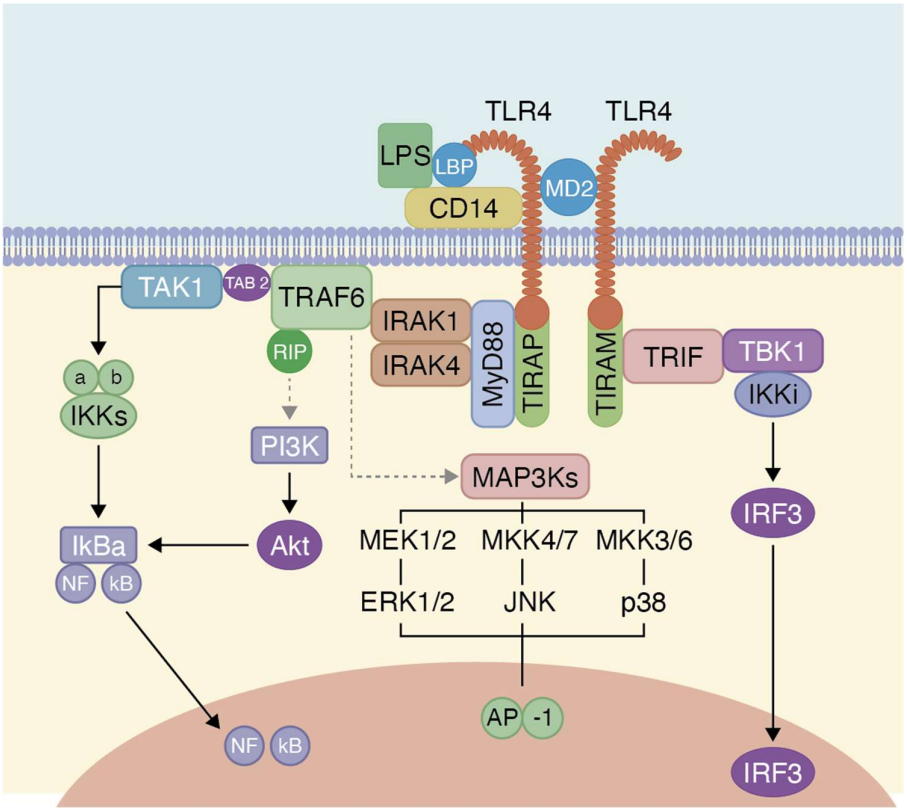

Figure 1.4. Toll-like receptor 4 (TLR4) signalling pathway. LPS binds to LBP protein, beginning the TLR4 pathway. This LPS-LBP complex facilitates the transfer of LPS to CD14, which subsequently allows the transfer of LPS to MD-2 protein. This process triggers TLR4 dimerization and conformational changes that trigger recruitment of downstream intracellular adaptor proteins that contain a TIR domain. These adaptors include MyD88, TRAM, TIRAP and TRIF. These adaptors activate various downstream signalling cascades including MAP kinases, AKT, NF-κB and AP-1 pathways, triggering a TLR4-mediated innate immune response.

1.15 Inflammasomes

Multiple cytosolic protein complexes exist that are designed to regulate immune responses to both microbial invasion or infection, environmental stresses and intracellular damage signals. These protein complexes are termed inflammasomes[114]. They were originally defined by *Tschopp et al* as high molecular weight complexes present in the cytosol of stimulated immune cells that mediate the activation of inflammatory caspases[115]. They have been identified as hugely important players in host defence against pathogens while on the flip side they have been shown to contribute to tumorigenesis, neurodegenerative disorders and metabolic syndromes under dysregulated conditions[116]. This heightens the importance for them to be tightly regulated in order that they can engage anti-

bacterial defences and launch an immune response without causing lasting effects to the body's tissues. While they differ in how they are triggered and the intermediate signalling networks that govern their function, they all ultimately coalesce in the proteolytic cleavage of two inert cytokines into their active forms. These cytokine precursors are known as pro-IL-1β and pro-IL-18[117]. Upon cleavage, they both become biologically active and play roles as highly potent pro-inflammatory mediators in a broad spectrum of immunogenic processes. These can include immune cell recruitment to the site of infection or invasion, regulation of immune cells and the activity of cytotoxic T cells[117]. As mentioned, inflammasomes are multi-protein complexes made up of several key components. An essential component of the complex is the PRR, with the majority of known inflammasomes containing a PRR from the NLR family. These receptors detect signals that can be extrinsic pathogen associated molecular patterns (PAMPS), danger signals released from damaged or necrotic cells called damage associated molecular patterns (DAMPS) or other stimuli such as particulate matter or crystalline structures (Asbestos, for example). As of today, we are aware of 5 inflammasomes that exist, and they can be defined by the PRR present in the complex. They are NACHT, LRR and PYD domains-containing protein 1 (NLRP1)[115], NACHT, LRR and PYD domains-containing protein 3 (NLRP3)[118], NLR family CARD domain-containing protein 4 (NLRC4)[119], absent in melanoma 2 (AIM2)[120-123] and the pyrin inflammasome[124]. NLRP1, NLRP3 and NLRC4 are all members of the NLR family but all five above-mentioned inflammasomes are called what we define as "canonical" inflammasomes. This set of canonical inflammasomes exist alongside another set defined as "non-canonical" inflammasomes, that differ in how they target caspase-4 and -5 in humans and caspase-11 in mice[125]. The above mentioned PRRs have been found to associate in specific complexes whose compositions are understood, emerging evidence suggests that there are more PRR's also capable of inflammasome formation, but these complexes compositions remain elusive at this point. The focus of this work is on the NLRP3 complex, one of the most studied and important inflammasomes. NLRP3 is unique in two ways; (1) how it responds to a very broad spectrum of stimuli ranging from extracellular ATP, pore-forming toxins, bacterial, viral and fungal PAMPs and (2) its requirement for a two-step activation process.

1.15.1 The non-canonical inflammasome

While the canonical inflammasomes result in caspase-1 autocatalysis and the secretion of activated or mature IL-1β, the non-canonical pathway operates via caspases-4, -5 (in humans) or -11 (in mice) in response to infection by Gram-negative bacteria (via LPS)[126]. Similarly, to canonical signalling they initiate pyroptosis. It has also been proposed that in contrast to the canonical pathway, the interactions between caspases and LPS are direct. The precise interaction between LPS and the caspases remains yet to be elucidated and there is interest into whether other additional factors are required here. Extracellular LPS binds and activates TLR4, inducing type 1 interferon alongside the complement system to activate caspase 11[127]. The direct binding of LPS to caspase 11 then triggers its oligomerization and auto-catalytic activation[128]. GSDMD is then cleaved by one of the activated non-canonical caspases allowing the subsequent K+ efflux that follows to activate caspase 1-NLRP3 mediated IL-1β maturation[129]. Interestingly, the existence of both canonical and non-canonical signalling pathways allows for different systems for host cells to recognize LPS in both extracellular and intracellular spaces.

1.16 The NLRP3 Inflammasome

The importance of NLRP3 was identified when it was shown that it was heavily linked to a series of autoimmune diseases such as cryopyrin-associated periodic syndrome (CAPS) and Muckle-Wells syndrome[130]. The NLRP3 inflammasome consists of three key components, a sensor (NLRP3), an adaptor apoptosis-associated speck-like protein containing a CARD (ASC) and an effector (pro-caspase-1). NLRP3 contains multiple key domains, namely an amino-terminal pyrin domain (PYD), a central NACHT domain, a C-terminal caspase-recruitment domain (CARD) and a C-terminal leucine-rich repeat domain (LRR domain). The NACHT and LRR domains are believed to be important for NLRP3 oligomerization and function with the former providing ATPase activity and the latter providing an autoinhibitory function, creating a sort of feed-back loop. NLRP3 also contains two protein interaction domains via its PYD and CARD regions[131].

1.16.1 NLRP3 Oligomerization

NLRP3 inflammasomes require a large-scale oligomerization process to become activated. The first step in this process is the homotypic oligomerization of NLRP3 units via their NACHT domains. This NLRP3 oligomer then recruits the NLRP3 complex adaptor protein, ASC, via homotypic PYD interactions. Subsequent ASC filamentation also occurs via PYD-PYD interactions[132]. This triggers an important event in which a mass-oligomerization and assembly of ASC occurs[133]. This structure is a macromolecular aggregate called a speck and is comprised largely of dimeric ASC multimers. ASC is often termed PYCARD because of the two important domains it contains, a PYD domain and a CARD domain. The ASC oligomers are arranged in long helical filaments that expose ASC on their surface to allow for caspase-1 recruitment to the complex. The assembled ASC specks recruits pro-caspase-1 via homotypic CARD interactions. This allows ASC to bring pro-caspase-1 monomers into close proximity to one other, which causes mass autocatalysis of pro-caspase-1 inducing pro-caspase cleavage and formation of the active form of caspase-1. Next, via its CARD domain, this activated caspase-1 can then go on to cleave the pro forms of IL-1β and IL-18. These active cytokines are the essential effector molecules of the NLRP3 inflammasome (and other inflammasomes). Advanced electron microscopy techniques identified that the NLRP3 complex adopts a similar wheel or disk like architecture to that seen in the apoptosome which contains 10-12 “spokes” that each correspond to an individual protomer[134, 135] (Figure 1.5).

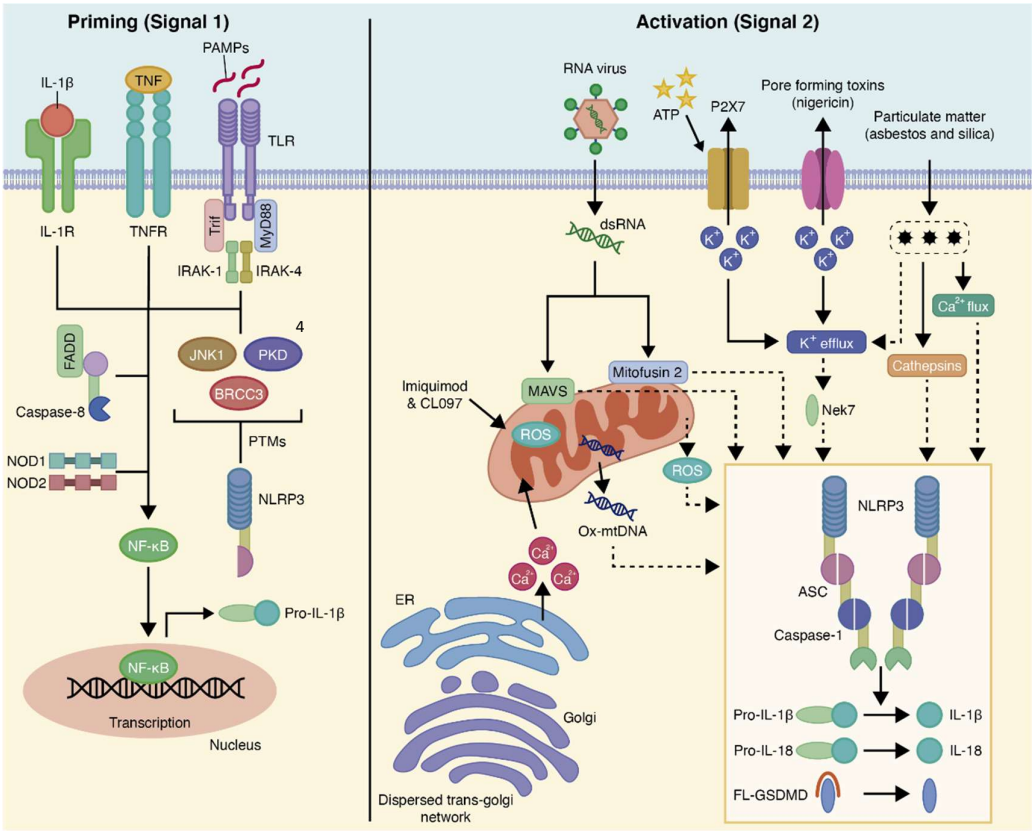

Figure 1.5: The NLRP3 inflammasome. The two-signal model for NLRP3 inflammasome activation consists of the priming signal (signal 1, left) and the activation signal (signal 2, right). Signal 1 is provided by microbial components (PAMPS) or endogenous cytokines, leading to the activation of the transcription factor NF-κB and subsequent upregulation of NLRP3 and pro-IL-1β. This activation begins with ligand-mediated activation of TLR4 (Toll-like receptor 4) amongst other cell surface receptors (TNFR (tumour necrosis factor receptor) and IL-1R(Interleukin 1 receptor). Caspase-8, FAS-mediated death domain protein (FADD), and NOD1/2 are also involved in the priming step by regulating NF-κB activity downstream of TLR4 stimulation. Post-translational modifications of NLRP3 have also been shown to regulate its activation and are induced by multiple factors including JNK1, BRCC3 and PKD. Signal 2 is more ambiguous but believed to be provided by a variety of stimuli including extracellular ATP, pore-forming toxins, RNA viruses, K^+ or Ca^{2+} efflux and particulate matter. Multiple molecular events such as ionic flux, mitochondrial dysfunction, reactive oxygen species (ROS) generation, and lysosomal damage, can activate the NLRP3 inflammasome. This activation leads to a mass oligomerization of key inflammasome components including NLRP3, ASC, Caspase-1 and NEK7 (Discussed in detail elsewhere). Definitions: TNFR (tumor necrosis factor receptor); IL-1R (IL-1β receptor); BRCC3 (BRCA1/BRCA2-containing complex subunit 3); JNK1 (JUN N-terminal kinase 1); PKD (protein kinase D); TLR (toll-like receptor);

1.16.2 NLRP3 Priming

NLRP3 has a unique two-step activation step, whereas other inflammasomes require only a single step activation process (Fig. 1.5). The first step is the transcriptional upregulation of key NLRP3 inflammasome components including NLRP3 itself and pro-IL1b[136]. This step is initiated by TLR4 activation via one of its many known ligands, such as *lipopolysaccharide* (LPS). TLR4 activation leads to nuclear factor kappa-light-chain-enhancer of activated B cells (NF-κB) transcriptional upregulation of NLRP3 inflammasome components[137]. NLRP3 priming also causes other changes in the cell such as a metabolic shift where oxidative phosphorylation switches to glycolysis and subsequently leads to hypoxia-inducible 1α (HIF1α) stabilization and increased IL1B transcription[138, 139]. There is also increasing evidence of the importance of post-translational modifications on NLRP3 in response to NLRP3 priming and its role in regulating NLRP3 assembly is likely to become important as research continues[140].

1.16.3 NLRP3 activation and assembly

The first priming step of NLRP3 inflammasome activation is often called a "licensing" step in that it gears the cell up for full activation if the subsequent demands are met. The second part of this two-part activation comes in the form of the "assembly step". There is much less understood about the specifics of this second step but what we do know is that it triggers the oligomerization and subsequent formation of the NLRP3 complex. This process begins after the initial NF-κB priming step and all required components have been transcribed. NLRP3 can be activated by bacterial, viral and fungal infections but also from endogenous DAMP signals. Some of these signals include nigericin, valinomycin, adenosine triphosphate (ATP), uric acid, asbestos and aluminium hydroxide[141-145]. This would suggest that NLRP3 assembly is not induced by these individual signals, but rather by a downstream signal common to them all. Likely signals that could result from these stimuli include reactive oxygen species (ROS) production, calcium signalling (Ca^{2+}), potassium efflux (K^{+}), lysosomal rupture, cell swelling and mitochondrial damage[146-150].

1.16.4 K^+ and Ca^{2+} efflux

It has been shown that K^+ efflux and Ca^{2+} are important activators of NLRP3 activity[151, 152]. The membrane cation channel, purinoceptor 7 (P2X7), can be stimulated by ATP to promote Ca^+ and Na^+ influx[153]. This then simultaneously activates the channel two-pore domain weak inwardly rectifying K^+ channel 2(TWIK2) allowing K^+ efflux[154]. It is worth noting that this efflux has been shown to be specific to NLRP3, with no effects seen in the other complexes examined. Despite this, it has also been shown that NLRP3 inflammasome activation is possible in the absence of K^+ efflux[155]. Ca^{2+} signalling is also influenced by NLRP3 stimuli and this effect is once again limited to the NLRP3 inflammasome[153]. In other studies, the role of Ca^{2+} signalling has been found to be largely dispensable as changes in cytosolic Ca^{2+} were shown to have no effect in comparison to that of K^+. Taken together, the literature suggests that both Ca^{2+} and K^+ efflux play important roles in NLRP3 activation and often through cooperative means. However, it has also been shown that in certain circumstances, both are redundant. It is likely that experimental conditions, models and third-party factors largely influence the roles of K^+ and Ca^{2+} here and further study and dissection of the pathway are necessary.

1.17 mtROS and mtDNA

Both mitochondrial ROS (mtROS) and mitochondrial DNA (mtDNA) are known upstream regulators of NLRP3 activity[150]. Cellular stress induced mtROS, expressed basally as by-products of oxidative phosphorylation but exacerbated during stress, are important activators of NLRP3[156]. Disruption of mitochondrial oxidative phosphorylation machinery was shown to induce NLRP3 activation and this activity was shown to be independent of K^+ efflux[157]. Potentially explaining this, it was shown in another study that ROS inhibitors inhibited the priming step but not the activation step.[158]. Similar to mtROS, mtDNA acts as a DAMP and induces NLRP3 activity[159]. The use of multiple known NLRP3 activators was shown to lead to the release of mtDNA into the cytoplasm, likely via MPT pores. mtROS and Ca^{2+}signalling have been shown to cooperate in the release of mtDNA via mitochondrial permeability transition (MPT) pores[160]. Interestingly, the oxidative state of cytosolic mtDNA determined whether it activated NLRP3 or the AIM2

inflammasome[161]. Oxidized mtDNA has been shown to immunoprecipitate with NLRP3 after activation while non-oxidized mtDNA preferentially stimulates AIM2.

1.18 IL-1β, function and release

IL-1β is cleaved into its active p17 form by caspase-1 and released into the extracellular space upon inflammasome activation[162]. Interestingly, IL-1β secretion does not occur via the traditional secretory pathway and how it reaches the extra cellular space to enact its functions remains a mystery to some extent[163]. To date many mechanisms have been proposed, for example, *Brough et al* suggest that caspase-1 selectively transports IL-1β across the plasma membrane[164, 165]. *Mackenzie et al* propose that the process involves microvesiculation of the membrane[166] while *Cullen et al* claim that the release simply occurs as a result of necrotic leakage[167]. While the path to secretion remains unclear it is well established that IL-1β is an essential effector of immunogenic processes once released.

1.19 Pyroptosis

Along with the production of inflammatory cytokines, NLRP3 inflammasome activation also leads to a rapid, lytic form of programmed cell death[168]. Previously referred to as caspase-1 mediated monocyte death, this form of cell death is termed pyroptosis. It operates as a general innate immune effector mechanism in that it relies on PRRs to detect an inflammatory stimulus. Pyroptosis is distinct from apoptosis and can be characterized by a number of morphological changes observed upon its induction[169]. These include cell swelling, lysis and the release of the cell's cytoplasmic components. This release is believed to be facilitated by the formation of membrane pores. This pore formation process has been shown to be dependent of a protein called gasdermin D (GSDMD)[170]. GSDMD belongs to a gene family of poorly understood genes called the gasdermin (GSDM) family. This family is comprised of four gene members in humans, namely gasdermin A (GSDMA), gasdermin B (GSDMB), gasdermin C (GSDMC) and GSDMD. The precise functions of these proteins remain elusive with the exception of GSDMD, which has now been shown to mediate pyroptosis. The mechanism remains poorly understood but it has been proven that GSDMD is comprised of an N-terminal cell death domain

(GSDMDNterm), a central short linker region and C-terminal autoinhibition domain. Caspase-1 mediated GSDMD cleavage and C-terminal removal alleviates the autoinhibitive domain allowing the protein to bind phosphatidylserine on the inner side of the membrane. This then allows GSDMD to form pores leading to cell death from within by disrupting osmotic potential and leading to cell swelling and lysis. Additionally, it may also serve as a release mechanism for active IL-1β and IL-18 via a form of non-conventional secretion[171].

1.20 Inflammation and cancer

Inflammation can be associated with a myriad of diseases, cancer being a well-documented example. Inflammation arises as a result of tissue injury and seeks to repair it, but in the case of cancer, it is said that tumorigenesis acts like a wound that the body fails to heal[172]. This chronic, dysregulated inflammation and how it leads to and propagates cancer, while generally accepted, is still being analysed on a mechanical or molecular scale. Tumour sites are home to a vast array of immune cell types that elicit immunoactive and immunosuppressive responses, the balance of which governs the body's response to neoplastic tissues. These responses are largely decided by signalling factors like cytokines. Continued inflammatory signalling brought on by a failure to eradicate the threat posed by neoplastic tissues ultimately leads to an inadvertent pro-tumorigenic inflammatory response that promotes tumour growth[173]. This response arises from infiltrating immune cells acting as potent secretors of pro-angiogenic and proliferative signalling factors such as VEGF and TGF-β[174, 175]. Additionally, chronically activated immune cells are also capable of releasing DNA-damaging agents such as ROS or NOS species which can genetically alter locally proliferating cells[176, 177]. In fact, many diseases such as irritable bowel disease, chronic pancreatitis and crohns disease all exhibit chronic immune responses that often lead to tumorigenesis in their respective organs[178-180]. The NLRP3 inflammasome, a key intracellular signalling platform for inflammatory pathways, has also specifically been associated with the progression of multiple cancer types and IL-1β levels often associate with poor disease prognosis. The NLRP3 inflammasome has been linked to colon, breast, prostate and pancreatic cancers with the proliferative, invasive and metastatic properties of IL-1β and IL-18

being the most commonly associated mechanisms[181]. Pro-inflammatory cytokines such as IL-6, TNF-α and IL-8 are all potent regulators of inflammatory responses and correlate heavily with the development and prognosis of multiple tumour types. Recent evidences in certain tumour types have highlighted a role for IRE1 in the regulation of key pro-inflammatory cytokines, creating an interesting link between IRE1, inflammation and cancer[86].

1.21 IRE1 and its role(s) in Cancer

The UPR has long been associated with cancer and IRE1 in particular has become associated with almost all of the "classical" hallmarks of cancer (Fig. 1.6)[182]. Since being first proposed in 2004 by *Ma et al,* our knowledge of the UPR's role here has evolved[183]. Intrinsic and extrinsic stressors trigger chronic UPR activation in certain tumours[184]. Intrinsic ER stress arises in the form of somatic mutations and to date such mutations have been identified in all three UPR sensors[185]. Extrinsically, the UPR provides the tumour with a support network allowing to cope with continuous proliferation and heightened protein folding demands. Our knowledge of UPR activation suggests that this sustained activity, further exacerbated by the toxic micro-environment associated with tumours, will lead to ER stress-induced apoptosis[186]. However, this is usually not the case. Tumours bypass UPR machinery to sustain pro-survival signalling and not engage the pro-apoptotic components of the UPR. IRE1 has been identified to play roles in all stages of cancer development, largely by acting as a coping mechanism for the side-effects of tumorigenesis on the tumour itself[187]. The roles, however, differ from tumour to tumour. IRE1 has been shown to be upregulated following oncogenic activation in multiple cancers with *c-MYC* driven-IRE1 activation becoming a hot topic in the field recently[188]. H-ras activity was also shown to drive a UPR response in melanocytes and keratinocytes[189]This oncogenic IRE1 activation may be a pro-survival response by the cell with the hope being to alleviate ER stress being generated by increased protein demand. There are many suggestions as to how tumour cells maintain this tight balance between UPR pro-life and pro-death mechanisms, and they include downregulation of apoptotic components. For example, H-RAS downregulates CHOP mRNA in RAS-transformed MEF's[190] and c-MYC induced PERK activity was linked

to increased autophagy which may alleviated cell death associated with ER stress via engulfment of misfolded proteins[191]. The tumour suppressor gene, *p53*, is capable of suppressing the IRE1/XBP1 axis under conditions of ER stress[192]. Alongside these potential functional roles of IRE1 in early-stage cancer activation there are also suggestions that IRE1 mutations may exist and be able to drive tumorigenesis. A study analysing the genomes from cancer patients (multiple tumour types) identified *Ire1* as one of the top twenty mutated kinases[193] and a more recent analysis of multiple cancer databases by *Chevet et al* confirmed the common occurrence of *Ire1* mutations[184]. Links between IRE1 and tumour growth and proliferation are well documented across multiple cancer types, including breast, prostate, glioblastoma and pancreatic[86, 194, 195]. The inhibition of IRE1 leads to reduced cellular proliferation in all cases but without the induction of cell death (Except in the case of pancreatic cancer, discussed more below[196]). Indeed, in colon cancer cells it has been shown that IRE1 inhibition causes G1 arrest via regulation of cyclin D1 and β-catenin signalling[197]. A similar role for IRE1 in cell-cycle regulation is seen in prostate cancer, where IRE1-mediated regulation of cyclin A1 showed a similar reduction in proliferation[198]. The cost of infinite proliferative potential for a tumour is the presence of a toxic tumour microenvironment. This microenvironment, present in most solid tumours, occurs as a result of how tumours quickly outgrow their blood supply leading to a hypoxic, nutrient deprived niche surrounding the tumour itself. Hypoxia leads to increased ROS levels in tumours, which is a known inducer of PERK activity[199, 200]. Mouse embryonic fibroblasts (MEFs) exposed to hypoxic conditions with deficient XBP1 levels exhibit reduced survival in vitro and reduced xenograft formation in recipient mice[201]. The role of IRE1 in regulating a tumours ability to withstand hypoxia may arise through its interactions with hypoxia inducible factor 1-alpha (HIF1α)[202]. Angiogenesis permits tumour expansion and growth and is regulated by several key factors such as vascular endothelial growth factor-A (VEGF-A)[203]. HIF1α is also known to induce VEGF-A production under hypoxic conditions and it is also now known that VEGF-A production by HIF1α is dependent on XBP1s as shown by *Chen et al[202]*. However, recent evidences in glioblastoma have shown that the IRE1-VEGF-A interaction can be further delineated by isolating IRE1's XBP1 and RIDD arms. *Lhomond et al* have shown that somatic IRE1

variants in glioblastoma differ in their angiogenic potential with mutations that give enhanced XBP1 signalling favour angiogenesis whilst mutations that favour RIDD activity supress angiogenesis[195]. The blood vessels formed during angiogenesis provide an escape route of sorts for tumour cells to escape the confines of the tumour mass and to metastasise to other organs. However, in order for this to occur, cells must undergo an epithelial to mesenchymal transition (EMT) to acquire their invasive phenotypes. This process is driven by a group of transcription factors (Snail1, Snail2, Twist) that down regulate cell adhesion markers like E-cadherin and N-cadherin whilst simultaneously upregulating mesenchymal markers, such as vimentin[204]. EMT has been linked to IRE1 signalling in breast cancer with XBP1 knockdown showing increased epithelial markers in the mesenchymal triple negative breast cancer (TNBC) cell line MDA-MB-231's[205]. However, IRE1 deficiencies in glioma cells and U87 cells showed increased invasion and migration likely as a result of increased levels of secreted protein acidic and rich in cysteine (SPARC), a known RIDD target[206]. This discrepancy could be a result of RIDD vs XBP1 mediated activity, as was the case when talking about glioblastoma angiogenesis above. IRE1 is also known to regulate tumour chemoresistance. Chemoresistance can be roughly described as a sub population of cells that persist after successful chemotherapy, after which the patient often enters remission and disease regression. What is left is a group of viable cells with the ability to withstand treatment. Many chemotherapies target cell division meaning that the largely quiescent cancer stem cell (CSC) population remains relatively untouched. IRE1 has been shown to play a role in sensitisation of CSC's to chemotherapy as MDA-MB-231 xenografts show tumour regrowth after doxorubicin treatment that can be stalled with the addition of the IRE1 RNase inhibitor, MKC8866[86]. This suggests a role for XBP1 in tumour regrowth. Coinciding with this is the report by *Chen et al* showed that XBP1 levels positively correlate with disease relapse and poor survival[202]. CSC's in breast cancer are major players in tumour relapse, and they are defined by their characteristic CD44high/CD24low expression along with their ability to form mammospheres, 3D tumour cell formations that can be grown in vitro. *Logue et al* have shown that XBP1 knockdown and MKC8866 treatment post-chemotherapy were both shown to reduce mammosphere formation, a model of disease relapse.

With very promising research into the molecular mechanisms of IRE1's role in tumorigenesis, there has been a strong focus on certain tumour types over others. Pancreatic cancer, a tumour type formed in an already highly secretory organ with an associated extensive UPR activation, remains relatively unexplored. While some isolated studies have examined the impact of IRE1 and specifically IRE1-ablation in pancreatic cancer, we still don't know much about its role. Combine this basally active ER with the inflammatory tumour-microenvironment associated with pancreatic cancers and one can easily hypothesize an important role for IRE1 here.

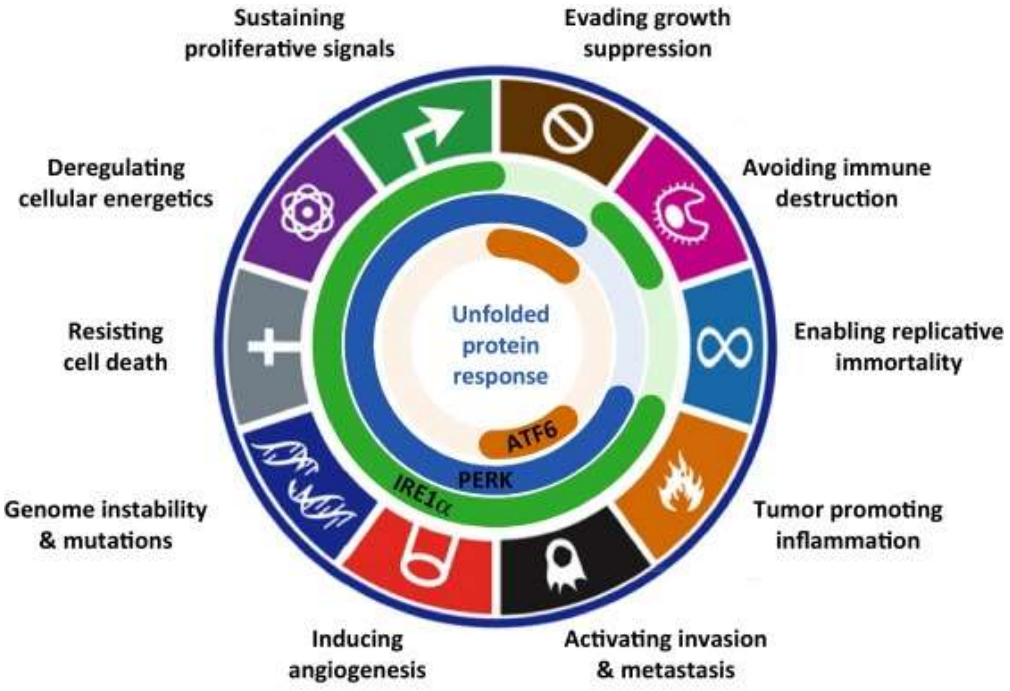

Figure 1.6: The role of the UPR in the classical hallmarks of cancer. All three arms of the UPR have become associated with cancer progression and linked to almost all cancer hallmarks defined by *Hanrahan et al.* IRE1 and PERK represent the arms with the most widespread roles in cancer development and maintenance with ATF6 also showing associations.[182]

1.22 Pancreatic cancer

The majority of pancreatic malignancies arise from the exocrine tissue with particular prevalence in the ductal cells. Within this cluster of malignancies, of which there are numerous variants, pancreatic ductal adenocarcinoma (PDAC) is by far the most common. In fact, PDAC is so common that it is often referred to simply as pancreatic cancer. Acinar cell carcinoma (ACC) is an example of a rare form exocrine derived cancer that accounts for only 1-2% of adult pancreatic tumours but exhibits a higher prevalence in paediatric patients. Pancreatic neuroendocrine tumours (NET) are an example of a pancreatic malignancy that arises in endocrine tissue. NET's cause disruptions to hormone levels which have a broad effect on bodily function. If NET's interfere with or alter hormone levels, they are termed functioning PNETS and can be further defined based on the specific issues that arise from them. For example, Gastrinomas can occur from any part of the pancreas and result in an over-production of the hormone gastrin which can lead to stomach ulcers and include symptoms such as abdominal pain, diarrhoea and heartburn.

1.22.1 PDAC

In 2015, there were 367,000 newly diagnosed PDAC patients with 359,000 of these dying in the same year. These staggering mortality rates means pancreatic cancer is the fourth leading cause of cancer-related deaths in developed countries with this expected to rise to second within the next decade or so. The five-year survival for PDAC patients is <7%[207]. The poor prognosis is due to multiple reasons but can be largely contributed to the commonly late-discovery due to the relatively asymptomatic nature of the malignancy. Symptoms of the disease are non-specific and include weight-loss, nausea and in some rare cases diabetes mellitus and migratory thrombophlebitis. This, alongside a lack of accurate biomarkers, difficulty in imaging early-stage disease and its aggressive nature make it a nightmare for clinicians to treat and the need for a targeted, molecular therapy is dire. Currently the only curative treatment is surgical resection if the disease is caught at an early stage, even in this circumstance; the five-year survival for these patients is only 15-25%. Pancreatic cancers have a unique, dense collagenous stroma that surrounds the tumour itself and subsequently makes drug delivery difficult. This layer is termed the

desmoplasia and is comprised of extra cellular matrix proteins-collagens, fibronectin and laminin that are produced by the activated pancreatic stellate cells, discussed in more detail later[208]. Interactions between stromal stellate cells and pancreatic cancer cells have been shown to be symbiotic in nature with one stimulating the growth and proliferation of the other. Stellate cells also play a role in granting these tumours the huge chemo resistance they exhibit by creating a physical barrier against drug delivery[209]. The current standard of chemotherapy is a nucleoside analogue called gemcitabine developed by Eli Lilly that causes a disruption to cellular replication and leads to apoptosis[210]. This drug grants 6 months extra life-expectancy to patients at most according to most studies[211]. While the molecular pathways involved in the development, progression and metastasis of pancreatic cancer have been slowly brought into the limelight over the years, we have yet to identify a targetable molecule that can be used effectively to treat the disease[212].

1.22.2 PDAC and the UPR: What we know

Research into the UPR in PDAC remains limited when compared to other tumour types. What is known, however, is that there is an overexpression of GRP78 levels in PDAC tumour that correlate with poor prognosis and the use of siRNA for GRP78 reduces proliferation and enhances chemotherapy induced cell death in cell lines[213, 214]. Regarding the PERK arm of the UPR, ATF4 and PERK levels are found to be overexpressed in neuroendocrine tumours[215] while in PDAC tumours, ATF4 levels can be induced after Gemcitabine treatment, a very common PDAC treatment[216]. Inhibition of the IRE1α/XBP1 axis using chemical inhibitors of the IRE1α RNase domain was also shown to reduce proliferation in PDAC cell lines but it is important to note that ER stress was artificially induced during these experiments also[217]. While the UPR seems to be activated in response to a tumour due to high protein turnover required for tumour growth and deleterious conditions associated with tumorigenesis ,like hypoxia and nutrient deprivation, evidences for UPR activity in PDAC onset and development have also been shown. The ER-associated protein anterior gradient protein 2 homolog (AGR2), has been demonstrated to correlate with early PDAC neoplasia's where its levels seem to increase while key UPR genes are simultaneously downregulated[218]. The authors hypothesize this may be an

important mechanism for tumours to circumvent ER-stress associated apoptosis. ER stress has also long been associated with chronic pancreatitis(CP), a condition that leads to PDAC development in patients more often than not. Specifically, ATF6 levels are found to be upregulated in murine models presenting CP and these were shown to influence p53 mediated apoptosis synonymous with CP cells[219]. Classical PDAC inducing carcinogens like smoking, alcoholism and poor diet have all also been linked to ER stress and UPR activity further strengthening the argument that analysing the role of the UPR in this model would be of great benefit to the betterment of current treatments and molecular understanding of the disease[220, 221].

1.23 PDAC tumour microenvironment

As knowledge about PDAC genetics, cellular biology and clinical responses advance we still only see incremental increases in survival rates and effective treatment strategies. A major roadblock in targeting PDAC tumours is the unique tumour microenvironment (TME) found in PDAC patients. The PDAC TME presents a dense stroma that surrounds the tumour in what is called a desmoplastic reaction. This stroma is comprised of many cell types and plays a role in PDAC tumorigenicity in many unique ways (Fig 1.7). While normal pancreatic tissues maintain basal levels of many TME components, it is upon injury or tissue damage that we see a large increase and upscaling of these components, where their physiological roles are often circumvented into pathological ones. Examples of these events include immune cell recruitment and activation or fibroblastic-mediated extra-cellular matrix (ECM) protein deposition. The primary components of the PDAC TME are cancer associated fibroblasts (CAF), acellular stroma, pancreatic stellate cells (PSC), immune cells and a wide range of soluble factors including cytokines, chemokines and growth factors. These components comprise a dense desmoplasia that surrounds the tumour and, in some cases, can account for 80% of total tumour volume[222].

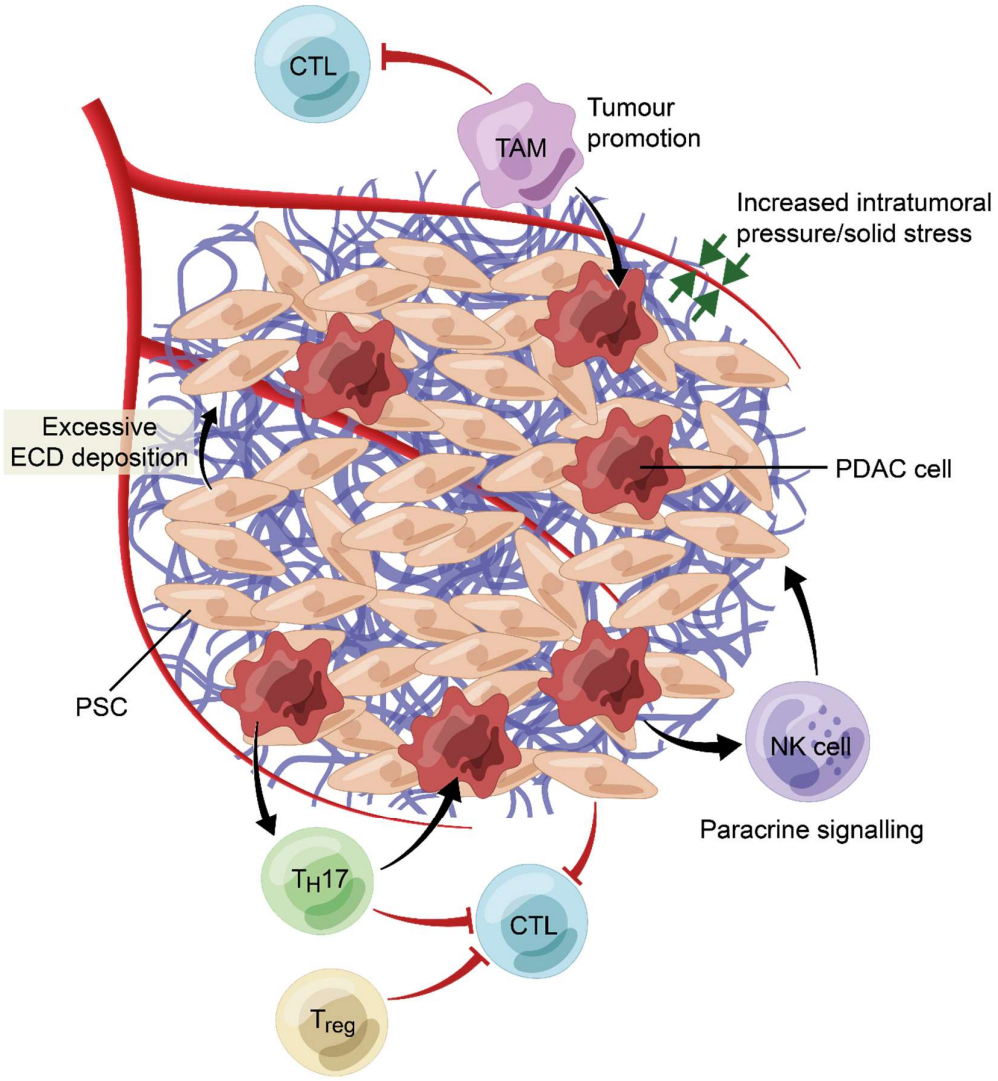

Figure 1.7: The pancreatic tumour microenvironment. The PDAC tumour microenvironment (TME) is a densely packed environment comprising of multiple cell types. Activated pancreatic stellate cells create excessive extracellular matrix deposits which causes intratumoural pressure, hypoxia, nutrient deprivation and the associated stresses. This enhanced desmoplasia is also believed to reduce effective drug delivery and reduce treatment efficiency. An immunosuppressive inflammatory infiltrate made up of regulatory tumour-associated macrophages (TAMs), T cells (Treg), and TH17 cells is recruited to the PDAC microenvironment. These cells enhance tumour promotion and dampen cytotoxic T lymphocyte (CTL) and natural killer (NK) responses to the tumour.

1.24 Pancreatic stellate cells

PSCs are periacinar star-shaped cells that form part of the pancreas under healthy conditions. They largely resemble hepatic stellate cells (HSC) found in the liver and share similar morphologies, vitamin A storage capacities and protein marker expression[223]. PSC's exist in two primary states; Quiescent (qPSC) and activated (aPSC). qPSCs express an array of specific markers that help define their state, such as desmin and synemin. The precise role(s) of qPSC remain elusive, but what is known is their vitamin A storage capacity, maintenance of pancreatic tissue structure and their potential roles in autophagy and immune regulation. In general, qPSCs are considered a sort of "housekeeper" cell in healthy pancreatic tissue that maintain its normal functions[224]. However, during pathological conditions, qPSCs undergo morphological and functional alterations upon detection of certain damage signals. These damage signals are released upon various pancreatic insults ranging from chronic pancreatitis, alcoholism and to PDAC formation. The factors themselves range from risk factors associated with things like alcohol consumption and smoking, environmental stresses such as hypoxia, hyperfusion and oxidative stress (associated with many pancreatic maladies) and cellular factors such as growth factors and/or cytokines[225]. In concert, these factors transform qPCRs into active myofibroblast-like cells called aPSCs. aPSC markers include vimentin, fibroblast activation protein-α(FAP-α) and α-smooth muscle actin (αSMA). aPSCs lose their vitamin A droplets, alter their protein expression markers and induce large scale production of extra-cellular matrix (ECM) proteins and signalling factors. The production of cytokines and growth factors allows continued PSC activation but also enhanced tumour cell growth, migration, invasion and metastasis via paracrine signals (Fig. 1.8)[226].

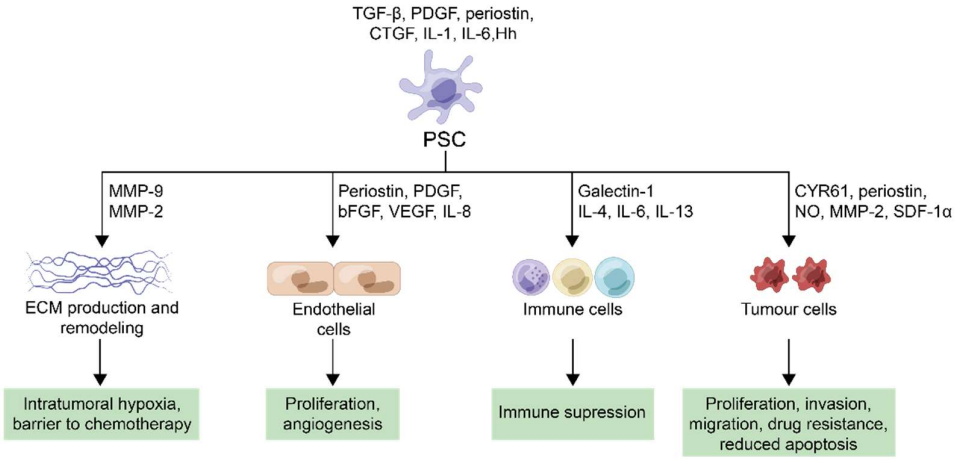

Figure 1.8: Active PSCs enhance PDAC tumourigenesis via secreted factors. Inactive and quiescent pancreatic stellate cells are activated under malignant conditions via cytokines and growth factors. They themselves subsequently release a myriad of secreted factors that are capable of influencing PDAC tumours and the surrounding stromal components. Adapted from *Schnittert et al* (2019)[227].

1.25 PDAC immune status

As pancreatic tissues progress towards full-blown tumourigenesis, alongside the expected genomic and fibrotic issues associated with PDAC, there is altered immune responses observed also. Inflammatory mediators such as IL-1β, IL-6 and TNFα are known promotors of chronic inflammation. These cytokines are heavily secreted from aPSC and PDAC cells, nurturing an inflammatory response in the local TME. Chronic inflammation alters cell biology of both normal pancreatic tissue but also inactive stellate cells in the damaged tissue and promotes malignant transformation. Chronic inflammation shifts the immune response towards that of an immunosuppressive phenotype which allows further tumour progression as a result of immune evasion by transformed cells[228]. PDAC patient tumours are largely considered immunosuppressive with large observed amounts of anti-inflammatory cytokines and factors found in the TME. Inversely, it has also been shown that patients can also exhibit significant levels of tumour associated lymphocytes whose levels correlate to a positive clinical prognosis[229]. It is worth noting that immune exhaustion is also common in PDAC patients meaning this initial activation may inevitably be reduced[230]. In fact, over 47 promising clinical trials involving immunotherapy on PDAC patients failed to show an improvement over standard chemotherapy[231]. These included the highly promising immune checkpoint inhibitors programmed cell death-ligand 1 (PD-L1) and cytotoxic T-lymphocyte associated protein 4 (CTLA-4)[232].

1.25.1 Natural killer cells

NK cells are innate immune cells with lytic functionality that provide the bodies initial line of defence against pathogens via the release of cytotoxic agents like perforin and granzyme B[233]. They make up about 5-15% of the total circulating cell population and were identified by their strong anti-cancer cytotoxicity[234]. NK cells are also capable of producing large numbers of inflammatory cytokines and chemokines which contribute further to the immune response[235]. Unlike T-cells, which mount antigen-specific immune responses, NK cells rely on germ-line encoded NK receptors (NKRs). NK cells recognise and kill tumour cells through a series of activating and inhibitory receptors, the “net” result of which induces NK cell mediated cell

death[234]. This means that they also respond very quickly to pathogenic insults, often within minutes to hours of detection. Research has shown that PDAC progression is linked to dysfunctional NK cells in circulation but compared to other solid tumour types, the overall infiltration percentage is lower in PDAC tumours in multiple studies[236]. This lower infiltrate of NK cells has potentially been linked to low expression of C-X-C motif chemokine receptor 2 (CXCR2), a chemokine receptor associated with immune cell trafficking[237]. Several studies have also shown that there is no significant difference in the number of NK cells when comparing healthy to diseased patient. Nonetheless, the debate regarding the total number of infiltrating NK cells withstanding, it has been shown that NK cells found associated with PDAC tumours display reduced cytotoxic potential as seen by reduced perforin and granzyme B levels[238]. Similarly, the hypoxic and metabolically dysregulated TME associated with PDAC tumours has also been shown to reduce NK cell functionality and survivability[236]. In some studies NK cell exhaustion has been shown to be a reason behind reduced NK cell lytic functionalities. Alongside a reduced cytolytic phenotype, PDAC associated NK cells display a reduced potential to secrete inflammatory cytokines like IL-6 and TNFα[239].

1.26 Aims

The overall aims and objectives of this thesis are to highlight novel roles for IRE1α in both the context of the NLRP3 inflammasome and in pancreatic cancer cells and their associated stromal cells. Given that IRE1α activity has previously been associated with NLRP3 activity, our studies will provide further detail elucidating this interaction. We will use TLR4 stimulation and nigericin treatment to activate the NLRP3 inflammasome and observe the effects of IRE1 ablation via chemical inhibition of the RNase domain and siRNA targeting IRE1α. It is of particular interest to us to try highlight if IRE1α regulates the NLRP3 inflammasome at signal I (LPS stimulation) or signal II (nigericin mediated K^+ efflux). We will perform our primary analysis in the THP-1 cell line but confirm results in primary PBMC's also. We hope that this analysis will help further define the role of IRE1α in this model and elucidate the mechanism behind its regulation of the NLRP3 inflammasome.

Regarding the role of IRE1α in pancreatic cancer, we hypothesized that due to the highly secretory nature of the pancreas, pancreatic cancer cells should exhibit high protein turnover and a subsequent active UPR. We will analyse basal UPR expression in a panel of commonly used pancreatic cancer cell lines alongside associated stromal cell lines, pancreatic stellate cells. The effects of IRE1α inhibition on PDAC/PSC proliferation, viability, cytokine secretion will be analysed by use of a chemical inhibitor of IRE1 RNase, MKC8866. Additionally, utilising co-culture conditions we will analyse the effects of MKC8866- conditioned PSC on pancreatic cancer and natural killer cell proliferation. We hope to analyse both the direct effect of IRE1 RNase inhibition on pancreatic cancer cells but also indirectly via conditioned media isolated from pancreatic tumour associated stellate cells. This will identify a novel role for IRE1α in pancreatic cancer, a disease with dire needs for novel therapeutics.

Chapter 2: Materials and methods

2.1 Cell lines and culture conditions

A panel of human pancreatic ductal adenocarcinoma (PDAC) cell lines (ATCC TCP-2060) was purchased from American Type Culture Collection (ATCC). This panel contained PANC1 (ATCC CRL-1469) cells derived from a male patient with PDAC, SW1990 (ATCC CRL-2172) cells derived from a spleen metastasized PDAC in male patient and BXPC3 (ATCC CRL-1687) cells derived from female PDAC patient.

PANC1 and SW1990 cells were maintained in high glucose DMEM (Sigma D6429) supplemented with 10% foetal bovine serum (FBS) (Sigma F7524), 100 U/ml penicillin (Sigma P0781) and 2 mM L-glutamine (Sigma G7513). BXPC3 cells were maintained in RPMI-1640 media (Sigma R0883) supplemented with 10% FBS (Sigma F7524), 100 U/ml penicillin (Sigma P0781) and 2 mM L-glutamine (Sigma G7513).

A human pancreatic stellate cell line (PSC) was kindly gifted from Dr. Rosa Hwang of the University of Texas, MD Anderson Cancer Centre. The PSC line was isolated from an untreated human PDAC resection and considered de-identified 'surgical waste' tissue under IRB approved protocols 03-189 and 11-104. Patients gave informed consent for tissue collection. Stromal cells that outgrew the cancer cells in culture were isolated by differential trypsinization and immortalized by infection with hTERT and SV40gp6 (Addgene plasmids #22396 and #10891, respectively) retro-viruses.[240] PSCs were cultured in high glucose DMEM (Sigma D6429) supplemented with 10% FBS (Sigma F7524), 100 U/ml penicillin (Sigma P0781) and 2 mM L-glutamine (Sigma G7513).

THP-1 (Sigma R0883) cells, a human monocytic cell line derived from an acute monocytic leukaemia patient, were maintained in RPMI-1640 media (Sigma R0883) supplemented with 10% FBS (Sigma F7524), 100 U/ml penicillin (Sigma P0781) and 2 mM L-glutamine (Sigma G7513). KHYG1 cells, a natural killer (NK) cell line isolated from a patient with aggressive NK leukaemia, were maintained in RPMI-1640 media (Sigma R0883) supplemented with 10% FBS (Sigma F7524), 100 U/ml penicillin (Sigma P0781) and 2 mM L-glutamine (Sigma G7513). KHYG1 cells obtained as a gift from Prof. Michael O' Dwyer and were previously purchased from Sigma by his lab.

All cells were cultured at 37˚C and 5% CO_2 in a humidified incubator. Cells were seeded at a 60-70% density 24 h prior to treatment for all experiments involving adherent cell lines and suspension cell lines were maintained at 0.5 x 10^6 cells/ml.

2.2 Isolation of human peripheral blood mononuclear cells (PBMCs)

Blood sampling of healthy volunteers was carried out following informed consent at the National University of Ireland, Galway (NUI Galway) under a protocol entitled "Immunological research using healthy human blood cells" approved by the NUIG Research Ethics Committee on 30/4/14 (Protocol No. 14/MAR/01). Human peripheral blood mononuclear cells (PBMCs) were isolated by Ficoll-Hypaque density gradient centrifugation (Sigma GE17-1440-02) from freshly drawn EDTA-anticoagulated peripheral venous blood. Briefly, 3 ml aliquots of EDTA-anticoagulated peripheral venous blood were layered over 3 ml of Ficoll Paque Plus in 15 ml tube and centrifuged at 400 x *g* for 22 min at 4˚C. The thin cloudy layer of PBMCs present at the interface of plasma and red blood cell layers was removed and transferred to a fresh 15 ml tube. The PBMCs were washed in 10 ml FACS buffer [2% FBS, PBS and 0.05% NaN3] and were pelleted by centrifugation at 300 x *g* for 10 min at 4˚C. The supernatant was discarded, and the cell pellet was re-suspended in 5 ml FACS buffer and washed a second time using the same protocol. The final cell pellet was re-suspended in 1 ml FACS buffer and counted using a haemocytometer. Freshly isolated PBMCs were diluted in complete media containing RPMI-1640 (Sigma R0883) supplemented with 1% L-glutamine (Sigma G7513) 100 U/ml penicillin/100 mg/ml streptomycin (Sigma P0781) and 5% clotted male human AB serum (Sigma H6914). All cells were grown at 37˚C and 5% CO_2.

2.3 Inflammasome activation

THP-1 cells were plated in 6-well plates at a density of 1 × 10^6 cells/ml and treated with 1 μg/ml LPS with or without MKC8866 (20 μM) for 24 h. After 24 h, LPS primed cells were treated with 10 μM NG for 45 min and cells and conditioned medium were collected for analysis. For inflammasome activation PBMCs were plated at a density of 1 × 10^6 cells/ml and primed with 1 ng/ml LPS for 2 h in the presence or absence of MKC8866. After 2 h of priming 5 mM ATP was added for 45 min and cells and conditioned medium were collected for analysis.

2.4 Drugs used

Tunicamycin ***(Tm)*** is a bacteria-derived compound which inhibits transfer of N-acetylglucosamine to dolichol, thereby perturbing N-linked glycosylation (Sigma T7765).

Thapsigargin ***(Tg)*** is a plant-derived inhibitor of the SERCA pump (Sigma T9033).

Dithiothreitol **(DTT)** is a reducing agent which impedes disulphide bond formation (Sigma D9779).

MKC8866 ***(MKC)*** is a potent IRE1 RNase inhibitor we obtained as a gift from Fosun Orinove (USA). MKC8866 has shown no off-target effects when tested against IRE1 RNase's closest homolog, RNase L. Work done previously in our lab has shown the specificity of the drug to the IRE1 arm[86].

Amgen PERK 44 **(Amg 44)** is a potent inhibitor of the PERK arm of the UPR. It functions through the prevention of PERK phosphorylation.

Lipopolysaccharide ***(LPS)*** is a component of the cell walls of Gram-negative bacteria. LPS stimulates innate immune cells via Toll-like receptor 4 which recognises common pathogen-associated molecular-patterns (PAMPS) (Sigma L2630).

Nigericin ***(NG)*** is a microbial toxin derived from streptomyces hygroscopicus that acts as a potassium ionophore in cells. NG induces a decrease in the levels of intracellular potassium that is crucial for NLRP3 inflammasome activity (Invivogen tlrl-nig)

Adenosine 5'-triphosphate ***(ATP)*** is an essential molecule involved in a variety of biological processes including signal transduction, neurotransmission and a source of energy potential. ATP can stimulate NLRP3 inflammasome via activation of the P2X7 cell surface receptor (Sigma A6419)

Phorbol 12-myristate 13-acetate ***(PMA)*** is a phorbol ester known to influence tumorigenicity via its roles in cell growth, gene transcription and immune cell differentiation. PMA is known to enhance the transfection efficiency of immune cells[241] (Sigma P8139).

2.5 Cell harvesting and sample preparation for protein analysis by SDS-PAGE

Cells were harvested and samples were prepared for SDS-PAGE analysis using two different methods, namely direct lysis in SDS-PAGE lysis buffer and lysis in RIPA buffer.

2.5.1 Direct cell lysis in SDS-PAGE buffer.

Cells harvested on ice using cell scraper to remove monolayer from culture flask or plate. Cells were pelleted by centrifugation in media at 4000 x *g* for 5 min at 4˚C. Supernatant stored at -20˚C or discarded. Pellet was resuspended and washed in 1 ml of ice-cold PBS (pH 7.4) and re-pelleted by centrifugation at 4000 x *g* for 5 min at 4˚C. Cell pellet was stored at -20˚C or kept on ice to continue with the next step. Pellet was lysed in 1X SDS-PAGE buffer **(Table 2.1)** by rapidly pipetting mixture up and down in tube. Samples kept on ice for 5 min before denaturing at 95˚C for 5 min. Volume of lysis buffer used based on cells being lysed at density of 5 x 10^6 cells/ml.

Table 2.1: SDS-PAGE buffer recipe

Stock solution	Volume	Final concentration
10% SDS	20 ml	4%
1 M Tris-HCl pH 6.8	5 ml	100 mM
Bromophenol blue	0.05 g	0.1%
100% Glycerol	10 ml	20%
dH_2O	Fill to 50 ml	N/A

Above recipe for 50 ml of Buffer (Store at room temp). 1X SDS prepared prior to lysis by diluting 2X SDS-PAGE in dH_2O and β-mercaptoethanol. Buffer can be stored for one week at 4˚C after dilution and addition of β-mercaptoethanol.

2.5.2 Cell harvesting and sample preparation in RIPA buffer

Cells harvested on ice using cell scraper to remove monolayer from culture flask or plate. Cells pelleted by centrifugation in media at 4000 x *g* for 5 min at 4˚C. Supernatant stored at -20˚C or discarded. Cell pellet resuspended and washed in 1 ml of ice-cold PBS (pH 7.4) and re-pelleted by centrifugation at 4000 x *g* for 5 min at 4˚C. Pellet stored at -20˚C or kept on ice to continue with the next step. Pellet lysed in Radioimmunoprecipitation assay buffer (RIPA) **(Table 2.2A-B)** with rapid pipetting of pellet and subsequent vortexing every ten min for forty min while samples are kept on ice. Samples quantified using Thermo Scientific™ Pierce™ BCA™ Protein

Assay (Thermo Scientific™ 23225). Specific quantity of protein lysed in Eppendorf tube with 5X Laemmli's Buffer **(Table 2.3)**. Samples denatured at 95˚C for 5 min and then stored at -20˚C or used in assay. **Table 2.2A: RIPA Lysis buffer recipe**

Stock solution	Volume (per 50 ml)	Final concentration
1 M Tris-HCl pH 8.0	2.5 ml	50 mM
1 M NaCl	7.5 ml	150 mM
10% NaDeox	2.5 ml	0.5%
10% SDS	500 µl	0.1%
10% NP-40	5 ml	1%
dH_2O	32 ml	N/A

The following reducing agents and protease inhibitors added prior to lysis:

Table 2.2B: RIPA buffer protease inhibitor supplements

Stock solution	Volume (per ml)	Final concentration
0.5 M DTT	1 µl	0.5 mM
100 mM PMSF	10 µl	1 mM
Pepstatin (1 mg/ml)	1 µl	1 µg/ml
Leupeptin (10 mM)	1 µl	10 µM
Aprotinin (2.3 mg/ml)	1.47 µl	1.47 µg/ml
ALLN (250 mM)	1 µl	250 µM

Table 2.3: 5X Laemmli's buffer recipe

Reagent	5X volumes (5 ml)
Tris-HCl (1 M, pH 6.8)	1.5 ml
SDS	0.5 g
Glycerol	1.0 ml
Mercaptoethanol	1.25 ml
PMSF (100 mM)	0.25 ml
Bromphenolblue (0.5%)	1.0 ml
H2O	Fill to 5 ml

2.6 SDS-PAGE gel electrophoresis

Gels were cast the day prior to running the gel or prepared fresh in the hours leading up to experiment. The percentage of SDS-PAGE gel determined the protein separation, lower percentage gels for high molecular weight molecules and higher percentages for smaller proteins. The SDS PAGE gels were then run in a tank with appropriate amounts of running buffer (25 Mm tris base, 250 Mm glycine, 0.1% SDS) at 50V until the sample passes through the stacking gel and 80V until the dye front reached the end of the gel. The gel was then sandwiched between a sponge, filter paper, gel, nitrocellulose paper, filter paper and sponge. The proteins were

transferred onto the nitrocellulose paper for 90 min at constant volts of 110V in transfer buffer (10 mM CAPS pH11 and 20% methanol). Membrane was blocked in 5% non-fat milk in PBS containing 0.1% tween (PBS-T).

2.7 Immunoblotting

Protein samples lysed and prepared according to previously described methods (2.5.1 and 2.5.2) and loaded onto SDS-PAGE polyacrylamide gels as outlined in **Table 2.4.** After gel electrophoresis proteins transferred to a nitrocellulose membrane. After transfer the membrane was analysed for transfer efficiency using Ponceau S solution (Sigma P7170) and then blocked for 1 h with 5% milk solution. Membrane probed with an appropriate primary antibody overnight **(Table 2.5)**. Blots were washed three times with PBS plus 0.1% Tween-20 and incubated with HRP-conjugated secondary antibody for 1 h at room temperature. Blots were washed again as previously. The membranes were incubated with Western Lightning ECL substrates (Perkin Elmer NEL105001EA) for 3 min. The signal was acquired in dark room after exposure of Agfa Medical X ray film blue 18×24 (Medray CP-BU) on the top of the membrane.

Table 2.4: Recipes for SDS-PAGE Polyacrylamide gels

8%	**5 ml**	**10 ml**	**15 ml**	**20 ml**	**25 ml**	**30 ml**
dH_2O	2.3	4.6	6.9	9.2	11.5	13.8
30% acrylamide mix	1.3	2.6	3.9	5.2	6.5	7.8
1.5 M Tris, pH 8.8	1.3	2.6	3.9	5.2	6.5	7.8
10% SDS	0.05	0.1	0.15	0.2	0.25	0.3
10% APS	0.05	0.1	0.15	0.2	0.25	0.3
TEMED	0.003	0.006	0.009	0.012	0.015	0.018
10%	**5 ml**	**10 ml**	**15 ml**	**20 ml**	**25 ml**	**30 ml**
dH_2O	2	4	6	8	10	12
30% acrylamide mix	1.7	3.4	5.1	6.8	8.5	10.2
1.5 M Tris, pH 8.8	1.3	2.6	3.9	5.2	6.5	7.8
10% SDS	0.05	0.1	0.15	0.2	0.25	0.3
10% APS	0.05	0.1	0.15	0.2	0.25	0.3
TEMED	0.002	0.004	0.006	0.008	0.01	0.012
12%	**5 ml**	**10 ml**	**15 ml**	**20 ml**	**25 ml**	**30 ml**
dH_2O	1.7	3.4	5.1	6.8	8.5	10.2
30% acrylamide mix	2	4	6	8	10	12
1.5 M Tris, pH 8.8	1.3	2.6	3.9	5.2	6.5	7.8
10% SDS	0.05	0.1	0.15	0.2	0.25	0.3
10% APS	0.05	0.1	0.15	0.2	0.25	0.3
TEMED	0.002	0.004	0.006	0.008	0.01	0.012

Table 2.5: Summary of primary antibodies used

Antibody	Company	Cat No.	Poly/ Mono	Species Reactivity	Raised In	Primary Dilution	Primary Incubation
Actin	Sigma	A2066	poly	H M R	rabbit	1: 2000	overnight at 4˚C
ATF4	CST	11815	mono	H M R	rabbit	1: 1000	overnight at 4˚C
total IRE1α	CST	3294	mono	H M	rabbit	1: 1000	overnight at 4˚C
PERK	CST	3192	mono	H M R Mk	rabbit	1: 2000	overnight at 4˚C
XBP-1s	Biolegend	619501	poly	H M R	rabbit	1: 1000	overnight at 4˚C
ATF6 α	Cosmo Bio	BAM-73-500-EX	mono	H	Mouse	1:1000	overnight at 4˚C
eIF2α	CST	5324	mono	H M R Mk	Rabbit	1:1000	overnight at 4˚C
Phospho-eIF2α (Ser51)	CST	D9G8	mono	H M R Mk Dm	Rabbit	1:1000	overnight at 4˚C
NLRP3	CST	D2P5E	mono	H	Rabbit	1:1000	overnight at 4˚C
NF-κB P-65	CST	8242	mono	H M R Hm Mk Dg	Rabbit	1:1000	overnight at 4˚C
Human IL-1 beta /IL-1F2	R&D	MAB201	mono	H	Mouse	1:1000	overnight at 4˚C
ASC	Santa cruz	sc-22514-R	poly	H M R	Rabbit	1:1000	overnight at 4˚C
Caspase-1	Santa cruz	Sc-662	poly	H	Rabbit	1:1000	overnight at 4˚C
caspase-1 p10	Santa cruz	sc-515	poly	H	Rabbit	1:1000	overnight at 4˚C
VDUP1 (TXNIP)	Santa cruz	sc-166234	mono	H M R	Mouse	1:1000	overnight at 4˚C

2.8 Enzyme linked immunosorbent assay (ELISA)

Cytokines of interest were analysed in cell supernatants using ELISA technique. DUOSET ELISA's for IL-6 (DY206), IL-8 (DY208), CXCL1 (DY275), TGFβ1 (DY240), TGFβ2 (DY302) and SDF-1 (DY350) were purchased from R&D Systems and carried out as per manufactures instructions **(Table 2.6)**. Conditioned media harvested from cells treated for 48-72 h and debris/cells removed by centrifugation at max speed for 5 min after harvest.

Table 2.6: Summary of Duoset ELISA kits from R&D Systems used

Cytokine	Product code
IL-6	DY206
IL-8	DY208
CXCL1 (GRO-α)	DY275
TGFβ1	DY240
TGFβ2	DY302
SDF-1	DY350
IL-1β	DY201
TNF-α	DY210

2.9 siRNA transfections and protein knockdown

I used an RNA interference approach to knockdown proteins of interest. PSCs transfected with siRNA using Lipofectamine™ 3000 Transfection Reagent (Thermo Fisher Scientific L3000008). Dharmacon On-Target SMARTpool Plus siRNA targeting XBP1 (L-009552-00), IRE1/ERN1 (L-004951-02-0005) and non-targeting control (D-001810-01-20) transfected by addition in dropwise fashion to culture media. Cells harvested after 72 h.

Prior to transfection, THP-1 monocytes treated with PMA for 24 h following which they were transfected with siRNA using TransIT-TKO (Mirus MIR 2154) according to the manufacturer's protocol. siRNAs (ON-TARGET plus smart pool) ERN1/IRE1 (L-004951-02-0005); Non-coding siRNA (D-001810-01-20) were obtained from Dharmacon. TransIT-TKO and siRNA mixtures added to media in dropwise fashion. Media was changed 6 h post-transfection and cells were left to recover for 72 h.

2.10 Propidium iodide uptake assay for assessment of cell death

THP-1 cells were plated in a 12-well plate at a density of 1×10^6 cells/ml and directly treated with 1 µg/ml LPS with or without indicated concentrations of MKC8866 for 24 h. After 24 h, LPS primed cells were treated with 10 µM NG for 45 min prior to cell death analysis. Cells were pelleted at 400 x *g* for 5 min and resuspended in 100 µl of ice-cold PBS. 5 min prior to analysis, 1.5 µg/ml Propidium Iodide (PI) (Sigma P4170) was added and PI uptake analysed using BD Accuri C6 flow cytometer (BD Biosciences).

PSC, PANC1, BxPC3 and SW1990 cell lines treated with MKC8866 or Amgen 44 inhibitors for 2, 4 or 6 days. On day of harvest, cells were trypsinized as per normal and allowed to recover in conditioned media that was collected prior to addition of trypsin for 10 min in 37˚C. After recovery, cells were pelleted by centrifugation at 400 x g for 5 min. Cell pellet was resuspended in ice-cold PBS. Five min prior to analysis, 1.5 µg/ml PI was added to cell suspension. PI uptake was analysed using BD Accuri C6 flow cytometer.

2.11 RNA extraction

After harvesting, cells transferred to an Eppendorf tube and centrifuged at 4000 x *g* for 4 min at 4˚C. Cell pellets resuspended in 1 ml TRI Reagent (Sigma T9424) and transferred to a 1.5 ml Eppendorf tube. Samples vortexed for 1 min, followed by incubation at room temperature for 5 min. Samples either stored at -20˚C at this point or the protocol was completed on same day. A 200 µl volume of chloroform (Sigma C2432) was added to the samples. Samples were vortexed for 30 sec and incubated at room temperature for 15 min. The samples were then spun at 17000 × *g* for 15 min at 4˚C. The upper aqueous layer of samples was removed to a new 1.5 ml Eppendorf carefully without disrupting the layers themselves. 1 volume of chilled isopropanol (Sigma I9516) was added dropwise to the samples. The samples were inverted ten times and incubated at room temperature for 10 min. The samples were spun at 17000 × *g* for 15 min. The supernatant was removed. 1 ml of 85% ethanol (Sigma 51976) in DEPC (Sigma D5758) treated water was added to the pellets. The samples were spun at 17000 × *g* for 15 min. The pellets were allowed to air dry until there was no excess liquid, but the pellet still appeared moist. Pellets were

resuspended in RNase free water and heated at 65˚C for 15 min to remove secondary structures. The samples were vortexed and centrifuged briefly and finally kept on ice. RNA was quantified using Thermo Scientific NanoDrop 2000 by measuring absorbance at 260 nm (A260 nm). RNA purity also assessed using A260 nm/A280 nm ratio to ensure nucleic acid/protein ratio was between 1.7 and 2.1 for all experiments.

2.12 Reverse Transcription (RT-PCR)

RNA dissolved to a final concentration of 500 ng-2000 ng in DEPC treated water based on nanodrop values gained with a final volume of 10 µl. 1 ul of 10X DNase buffer and 1 µl of Mol. Grade DNase added to side of tube (Sigma AMPD1). Samples spun to allow simultaneous addition of DNase to each sample. Samples were then incubated at room temperature for 15 min. 1 µl of DNASE stop buffer (Sigma AMPD1) added to side of tube and spun down. Samples were then incubated at 65˚C for 2 min followed by another 2 min at 42˚C. Reverse transcription master mix comprised of sterile ddH2O (Sigma W4502), 5X 1st strand buffer (Invitrogen), 100 mM DTT (Sigma D9779), 10 mM dNTPs (Invitrogen 10297018), and superscript III (Invitrogen 18080044) **(Table 2.7)**. 10 µl of Reverse transcription master mix then added to samples and reverse transcription was performed using Biometra T3 thermocycler.

Table 2.7: Reverse transcription master mix recipe

Reagent	Volume per reaction (µl)
ddH_2O	2.6
5X 1st strand buffer	4
DTT	2
dNTP's	1
Superscript III	0.4

2.13 Conventional PCR

For conventional or classical PCR, a reaction mixture was made up, containing cDNA product, 100 nM forward and reverse primers, ddH2O and GoTaq master mix (Promega M7123) **(Table 2.8)**. The reaction mixtures underwent 25- 35 cycles, depending on the product, for 1 min denaturation at 95˚C, 1 min annealing at 60˚C and 1 min extension at 72˚C in Biometra T3 thermocycler. PCR products run on 1% agarose gels at 100 V unless analysing XBP1s/u which was run on 3% agarose gel to

allow sufficient separation of XBP1 isoforms (Invitrogen 16500500). Gels were imaged using the BioRad Pharos FXTM plus Molecular Imager and Densitometry was carried out using ImageJ software. Primer sequences detailed below **(Table 2.9)**

Table 2.8: Conventional PCR master mix recipe

Reagent	Volume per reaction (µl)
ddH_2O	6.5
Forward primer (100 nM)	2
Reverse primer (100 nM)	2
GoTaq mastermix	12.5
cDNA	2

Table 2.9: Primer sequences

Transcript	FWD 5' - 3'	REV 5' - 3'
GAPDH	ACCACAGTCCATGCCATC	TCCACCACCCTGTTGCTG
XBP1s	TCTGCTGAGTCCGCAGCAGG	CTCTAAGACTAGAGGCTTGG
XBP1u	CAGACTACGTGCGCCTCTGC	CTTCTGGGTAGACTTCTGGG
Conventional *XBP1* Splicing	CCTGGTTGCTGAAGAGGAGG	CCATGGGGAGATGTTCTGGAG
Total *XBP1*	CCTGGTTCTCAACTACAAGGC	AGTAGCAGCTCAGACTGCCA

2.14 Quantitative PCR (qPCR)

Specific cDNA targets were detected using PrimeTime TaqMan qPCR assays (IDT). Takyon ROX Master Mix (Eurogentec UFRP5XC0501) was used for qPCR reactions. Applied Biosystems 7500 and StepOne Plus qPCR platforms were used for running the experiment. The data was analysed manually using the ΔΔCt method using the endogenous control stated in the relevant figures. qPCR primer sequences outlined in **Table 2.10**.

Table 2.10: Summary of qPCR probe sequences used

NLRP3	
Probe:	5'-TGCAGGTTACACTGTGGATTCTTGGC-3'
Primer 1:	5'-AGATTCTGATTAGTGCTGAGTACC-3'
Primer 2:	5'-GAATGCCTTGGGAGACTCAG-3'
IL1β	
Probe:	5'-AGAAGTACCTGAGCTCGCCAGTGA-3'

Primer 1:	5'-GAACAAGTCATCCTCATTGCC-3'
Primer 2:	5'-CAGCCAATCTTCATTGCTCAG-3'
Caspase1	
Probe:	5'-AGTCTTCCAATAAAAACAGAGCCCATTGTG-3'
Primer 1:	5'-CACATCACAGGAACAGGATA-3'
Primer 2:	5'-TGAAGGACAAACCGAAGGTG-3'
TXNIP	
Probe:	5' TTGCGGAGTGGCTAAAGTGCTTTG-3'
Primer 1:	5'-GTGATAGTGGAGGTGTGTGAAG-3'
Primer 2:	5'-CAGGTACTCCGAAGTCTTTTG-3'
GAPDH	
Probe:	*5'-AAGGTCGGAGTCAACGGATTTGGTC-3'*
Primer 1:	*5'-ACATCGCTCAGACACCATG-3'*
Primer 2:	5'-*TGTAGTTGAGGTCAATGAAGGG-3'*
CXCL1	
Probe:	*5'-AAGCTCACTGGTGGCTGTTCCT-3'*
Primer 1:	*5'- TCTCTCTTTCCTCTTCTGTTCCTA-3'*
Primer 2:	*5'-CATCCCCCATAGTTAAGAAAATCATC-3'*
IL6	
Probe:	*5'-CAACCACAAATGCCAGCCTGCT-3'*
Primer 1:	*5'- GCAGATGAGTACAAAAGTCCTGA-3'*
Primer 2:	*5'- TTCTGTGCCTGCAGCTTC-3'*

2.15 ASC Crosslinking assay

THP-1 cells were resuspended in 500 µl of ice cold buffer (20 mM HEPES-KOH, pH 7.5, 150 mM KCl, 1 mM Na_3VO_4, 0.1 mM PMSF, 1% NP40, and a protease inhibitor cocktail) and lysed by shearing 10 times using a 21 gauge needle. Lysate was centrifuged at 300 *x g* for 5 min at 4 ˚C. Supernatants were filtered through 5 µM filter (GE Healthcare, 6784-1350). Filtrates were centrifuged at 6800 *x g* for 15 min at 4 ˚C to pellet ASC insoluble specks. Supernatants were transferred to new tubes (ASC-soluble fractions). The ASC-insoluble pellets were washed with PBS twice and then suspended in 200 µl PBS. The ASC-insoluble pellets were cross-linked at room temperature for 30 min by adding 2 mM bis[sulfosuccinimidy]suberate (BS3). The cross-linked ASC were centrifuged at 6800 *x g* for 15 min at 4 ˚C to pellet the cross-linked ASC and dissolved directly in SDS sample buffer.

2.16 Caspase-1 activity assay (FLICA)

THP-1 cells and PBMCs were treated as indicated and whole-cell caspase-1 activity was determined using FLICA 660 *in vitro* Caspase-1 detection Kit (Immunochemistry Technologies, 9122) on BD Accuri C6 Flow Cytometer. Cell suspensions were aliquoted into 96-well flat-bottom cell culture plates at a final concentration of 1 x 10^6 cells/ml in complete media and a total incubation volume of 200 µl. At the time of signal II addition, 10 µl of FLICA reagent (reconstituted as directed by manufacturer) and diluted to 1:10 in FACS buffer 5 min prior to staining were added to each tube. The cells were incubated for 45 min at 37 ˚C, 5% CO_2 then washed using 1 ml PBS and pelleted by centrifugation at 300 *x g* for 5 min at 4˚C. The cells were then resuspended in FACS buffer and analysed on BD FACSCanto II (BD Biosciences). PBMCs were co-stained with CD14-PerCP-Cy5.5 (Miltenyi Biotec) and CD45-V500 (BD Biosciences) antibodies and caspase-1 activity in CD14/CD45 positive population.

2.17 Biochip array technology for XBP1s/u analysis

XBP1 Biochip assay kit was obtained from Randox Laboratories (XBP1 Array (EV4357), Randox Laboratories Ltd., Crumlin, UK). This array was obtained as part of a collaborative project with Randox Laboratories Ltd. RIPA lysed samples were diluted to 100 µl in RIPA buffer followed by dilution to 200 µl in XBP1 assay buffer and mixed well with gentle pipetting. 200 µl of XBP1 assay diluent was then applied to the surface of the biochip followed by 200 µl diluted sample or 100 µl calibrator/control per well. Following a 60 min incubation at 37˚C, 370 RPM in a thermoshaker (Randox Laboratories Ltd., Crumlin, UK) liquid contents were removed with a sharp flick and washed in a PBS-T, 4 x 2 min wash steps. 300 µl of HRP conjugated pan-XBP1 detector was applied to each well and another 60 min incubation at 37˚C, 370 RPM in a thermoshaker was performed. Following another wash as above, 250 µl of a 1:1 ratio of EV841 luminol and peroxide was applied to the surface of each biochip in a carrier and incubated away from direct light for 2 min. Carriers are then submitted to the Evidence Investigator, light emitted from each DTR is detected by the CCD camera and signal quantified by the instrument software. Final values in pg/mg were obtained by dividing reported value (in pg) by total protein loaded per well, as determined by bicinchoninic acid (BCA) assay.

2.18 Cell counting assay

Cells seeded at optimal density to allow constant growth over period of assay (Usually six days) without reaching a confluent state. Cells counted using haemocytometer during assay after removal and storage of conditioned media in labelled Eppendorf tubes, wash in Hanks balanced salt solution (Sigma H9394-500 ML) and trypsinization using Trypsin-EDTA solution (T4174-100ML). Cells then returned to wells alongside conditioned media until completion of assay. Haemocytometer counts performed in triplicate for each experimental repeat and average taken. Cells allowed to recover for 24 h after seeding before addition of drugs.

2.19 Generation of conditioned media from PSCs and media swap experiments

To generate conditioned media PSC's were cultured as outlined in section 2.1. Cells were then treated with either DMSO or MKC8866 for 48 or 72 h. Conditioned media then filtered with 0.2 µm filters to remove any cellular debris and then concentrated using 3 KDa cut-off centrifugal columns (Sigma Z629405) to concentrate soluble factors. Cells to receive conditioned PSC media were washed with Hanks to remove residual media or FBS before conditioned PSC media was added to wells. PDAC cell lines cultured with conditioned PSC media for 5 days prior to cell counts and KHYG1 cells cultured in PSC conditioned media for 24 h.

2.20 Densitometry analysis

ImageJ software was downloaded from (lukemiller.org2013). The rectangle tool was used to select bands and intensity of pixels was converted to graph format and the area under the curve was quantified using the wand tool. Levels of target gene expression was normalised to the relevant control gene, and target gene/control gene for each sample was normalised to the relevant control sample.

2.21 SDF-1α promotor binding partner prediction analysis

In order to predict as to whether SDF-1α could be potentially regulated by the XBP1s transcription factor we used free online databases as follows. https://www.ensembl.org/index.html used to identify 1000 bp region upstream of SDF-1α promotor region. http://tfbind.hgc.jp/ was then used to predict and identify

potential transcription factors capable of binding to SDF-1α. The number of total predicted sites for each factor was also recorded.

2.22 Large scale cytokine array

PANC1 cells seeded at 450,000 cells in a T- 25 flask and PSC seeded at 250,000 cells in a T-25 flask. Cells treated with 20 µM MKC8866 or DMSO after 24 h. After 72 h of treatment, media was transferred into Eppendorf tube. Samples were centrifuged for 5 min at 4000 x *g* at 4˚C to remove any cellular material. Samples stored at -20 ˚C until needed. Samples analysed for cytokine secretion using Proteome Profiler Human XL Cytokine Array Kit (ARY022B) from R&D systems. Cytokines present for analysis on this array are outlined in **table 2.11** below. A 2 ml volume of blocking buffer (Array Buffer 6) added into each well of the 4-well multi-dish. Array membranes placed into separate wells containing blocking buffer and incubated on a shaker for 1 h at RT. After 1 h the blocking buffer was aspirated and membranes incubated in supernatant samples overnight at 4˚C on a shaker. The next day the samples were aspirated and membranes were washed 3 times for 10 min with 20 ml 1X washing buffer. After removing the washing buffer, Detection Antibody with 1.5 ml of 1X Array Buffer 4/ 6 was added to membranes. Membranes incubated for 1 h at RT and placed on the shaker. Washing step repeated. Next, 2 ml of 1X Streptavidin-HRP added to membranes and left to incubate at RT for 30 min on a shaker. The washing step repeated as described previously after incubation. Next chemo reagent mix was added to membranes and distributed over the entire membrane surface with a pipette for one minute. Exposed membranes to X-ray film for 1-10 min.

Table 2.11. List of cytokines analysed using XL cytokine array (ARY022B)

Adiponectin/Acrp30	Endoglin/CD105	IL-3	IL-34	CXCL4/PF4
Angiogenin	EMMPRIN	IL-4	CXCL10/IP-10	RAGE
Angiopoietin-1	Fas Ligand	IL-5	CXCL11/I-TAC	CCL5/RANTES
Angiopoietin-2	FGF basic	IL-6	Kallikrein 3/PSA	RBP4
Apolipoprotein A1	KGF/FGF-7	IL-8	Leptin	Relaxin-2
BAFF/BLyS/TNFSF13B	FGF-19	IL-10	LIF	Resistin
BDNF	Flt-3 Ligand	IL-11	Lipocalin-2/NGAL	CXCL12/SDF-1 alpha

CD14	G-CSF	IL-12 p70	CCL2/MCP-1	Serpin E1/PAI-1
CD30	GDF-15	IL-13	CCL7/MCP-3	SHBG
CD31/PECAM-1	GM-CSF	IL-15	M-CSF	ST2/IL1 R4
CD40 Ligand/TNFSF5	CXCL1/GRO alpha	IL-16	MIF	CCL17/TARC
Chitinase 3-like	Growth Hormone (GH)	IL-17A	CXCL9/MIG	TFF3
Complement Component C5/C5a	HGF	IL-18 BPa	CCL3/CCL4 MIP-1 alpha/beta	TfR
Complement Factor D	ICAM-1/CD54	IL-19	CCL20/MIP-3 alpha	TGF-alpha
C-Reactive Protein/CRP	IFN-gamma	IL-22	CCL19/MIP-3 beta	Thrombospondin-1
Cripto-1	IGFBP-2	IL-23	MMP-9	TIM-1
Cystatin C	IGFBP-3	IL-24	Myeloperoxidase	TNF-alpha
Dkk-1	IL-1 alpha/IL-1F1	IL-27	Osteopontin (OPN)	uPAR
DPPIV/CD26	IL-1 beta/IL-1F2	IL-31	PDGF-AA	VCAM-1
EGF	IL-1ra/IL-1F3	IL-32 alpha/beta/gamma	PDGF-AB/BB	VEGF
CXCL5/ENA-78	IL-2	IL-33	Pentraxin 3/TSF-14	Vitamin D BP

2.23 Analysis of XL cytokine array data

HLImage++ software from Western vision was used to analyse data obtained from Proteome Profiler Human XL Cytokine Array Kit (ARY022B). HLImage++ generated pixel density values for each spot on the array and calculated the average for both technical replicates. The values were then assessed and passed through a high and low cut-off point of <25000 and >2500 pixel density to remove anything overexposed or underexposed. Cut-off points obtained from comparing to control spots. Next the relative fold-change compared to control treated samples (DMSO vs MKC treated) was calculated and a second filter of value cut-off's was applied. In this second analysis fold change increases of less than 1.2 and fold change decreases of less than 0.8 were removed. Further analysis of data and the generation of heat maps was performed using the following R-packages; RColorBrewer, GGally, ggplot2 and pheatmap.

Chapter 3: Inhibition of IRE1 RNase activity reduces NLRP3 inflammasome assembly and processing of pro-IL1β

The work in this chapter is part of a manuscript published to the journal *Cell death and disease* in August 2019.

Aaron Talty, Shane Deegan, Mila Ljujic, Katarzyna Mnich, Serika D. Naicker, Dagmar Quandt, Qingping Zeng , John B. Patterson , Adrienne M. Gorman, Matthew D. Griffin, Afshin Samali and Susan E. Logue. Inhibition of IRE1alpha RNase activity reduces NLRP3 inflammasome assembly and processing of pro-IL1beta. Cell Death Dis **10**(9): 622. (2019)

The contributions to this experimental work are as follows:

Fig. 3.1-Shane Deegan and Mila Ljujic

Fig. 3.2-Katarzyna Mnich

Fig. 3.3-Shane Deegan

Fig. 3.7-Shane Deegan

Fig. 3.9-Mila Ljujic

Fig. 3.10-Shane Deegan

Fig. 3.11-Shane Deegan

Introduction and background

Although IRE1 has a well-established role in the UPR, its influence may extend beyond monitoring ER homeostasis. IRE1 signaling contributes to the development of several immune cell types, including secretory plasma cells[242] and dendritic cells[243]. IRE1-mediated regulation of macrophage polarization under conditions of metabolic stress has also been reported[244]. In addition to immune cell development, several studies have also demonstrated that IRE1-XBP1 signalling contributes to innate immune responses triggered by various toll-like receptor (TLR) ligands including lipopolysaccharide (LPS)[245], attenuated *Brucella abortus* strain[246] and Methicillin-resistant *Staphylococcus aureus* (MRSA)[247] infection. Furthermore, IRE1 activity was also shown to be upregulated in inflammatory arthritis[248] as well as in lipid-induced inflammation. In this study, we examined the contribution of IRE1 RNase activity to inflammasome formation and in particular the Nucleotide-Binding Oligomerization Domain, Leucine Rich Repeat and Pyrin Domain Containing 3 (NLRP3) inflammasome. Structurally, the NLRP3 inflammasome is composed of three components – NLRP3 that functions as a sensor protein; the adaptor apoptosis-associated speck-like protein containing a caspase recruitment domain (ASC) and pro-caspase-1. Activation is achieved *via* a two-step mechanism with the first step (priming step) involving transcriptional upregulation of key components including NLRP3 as well as pro-IL-1β through TLR activation and subsequent NF-κB signaling. The second step (signal II) promotes NLRP3 inflammasome assembly and activation. The precise mechanisms facilitating NLRP3 inflammasome activation remain unclear with several models proposed. Ultimately, signal II enables structural assembly of the inflammasome with NLRP3 recruiting ASC via pyrin:pyrin domain interactions, which in turn triggers ASC oligomerisation leading to the formation of long ASC filaments. Pro-caspase-1 is recruited to ASC via CARD:CARD interactions leading to auto-processing resulting in the generation of activate caspase-1. We now report that inhibition of IRE1 RNase activity, while not impacting on inflammasome priming, selectively reduces structural assembly of the inflammasome. This suggests that small molecule inhibitors of IRE1 RNase activity

offer a new therapeutic opportunity for diseases mediated by excessive or prolonged NLRP3-inflammasome activity.

Aims and objectives

In this study, we examined the contribution of IRE1α RNase activity to inflammasome formation and in particular the nucleotide-binding oligomerization domain, leucine rich repeat and pyrin domain containing 3 (NLRP3) inflammasome. Structurally, the NLRP3 inflammasome is composed of three components— NLRP3 that functions as a sensor protein; the adapter apoptosis-associated speck-like protein containing a caspase recruitment domain (ASC) and pro-caspase-1. Activation is achieved via a two-step mechanism with the first step (priming step) involving transcriptional upregulation of key components including NLRP3 as well as pro-IL-1β through TLR activation and subsequent NF-κB signalling. The second step (signal II) promotes NLRP3 inflammasome assembly and activation. The precise mechanisms facilitating NLRP3 inflammasome activation remain unclear with several models proposed. Ultimately, signal II enables structural assembly of the inflammasome with NLRP3 recruiting ASC via pyrin:pyrin domain interactions, which in turn triggers ASC oligomerisation leading to the formation of long ASC filaments. Pro-caspase-1 is recruited to ASC via CARD:CARD interactions leading to auto-processing resulting in the generation of activate caspase-1. We now report that inhibition of IRE1α RNase activity, while not impacting on inflammasome priming, selectively reduces structural assembly of the inflammasome. This suggests that small molecule inhibitors of IRE1α RNase activity may offer a new therapeutic opportunity for diseases mediated by excessive or prolonged NLRP3 inflammasome activity. Specifically, we wish to investigate the following:

- Does TLR4 stimulation selectively upregulate the IRE1 arm of the UPR in THP-1 cells?
- Does IRE1 inhibition reduce NLRP3 activity as assessed by caspase-1 activity or il-1β release?
- Does IRE1 regulate the NLRP3 inflammasome via the priming or assembly steps of activation?
- Can we recapitulate our results in primary PBMC's?

3.1 Inflammasome activity induced by signal I and signal II conditions in human monocytic cell line THP-1

The human monocytic cell line THP-1[249] was treated with LPS alone or with LPS in combination with a short incubation with the K^+ ionophore, Nigericin (NG). These two treatments represent signal I (priming) and signal II (assembly) in NLRP3 inflammasome activation, respectively. In combination, they induce NLRP3 inflammasome assembly as indicated by an increase in caspase-1 cleavage in conditioned medium isolated from treated cells (alongside enhanced IL-1β processing) (Fig. 3.1A). The addition of NG also gave an increase in the levels of IL-1β as assessed by immunoblot analysis, further supporting that our model is inducing NLRP3 inflammasome activity (Fig. 3.1B). Additionally, enhanced IL-1β levels were observed by ELISA under combination treatment conditions (Fig. 3.1C). We observed that the addition of NG to LPS-stimulated cells did not alter the levels of LPS-induced inflammatory cytokines IL-6, IL-8 and TNFα (Fig. 3.1D-I).

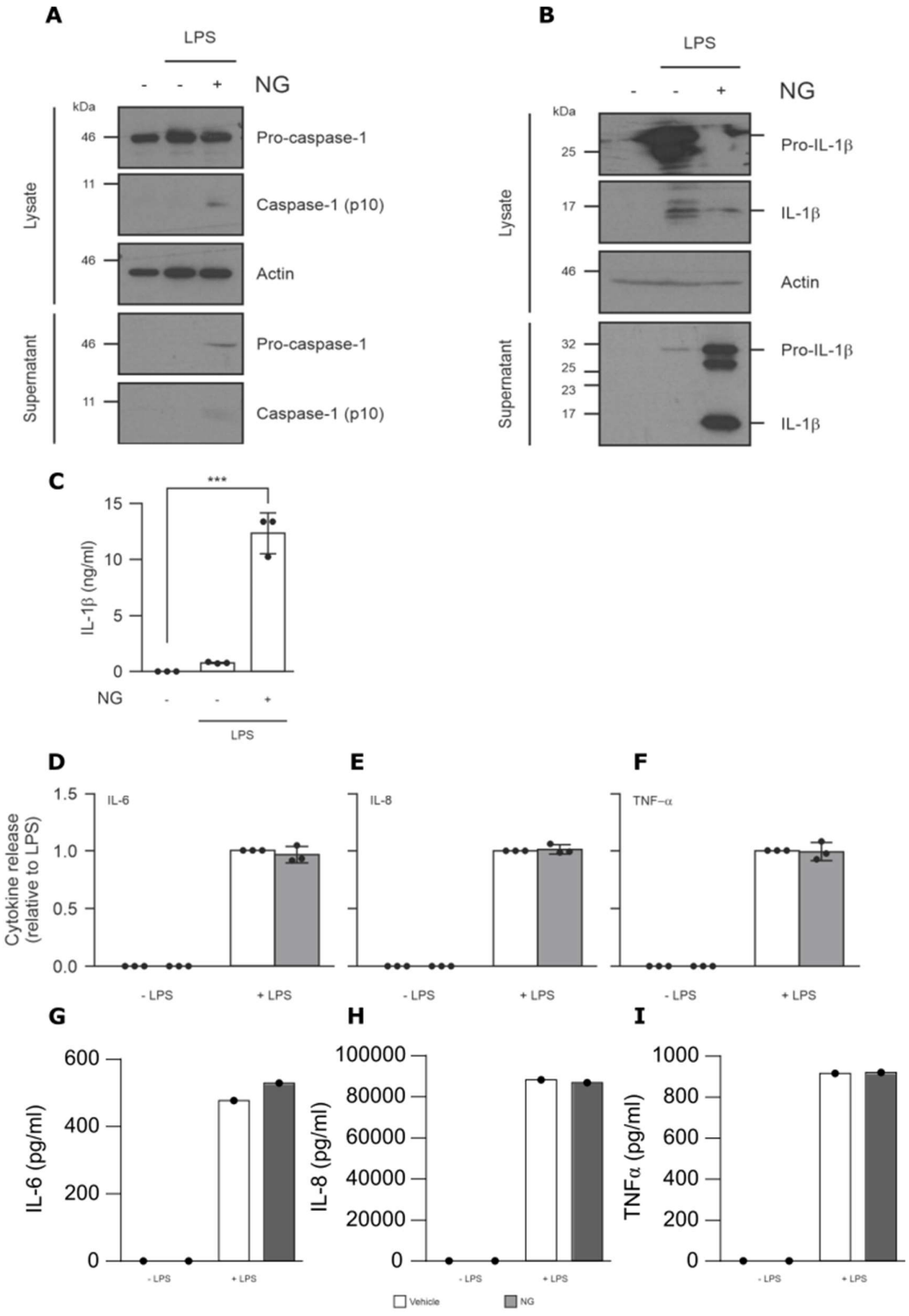

Figure 3.1. Inflammasome activity induced by signal I and signal II conditions in human monocytic cell line THP-1. THP-1 cells were primed with either 1 µg/ml LPS alone for 24 h or 1 µg/ml LPS for 24 h followed by addition of 10 µM NG for 45 min. **(A)** Processing of caspase-1 was analysed in cell lysates and supernatants using by immunoblotting for full pro-caspase-1 (p45) and processed p10 caspase-1. **(B)** Processing of pro-IL-1β was analysed in cell lysates and

supernatants using by immunoblotting for full-length pro-IL-1β and processed p17 IL-1β. **(C)** Levels of IL-1β were quantified in supernatants from untreated, LPS and LPS/NG treated THP-1 cells by ELISA (n=3). Levels of listed inflammatory cytokines were quantified in supernatants from untreated, LPS and LPS/NG treated THP-1 cells by ELISA; **(D)** IL-6, **(E)** IL-8 and **(F)** TNF-α (n=3). Representative quantitative ELISA shown for **(G)** IL-6, **(H)** IL-8 and **(I)** TNF-α. ***P < 0.001 based on a Student's t test. Error bars represent SD.

3.2 IRE1-XBP1 axis of the UPR is selectively activated upon TLR4 stimulation

In order to assess the status of the UPR during inflammasome activating conditions, we analysed the activity of the three arms of the UPR during LPS and LPS/NG treated conditions in THP-1 cells. We observed activation of the IRE1 arm during LPS and LPS/NG conditions, indicated by increased XBP1 splicing (Fig. 3.2). We also observed no changes to the activation status of the other two UPR arms , PERK and ATF6, under the same treatment conditions. PERK activation was measured by both an upshift in the molecular weight of PERK, indicative of PERK phosphorylation, and also by the induction of ATF4 expression. ATF6 was analysed by processing of its full form to a cleaved form and a subsequent reduction in molecular weight. Each of these responses is also confirmed in Tunicamycin (Tm) treated THP-1 cells, an ER stress inducing agent used as a positive control. Collectively, these data suggested that the IRE1 arm of the UPR is selectively upregulated during conditions in which we also observe inflammasome activation. This selectivity mirrors that observed by *Martinon et al[245]*.

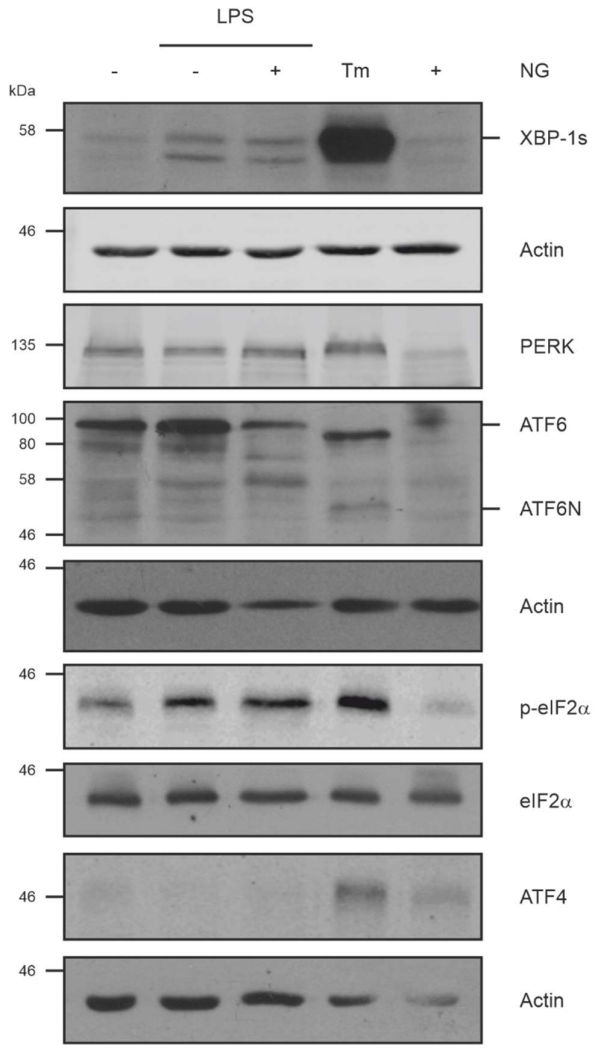

Figure 3.2. IRE1-XBP1 axis of the UPR is selectively activated upon TLR4 stimulation. Immunoblot analysis of UPR markers ATF6, XBP1s, PERK, eIF2α, p-eIF2α and ATF4 were analysed THP-1 post-treatment with LPS alone or LPS/NG (n=3). Tunicamycin (Tm) treated THP-1 cells served as a positive control for UPR activation. Actin was used a loading control.

3.3 Knockdown of IRE1 reduces NLRP3 inflammasome activity in THP-1 cells.

As our results confirmed that LPS selectively upregulates IRE1 signalling in THP-1 cells while simultaneously not affecting the other two UPR arms, we wanted to next test the effects of inhibiting IRE1 signalling and the effects it has on downstream inflammasome formation and activity. Firstly, THP-1 cells were transfected with IRE1 targeting siRNA. An efficient knockdown of IRE1 was achieved after 72 h treatment and this was verified by immunoblotting (Fig. 3.3A). To investigate inflammasome activity under these same IRE1-deficient conditions we first analysed pro-IL-1β processing after LPS/NG stimulation and found that IRE1 knockdown could reduce levels of bioactive p17 IL-1β present in the conditioned medium of cells (Fig. 3.3B). Quantification of IL1b levels by ELISA revealed a similar pattern with lower IL1b present in the conditioned medium of IRE1 knockdown cells compared to non-coding counterparts (Fig. 3.3C-D). This data indicated that IRE1 signalling may contribute in to NLRP3 inflammasome formation.

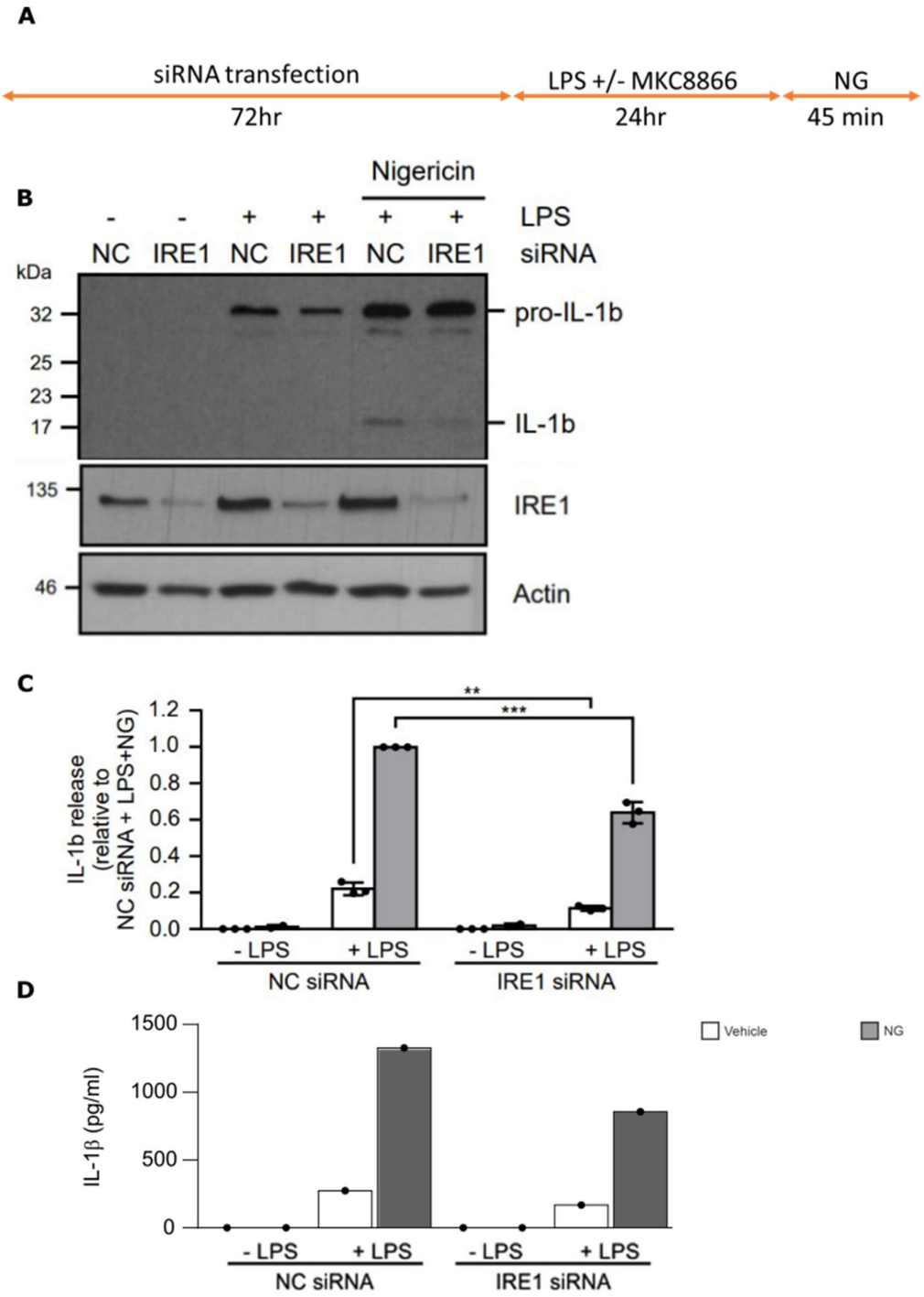

Figure 3.3. Knockdown of IRE1 reduces NLRP3 inflammasome activity in THP-1 cells. **(A)** THP-1 cells transfected with either non-coding or IRE1 targeting siRNA were treated with either 1 µg/ml LPS alone for 24 h or 1 µg/ml LPS for 24 h followed by addition of 10 µM NG for 45 min (n=3). **(B)** Cell lysates were analysed via immunoblotting for IRE1 and pro-IL-1β. Actin was used as a loading control. **(C)** Levels of IL-1β were assayed in cell conditioned medium by ELISA (n=3). **(D)** Representative quantitative ELISA shown for IL-1β. **P < 0.01, and ***P < 0.001 based on a Student's t test. Error bars represent SD.

3.4 IRE1 regulates secreted levels of pro-inflammatory cytokines

TLR4 stimulation leads to release of other pro-inflammatory cytokines other than IL-1β[250]. We also investigated the levels of the key inflammatory cytokines IL-6, IL-8 and TNFα under IRE1 knockdown and LPS or LPS/NG stimulated conditions. We observed reduced amounts of secreted IL-6 and TNFα under siIRE1 conditions with no changes in IL-8 levels observed (Fig. 3.4A-F). LPS stimulated TLR4 activation is a known inducer of NF-κB regulated transcription, of which these cytokines are transcriptional targets. Given that IRE1 has also been linked, via its kinase domain activity, to NF-κB activity, we next examined the effects that LPS and LPS/NG treatment have on NF-κB activity. We questioned whether reduced IRE1 signalling could dampen NF-κB mediated-transcription of key inflammasome components, leading to reduced complex assembly and IL-1β secretion. The induction of NF-κB activity, assessed by phospho-p65 levels, after LPS and LPS/NG treatment is not influenced by IRE1 activity (Fig. 3.4G). These results indicate; (1) The effects on NLRP3 inflammasome activity in IRE1 deficient conditions upon LPS or LPS/NG treatment are not influenced by the NF-κB mediated "priming" step and (2) IRE1 signalling mediates the production of other cytokine targets independently of signal II inflammasome assembly. It is important to note that while p65 phosphorylation is indicative of NF-κB activation, other transcription factors operate downstream of NF-κB upon activation of the pathway and analysing them in future could be of importance[111]

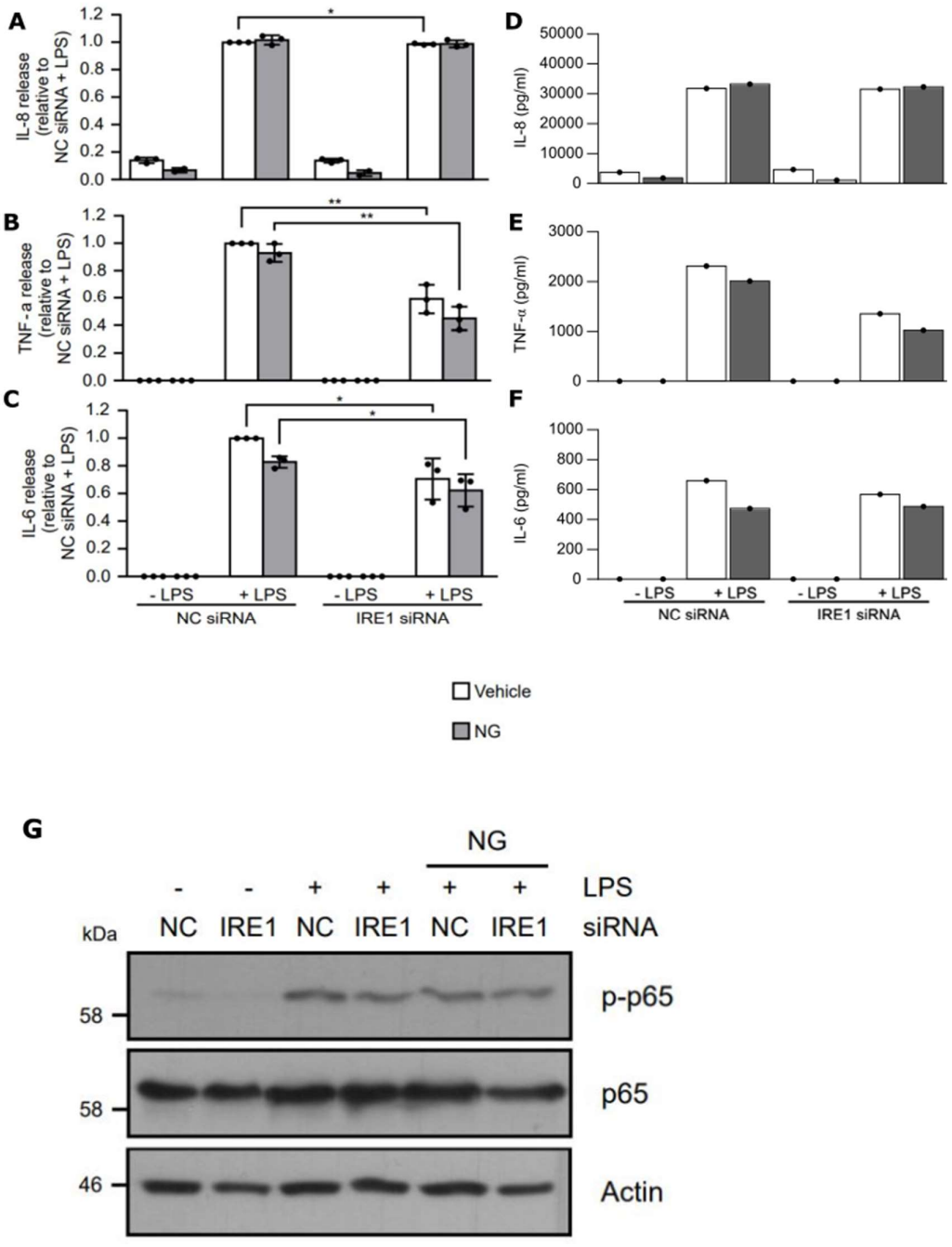

Figure 3.4. IRE1 regulates secreted levels of pro-inflammatory cytokines. THP-1 cells transfected with either non-coding or IRE1 targeting siRNA were treated with either 1 µg/ml LPS alone for 24 h or 1 µg/ml LPS for 24 h followed by addition of 10 µM NG for 45 min. **(A-C)** Levels of IL-8, TNF-α and IL6 were assayed in cell conditioned medium by ELISA (n=3). Representative quantitative ELISA shown for **(D)** IL-6, **(E)** IL-8 and **(F)** TNF-α. **(G)** Cell lysates were analysed via immunoblotting for total p65 and phospho-p65. Actin was used as a loading control. *P < 0.05, **P < 0.01 based on a Student's t test. Error bars represent SD.

3.5 Addition of IRE1 RNase inhibitor reduces LPS-induced IRE1 signalling and suppresses NLRP3 inflammasome activation in THP-1 cells

The small molecule inhibitor of the IRE1 RNase domain known as MKC8866 was first described by Patterson et al in 2011[251]. MKC8866 is a salicyaldehyde derivative and is thought to act primarily by my forming a Schiff base with a lysine (K907) residue in the RNase domain of IRE1, though it also interacts with other residues within the RNase domain[252] (Fig. 3.5A) It has been demonstrated to have an *in vitro* IC_{50} of 0.38 μM[253]. MKC8866 was used to identify whether blocking IRE1 RNase activity could potentially effect inflammasome activation. Addition of MKC8866 efficiently reduced LPS-induced activation of IRE1 RNase activity as determined by a reduction in XBP1s. (Fig. 3.5B). Pro-caspase-1 cleavage in LPS/NG treated conditions was also decreased in cells treated with MKC8866, as evidenced by reduced p10 caspase-1 (Fig. 3.5C). Similar to the effects observed upon IRE1 knockdown, MKC8866 significantly reduced the levels of IL-1β detected in the conditioned media under LPS/NG treated conditions in a dose dependent manner (Fig. 3.5D-E). The levels of XBP1s inhibition observed at the lower concentrations of MKC8866 (1 μM, for example) do not correlate with a similar reduction in IL-1β levels. While it is difficult to say exactly why, perhaps IRE1 regulates the NLRP3 inflammasome via one of its other core mechanisms. This could be through its kinase domain, which is required for RNase activity (discussed in introduction) or through RIDD activity which cannot be measured using XBP1s levels as a readout. Taken together these results suggest that IRE1 RNase inhibition reduces IL-1β processing by reducing caspase-1 cleavage.

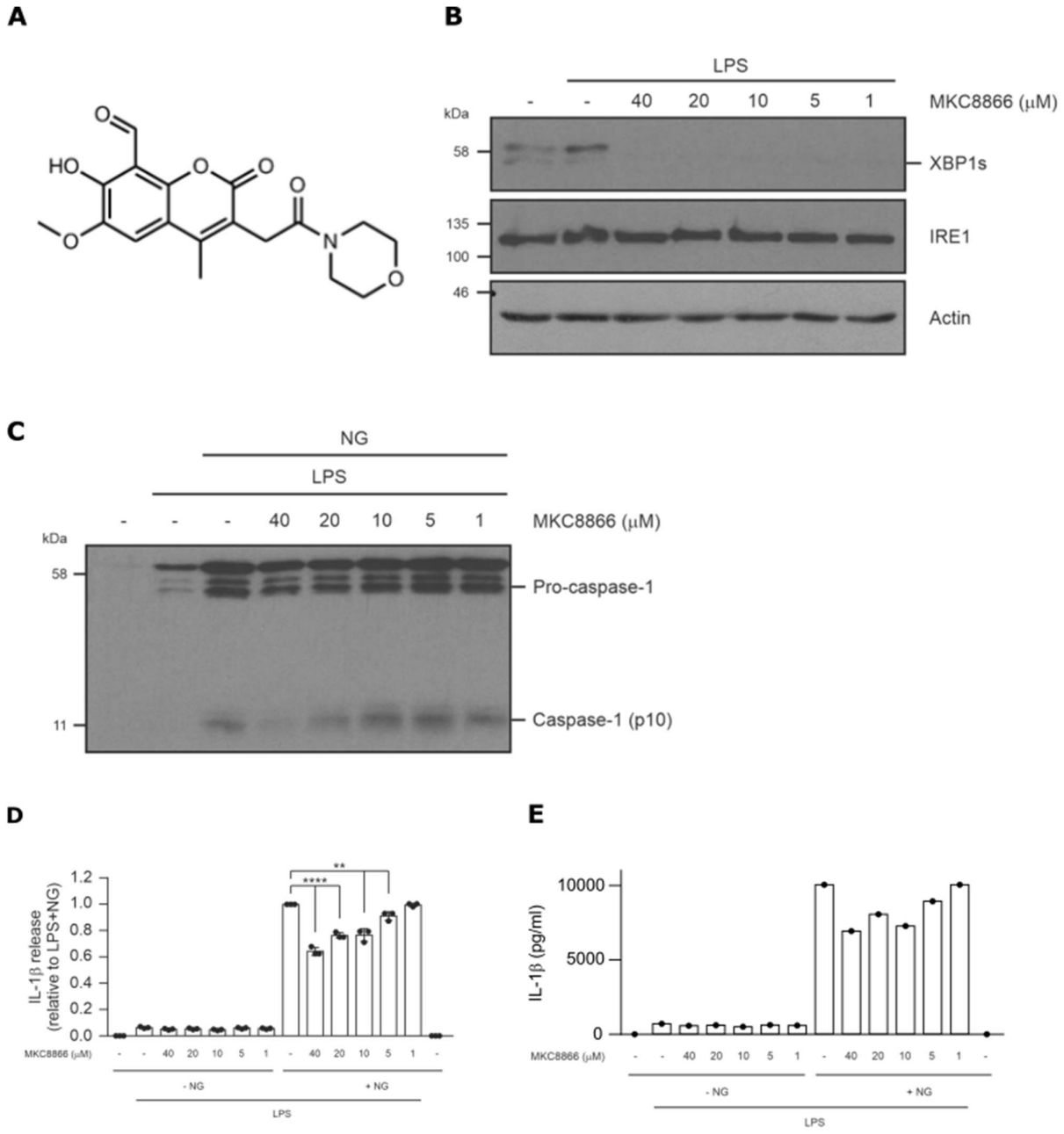

Figure 3.5. Addition of IRE1 RNase inhibitor reduces LPS-induced IRE1 signalling and suppresses NLRP3 inflammasome activation in THP-1 cells. (A) Chemical structure of MKC8866. THP-1 cells were treated with 1 μg/ml LPS alone or in combination with indicated concentrations of IRE1 inhibitor (MKC8866) for 24 h **(B)** after which cell lysate was collected and analysed via immunoblotting for XBP1s and IRE1. Actin was used as a loading control. **(C)** Levels of caspase-1 (pro- and cleaved p10) were assessed via immunoblotting in cell supernatant following indicated treatments. **(D)** Conditioned medium from THP-1 cells treated with LPS alone or LPS/NG combination in the presence or absence of indicated concentrations of MKC8866 were analysed by ELISA for IL-1β (n=3). **(E)** Representative quantitative ELISA shown for IL-1β. **P < 0.01 and ****P < 0.0001 based on a Student's t test. Error bars represent SD.

3.6 Reduced IL-1β levels found in conditioned media from THP-1 cells after LPS/NG treatment is not due to increased cell death.

The literature surrounding the precise mechanism by which IL-1β is secreted from the cell is ambiguous[254]. Recent evidence has suggested that the release occurs after pyroptosis[167] and in order to test this model in our system we analysed the effects of MKC8866 on cell viability during inflammasome stimulated conditions. We assayed uptake of propidium iodide in THP-1 cells after LPS/NG treatment in the presence or absence of MKC8866. While we observed a significant increase in PI uptake in cells post-NG treatment, this was not altered by incubation with MKC8866 (Fig. 3.6A). This suggests that the IRE1 RNase domain mediated regulation of IL-1β is not as a result of increased cell death. A reduction in IL-1β levels analysed by ELISA from supernatant isolated from same experiment conditions also confirms efficient reduction in NLRP3 inflammasome activity by MKC8866 (Fig. 3.6B).

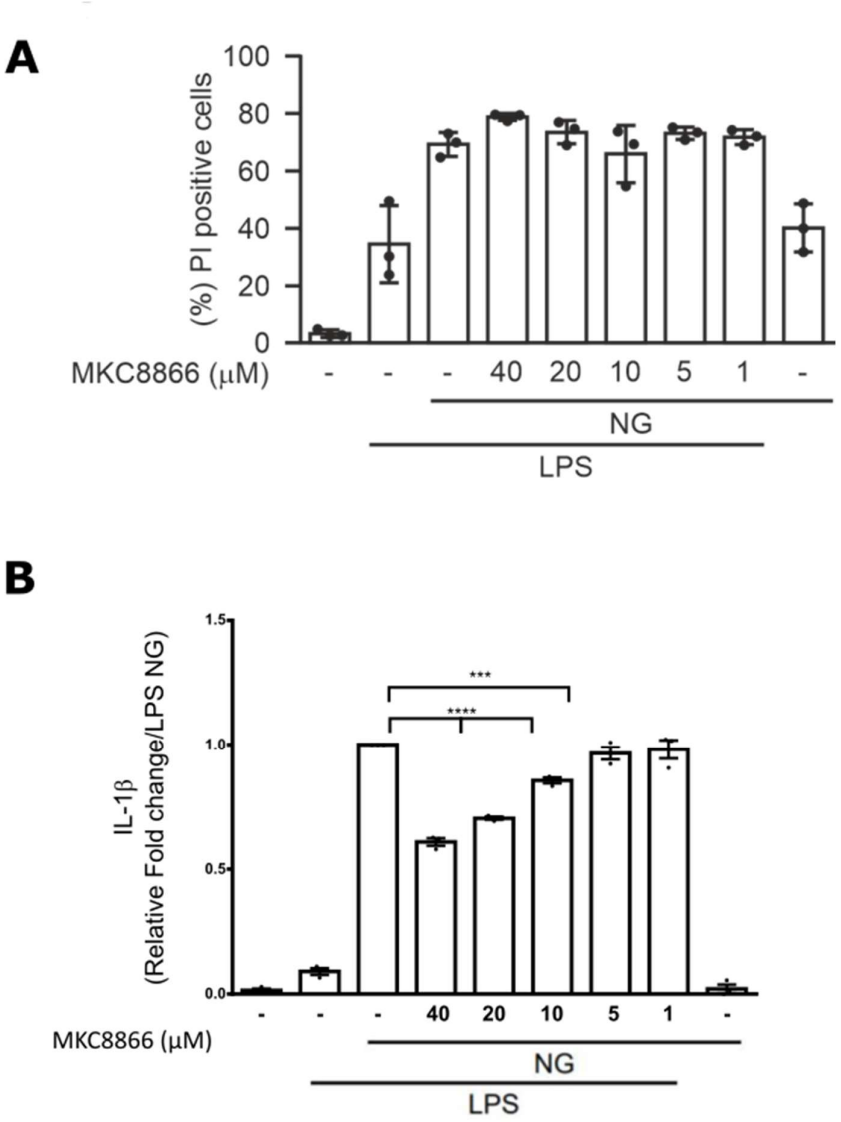

Figure 3.6. Reduced IL-1β levels found in conditioned media from THP-1 cells after LPS/NG treatment is not due to increased cell death. THP-1 cells were treated with either 1 μg/ml LPS alone for 24 h or 1 μg/ml LPS for 24 h followed by addition of 10 μM NG for 45 min, **(A)** propidium iodide uptake was assessed in THP-1 cells following treatment with LPS alone or LPS/NG combination in the presence or absence of indicated concentrations of MKC8866 (n=3)**. (B)** Conditioned medium isolated from THP-1 cells were analysed by ELISA for IL-1β secretion (n=3). ***P < 0.001 and ****P < 0.0001 based on a Student's t test. Error bars represent SD.

3.7 Inhibition of IRE1 RNase by MKC8866 does not impact LPS-mediated priming of *CASP1, IL1β* or *NLRP3*

The data thus far indicates that IRE1 regulates the activation of the NLRP3 inflammasome and we next sought to determine at which point in the two-step activation it was occurring. We examined the transcript levels of the core NLRP3 inflammasome complex under LPS treated conditions in the absence or presence of MKC8866 at 4 h, 10 h and 24 h timepoints. We observed that there were no significant changes upon inhibition of the IRE1 RNase domain to the transcript levels of *CASP1, IL1β* or *NLRP3* (Fig. 3.7A-C). An increase in the transcript levels of pro-IL-1β after 4 hours indicated we have stimulated NLRP3 inflammasome priming and we also confirmed the efficiency of MKC8866 in these experiment conditions by monitoring XBP1s levels via PCR (Fig. 3.7D). However, no significant changes in the protein levels or transcripts of any core inflammasome component under MKC8866 treated conditions suggests that the role of IRE1 in this model is independent of altered expression of the core inflammasome via signal I priming.

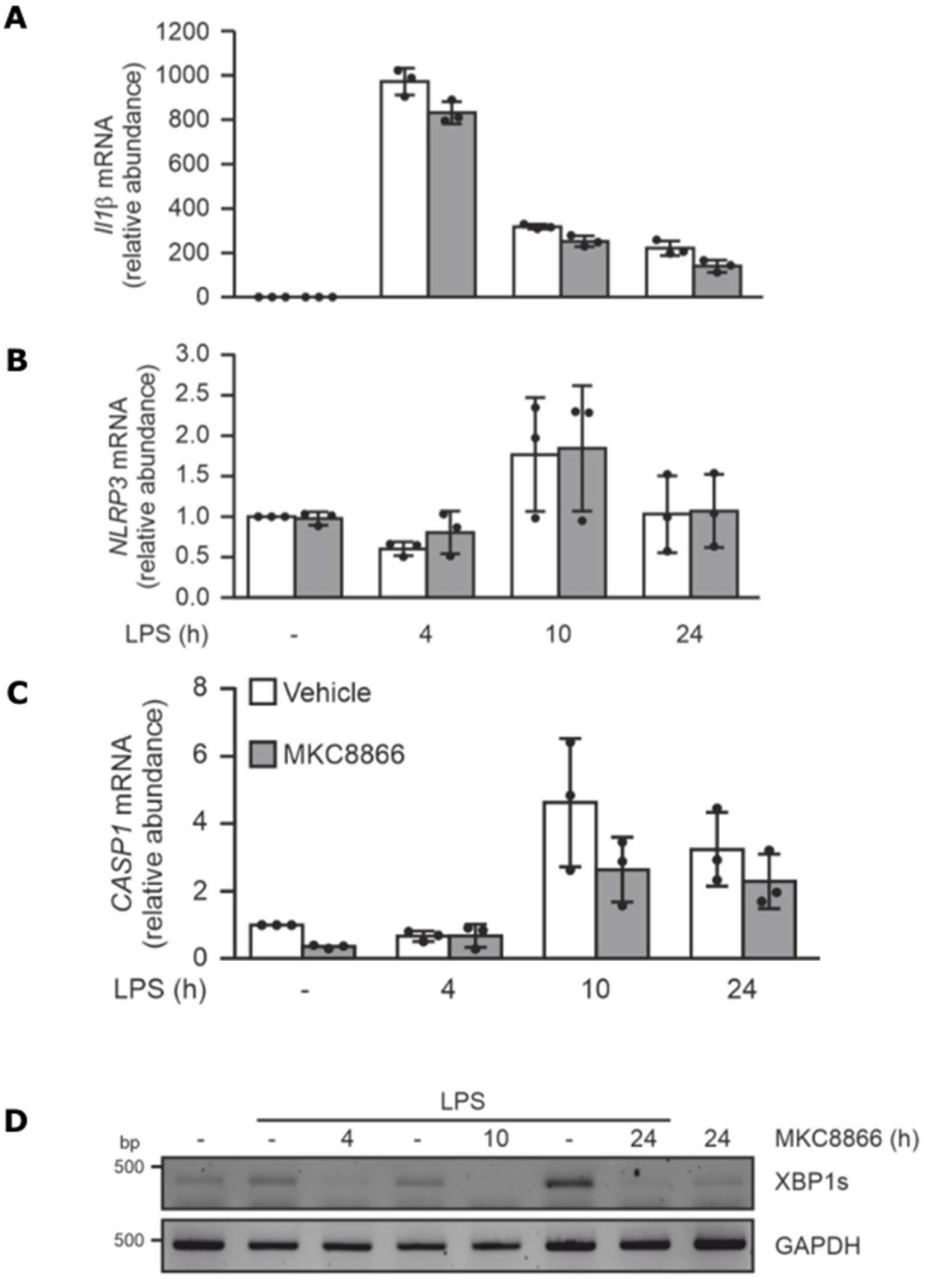

Figure 3.7. Inhibition of IRE1 RNase by MKC8866 does not impact LPS-mediated priming of CASP1, IL1β or NLRP3. THP-1 cells were treated with 1 µg/ml LPS alone for 24 h in the presence or absence of 20 µM MKC8866 for the indicated times after which RNA was extracted and qPCR carried out to assess relative transcript expression of **(A)** *IL1β,* **(B)** *NLRP3* and **(C)** *CASP1* (n=3). **(D)** cDNA used in qPCR analysis of target transcripts was also used in classical PCR to analyse and confirm MKC8866 (20 µM) efficiency via XBP1s levels across samples. Error bars represent SD.

3.8 Inhibition of IRE1 RNase domain does not alter levels of key inflammasome components

In addition to analysing the transcript levels of the core inflammasome components, we also sought to analyse them at the protein level. THP-1 cells were treated with LPS in the presence or absence of MKC8866 and under siIRE1 treated conditions. We observed that there were no changes in the protein level of pro-IL-1β, pro-caspase-1, ASC and NLRP3 under either condition (Fig. 3.8A-B). This suggests the inhibition observed following inhibition of IRE1 RNase activity via MKC8866 or a reduction in overall IRE1 protein expression via siRNA does not alter expression of core inflammasome components. Therefor the reduction in IL1b processing efficiency observed is unlikely to be a consequence of a deficit in signal 1. However, it is also important to note that NLRP3 expression seems to be present even in the absence of LPS treatments. The reason behind this is not clear but it would suggest that the THP-1 cells are “partially primed” or exhibit basal levels of NLRP3. We still observe enhanced IL-1β and caspase-1 levels upon LPS treatment which signifies successful signal 1 induction, however. The basal levels of NLRP3 being observed could be an important avenue you optimization for future experiments.

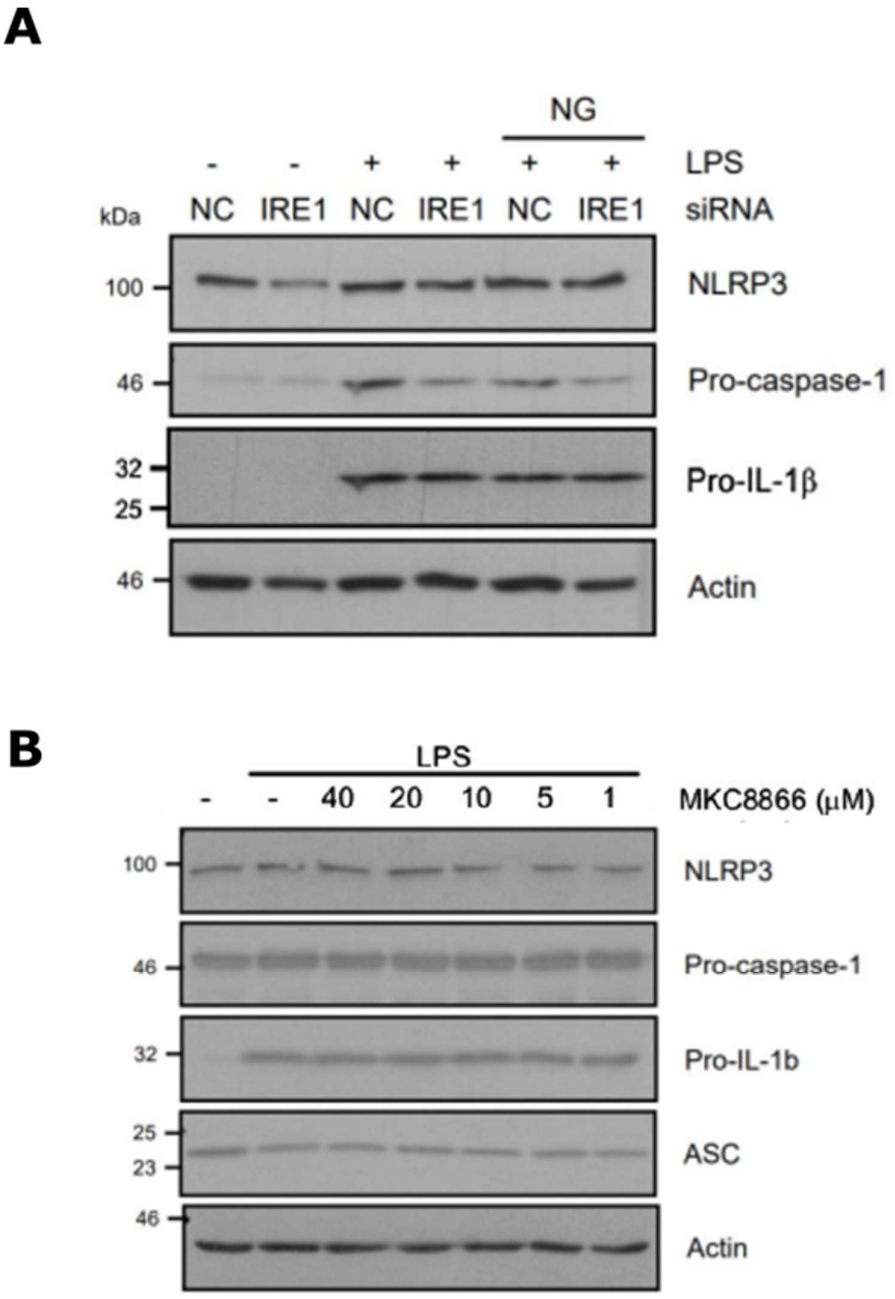

Figure 3.8. Inhibition of IRE1 RNase domain does not alter levels of key inflammasome components. (A) THP-1 cells transfected with either non-coding or IRE1 targeting siRNA were treated with either 1 μg/ml LPS alone for 24 h or 1 μg/ml LPS for 24 h followed by addition of 10 μM NG for 45 min. Cell lysates were analysed via immunoblotting for pro-IL-1β, pro-caspase-1, ASC, NLRP3, phospho-p65 and total p65. Actin was used as a loading control. **(B)** THP-1 cells were treated with 1 μg/ml LPS alone or in combination with indicated concentrations of MKC8866 for 24 h following which cell lysate was collected and analysed via immunoblotting for pro-IL-1β, pro-caspase-1, ASC, NLRP3, phospho-p65 and total p65. Actin was used as a loading control.

3.9 Addition of MKC8866 reduces LPS/NG-induced NLRP3 inflammasome formation

To investigate the role of the IRE1 RNase domain in the regulation of signal II of inflammasome activation we analysed the effects of MKC8866 treatment on ASC oligomerization, a readout for NLRP3 inflammasome assembly. Treatment of THP-1 cells with LPS/NG triggers an expected increase in ASC oligomerization compared to that of LPS alone (Fig. 3.9A). Treatment of cells with MKC8866 reduces oligomerization after LPS/NG treatment (Fig. 3.9A). Extracellular K^+ was used as a positive control and as previously demonstrated showed almost complete impairment of oligomer formation[148]. Following ASC oligomerization, pro-caspase-1 is recruited to the complex via CARD-CARD interactions with ASC. This causes proximity-induced autocatalysis of the now closely oriented pro-caspase-1 monomers[255]. Any disruption in this oligomerization process will also disrupt optimal pro-caspase-1 cleavage. Upon MKC8866 treatment in THP-1 cells stimulated with LPS/NG we also observed decreases in cleaved or active p10 caspase-1 along with reduced cleaved IL-1β, both analysed in the supernatant harvested from samples (Fig. 3.9B). We also analysed IL-1β via ELISA method from the same supernatant and observed a similar reduction in IL-1β levels (Fig. 3.9C) indicating a reduction in the efficiency of inflammasome formation.

We also assessed structural formation of the inflammasome by accessing processing of pro-caspase-1. Using a FLICA assay specific for caspase-1 like caspases we compared caspase-1 like activity in cells treated with LPS/NG to those treated with LPS/NG in combination with MKC8866 (Fig. 3.9D). This data demonstrated an inhibition in pro-caspase-1 processing following addition of MKC8866. Collectively, this data indicated treatment with MKC8866 reduces inflammasome assembly and formation as evidenced by reduced ASC oligomerization and caspase activity and as a result of this, reduced IL-1β processing.

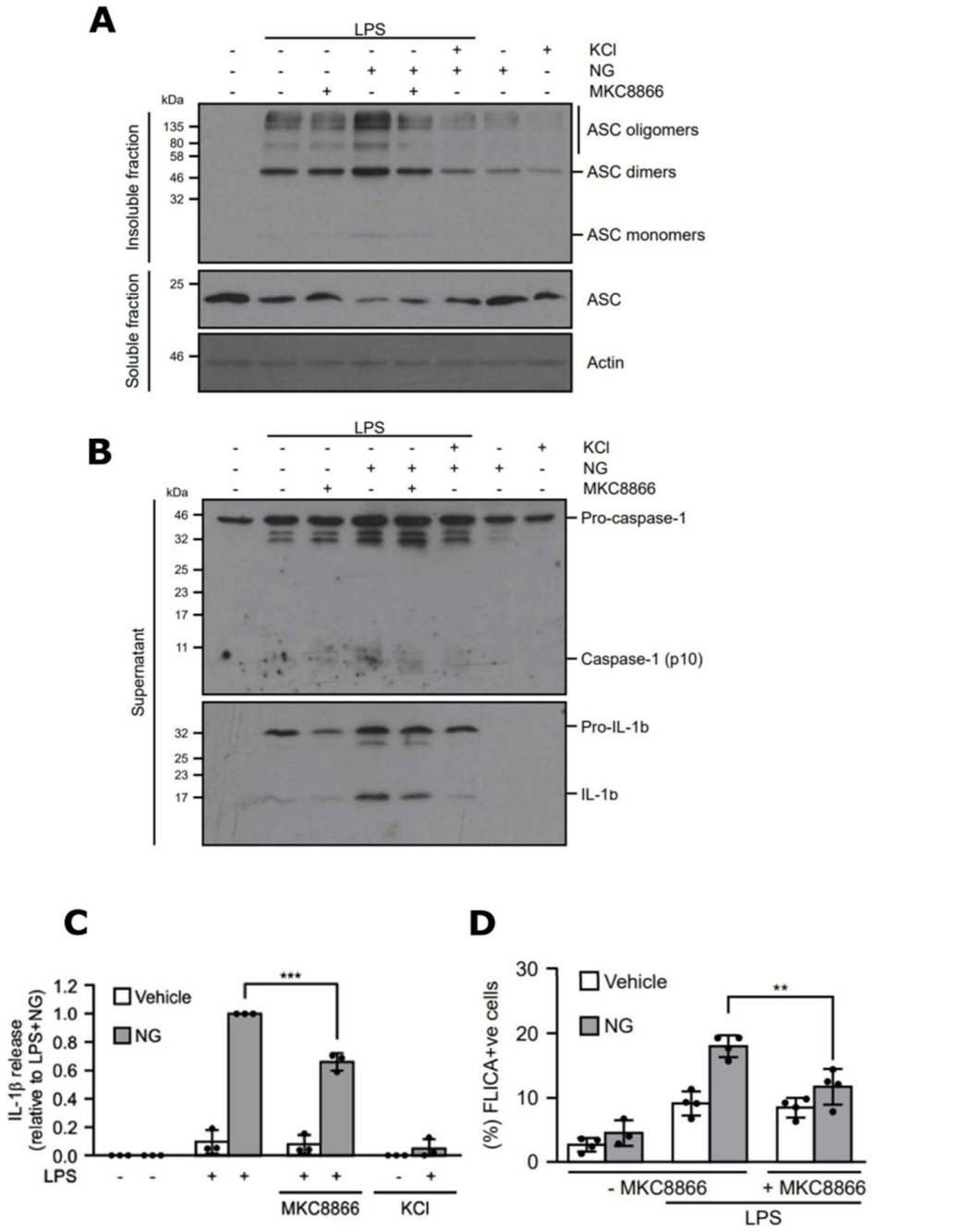

Figure 3.9. Addition of MKC8866 reduces LPS/NG-induced NLRP3 inflammasome formation. THP-1 cells were treated with LPS alone, LPS/NG or LPS/NG plus MKC8866 or KCL. Cells and conditioned medium harvested after 24 h. **(A)** ASC oligomerization was assessed in THP-1 cells following the above-described treatments by immunoblotting for ASC oligomers. **(B)** Caspase-1 and IL-1β, both pro and cleaved forms, were assessed by western blotting in supernatant harvested after treatment. **(C)** IL-1β protein in the supernatant also analysed by ELISA method following outlined treatments (n=3). **(D)** Caspase-1 activity assessed following the indicated treatments using a FLICA assay (n=3). **P < 0.01, and ***P < 0.001 based on a Student's t test. Error bars represent SD.

3.10 MKC8866 restores TXNIP protein and transcript levels in THP-1 cells after LPS-induced depletion

Thioredoxin-interacting protein (TXNIP) has been demonstrated to bind NLRP3 during oxidative stress, leading to increased inflammasome activation[256]. Furthermore, several reports have proposed that IRE1 signalling increased TXNIP expression and, thereby, inflammasome formation[73, 256, 257]. Based on these studies, we asked if IRE1 activity promotes inflammasome formation via TXNIP in our model. To answer this, we examined TXNIP expression following NLRP3 inflammasome stimulation in the presence or absence of MKC8866. Contrary to what has been observed in the literature, rather than LPS causing an increase in TXNIP, we found that it led to a decrease in TXNIP transcript levels (Fig. 3.10A)[256]. Interestingly, this reduction was also partially rescued by MKC8866. We also observed a similar response in protein analysis via immunoblotting for TXNIP (Fig. 3.10B). Therefore, in our model, TXNIP does not seem to be playing a role in IRE1's regulation of NLRP3 inflammasome activation. It is important to note that while the evidences of IRE1, TXNP1 and NLRP3 interacting with one another is somewhat accepted in the field, a caveat found in most studies linking these factors is that they rely on artificial means of ER stress induced by ER stress agents. We believe that this could play a role in altering the state in which TXNIP interacts with IRE1 and NLRP3, or *vice versa*. Therefore, this may explain the differences in our results compared to that already published.

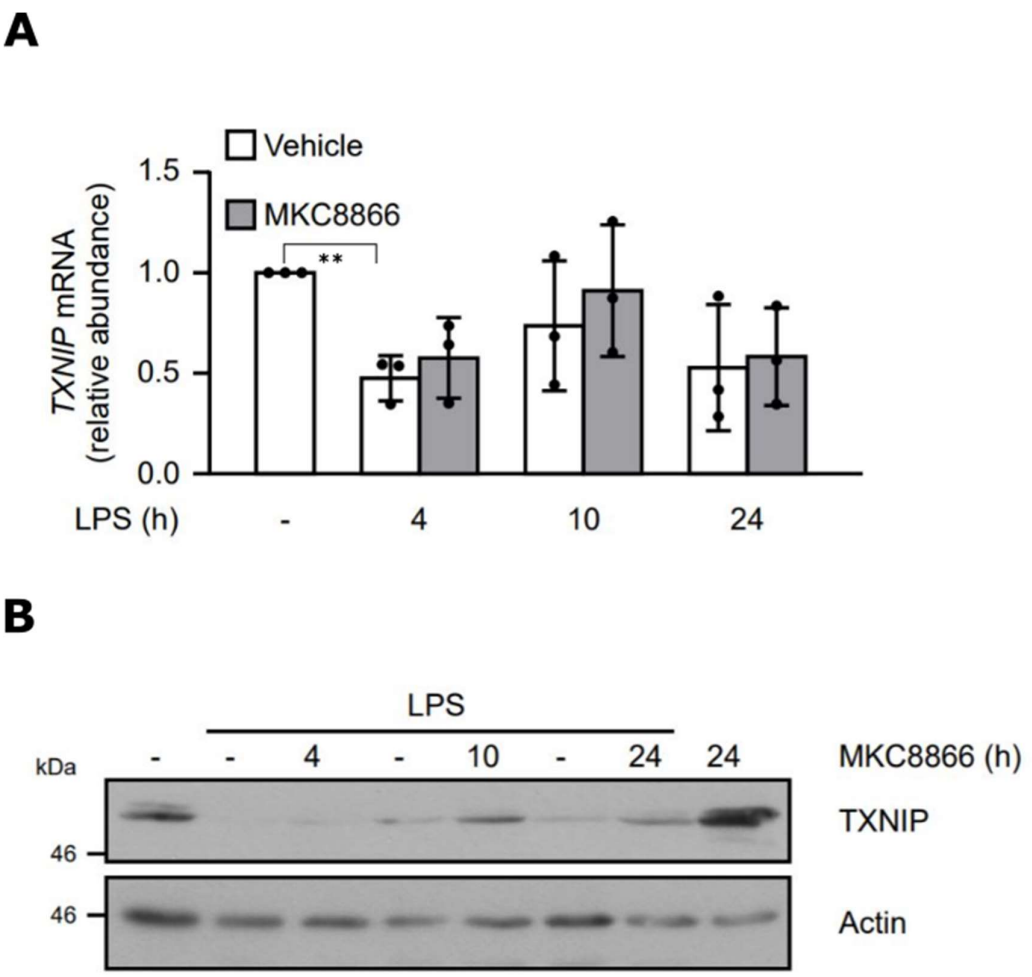

Figure 3.10. MKC8866 restores TXNIP protein and transcript levels in THP-1 cells after LPS-induced depletion. THP-1 cells were treated with 1 µg/ml LPS alone or in combination with 20µM MKC8866 for the indicated time-points after which cells were harvested and TXNIP expression monitored **(A)** at transcript levels by qPCR (n=3), **(B)** and protein levels by immunoblotting. **P < 0.001 based on a Student's t test. Error bars represent SD.

3.11 MKC8866 reduces inflammasome activation in primary PBMC's

In order to verify that the role we observe for IRE1 in NLRP3 inflammasome formation was not restricted to THP-1 cells, we analysed its role in PBMC's isolated from healthy individuals. Primary PBMCs were stimulated with 0.5 μg/ml LPS for 2h to facilitate signal I priming. Post LPS treatment, PBMC's received signal II stimulation in the form of 5mM ATP. ATP produces a similar K^+ efflux to NG but its mechanism has been specifically identified as activation of the P_2X_7 receptor, in contrast to the ambiguous role played by NG[258]. Firstly, we observed that PBMC's stimulated with both signal I and II displayed increased IL-1β levels compared to those stimulated with LPS only (Fig. 3.11A). Importantly, the treatment of stimulated PBMC's with MKC8866 both reduced XBP1s by PCR and IL-1β levels by ELISA (Fig. 3.11A-B, 3.11D). Western blotting analysis also revealed reduced levels of cleaved p17 IL-1β and p10 caspase-1 in the conditioned media from LPS/ATP stimulated PBMC's in the presence of MKC8866 compared to those without (Fig. 3.11C). Taken together, these data suggest that IRE1 RNase mediated regulation of the NLRP3 inflammasome is also functional in primary PBMC's.

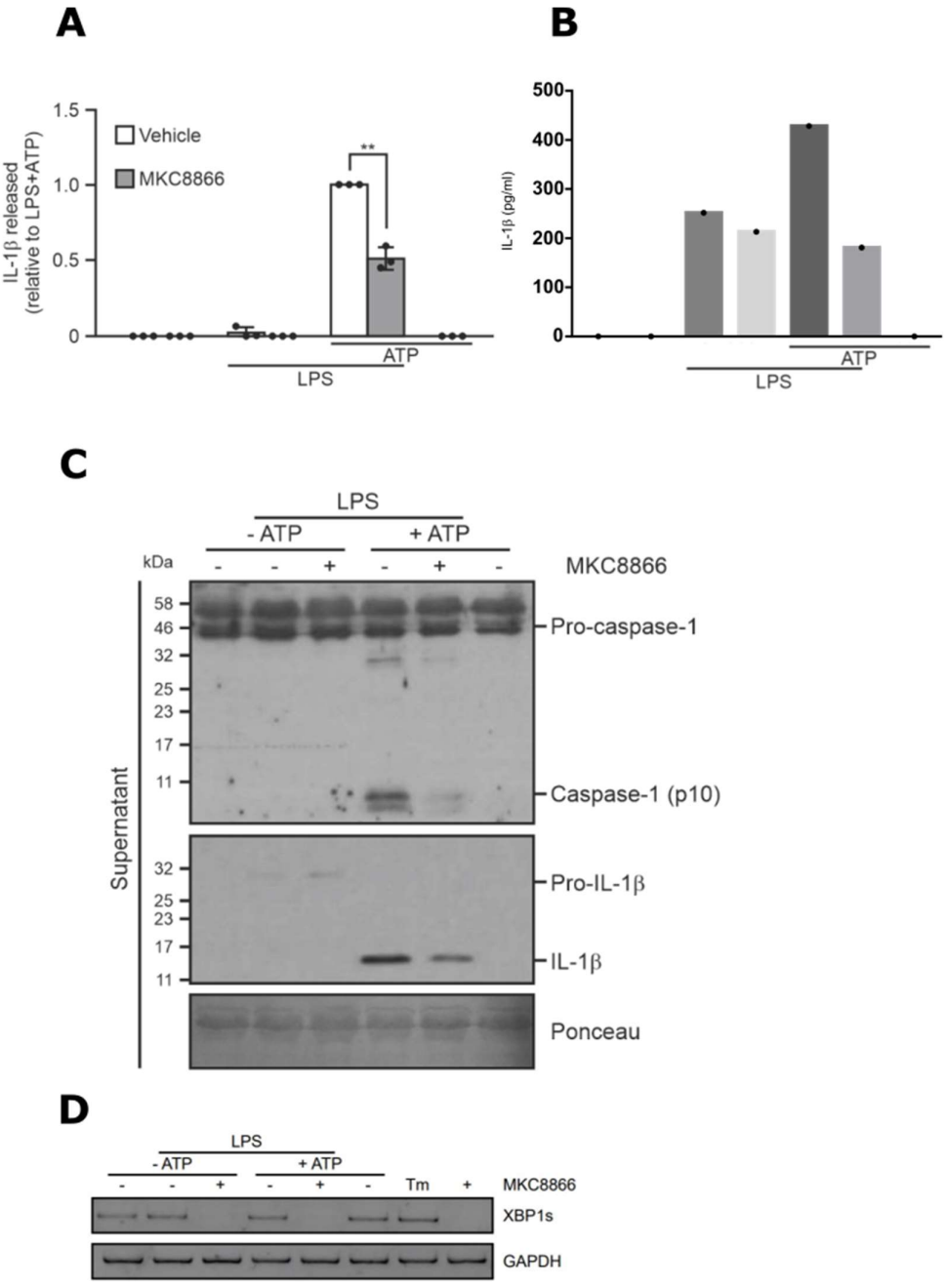

Figure 3.11. MKC8866 reduces inflammasome activation in primary PBMC's. PMBCs isolated from healthy individuals were treated with either 0.5 µg/ml LPS alone or 0.5 µg/ml LPS followed by addition of 5mM ATP, following which cell lysates and supernatant was collected. **(A)** Levels of IL-1β were quantified by ELISA in PBMC conditioned medium following indicated treatments (n=3). **(B)** Representative quantitative ELISA shown for IL-1β. **(C)** Immunoblotting of cell lysates and supernatant for caspase-1 (pro- and p10) and IL-1β (pro- and p17). **(D)** XBP1s levels analysed by PCR to confirm IRE1 RNase inhibition in PBMC's. Actin was used as a loading control for cell lysates (upper panel). **P < 0.01 based on a Student's t test. Error bars represent SD.

3.12 Inflammasome activity in stimulated THP-1 cells can be reduced by blocking antibodies for IL-6 and CXCL1

It has been shown in the literature that CXCL1 is a regulator of the NLRP3 inflammasome[259]. Additionally, in breast cancer cells we have recently demonstrated IRE1-dependent regulation of CXCL1[86]. This led us to ask whether IRE1 also regulated CXCL1 production in THP-1 cells following stimulation with LPS/NG and whether it was possible that the inflammasome regulation we observe upon IRE1 deficiency could be caused by disrupting feedback loops with other cytokines. To test this, we treated THP-1 cells stimulated with LPS/NG in the presence or absence of MKC8866 and analysed CXCL1 levels in the conditioned media (Fig 3.12A). In order to test whether CXCL1 could be regulating NLRP3 inflammasome activation in a feedback mechanism, we treated LPS/NG stimulated THP-1 cells with blocking antibodies for CXCL1. In addition to this we also used blocking antibodies for IL-6 and IL-8 due to their associations with IRE1 and as they are also TLR4 stimulated. ELISA analysis of CXCL1(B), IL-6(C), IL-8(D) and IL-1β(E) in conditioned media revealed both successful cytokine neutralization by their respective neutralizing antibody but also that reductions in IL-6 and CXCL1 levels could subsequently reduce IL-1β levels (Fig. 3.12B-E). This suggests that the published data identifying CXCL1 as an NLRP3 regulator may be relevant in our system but also suggests a novel role for IL-6 in inflammasome regulation. Interestingly, we also see a consistent increase in IL-1β levels upon IL-8 blocking antibody treatment suggesting a negative feedback loop. It is possible that IRE1-mediated regulation of an inflammatory cytokine induced during signal I of NLRP3 inflammasome activation has a subsequent effect on signal II activation and impacts efficient complex assembly in some manner. The possibility of one of these cytokines being a regulator of NLRP3 inflammasome activation downstream of their signal I induction is an interesting one. However, the complex nature of cytokines and their interactions cannot be understated meaning further elucidation of these interactions are absolutely required.

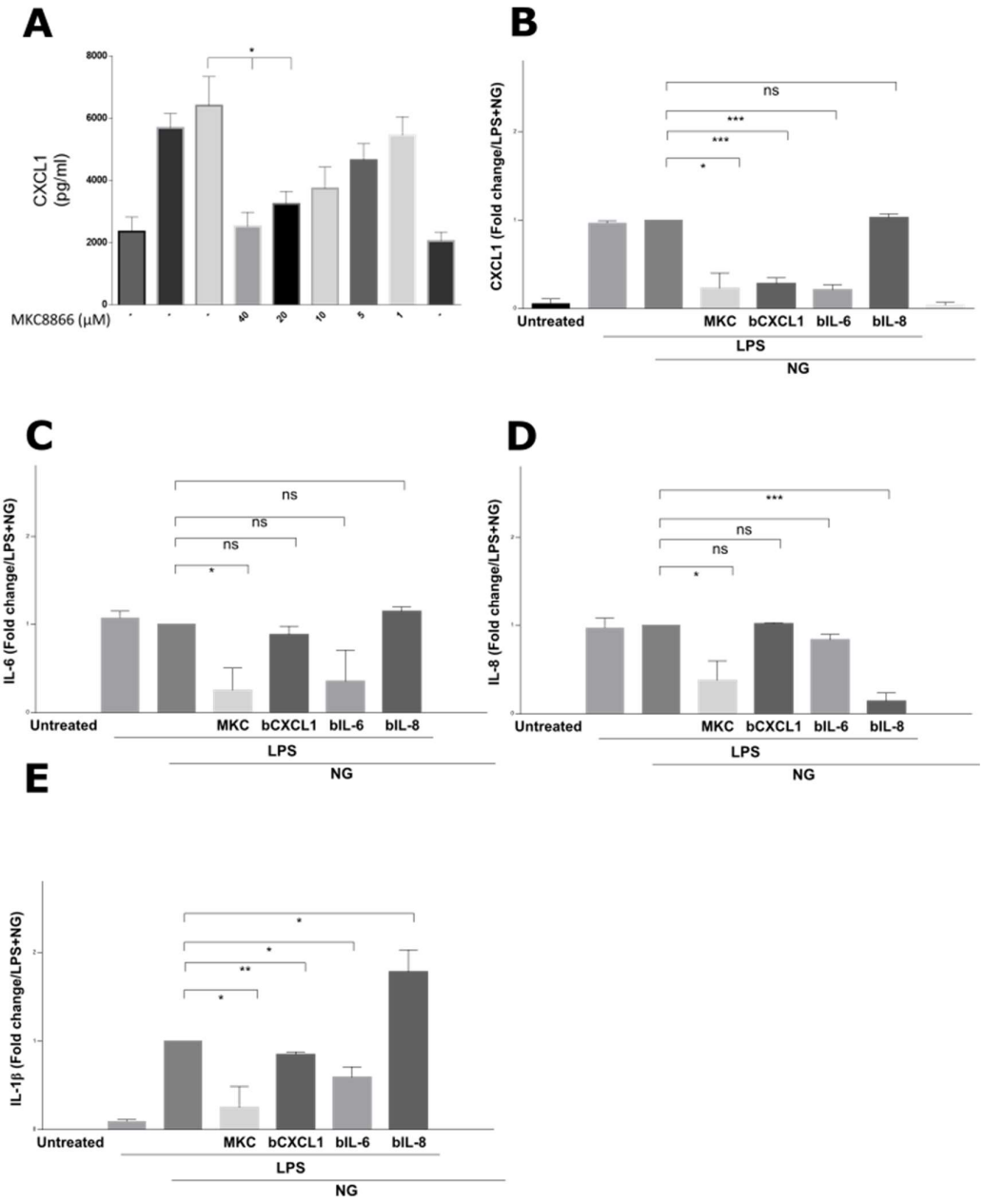

Figure 3.12. Inflammasome activity in stimulated THP-1 cells can be reduced by blocking antibodies for IL-6 and CXCL1. (A) THP-1 cells were treated with LPS alone for 24 h followed by addition of 10 μM NG for 45 min in the presence or absence of various doses of MKC8866 analysed by ELISA for CXCL1 secretion levels (n=3). **(B-E)**THP-1 cells treated with LPS for 24 h followed by 10 μM NG for 45 min in the presence or absence of blocking antibodies for CXCL1 (25 μg/ml), IL-6 (500 ng/ml) and IL-8 (5 μg/ml). Conditioned medium isolated from THP-1 cells after 24 h were analysed by ELISA for CXCL1, IL-6, IL-8 and IL-1β secretion (n=3). *P < 0.05, **P < 0.01, ***P < 0.001 based on a Student's t test. Error bars represent SD.

3.13 Application of a new multiplexed array for rapid, sensitive, simultaneous and quantitative assessment of spliced and unspliced XBP1

As therapies targeting the UPR enter clinical trials and evidence for the use of XBP1s as a pathologically relevant biomarker grows, effective means of monitoring XBP1 splicing and expression of the XBP1 isoforms has become a clinical need. None of the methods currently employed for XBP1s or XBP1u detection are suitable for routine use in a clinical laboratory. RT-PCR and RT-qPCR are often used to assess *XBP1* splicing, using primers flanking the spliced intron sequences where variant specificity is required[86]. Whilst more specialised laboratories can utilise qPCR to get a quantitative measurement of XBP1s/XBP1u ratios, this method could have far less reliable results in a routine clinical setting. Factors such as extended sample preparation, potential for contamination and requirements for standardisation and normalisation of results make RT-qPCR unsuitable for medium-high throughput in non-sterile clinical laboratories[260]. At the protein level, standard assessment of XBP1s (and less commonly XBP1u) is performed by immunoblotting. Medium-high throughput is not practical with this time-consuming and technically laborious method. Western blots are also largely unsuitable for quantification or inter-blot comparison with variation due to detection mechanism, reagents and analysis methods.

Biochip Array Technology (BAT) is commonly used in both clinical and research settings to simultaneously, quantitatively determine protein levels in serum and other biological matrices. The XBP1 Biochip assay kit was obtained from Randox Laboratories (XBP1 Array (EV4357), Randox Laboratories Ltd., Crumlin, UK). The multiplexed sandwich immunoassay system provides a platform to assess multiple protein levels in a single sample. An assay system was proposed using the unique principles of sandwich-BAT to simultaneously capture the two XBP1 isoforms utilising their different C-termini, and detecting the captured protein using an enzyme labelled antibody, Horse Radish Peroxidase (HRP) conjugated pan-detector, targeted to their common N-terminus (Fig. 3.13A). Here we demonstrate the application of a biochip to simultaneously detect the two XBP1 isoforms in THP-1 cells under LPS/NG stimulated conditions (Fig. 3.13B-C). We achieved a simple, reproducible method of

analysing XBP1s but also XBP1u at the protein level, something which has been a difficulty for work done prior in this project due to antibody specificity issues and difficulties in obtaining strong signal during immunoblotting. We also confirmed the efficiency of MKC8866 on the levels of XBP1s by traditional PCR in the same experiment (Fig. 3.13D).

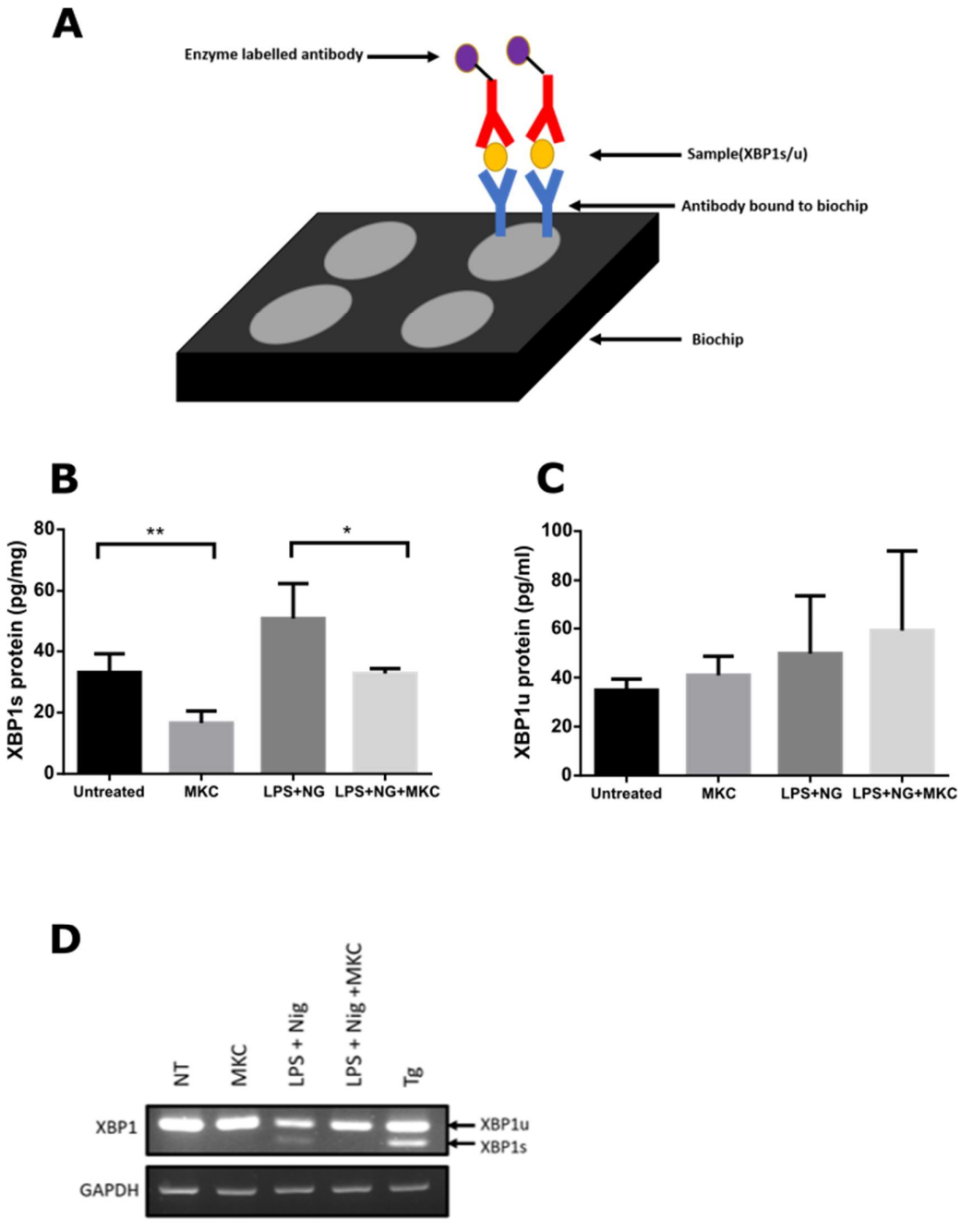

Figure 3.13. Application of a new multiplexed array for rapid, sensitive, simultaneous and quantitative assessment of spliced and unspliced XBP1. THP-1 cells treated with LPS (1 µg/ml) for 4 h followed by 10 µM NG for 45 min in the absence of presence of MKC8866. **(A)** Sandwich BAT assays utilise a solid state immobilised multiplexed ELISA based system. **(B-C)** Levels of XBP1s and XBP1u measured using XBP1 biochip (N=4)**. (D)** Levels of *XBP1* mRNA analysed from same samples as *(a)***.** *P < 0.05, **P < 0.01 based on a Student's t test. Error bars represent SD.

3.14 Discussion

Classically IRE1 activation is associated with resolution of ER stress via activation of the adaptive, pro-survival unfolded protein response. However, an important role for IRE1 signalling is emerging within the innate immune system where it has been linked to the function of several cell types including dendritic cells, macrophages and natural killer cells [243]. In this study we asked whether IRE1 signalling contributed to activation of the NLRP3 inflammasome in monocytic cells. Similar to the findings reported by Martinon and colleagues, using murine bone marrow derived macrophages (BMDMs) [245], we observed selective activation of the IRE1-XBP1 axis in the human monocytic cell line, THP-1 following stimulation with LPS. Induction of signal II, via nigericin treatment, while not altering IRE1-dependent signalling, significantly enhanced inflammasome activation and pro-IL-1β processing. By selectively inhibiting IRE1 signalling using a small molecule IRE1 RNase inhibitor we observed a substantial reduction in processing of pro-IL-1β in both THP-1 cells and primary PBMCs. Similar to our findings, Tufanli and colleagues recently reported blocking IRE1 RNase signalling reduced pro-IL-1β processing in PBMCs and NLRP3 inflammasome activation in murine BMDMs [261] but did not explore the mechanism underpinning these observations.

By assessing the various signalling steps driving NLRP3 inflammasome assembly we demonstrate IRE1 signalling, while not required in THP-1 cells for priming of inflammasome components or induction of pro-IL1β expression, is required for efficient assembly of the NLRP3 inflammasome complex. The reduction we observe in inflammasome assembly, upon IRE1 RNase inhibition, while substantial is not complete (Fig. 3.3, 3.5). This suggests that IRE1 signalling likely promotes the efficiency of inflammasome assembly by fine-tuning it in some manner but is not an absolute requirement. Similar results were obtained in primary PBMCs where treatment with MKC8866 reduced but did not inhibit pro-IL1β processing and release in response to LPS/ATP treatment (Fig. 3.11).

The signalling pathways initiating structural assembly of the inflammasome are not fully understood, with diverse processes including ion efflux, generation of mitochondrial reactive oxygen species (mtROS) and post-translational modification

of inflammasome components including NLRP3 and ASC implicated [262]. Recent reports have suggested that IRE1 RNase activity can increase NLRP3 inflammasome formation in the pancreatic B cell line INS-1 via regulation of thioredoxin-interacting protein (TXNIP) expression [256, 257]. Increased IRE1 RNase activity induced in INS-1 cells via treatment with pharmacological inducers of ER stress, was demonstrated to degrade miR-17, a microRNA that normally represses TXNIP mRNA resulting in increased TXNIP expression and enhanced inflammasome formation [256]. Similarly, Oslowski and colleagues reported addition of thapsigargin or tunicamycin to INS-1 cells induced TXNIP expression, which increased levels of pro-IL-1β [257].

In assessing the contribution of TXNIP in our system, we found that LPS treatment decreased TXNIP expression in THP-1 cells. Furthermore, LPS-induced decreases in TXNIP expression were partly blocked upon addition of MKC8866 suggesting that IRE1-mediated signalling leads to a loss of TXNIP expression in our system (Fig. 3.10). The discrepancy between our work and previously reported results may be a consequence of several factors including the amplitude of IRE1 signalling triggered and the cell types used. We have modelled physiological activation of IRE1 signalling within the innate immune system rather than IRE1 signalling induced by pharmacological inducers of ER stress. Although we have clearly demonstrated a role for IRE1 signalling in fine-tuning assembly of the NLRP3 inflammasome in monocytes following TLR ligation, further studies are required to determine the mechanisms underpinning this observation (Fig.3.14).

While our results indicate that IRE1 signalling contributes to, but is not an essential requirement, for inflammasome activation in LPS-stimulated monocytes it is likely that the importance of this pathway may be heightened in particular settings. Elevated IRE1 signalling, as determined by increased XBP1 splicing, has been reported in monocytes obtained from rheumatoid arthritis and tumour necrosis factor receptor associated periodic syndrome (TRAPS) patients [263, 264]. Within these specific disease settings, it is plausible that constitutively elevated IRE1 signalling helps drive hyper-stimulation of the inflammasome leading to excessive production of IL-1. Therefore, selective, targeted use of IRE1 inhibitors could yield benefits in these clinical settings. Indeed, genetic ablation of IRE1 signalling in a mouse model

of rheumatoid arthritis has been demonstrated to confer significant therapeutic benefits [248].

Additionally, we have also shown that under stimulated conditions, IRE1 ablation also leads to a significant reduction in the secretion of key inflammatory cytokines, as already seen in the literature (Fig. 3.4). While this regulation is strictly LPS/TLR4 mediated and unrelated to signal II activity, we sought to question as to whether any cytokine regulated at this level could subsequently disrupt inflammasome assembly via IL-1β. Interestingly, through the use of blocking antibodies for IL-6, IL-8 and CXCL1 we observed that a reduction in IL-6 and CXCL1 levels had a knock-on effect on secreted IL-1β levels in stimulated conditions (Fig. 3.12). While this remains to be further investigated, it is interesting to speculate whether there is an important mechanism here.

In summary, our study highlights a previously unknown role for IRE1 dependent signalling in the structural assembly of the NLRP3 inflammasome. We demonstrate blockade of IRE1 signalling, through the use of a small molecule inhibitor, efficiently reduces NLRP3 inflammasome formation and pro-IL1β processing in both THP-1 cells and primary PBMCs. Our findings further support the emergence of IRE1α as a driver of innate immune responses and suggest therapeutically targeting IRE1 could yield clinical benefit in conditions characterised by excessive NLRP3 inflammasome formation.

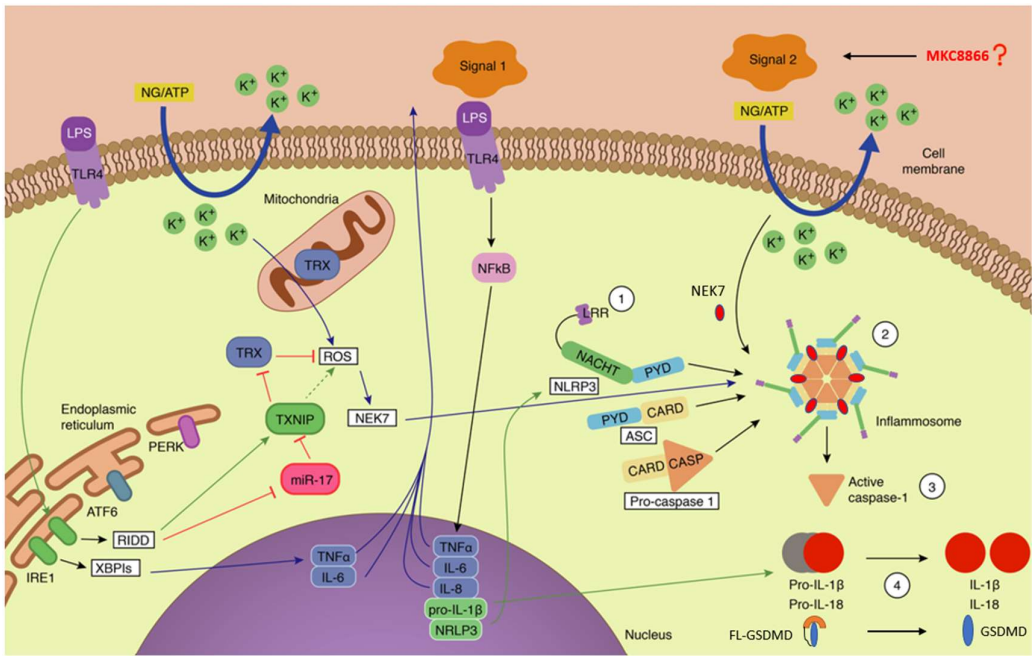

Figure 3.14. IRE1 regulates NLRP3 inflammasome activation efficiency. While it has been demonstrated by *Martinon et al[245]* that IRE1 regulates inflammatory cytokine production upon LPS-mediated stimulation of TLR4, the precise mechanism behind IRE1's role in NLRP3 inflammasome formation was previously unreported. We have shown that **(1)** IRE1 does not regulate the transcript or protein levels of key inflammasome components (NLRP3, ASC, pro-caspase-1) suggesting IRE1 does not regulate NLRP3 priming (signal 1). **(2)** We have shown, using ASC oligomerization as the primary method of analysis, that IRE1 inhibition reduces NLRP3 complex assembly which suggests IRE1 plays a role in the NLRP3 activation step (signal 2). We also show that **(3)** IRE1 inhibition reduces activated caspase-1, suggesting that the terminal outputs of NLRP3 inflammasome activity are also hindered. Finally, **(4)** we have shown that IRE1 inhibition reduces levels of secreted, activated IL-1β independently of pyroptosis. It is worth noting that our study did not analyse the key NLRP3 component NEK7, essential to complex formation and the pyroptosis regulating protein GSDM (caspase-1 substrate). These should be examined in future.

3.15 Future directions

Having identified a role for IRE1 in the activation of the NLRP3 inflammasome we now need to question the specifics of this interaction. Below are possible future avenues of research that could help elucidate the mechanisms involved and increase our understanding of IRE1's role in NLRP3 inflammasome assembly.

3.15.1 Does IRE1 regulate other inflammasome complexes?

As briefly mentioned in the introduction of this thesis, multiple inflammasomes exist. Considering the role of IRE1 in the NLRP3 inflammasome activation step, it's interesting to consider if other Inflammasomes could also be influenced by IRE1 RNase activity. The NLRP1 inflammasome is stimulated by the agent behind anthrax disease, *B. anthracis* lethal toxin (LeTx)[265]. It has been shown that IRE1 and PERK signalling contributes to NLRP1 expression via ATF4 transcription factor and independently of XBP1[266]. IRE1 has also been reported to regulate NLRP1 expression via cAMP responsive element binding protein (CREB) phosphorylation[267, 268]. Given this process's independence from XBP1 signalling and that IRE1 knockdown reduced CREB phosphorylation and NLRP1 expression, IRE1 may regulate NLRP1 via its kinase domain. Other key inflammasomes like AIM2, NLCR4 and the pyrin inflammasome are all induced by various stimuli and composed of different complex components[114]. There is no evidence linking them to IRE1 activity currently in the literature. However, they all share in common the ability to induce IL-1β and IL-18 cleavage and it would be of great interest to observe if similar effects upon MKC8866 treatment were observed here.

3.15.2 Novel NLRP3 interactors

While much is known about inflammasome regulation, research continues to identify newly associated regulatory proteins that are continuing to make the picture clearer. In recent years, one of these proteins, has been identified as NIMA-related kinase 7 (NEK7). In terms of the NLRP3 inflammasome it has been shown that NEK7 is essential for NLRP3 activation. It occurs downstream of K+ efflux and it is now believed to be part of the NLRP3 inflammasome complex as it has been shown to directly bind NLRP3 and controls its oligomerization[269]. NEK7 seems to also bind exclusively with the NLRP3 inflammasome as it has been shown to be dispensable for AIM2 and

NLRC4 inflammasomes. Future work should hopefully help elucidate the role of NLRP3's newest binding partner and maybe give rise to a potential new therapeutic target. No evidences link IRE1 to NEK7 in the literature to date, however. TXNIP was originally identified as a negative regulator of the expression and function of thioredoxin (TRX). Thioredoxins are a class of proteins that exhibit antioxidant functions by causing the reduction of other proteins via cysteine thiol-disulphide exchange. TXNIP interacts with thioredoxin and negatively regulates its antioxidant activity. Low levels of TXNIP in tumours suggest it may act as a tumour suppressor, with links to cell tumour growth inhibition, glucose metabolism regulation and decreased metastasis being associated with TXNIP activity to date[270]. TXNIP can bind to NLRP3 under oxidative stress whereupon TXNIP dissociates from TRX and binds to NLRP3 in a ROS dependent manner[256]. LPS treatment reduces TXNIP expression and allows for a simultaneous upregulation of iNOS and the author suggests that it may be that reducing TXNIP levels creates favourable conditions for iNOS induction upon LPS stimulation[271]. iNOS is a member of the nitric oxide synthase family, a protein family that regulate the production of nitric oxide (NO), a cell signalling molecule with roles in a huge range of biological processes. *Park et al* have shown that TXNIP regulates iNOS expression via NF-κB activation and translocation[271]. It is also known that excess NO levels S-nitrosylate and inhibit NLRP3 activity[272]. We have already briefly analysed TXNIP in our system and observed that the effects of LPS treatment and IRE1 inhibition on TXNIP do not comply with what is reported in the literature. The abundance of data linking TXNIP to NLRP3 regulation in the literature may be enough to warrant a further analysis of TXNIP in future. Given that it appears to not play a role in our system does makes us question what conditions are required for TXNIP/NLRP3/IRE1 interactions to occur and whether it is important under physiological conditions.

Chapter 4: Investigating the role of IRE1 in PDAC

Introduction and background

The emergence of effective treatments seen for many cancer types has not occurred for PDAC patients to the same extent[273]. Late diagnosis and the associated terminal metastasis, poor molecular understanding of the disease, and ineffective drugs all contribute to staggering mortality rates associated with pancreatic cancer. PDAC patient tumours also exhibit a stromal phenotype that presents a sort of "shield" or "shell" that surrounds and protects the tumour, furthering tumour development whilst simultaneously slowing effective treatments[274]. This stroma consists of multiple cell types such as fibroblast or fibroblast-like cells, an immune infiltrate and local endothelial cells. PDAC patients present a highly active fibroblast-like cell unique to the pancreas called a pancreatic stellate cell[275]. These stellate cells promote tumourigenesis via acting as a protective barrier to chemotherapy but also via the promotion of tumour growth using secreted factors like cytokines/chemokines[276]. In terms of immune infiltration, PDAC tumours are diverse as to whether they present a pro- or anti- tumour inflammatory response but it is largely considered to fall under a more anti-inflammatory environment in most cases[277]. The role of tumour associated macrophages, lymphocytes and NK cells ultimately depends on the tumour microenvironment and how immune infiltration plays a role in tumorigenesis is something that is becoming increasingly studied. The UPR, now increasingly associated with disease progression in multiple cancer types could represent a novel therapeutic target which remains largely unexplored in PDAC patients or cell lines[86, 194, 195]. The exocrine and secretory nature of the pancreas suggests a high-protein demand would necessitate a basally active UPR, something that would theoretically only become further exacerbated upon the development of a tumour.

Given the knowledge gained from my own work on IRE1-mediated cytokine signalling in inflammasome activation, in chapter 3 of this thesis, and the emerging literature connecting IRE1 to cytokine regulation in breast and prostate cancers, we sought to explore similar pathways in PDAC cells. Due to the importance of cytokine signalling to PDAC tumorigenesis and intra-tumoral cell signalling it seems likely there may be another pivotal role for IRE1 under this disease circumstance. Specifically, the

interactions between PDAC cells and their stromal neighbours is a key area of ongoing cytokine research in PDAC studies[240]. If there is a role for IRE1 in mediating these interactions it may present a potential therapy down the line. Importantly it will expand our knowledge of the role IRE1 plays in PDAC, the role IRE1 plays in cytokine regulation and how different cell types of the PDAC TME interact via signalling factors.

In this study, we identified IRE1 as an important regulator of cytokines, both positively and negatively, in PSC and PDAC cell lines. We found that IRE1 RNase impairment in PSC could reduce PDAC proliferation upon indirect co-culture with conditioned media, suggesting that IRE1 disrupted important signalling pathways between the two cell types. We also saw that the same IRE1-deficient PSC supernatant had an opposite, pro-proliferative effect on NK cells. This discovery coupled with the reduced proliferation and cell viability shown upon IRE1 RNase activity ablation highlights a potential dual-role for IRE1 inhibitors in PDAC.

Aims and objectives

In this chapter we will be analysing the role of IRE1 in pancreatic cancer. Our hypothesis is that pancreatic cancer cells will exhibit a basal UPR activation based on their secretory nature (owing to their origins in the pancreas) in combination with the added protein demands associated with cancer. We also speculate that IRE1 could potentially play an important role in cytokine regulation in pancreatic cancer, cytokines being important regulators of PDAC tumorigenesis. PDAC tumorigenesis is heavily mediated by paracrine interactions between pancreatic cancer cells and their associated stroma. Therefore, based on IRE1's established role in cytokine regulation (detailed previously) we suggest it may play important roles in PDAC cells but also in the inter-cellular interactions of PDAC cells. We will analyse basal UPR activity in a panel of PDAC cell lines alongside a transformed pancreatic stellate cell line. We will determine the effects of IRE1 and PERK inhibition on PDAC and stellate cell proliferation, viability and cytokine secretion. Using a large scale cytokine array, we will be able to identify potential secreted factors regulated by IRE1 in both pancreatic cancer cells and pancreatic stellate cells. Finally, using conditioned media generated from stellate cells which have been treated with an IRE1 RNase inhibitor, we will analyse the effects of this conditioned media on PDAC proliferation. It will also be interesting to expand this conditioned media experiment to NK cells, an immune cell type known to be dysregulated in pancreatic cancer. This analysis will be performed with western blot, PCR, qPCR, flow cytometry, cytokine array analysis and ELISA techniques. In summary:

- Do pancreatic cancer and pancreatic stellate cell lines exhibit basal UPR activity?
- What are the effects of IRE1 and PERK inhibition on PDAC/PSC cell numbers and viability?
- Does IRE1 regulate cytokine secretion in PDAC/PSC lines?
- Does IRE1 ablation in PSC effect the proliferation of PDAC and NK cells cultured indirectly with conditioned media?

4.1 PDAC and PSCs exhibit basal PERK and IRE1 activity

To determine whether key UPR sensors, PERK and IRE1, were basally active in a panel of PDAC cell lines and in a transformed, non-cancerous PSC cell line we analysed a panel of UPR markers. The third arm of the UPR, ATF6, was not focused on for this study because of a poor availability of effective tools for its study. The three PDAC cell lines, PANC1[278], BxPC3[279] and SW1990[280], were used in this study. PANC1 and BxPC3 representing primary tumours and SW1990 being isolated from a spleen metastasis. The PSC cells were immortalised by infection with human telomerase reverse transcriptase (hTERT) and simian vacuolating virus 40(SV40) retroviruses[240]. Immunoblotting analysis revealed enhanced GRP78 expression, similar to control levels across all cell lines, indicative but not proof of basal UPR. The levels of PERK activity across cell lines differed, with PANC1 and PSC cells displaying the highest levels of PERK phosphorylation (as indicated by an upshift in the molecular weight of total PERK) and levels of ATF4 expression. (Fig.4.1A) IRE1 protein expression was comparable across all cell lines but analysis of XBP1s mRNA by PCR identified higher levels of IRE1 RNase activity in PANC1 and PSC lines (Fig. 4.1B). PERK and IRE1 activation were present in all cell lines to varying degrees suggesting PDAC cell lines and their associated stellate cells exhibit basal activation of the UPR. It will be important in future to assess the levels of UPR activation in a non-cancerous cell line and compare it to our PDAC cell lines. This will tell us if there is a hyperactivation of UPR activity in cancerous pancreatic cells, as we theorized.

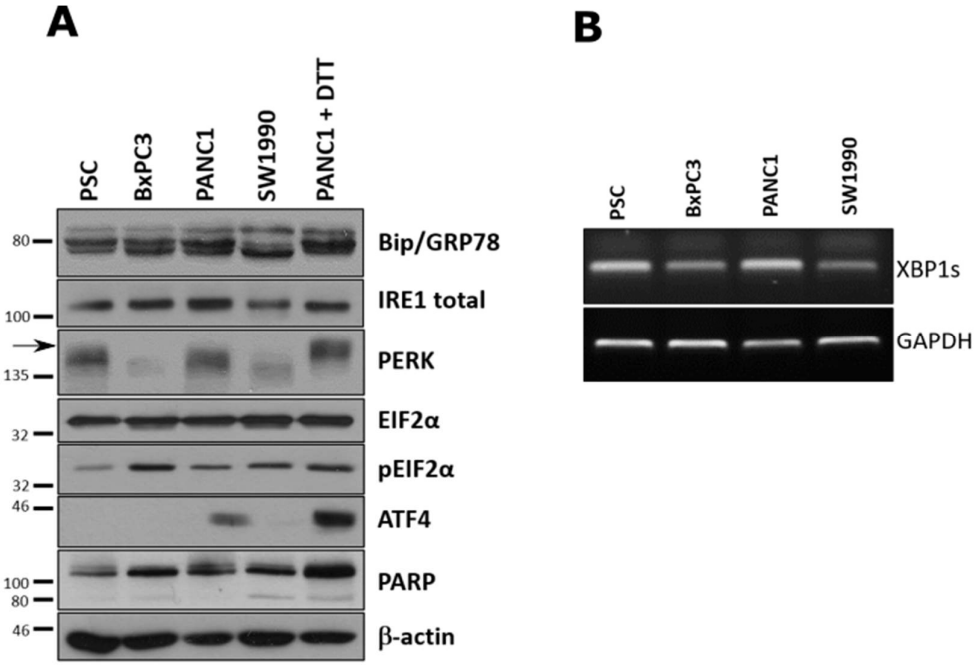

Figure 4.1. PDAC and PSCs exhibit basal PERK and IRE1 activity. **(A)** Immunoblot analysis of the basal expressions levels of UPR markers, GRP78, IRE1, PERK, total eIF2α, phospho-eIF2α, ATF4 and PARP in PSC, BxPC3, PANC1 and SW1990 cell lines in basal conditions. PANC1 cells treated with 1 mM DTT for 2 h served as a positive control for UPR activation. Actin was used as a loading control (n=3). **(B)** RT-PCR analysis of XBP1s levels in PSC, BxPC3, PANC1 and SW1990 cell lines under basal conditions. GAPDH was used as a loading control. Arrow indicates PERK phospho-upshift.

4.2 MKC8866 and Amgen 44 reduce XBP1s and PERK phosphorylation in PDAC

The IRE1 RNase inhibitor MKC8866 has been demonstrated to effectively reduce IRE1 RNase activity in multiple systems to date[86, 188, 253]. To test if MKC8866 could efficiently reduce XBP1s levels in our panel of PDAC cell lines we treated all cell lines with 20 µM MKC8866 for 48 h and analysed XBP1s protein by Immunoblotting (Fig. 4.2). Immunoblotting analysis of basal XBP1s levels of all PDAC cell lines revealed similar XBP1s levels as was observed in PCR analysis in Fig. 4.1b. The use of a PERK phosphorylation inhibitor, Amgen 44, was also used in our panel under same conditions as MKC8866 at a concentration of 2 µM and PERK levels were analysed by immunoblotting (Fig. 4.2). SW1990 and BxPC3 cell lines were shown to display low PERK pathway activity but PANC1 cells, previously identified as having the highest PERK phosphorylation, display a reduction in PERK phospho-upshift upon Amgen 44 treatment suggesting successful inhibition of the arm, albeit the total activity appears to be low. BxPC3 cells total PERK levels were too low to be displayed at a low exposure compared to other cell lines.

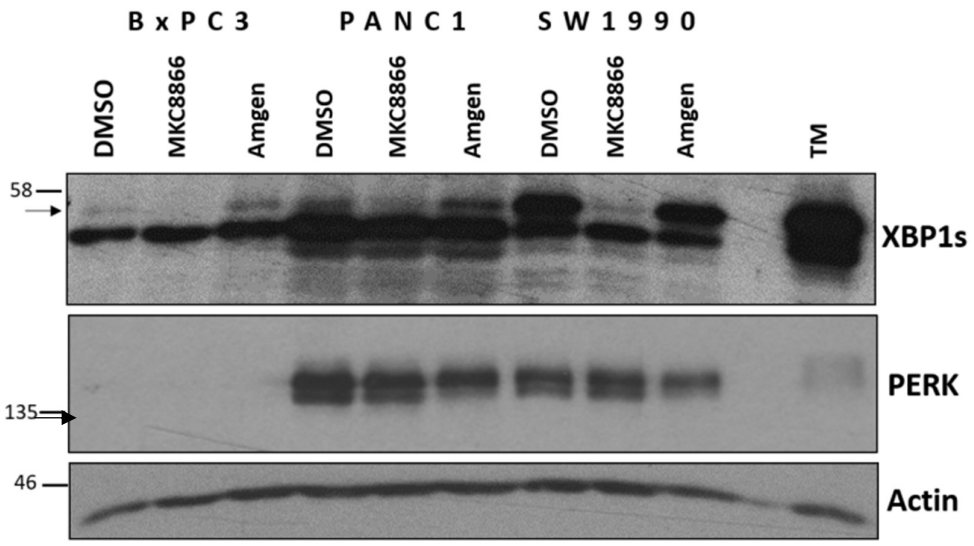

Figure 4.2. MKC8866 and Amgen 44 reduce XBP1s and PERK phosphorylation in PDAC, respectively. Immunoblotting analysis of XBP1s and PERK in BxPC3, PANC1 and SW1990 cell lines after 48 h treatment with 20 µM MKC8866 and 2 µM Amgen 44 (n=3). PANC1 cells treated with 0.5 µg/ml Tunicamycin ™ as positive control. Actin used as loading control. Arrows indicate XBP1s band and PERK phosphorylation upshift.

4.3 MKC8866 and Amgen 44 reduce XBP1s and PERK phosphorylation in PSCs

The PSC cell line analysed for this study displayed both basal PERK and IRE1 levels in our initial analysis and we wished to test both our UPR inhibitors on this cell line before continuing with the study. MKC8866 and Amgen 44 were used at concentrations of 20 μM and 2 μM individually for 48 hours and the IRE1 and PERK pathways were analysed by immunoblotting (Fig. 4.3A). Reductions in levels of PERK phosphorylation by Amgen 44 is stark and suggest it is capable of successfully inhibiting the PERK arm in PSC's. Both ATF4 and P-eIF2α are similarly reduced upon Amgen 44, suggesting successful inhibition of PERK's downstream pathway. In contrast, protein levels of XBP1s appeared to be low in this analysis but the reduction in XBP1s levels observed with MKC8866 is clear. To confirm this, we also analysed XBP1s at the mRNA level by classical PCR and confirmed its basal expression and effective inhibition using MKC8866 (Fig. 4.3B). It is perhaps of interest to a tumour to maintain relatively low/balanced levels of XBP1s as it is hypothesized that hyperactivation of IRE1 leads to a pro-death modality, although this is just speculation[59]. Additionally, the difficulties in obtaining clear signals with available XBP1s antibodies is perhaps underestimating total XBP1s levels here as it is readily observed by PCR methods. In future we hope to employ the multiplex array technology outlined in Fig. 3.13 for XBP1 analysis to avoid these issues.

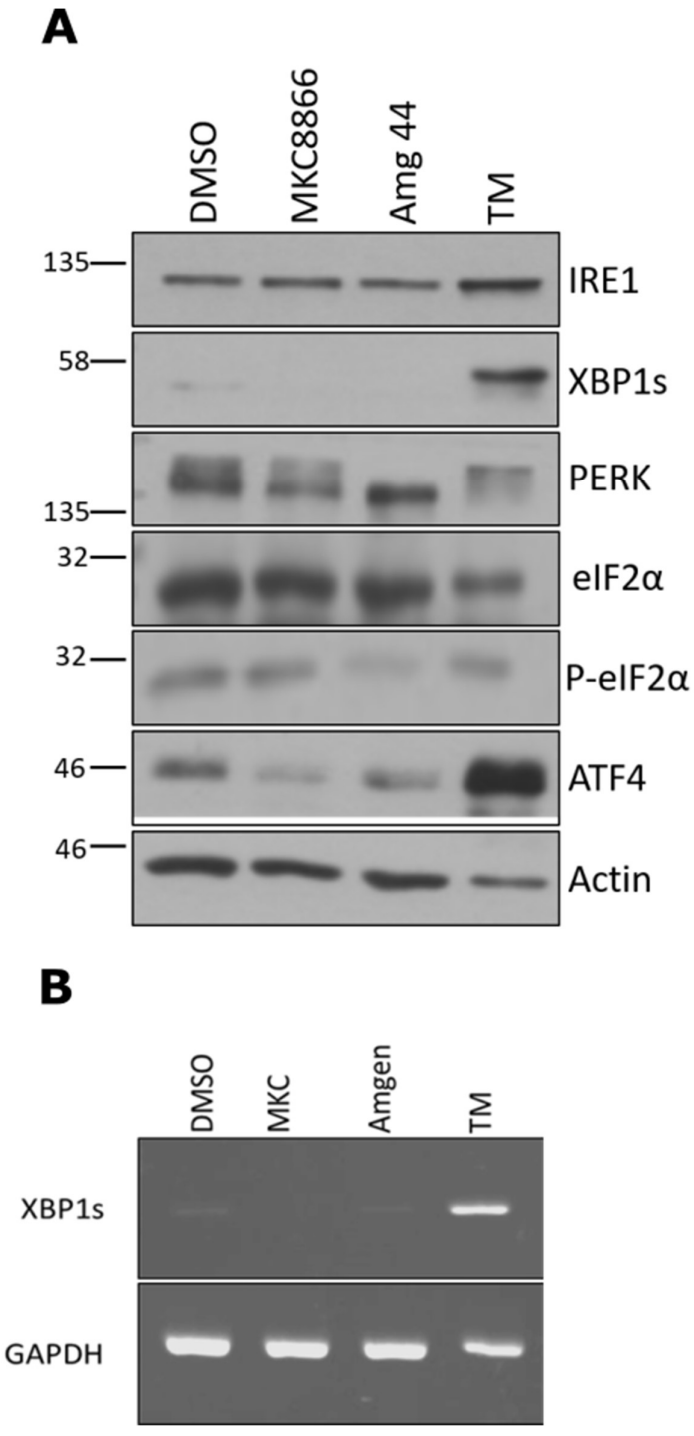

Figure 4.3. MKC8866 and Amgen 44 reduce XBP1s and PERK phosphorylation in PSCs, respectively. (A) Immunoblotting analysis of both IRE1 and PERK pathways in PSC after 48 h treatment with 20 µM MKC8866 or 2 µM Amgen 44 (n=3). **(B)** XBP1s levels analysed by PCR under same treatment conditions as (*a*). PSC treated with 0.5 µg/ml TM for 24 h as positive control. Actin used as loading control

4.4 MKC8866 and Amgen 44 treatment reduce total cell number of PDAC and PSCs lines

Having determined that PDAC and PSC cell lines exhibit basal PERK and IRE1 activity to varying extents, we sought to determine the effects of inhibiting these proteins on cell proliferation. Recent work by our group in breast cancer and work by others in prostate cancer has identified that IRE1 inhibition can hinder cell proliferation without inducing cell death and we wished to observe whether similar responses could occur in our PDAC and PSC models[86]. To do this we used the aforementioned IRE1 RNase domain inhibitor MKC8866 and the PERK phosphorylation inhibitor, Amgen 44. PSC, BxPC3, PANC1 and SW1990 cell lines were treated with 20μM MKC8866 and 2μM Amgen 44, 24 h after seeding. All cell lines exhibit reduced cell numbers after 6 days MKC8866 treatment and this is consistent with the expression of XBP1s levels observed in all cell lines. BxPC3 and SW1990 cells exhibited little or no reduction in cell counts upon Amgen 44 treatment, perhaps attributable to their low PERK phosphorylation (Fig. 4.4). In order to determine if the reduced cell numbers we observed in response to MKC8866 treatment were outcomes of reduced proliferation or increased cell death we decided to analyse cell viability by PI uptake.

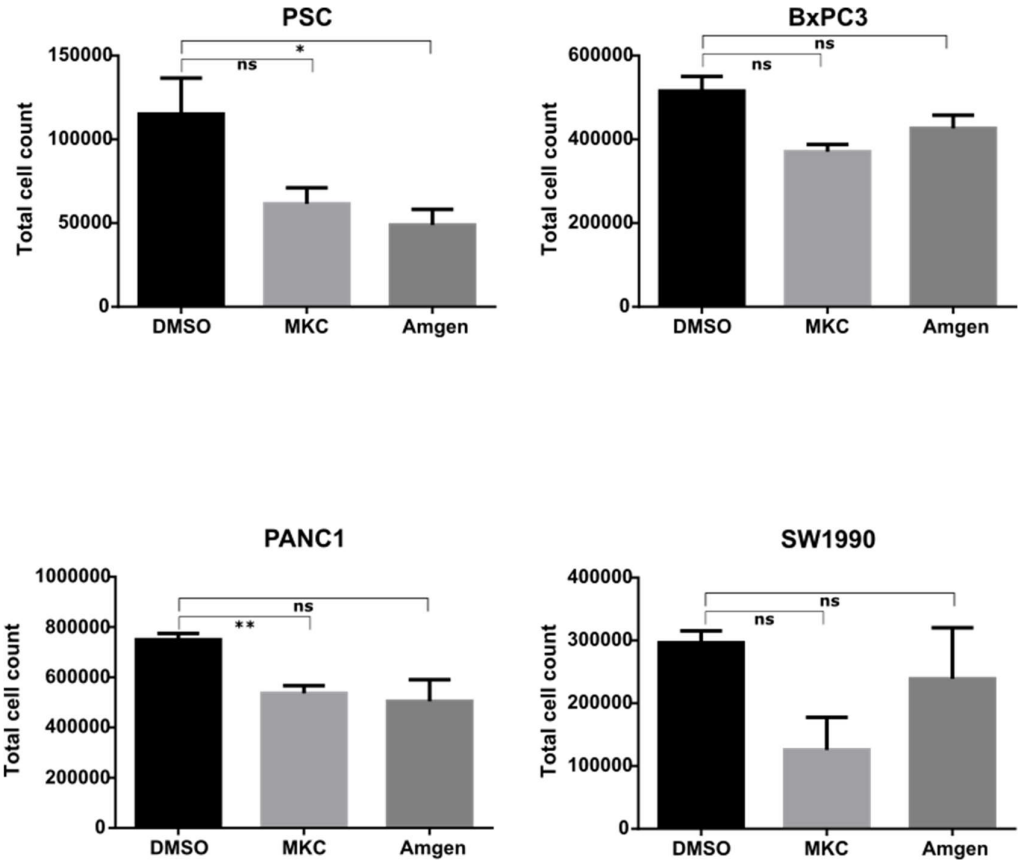

Figure 4.4. MKC8866 and Amgen 44 treatment reduce total cell number of PDAC and PSCs lines. PSC, BxPC3, PANC1 and SW1990 cells seeded in 6 well plates and treated with 20 µM and 2 µM Amgen 44 24 h post seeding. Cells were harvested and counted after 6 days treatment (n=3). *P < 0.05 and **P < 0.01 based on a Student's t test. Error bars represent SEM.

4.5 Addition of MKC8866 or Amgen 44 reduces the viability of some PDAC and PSC cell lines

Using propidium iodide (PI), we analysed PDAC and PSC cell viability following days 2, 4 and 6 post treatment with MKC8866 or Amgen 44. PSC cell viability was slightly reduced upon MKC8866 treatment in a time-dependent manner albeit not statistically significantly, whereas Amgen 44 did induce slight cell death, the effects did not significantly increase in a time-dependent manner (Fig 4.5). Similarly, to PSC, BxPC3 cells displayed enhanced cell death with MKC8866 treatments in a time-dependent manner and no response to Amgen 44, similar to the reduced proliferation seen in cell counting experiments (Fig 4.5). PANC1 cells displayed the inverse response to MKC8866 and Amgen 44 seen in previously mentioned cell lines, with Amgen 44 inducing significant cell death levels in a time-dependent manner while MKC8866 had no obvious effects on cell viability (Fig. 4.5). SW1990 cells presented little or no changes compared to control cells. While the results from PI analysis do not indicate a strong statistical significance, there seems to be a varied response between cell lines when treated with either inhibitor. The precise reason for the low significance and disparity in responses between cell lines will need to be further examined in future. Taking cell counts and PI-uptake into account, it is likely that there is a mix of both anti-proliferative and reduced viability effects occurring here. Importantly, there seems to be an important role for IRE1 and PERK in maintaining a healthy cell in PDAC and PSC lines. The diverse response to Amgen 44 is particularly interesting, for example, PANC1 and PSC cell lines displayed the highest levels of PERK activity but the effects of its inhibition on their viability was drastically different. It is well documented that PERK inhibitor toxicity exists in pancreatic cells[281]. We hypothesized that perhaps some effects of PERK inhibitor associated reduced viability could be a result of off-target effects rather than due to UPR deficiency in the cell. In the interest of narrowing the scope of this research and removing any potential doubts from our analysis for now, we chose to focus on IRE1 signalling from this point forward. Analysing the role of PERK in the future is still something of great interest to our research, however.

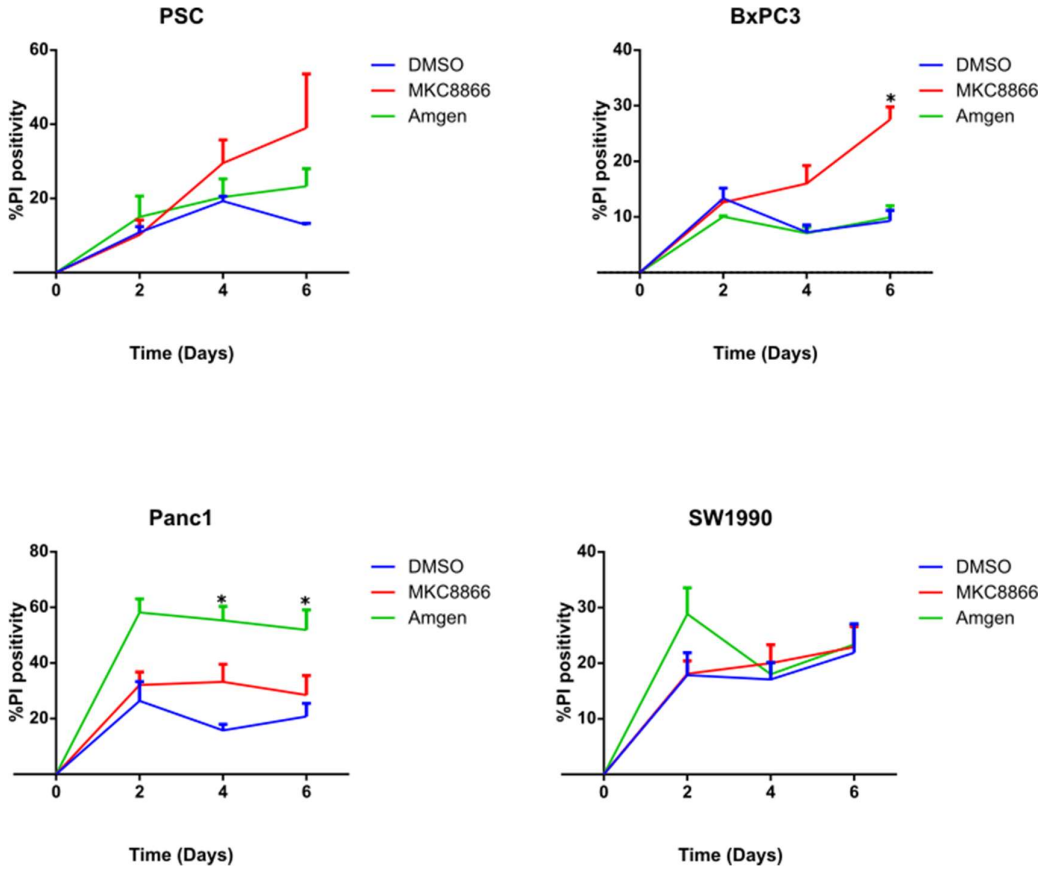

Figure 4.5.Addition of MKC8866 or Amgen 44 reduces the viability of some PDAC and PSC cell lines. Propidium iodide (PI) analysis of PDAC and PSC cell lines treated with 20 µM MKC8866 and 2 µM Amgen 44 inhibitors for up to 6 days, with analysis on days 2, 4 and 6. Cell viability was analysed by measuring PI uptakes by cells using flow cytometry (n=3). Statistical analysis performed on MKC8866/Amgen treated samples against DMSO controls on each day of analysis. Data not significant unless otherwise stated. *P < 0.05 based on a student's t test. Error bars represent SEM.

4.6 MKC8866 treatment does not alter α-SMA levels in PSC

Another key aspect to consider when analysing PSCs is their activation state. Under normal conditions PSCs exist in an inactive, quiescent state from which they transition to an activated state upon detection of certain stimuli[282]. Alpha smooth muscle actin (α-SMA) is a commonly used activation marker often used to identify the activity state of a PSC[283]. To determine the activation state of the PSC cell line and determine the outcome of MKC8866 addition we assessed α-SMA levels by immunoblotting. The addition of MKC8866 reduced XBP1s levels indicating IRE1 RNase was successfully inhibited and we saw no change in PERK levels or phosphorylation. α-SMA levels were unaffected by MKC8866 addition after 48 h which suggests that IRE1 RNase ablation does not affect PSC activation status (Fig. 4.6). It would be interesting in future to examine α-SMA levels after MKC8866 treatment over a time-course and longer treatment time.

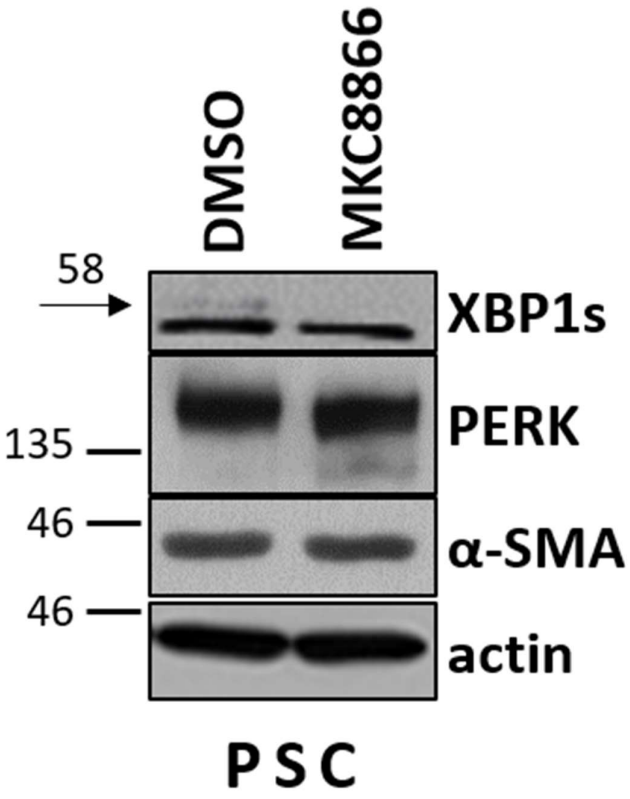

Figure 4.6 MKC8866 treatment does not alter α-SMA in PSCs. Immunoblotting analysis of XBP1s, PERK and α-SMA in PSC treated with 20 µM MKC8866 for 48 h (n=3). Actin used as a loading control. Arrow indicates XBP1s band.

4.7 MKC8866 reduces cytokine levels in PANC1 cells

As described in the introduction chapter, the relationship between PDAC and PSC relies heavily on secreted factors like cytokines and growth factors. These factors mediate communication between the two cell types to encourage a symbiotic relationship that induces the continued growth, proliferation and migration of the recipient cell type while also maintaining the donor cell in an endless activation state[284]. Whether you look at the effects of the PSC secretome on PDAC biology or *vice versa,* the influence of cytokines in this interaction are a hugely important target in current research surrounding PDAC tumorigenesis as a whole. Given the recent evidences in breast cancer highlighting IRE1's role in cytokine production[86] from our lab and my own studies into IRE1's ability to regulate cytokine production under inflammatory conditions, we decided it was relevant to the current PDAC study to also perform a similar analysis on cytokine levels after IRE1 RNase inhibition. Based on our initial study on basal UPR levels, PANC1 cells were chosen for the following study due to its high basal IRE1 levels and the low levels of cell death that was observed after MKC8866 addition. PANC1 cells were grown in 3% serum to reduce any potential background noise from FBS that could affect cytokines levels for 48 h in the presence or absence of MKC8866. Immunoblotting of the cell pellet obtained from same experiment as supernatant that was used in array revealed sufficient reduction in XBP1s levels confirming inhibition of the IRE1 RNase domain upon addition of MKC8866 (Fig. 4.7A). Conditioned supernatant was collected after 48 h and applied to XL cytokine array as described in materials and methods. Analysis of array data revealed a large cohort of cytokines reduced upon the addition of MKC8866 that have been previously associated with PDAC, some of which have been highlighted on the dot blot for illustration purposes and represent interesting targets (Fig 4.7B). Using pixel density cut-off values (to remove over and under exposed cytokine expression values) and fold-change cut-off values to define downregulation in our analysis we found 15 cytokines to be significantly downregulated with MKC8866 treatment in our model and represented it on a pie chart. Cytokines that fell below detectable levels highlighted as "low expression" on pie chart (Fig. 4.7C). Analysis of all cytokines with suitable expression levels (outlined in detail in Materials and methods chapter) by R-packages used to generate heat maps displaying the

average intensity and the log 2 fold change (FC) between DMSO/MKC8866(Fig. 4.7D-E). The addition of MKC8866 reduced the secretion of numerous cytokines associated with PDAC progression, prognosis and interactions with PSC's. These cytokines have the potential to act both through autocrine and paracrine avenues meaning they themselves could potentially be responsible for the reduced proliferative potential we see upon MKC8866 addition. Interestingly however, they are also known to regulate PSC functionality via paracrine signalling and this led us to hypothesise that IRE1 RNase inhibition could potentially not only interfere with PDAC and PSC proliferation and survival directly but also disrupt communication between the two cell types.

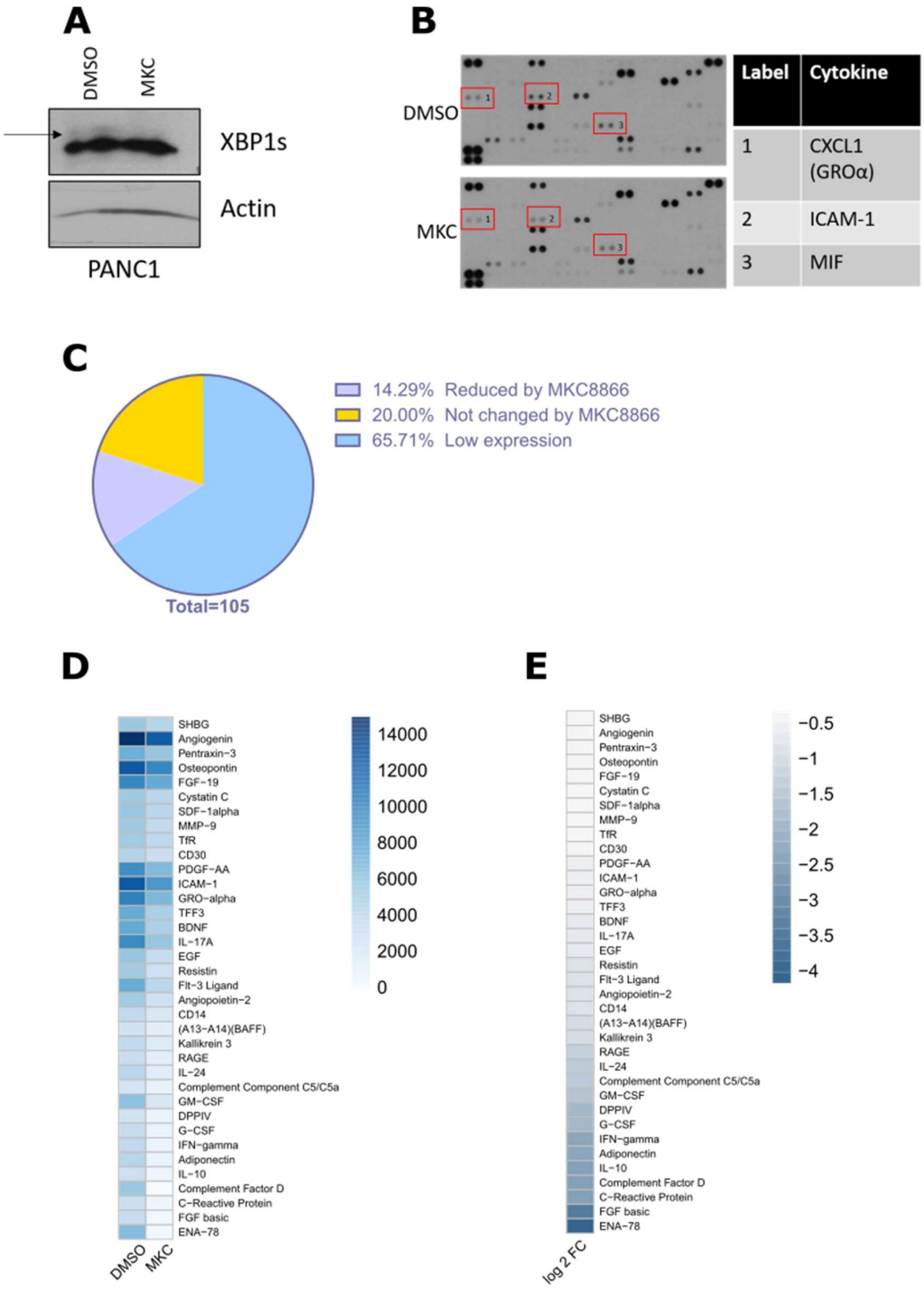

Figure 4.7. MKC8866 reduces cytokine levels in PANC1 cells. PANC1 cells treated with 20 µM MKC8866 or DMSO for 48 h and conditioned media was collected and filtered. XL cytokine array protocol followed as described in materials and methods. **(A)** Immunoblotting for XBP1s in PANC1 cells treated with or without 20 µM MKC8866 for 48 h to confirm drug efficiency. **(B)** Expression profile of cytokines in vehicle alone versus MKC8866-conditioned medium was determined by chemiluminescence. CXCL1, ICAM-1 and MIF levels highlighted on dot blot for representation. **(C)** All 105 cytokines on array analysed and anything that did not fit

within minimum densitometric values designated in materials and methods chapter are highlighted as low expression on this pie chart. Others classified based on fold change differences between DMSO and MKC8866 treated datasets. **(D-E)** Target cytokines regulated by MKC8866 (highlighted on pie chart) average pixel density (densitometry) and Log2 fold change (MKC/DMSO) calculated and represented as heat maps. Arrow indicates XBP1s band.

4.8 MKC8866 differentially regulates cytokine levels in PSCs

In addition to investigating PDAC cells we also analysed the impact of MKC8866 addition on cytokine and chemokine production in PSC cells. Similar to the PANC1 experiment, we cultured PSCs in 3% serum and confirmed there was no significant reduction in cell number after 48 h of treatment with MKC8866 that could exacerbate any cytokine changes we observe in the array. Immunoblotting analysis of the PSC pellet obtained from experiment reveals sufficient reduction in XBP1s levels to indicate MKC8866 inhibited IRE1 RNase functionality (Fig. 4.8A). A similar analysis of densitometric data obtained from array to remove outliers was performed as in Fig. 4.7 (Fig. 4.8B-D). In contrast to the array data obtained from PANC1 cells, cytokine levels in PSCs were both upregulated and downregulated upon MKC8866 treatment (Fig. 4.8B) and the fold change was calculated in a similar manner to before (Fig. 4.8D). This divergent regulation of cytokines in response to MKC8866 addition is a very interesting prospect as it suggests that, at least in PSC, IRE1 regulates cytokines in both a positive and negative manner. The functions or roles of cytokines will determine as to whether the use of MKC8866 will give rise to beneficial changes in the PSC secretome. Both cytokine cohorts, upregulated or downregulated in response to MKC8866, will be examined in more detail in the coming pages.

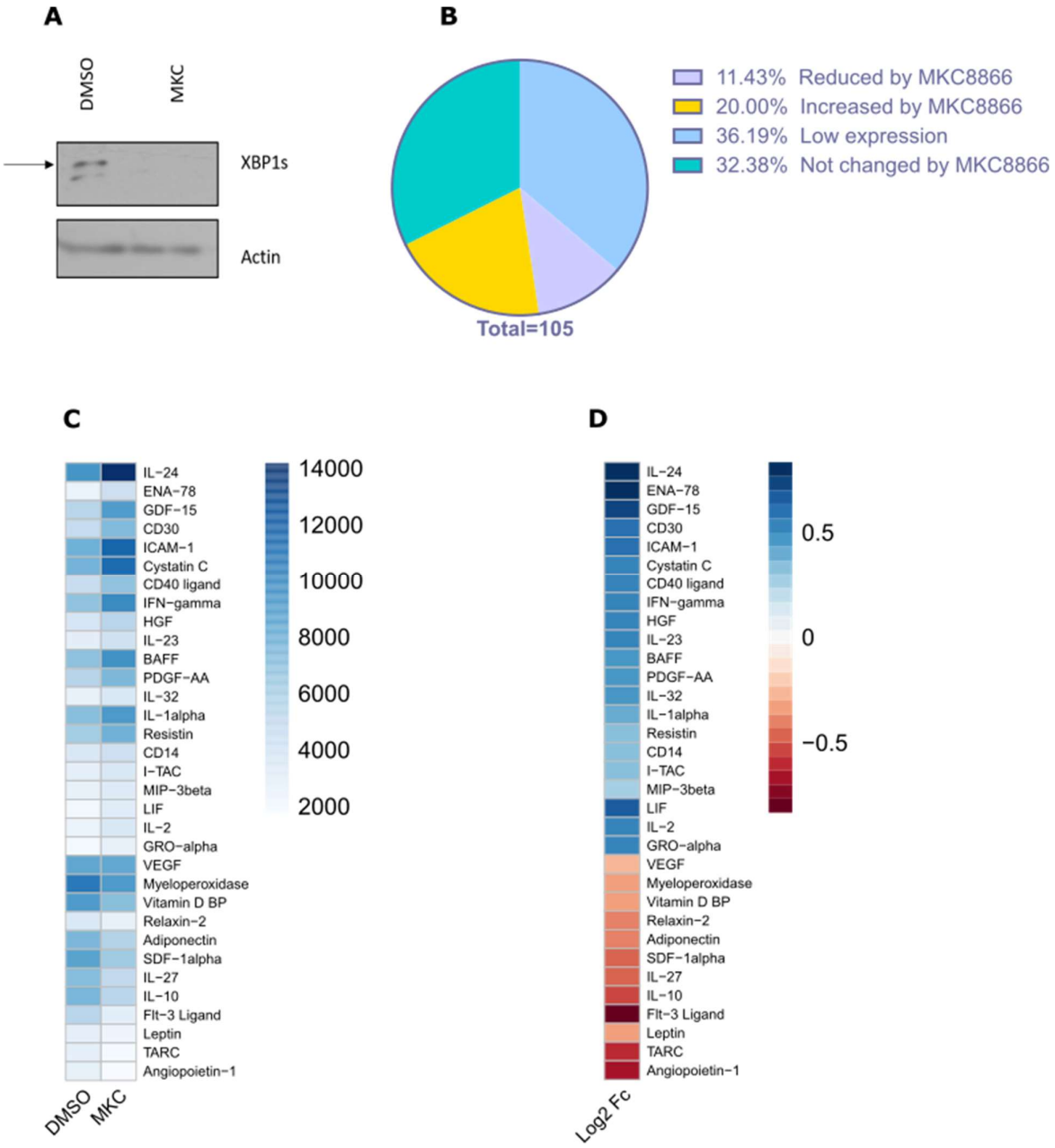

Figure 4.8. MKC8866 differentially regulates cytokine levels in PSCs. PSC cells treated with 20 µM MKC8866 or DMSO for 48 h and conditioned media was collected and filtered. XL cytokine array protocol followed as described in materials and methods. **(A)** Immunoblotting for XBP1s in PANC1 cells treated with or without 20 µM MKC8866 for 48 h. **(B)** All 105 cytokines on array analysed and anything that did not fit within minimum densitometric values designated in materials and methods chapter are highlighted as low expression on this pie chart. Others classified based on fold change differences between DMSO and MKC8866 treated datasets. **(C)** Densitometry data for individual cytokines that were either increased or decreased in response to MKC8866 represented above. **(D)** Cytokines outlined in *(C)* Log2 fold change (MKC/DMSO) calculated and represented as heat map. All analysis performed using R program. Red colour indicates reduction in fold change and blue indicates an increase in part (D). Arrow indicates XBP1s band.

4.9 MKC8866 reduces levels of select cytokines in PSC that are associated with PDAC tumorigenesis

When we examined the list of downregulated cytokines after MKC8866 addition we found that in general, we see a reduction in important cytokines that have been associated with the promotion of PDAC tumorigenesis. Once again, analysis of the dot blot from the XL cytokine array itself reveals there is a reduction in the levels of key cytokines that are associated with PSC activity and with signalling networks connected to PDAC cells (Fig 4.9A-B). IL-17A, a pro-inflammatory cytokine that is known to enhance tumorigenesis in tumours via upregulation of other cytokines such as IL-6 and via NF-κB pathway activation[285, 286]. It has also recently been linked to PDAC development by enhancing stemness in pancreatic interepithelial neoplasia (PaNIN)[287]. SDF-1α is a chemokine that is heavily linked to PSC-mediated enhancement of PDAC proliferation, migration, EMT and invasion through its CXCR4 receptor[288]. Targeting SDF-1α levels in the tumour microenvironment is a very popular theme in the current PDAC therapy literature (Detailed later in discussion). Finally ,VEGF, a pro-angiogenic factor, has been heavily associate with poor disease prognosis in PDAC and its inhibition has been shown to reduce tumour growth and reduce metastasis[289, 290]. Similar to PDAC, MKC8866 treatment reduces the levels of certain cytokines that could prove beneficial to PDAC patients.

A

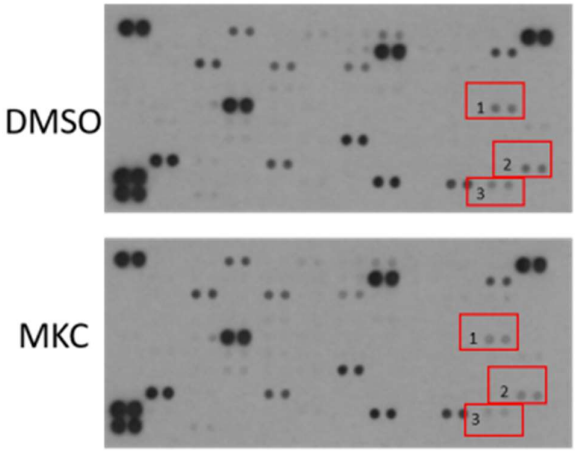

Label	Cytokine
1	IL-17A
2	SDF-1α
3	VEGF

B

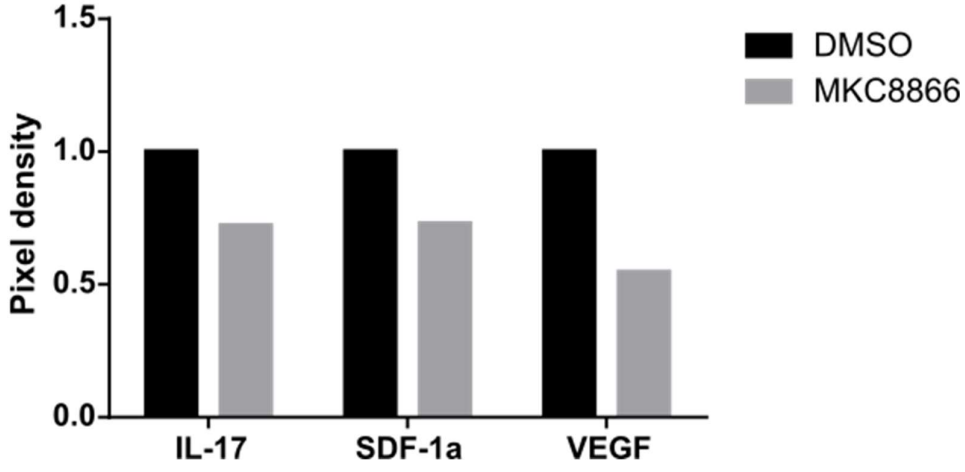

Figure 4.9 MKC8866 reduces levels of select cytokines in PSC that are associated with PDAC tumorigenesis. (A) Expression profile of cytokines that showed a reduction in MKC8866-conditioned medium was determined by chemiluminescence. IL-17A, SDF-1α and VEGF levels highlighted on dot blot. **(B)** IL-17A, SDF-1α and VEGF levels represented as graphs showing average pixel density determined by densitometry analysis.

4.10 Key cytokines regulated by IRE1 confirmed via ELISA technique in PSC

Focusing on PSC cytokine regulation by IRE1, we chose to analyse extra cytokine targets from the literature and to validate some identified by our array analysis. We treated PSC with 20 μM MKC8866 for 48 h and collected the supernatant and pellet afterwards. PCR analysis of XBP1s in the cell pellet confirmed that MKC8866 successfully reduced XBP1s in our experiment (Fig 4.10F). We then analysed cytokine levels of IL-6, SDF-1α, IL-8, TGF-β1 and CXCL1 in the conditioned media obtained by ELISA technique (Fig 4.10A-E). IL-6 was present on our array data but did not show a significant reduction due to variation between different exposure times. However, it was decided to be further analysed based on its importance to PDAC signalling[291] and the fact it has previously been found to be IRE1-regulated under different contexts[86, 245]. Here, we see a significant reduction in IL-6 levels suggesting another role for IRE1 in IL-6 regulation. TGF-β1 was not present on the array and due to its known association with PDAC-PSC interactions[292, 293] it was also examined and found to be significantly reduced upon MKC8866 treatment. IL-8 levels were far too high to be analysed on the cytokine array as they fell outside of the signal parameters we set. Upon analysis of the effects of MKC8866 on IL-8 levels in PSC, we see a significant reduction also. CXCL1 levels were shown to be very slightly upregulated in our array upon IRE1 RNase domain inhibition but also fell below acceptable fold change levels to be evaluated further by array. ELISA analysis revealed that CXCL1 levels were not significantly up or down regulated under MKC8866 treated conditions suggesting they do not play a role here, which contrasts what we see in PANC1 array. SDF-1α was also further examined due to its importance to the literature surrounding PDAC and PSC interactions. We also saw a significant reduction in SDF-1α levels by ELISA similar to what was observed by array analysis. SDF-1α and its roles in PDAC will be discussed in great detail later.

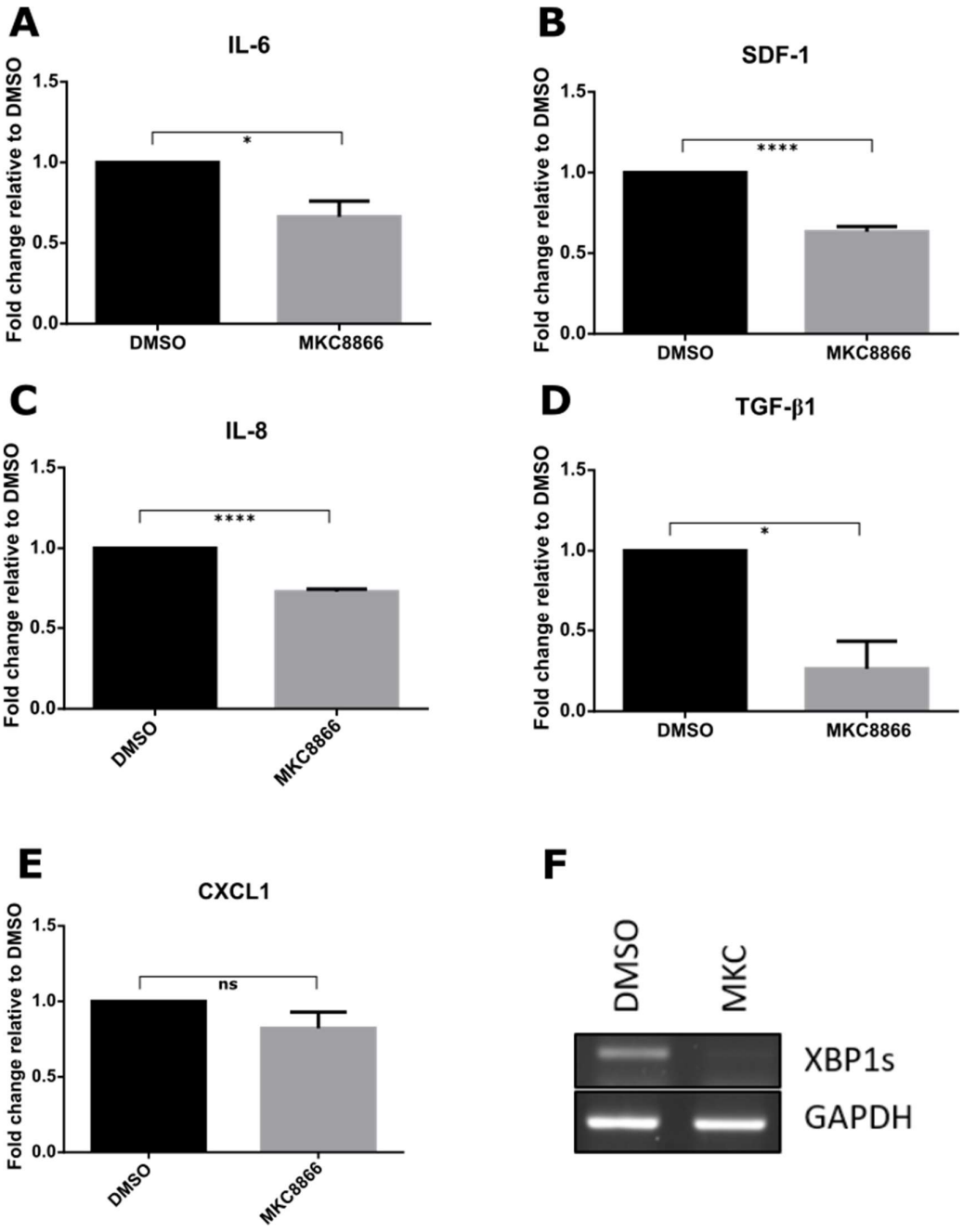

Figure 4.10. Confirmation of MKC8866 regulated cytokine targets identified in large scale array analysis plus additional targets not found on array(A-E) Levels of IL-6, SDF-1, IL-8, TGF-β1 and CXCL1 analysed by ELISA in supernatant of PSC cells treated with 20 µM MKC8866 for 48 h. (n=3) **(F)** Levels of XBP1s analysed in pellets from PSC treated with 20 µM MKC8866 for 48 h to confirm inhibition of IRE1 RNase. *P < 0.05 and ****P < 0.0001 based on a Student's t test. Error bars represent SEM.

4.11 IRE1 and XBP1 knockdown reduces total cell number and cytokine levels in PSC

To further validate the link between IRE1 and 1) PSC proliferation and 2) cytokine regulation we sought to analyse the effects of IRE1 and XBP1 knockdown on both. This would both allow us to rule out off target effects induced by MKC8866 but also would help identify as to whether IRE1 exerts its function via its XBP1s or RIDD pathways. If a target was RIDD regulated, one would expect that upon siIRE1 treatment you would see an increase in total protein levels. In contrast to this, siXBP1 should theoretically have no effect on target cytokine levels if it is RIDD regulated or potentially we would see a further decrease in levels as it is hypothesized by some that reducing XBP1s leads to a knock-on increase in RIDD signalling. PSC cells were transfected with siIRE1 or siXBP1 in the presence or absence of MKC8866 for 72h before cell pellet was collected, a proportion of cells were kept for cell counts and the supernatant stored for ELISA analysis. Immunoblotting for IRE1 and XBP1s revealed successful knockdown of IRE1 and XBP1 were achieved in the 72 h timepoint (Fig. 4.11A). Cell counts of cells after their 72 h siRNA transfection revealed that siIRE1 significantly reduced cell number in both the presence and absence of MKC8866 (Fig. 4.11B). A treatment with siXBP1 alone reduced proliferation, albeit not significantly . The effect of siXBP1 on PSC proliferation was enhanced by the addition of MKC8866 suggesting either an incomplete knockdown or that IRE1's regulation of proliferation is not entirely via XBP1s, if at all (Fig. 4.11B). We also analysed the levels of three cytokines, IL-6, CXCL1 and SDF-1α, under siIRE1 and siXBP1 conditions and found that there were reductions in all three under IRE1/XBP1 knockdown conditions (Fig. 4.11C-e). Interestingly, we see a significant reduction in CXCL1 levels under siRNA conditions in contrast to that seen with MKC8866 treatment. This could potentially be explained by the fact that under siRNA treated conditions we see a 3 to 4-fold increase in total CXCL1 levels, perhaps due to the known immunostimulatory effects associated with siRNA transfections[294]. If CXCL1 production is severely enhanced, perhaps the effects of disrupting IRE1 activity could be similarly enhanced and give rise to a noticeable drop in CXCL1 levels detected.

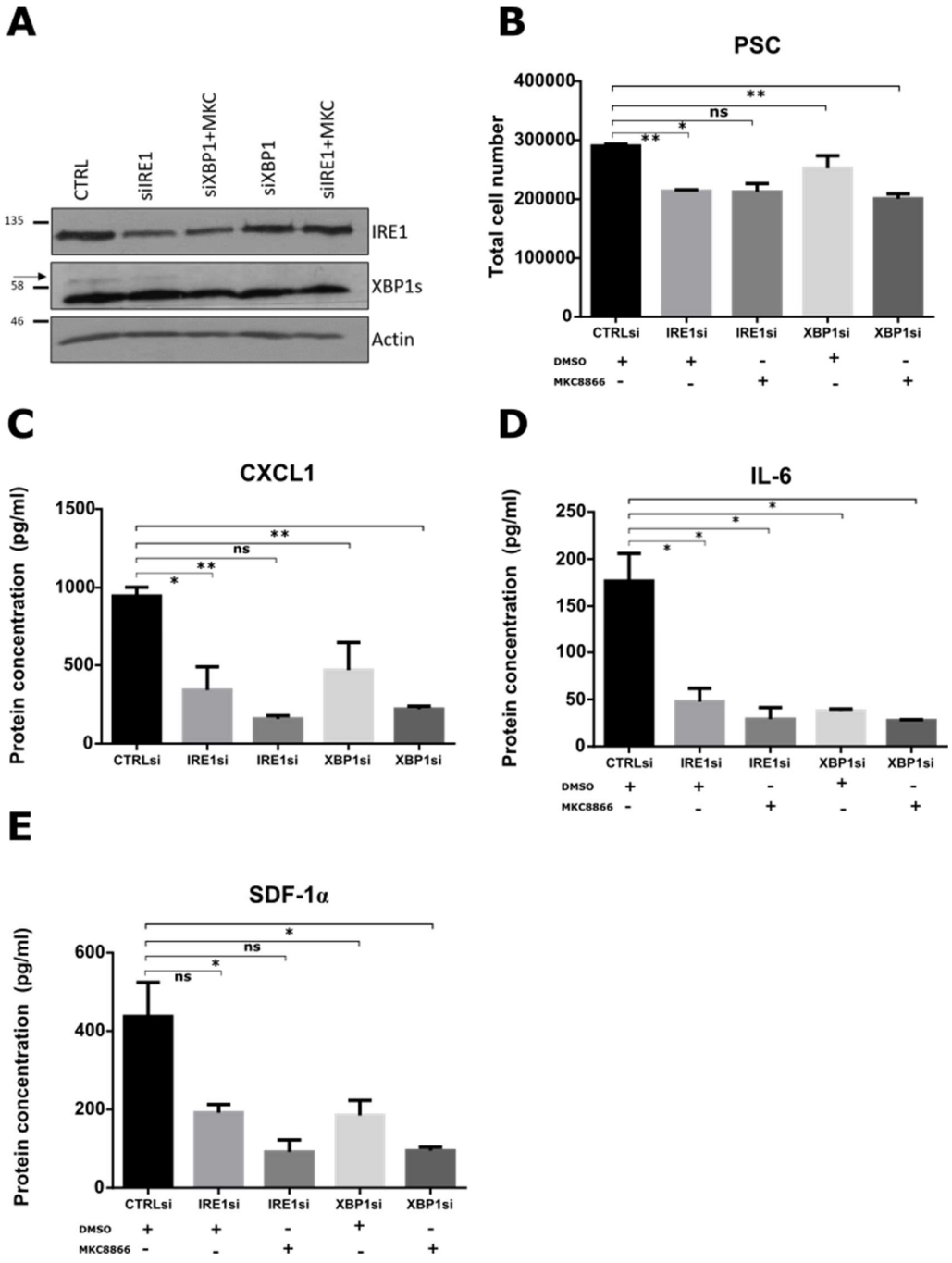

Figure 4.11. IRE1 and XBP1 knockdown reduces proliferation and cytokine levels in PSC. (A) PSCs transfected with siRNA targeting IRE1 or XBP1 in the presence or absence of 20 µM MKC8866 for 72 h following which XBP1 and IRE1 levels were analysed by immunoblotting. **(B)** PSC cell number counted using haemocytometer after 72 h transfection with siIRE1 and siXBP1 in the presence or absence of MKC (n=3). **(C-E)** CXCL1, IL-6 and SDF-1α levels analysed by ELISA technique in the supernatant of transfected PSC after 72 h (n=3). *P < 0.05 and **P < 0.01 based on a Student's t test. Error bars represent SEM.

4.12 MKC8866 reduces transcript levels of *SDF1* in PSCs

We wished to identify if the reduction in the levels of our target cytokines upon MKC8866 treatment was due to reduced cytokine production (likely via XBP1s mediated transcriptional regulation) or through a reduction in the actual secretion of the cytokine. To do this we treated PSC with MKC8866 for 48 h and analysed XBP1s levels by PCR to confirm MKC8866 efficiency (Fig. 4.12a). The remaining cDNA was used to analyse *CXCL1*, *IL6* and *SDF1* transcript levels under conditions in which IRE1 RNase activity was impaired. We observed that levels of *CXCL1* were largely unchanged after the addition of MKC8866, similar to array and ELISA data (Fig. 4.12b). *IL6* transcript levels were not altered under MKC8866 treated conditions, similar to what we observe under array conditions and contrasting the ELISA data (Fig. 4.12c). In contrast to the first two targets analysed, *SDF1* transcript levels were significantly reduced upon the addition of MKC8866 (Fig. 4.12d). Having shown SDF-1α can be regulated by IRE1 RNase at both protein and transcript level we speculated it may be under transcriptional control by XBP1. In order to investigate this, we analysed the *SDF1* promotor sequence for potential binding sites for XBP1s transcription factor. This analysis revealed that there were in fact two potential binding sites for XBP1 (Fig. 4.12e). This analysis also revealed that *SDF1* could potentially be regulated by other transcription factors that have been previously associated with IRE1 or UPR activity in the literature, including *p53*, *NRF2* and *NMYC[192, 295, 296]*. In conclusion, based on our data to this point, while multiple cytokines appear to be IRE1 RNase regulated in PSC, it seems that the most promising target to potentially pursue in the future would be SDF-1α.

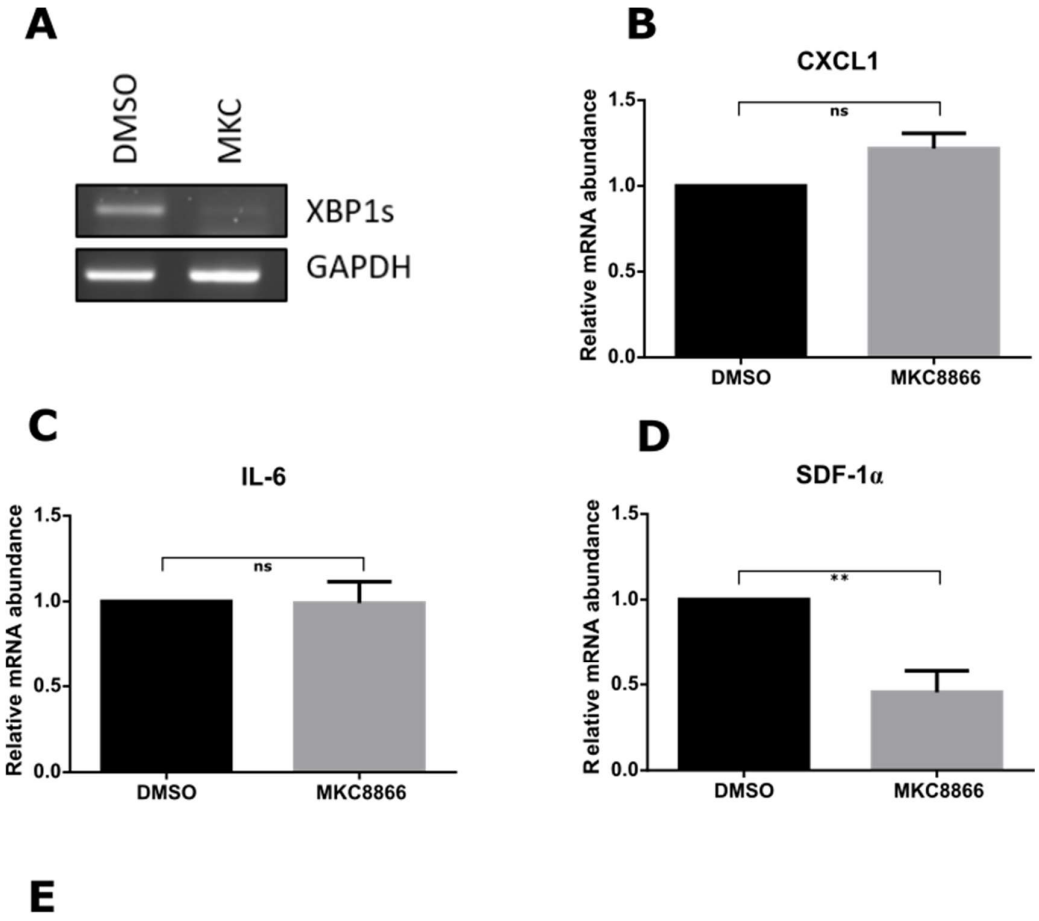

E

Predicted binding partners to SDF-1α promotor	No. of predicted binding sites
XBP1	2
NRF2	9
NMYC	17
P53	19

Figure 4.12. MKC8866 reduces transcript levels of *SDF1* in PSCs. (A) RT-PCR analysis of XBP1s levels to confirm efficiency of MKC8866 treatment in samples. **(B-D)** Transcript levels of *CXCL1*, *IL6* and *SDF1* analysed after MKC8866 treatment for 48 h in PSC cells by qPCR. GAPDH was used as the endogenous control gene (n=3). **(E)** *SDF1* promotor sequence analysed for potential transcription factor binding sites. **P < 0.01 based on a Student's t test. Error bars represent SEM.

4.13 The effect of MKC8866 treated PSCs on PDAC cell lines

It has been shown that conditioned medium generated from cultured PSC can strongly influence the growth, proliferation, migration and invasion of PDAC cells via secreted factors including cytokines and growth factors[226, 297]. Given that we have generated data indicating that IRE1 is capable of regulating several of these factors we next sought to identify if IRE1 RNase inhibition was capable of affecting PDAC proliferation via PSC-conditioned media. In order to observe the effects of IRE1 on this interaction we treated PSC with or without MKC8866 for 72 h and collected the conditioned media. This media was then filtered and concentrated using centrifugal columns after which it was placed on BxPC3, PANC1 and SW1990 cell lines. PDAC cell proliferation was measured using cell counts after 5 days of co-culture with conditioned PSC media (Fig 4.13a). Conditioned media generated from MKC8866 treated cells significantly reduced PDAC cell proliferation across all three cell lines analysed suggesting that IRE1 played an important role in regulating PSC-mediated PDAC proliferation (Fig. 4.13b-d). Additionally, the PDAC cell pellets were harvested at the end of the 5-day growth period to be analysed by PCR for XBP1s (Fig 4.13e). Interestingly, the levels of XBP1s seemed to be lower in the MKC8866 treated samples compared to controls which made us question as to whether residual MKC8866 was affecting PDAC proliferation. The cut-off point for filters used to generate conditioned medium was 5 KDa, meaning MKC8866 (300 DA) should have been washed out during concentration progress. Whether this effect is in fact residual MKC8866 that is somehow escaping the filter process remains unclear. What is interesting is that comparison between the control cells (DMEM cultured) and PSC-DMSO revealed that in SW1990 and PANC1 cells there was a trend indicating that PSC-DMSO cells exhibited higher XBP1s levels (Data not significant) (Fig. 4.13f-h). This could possibly be suggesting that there is some transmissible ER stress occurring under these conditions, a phenomenon in which cells grown in direct or indirect co-culture are capable of transmitting signals that regulate the UPR activation of the recipient cell[182].

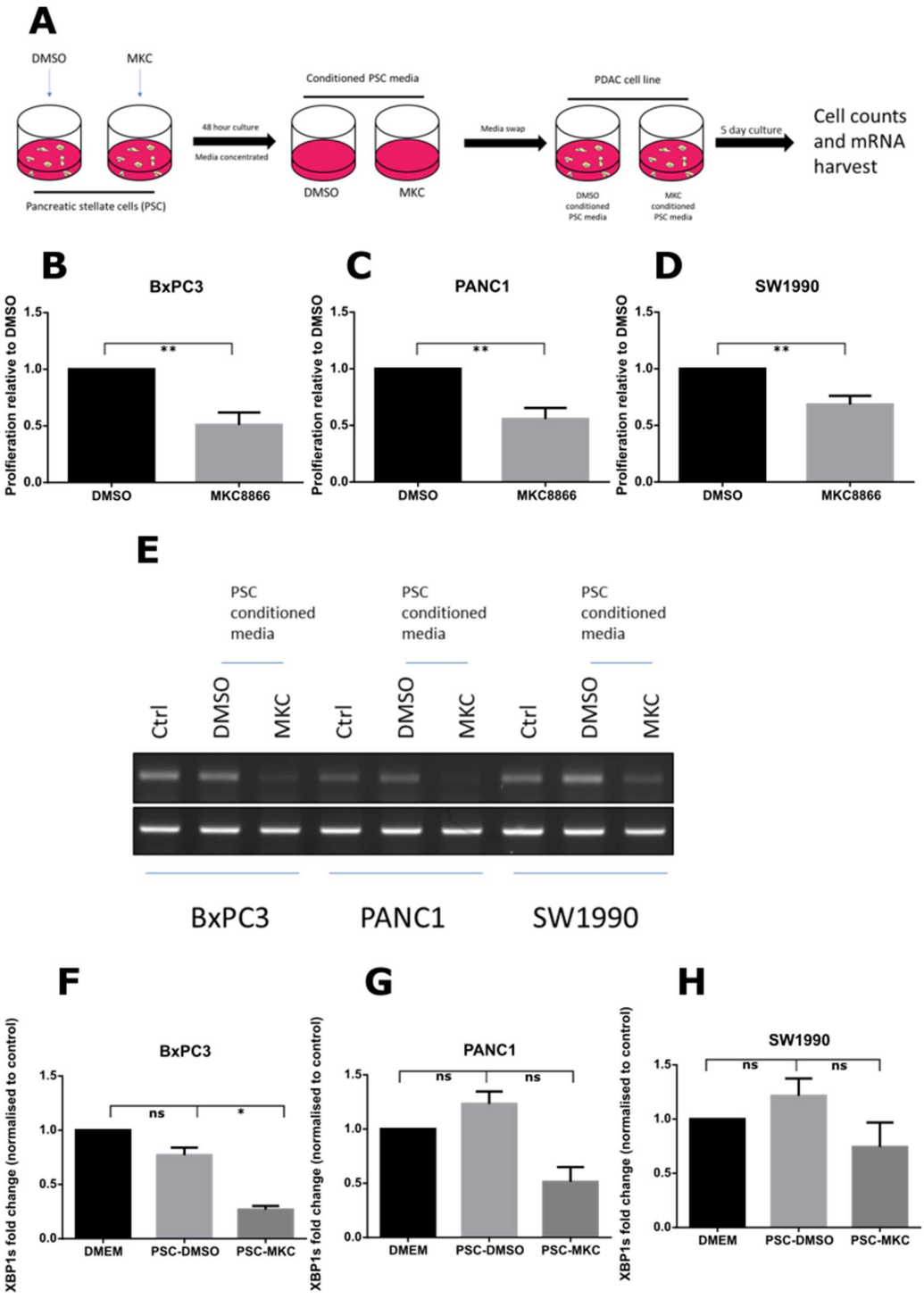

Figure 4.13. The effect of MKC8866 treated PSCs on PDAC cell lines. (A) PSC cells seeded to 80% confluency over 48 h in presence or absence of 20 µM MKC8866. Conditioned media collected, filtered to remove cell debris and added to PDAC cell lines to be further cultured for 5 days. **(B-D)** PDAC cells counted after 5 days of indirect co-culture with PSC (n=3) and **(E)** cell pellets harvested and analysed for XBP1s levels by classical PCR. **(F-H)** Levels of XBP1s transcript quantified by

densitometry in BxPC3, PANC1 and SW1990 cell lines (n=3). **P < 0.01 based on a student's t test. Error bars represent SEM.

4.14 MKC8866 increases levels of NK-associated cytokines in PSC

When we examined the list of upregulated cytokines that emerged from the array, we also found that there was a particular trend of immune-regulating cytokines that appeared to be enhanced by the addition of MKC8866. Upon a closer look at the function of said factors, we found that there were many cytokines associated with the activation and/or proliferation of natural killer cells (NK). Factors like IL-15[298], IL-2[299] and IFN-γ[300] have all been shown to regulate NK cell expansion and cytolytic functions and looking at the dot blot, it is apparent that some of these cytokines exhibit an upregulation upon treatment with MKC8866 (Fig.4.14A-B). The presence of NK cells in PDAC is well studied and it is generally considered that NK cells are present in low numbers in PDAC tumour sites[236], exist in an exhausted state and contribute to the immune-suppressive phenotype associated with PDAC tumour microenvironments[237]. The increase in the levels of these factors under IRE1 RNase deficient conditions, in combination with a reduction in the levels of factors associated with enhanced tumorigenesis in PDAC, no doubt represents a very interesting result.

A

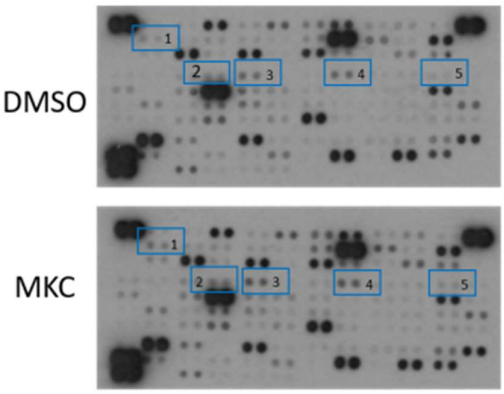

Label	Cytokine
1	CD40
2	ICAM-1
3	IFN-γ
4	IL-2
5	IL-15

B

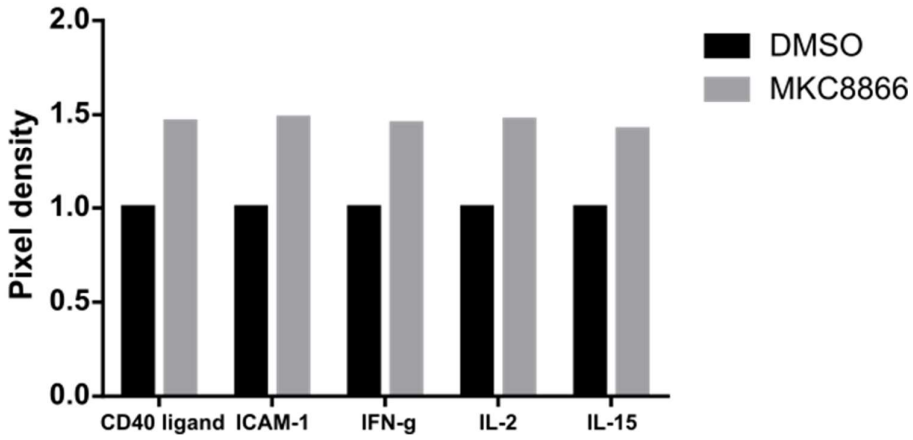

Figure 4.14. MKC8866 increases levels of certain cytokines in PSC (A) Expression profile of cytokines that showed an increase in MKC8866-conditioned medium was determined by chemiluminescence. CD40 ligand, ICAM-1, IFN-γ, IL-2 and IL-15 levels highlighted on dot blot. **(B)** CD40 ligand, ICAM-1, IFN-γ, IL-2 and IL-15 levels represented as graphs showing average pixel density determined by densitometry analysis.

4.15 The effect of conditioned medium from MKC8866-treated PSCs on KHYG1 cells proliferation

We next wished to explore the second highlighted cohort of IRE1 regulated factors identified from our array, those that were upregulated upon MKC8866 treatment and associated with NK cell activity. NK cells are an innate immune cell line that engage in early response to pathogens and are known to be dysregulated in PDAC tumours. Using the commonly used cell line, KHYG1[301], for our analysis we performed a similar experiment to analysed PSC-conditioned media on NK proliferation as was done in Fig.4.13B-D. Initially, we decided to observe the effects of MKC8866 alone on KHYG1 proliferation. We treated KHYG1 cells with 20 µM MKC8866 for only 24 h and performed cell counts. We observed a significant reduction in KHYG1 cell number after this short timepoint, something not observed in other cell lines until later timepoints (Fig. 4.15A). Cell pellets from KHYG1 cells treated with MKC8866 for 24 h alone were analysed by PCR for XBP1s (Fig. 4.15B). We then generated MKC8866-conditioned PSC media by treating PSC cells for 48 h followed by filtering and concentrating via centrifugal columns. We then cultured KHYG1 cells in PSC-conditioned media and very interestingly noticed an increase in KHYG1 proliferation in the presence of MKC8866-conditioned media compared to DMSO control (Fig. 4.15C). Similar to before, we analysed XBP1s levels by classical PCR in KHYG1 cells after 24 hour co-culture period and observed similar reductions in XBP1s under MKC8866-conditioned PSC media conditions (Fig. 4.15D). The reduction in XBP1s levels once again suggests that MKC8866 is somehow escaping the filtering process and remaining in the conditioned media. Overall, what we observed was that MKC8866 alone reduces KHYG1 cell proliferation while MKC8866-conditioned media from PSC, increases it. This stark difference is incredibly interesting even if somewhat hindered by the puzzling MKC8866 issues. Regardless, even if MKC8866 is somehow retained in the media despite the size exclusion, it is likely that other factors in the conditioned media are strong enough to mask the anti-proliferative effects of MKC8866 alone. The use of siIRE1 to analyse the effects of conditioned media on KHYG1 cells and on the PDAC panel could prove to resolve this issue in the future.

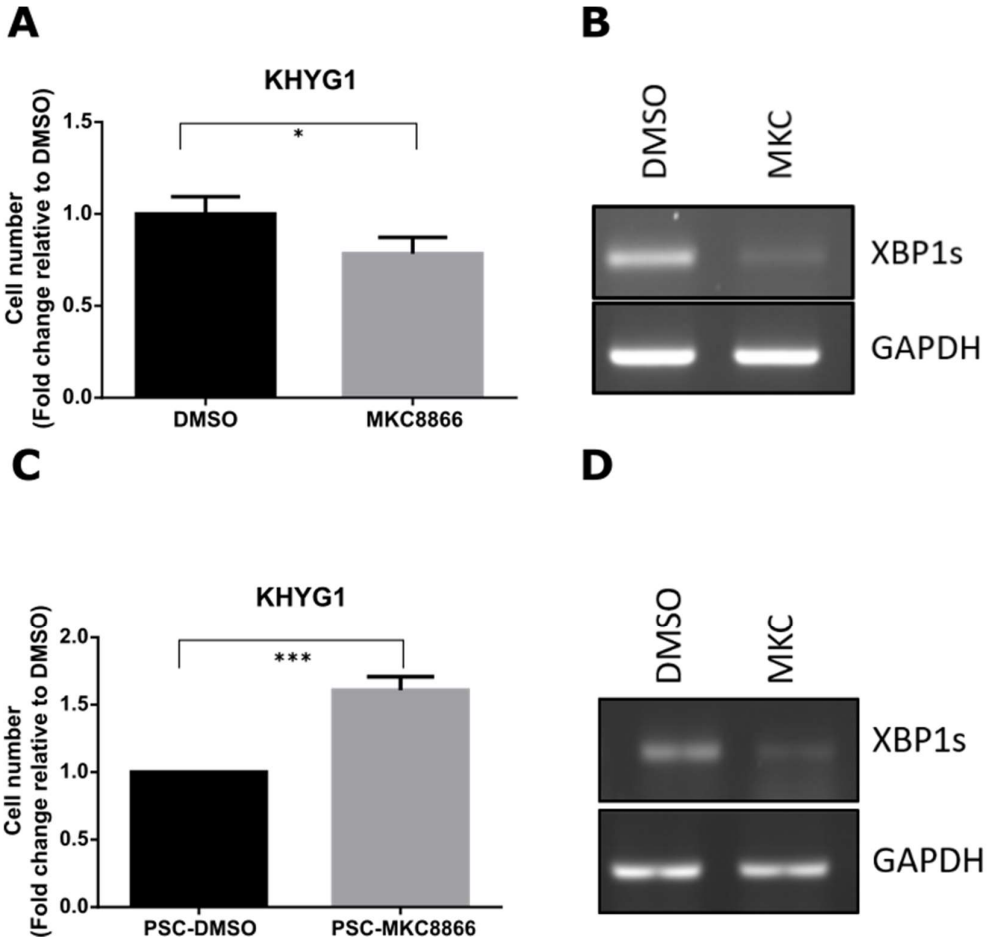

Figure 4.15. The effect of conditioned medium from MKC8866-treated PSCs on KHYG1 cells proliferation. KHYG1 cell were treated with 20 µM MKC8866 for 24 h, after which cells were harvested and **(A)** counted to determine cell numbers, or **(B)** were subjected to RT-PCR analysed to determine XBP1s levels PCR (n=3). PSC cells were treated 20 µM MKC8866 or DMSO for 48 h. KHYG1 cultured with PSC conditioned-media for 24 h after which cell were harvested and **(C)** counted to determine cell numbers (n=3). **(D)** Cell pellets obtained from counts were subjected to RT-PCR analysis for XBP1s levels. *P < 0.05 and ***P < 0.001 based on a Student's t test. Error bars represent SEM.

4.16 Discussion

As the number of roles played by IRE1 in disease contexts expands outside of its traditional ER stress resolution niche, one of the more interesting associations to arise is its role in cytokine signalling. This means IRE1 likely plays a role in many more disease models than we are currently aware due to the widespread effects of cytokine pathways. The hypoxic, nutrient deprived and highly dense PDAC TME has been shown to present basal ER stress levels and its continued maintenance is dependent on signalling pathways between different cell types[302]. To date, there is very limited data as to what role IRE1 plays in PDAC. While IRE1 RNase inhibition has been shown to reduce proliferation in one study[196], the use of multiple cell types inconsistently throughout the study, the fact that ER stress is artificially induced via chemical means and a lack of follow up mechanistic studies leaves a lot to investigate in this area. We first found that all cell lines examined, both cancer and stellate, exhibit basal IRE1 activation evidenced by the presence of XBP1s at both transcript and protein levels (Fig. 4.1). PERK activation in comparison was only found to be active in the stellate cells and a single PDAC cell line, PANC1, as evidenced by an upshift in PERK molecular weight. Basal UPR activity in a cancer cell line can be attributed to its role in maintaining the infinitive replication of a cancer cell and the huge protein demands associated. Similar to the aforementioned previous studies, the use of a pharmacological inhibitor of IRE1 RNase leads to a reduction in the proliferation of PDAC cell lines and we also report a reduction in PSC proliferation (Fig. 4.4). Additionally, we used an inhibitor of PERK phosphorylation, Amgen PERK 44, to address whether a similar reduction in proliferation can be observed and found that the cell lines who exhibit PERK phosphorylation displayed a reduction in proliferation, similar to that seen with pharmacological IRE1 RNase inhibition. However, it was important to understand whether the reduction in cell number was a result of reduced proliferation or decreased cell viability. While we initially stained cells used in counting with trypan blue for cell viability analysis, the issues of human error and difficulties in discerning whether a cell was stained positive or not, led us to expanding our analysis to other methods in order to answer this question. To do this we analysed the inhibitors effects on cell viability through the use propidium iodide (PI) uptake. PI uptake trends suggested that there was a mixture of both

reduced proliferation and reduced cell viability in play here (Fig. 4.5). For example, PANC1 cells display reduced cell number in response to MKC8866 treatment that does not correlate with a similar level of cell death by PI uptake. Oppositely, PSC showed a reduction in cell number by counting that also indicated similar levels of cell death. While it remains to be determined if the reduced cell number is due to a reduction in cell viability or reduced proliferative capacity and whether the reductions observed are significant enough to be physiologically relevant. What remains certain is that PERK and IRE1 inhibition reduce PDAC and PSC cell number by some means. The reasoning behind this altered proliferation/viability after inhibition of IRE1 RNase activity is not certain but there are multiple plausible explanations. These include that IRE1 has links to cell cycle regulators[198], cytokines associated with autocrine signalling pathways in PDAC that promote proliferation[245] and the importance of maintaining a healthy ER for cell viability. IRE1 ablation in breast cancer has been identified by our lab to reduce proliferation[86] but not effect cell viability whereas recent work in prostate cancer highlighted reduced proliferation alongside enhanced apoptosis[253]. These differences highlight the diverse response to UPR inhibition in different models. In terms of PERK inhibition and decreased cell viability, we see similar patterns but also cell lines lacking obvious PERK activity display reduced cell viability. This could potentially be explained by the pancreatic toxicity associated with PERK inhibitors that is believed to act through altered interferon signalling[281]. Given the possibility that PERK inhibition may be leading to off-target cytotoxicity and examining this was not within the scope of this research, we chose to focus the remainder of our work on the IRE1 arm. It is also worth noting that not all cell lines examined displayed activated PERK pathways, suggesting it may not be as important as IRE1 activity in the cell lines used for this study.

Upon identifying a role for IRE1 inhibition in PDAC and PSC viability/proliferation we sought to expand our analysis to inter-cellular interactions important to pancreatic cancer. These interactions being largely mediated by cytokines, we initially opted to perform a large scale array analysis on secreted factors potentially regulated by IRE1 that could hypothetically regulate other cell types found in the PDAC milieu. Taking

PSC and using PANC1 as a representative cell line for PDAC (based on its basal IRE1 activity and use in experiments relating to PSC interactions) we analysed cytokine levels after MKC8866 treatment (Fig. 4.7, 4.8). Our PANC1 array analysis led to us identifying a large number of downregulated factors upon the addition of MKC8866, many of which are heavily linked to PDAC in the literature. These cytokines have been associated with PDAC progression via multiple pathways including metastasis, epithelial to mesenchymal transition, migration, invasion, proliferation and angiogenesis. The most exciting and important of these is stromal cell derived factor 1 (SDF-1α). It is important because 1) this is the first report of SDF-1α being regulated by IRE1 and 2) SDF-1α is known to be a major regulator of PDAC disease progression by activating the C-X-C motif chemokine receptor 4 (CXCR4) receptor, which is overexpressed in PDAC tissues and associated with poor prognosis[303]. Additionally, using qPCR and ELISA methods on cDNA generated from MKC8866 treated PSC, we were also able to confirm the transcriptional regulation of *SDF1* (Fig. 4.9, 4.12). The other two cytokines analysed by qPCR, *IL6* and *CXCL1*, showed no changes in mRNA abundance upon MKC8866 treatment despite reduced levels after MKC8866 treatment being shown upon array and ELISA analysis. The levels of these transcripts analysed were very low, something known to create unreliable qPCR analysis, which may explain the results as both *IL6* and *CXCL1* have been reported to be transcriptionally regulated by the IRE1 pathway[86]. Alternatively, although no evidence exists of IRE1 regulating the cytokine secretory pathways, it is interesting to speculate a potential role here especially considering the relationship the ER shares with the Golgi and its exosome functions. In contrast, upon analysing the array data from our PSC cell line we observed cytokines being both upregulated and downregulated upon MKC8866 treatment. The cytokines could largely be broken into downregulated factors associated with enhancing PDAC tumorigenesis via increased migration, invasion, proliferation etc and upregulated immunoregulatory cytokines largely associated with NK cell activity and proliferation. This represents an exciting prospect as this kind of double-edged response to IRE1 inhibition represents promising prospects regarding IRE1 as a therapeutic target in PDAC in the future but also it is to my knowledge the first time such a response to MKC8866 has been observed. Having identified target cytokines that are either reduced or enhanced

upon IRE1 RNase ablation in PSC we then needed to identify if this could also lead to any functional effects during co-culture conditions. Given that PSC are known inducers of PDAC proliferation[225] we chose to examine the effects of MKC8866-conditioned PSC media on PDAC cell proliferation. To do this used indirect co-culture methods and we found MKC8866-conditioned PSC media could reduce the proliferation of PDAC cell lines when compared to a control (Fig. 4.13). We also examined XBP1s levels in PDAC cells after their incubation with PSC-conditioned media and found that XBP1s levels increased slightly (not significant) over cells cultured under normal fresh media conditions. This suggests that the transmissible ER stress (TERS) phenomena described in the literature (and described here in detail later) could potentially be at play here. The specifics of the mechanism, if any, behind this would need to be thoroughly investigated but it is interesting to speculate that PSC-conditioned media contains factors capable of altering the UPR status in PDAC cells, leading to enhanced survival. The ability of cells to influence the UPR status of their neighbours could have huge implications. Given the huge role secretory signalling has across the board on PDAC tumorigenesis, the possibility that PSC alter other stromal components by regulating their UPR is tempting.

As already mentioned, we also observed a strong trend of cytokines that were increasing in response to MKC8866 treatments (Fig. 4.14). Interestingly many of the upregulated factors could be attributed to roles in natural killer cell biology. When examining KHYG1 cells, a natural killer cell line, we found that indirect co-culture with MKC8866-conditioned PSC media for a short 24 h period led to a significant increase in cell numbers (Fig. 4.15). This was made more interesting by the fact that treating KHYG1 cells with MKC8866 alone for the same 24 h period led to only a slight reduction in proliferation, the inverse response. It is also important to note that this 24 h period is much shorter compared to the 5 days used to analyse PDAC-PSC interactions, suggesting NK cells may be more responsive to factors contained in the PSC-conditioned media. This also supports that the factors contained in the conditioned media are having a strong effect on cell functions. Even if MKC8866 is hypothetically retained in conditioned media, despite its molecular weight suggesting it should be washed out, the fact that MKC8866 alone vs MKC8866-

conditioned PSC media gives the opposed response suggests to us that its effects are masked by factors contained in the media anyway. From this it seems that there are clearly important secreted factors being secreted from PSC that play important and strikingly diverse roles in PDAC and NK cell lines (Fig. 4.16). While this result only represents preliminary data, it is an extremely exciting prospect to consider in future and could be why we see enhanced KHYG1 proliferation upon MKC8866 treatment.

In summary, our study has shown that IRE1 inhibition leads to reduced proliferation and/or cell viability in a panel of PDAC cells and a PSC line. We also highlighted another model in which IRE1 is capable of regulating multiple cytokines associated with key roles associated with disease progression. Strikingly, unlike as observed in other tumour types, IRE1 RNase ablation leads to differential regulation of cytokines suggesting different cell types in the PDAC TME respond differently to the drug. We showed that co-culturing PDAC cell lines and the NK cell line, KHYG1, with MKC8866-conditioned PSC media led to reduced and enhanced proliferation, respectively. This difference could prove hugely important when considering IRE1 as a potential target for PDAC in future. We hypothesize that the differential regulation of cytokines caused by MKC8866 could lead to different phenotypes in different cell types. Cytokines are capable of regulating cell proliferation in an autocrine manner but given the already established importance of cell-cell signalling in PDAC that is largely mediated by cytokines, it is likely that a combination of autocrine and paracrine signalling gives rise to the responses to IRE1 inhibition that we observed in our model.

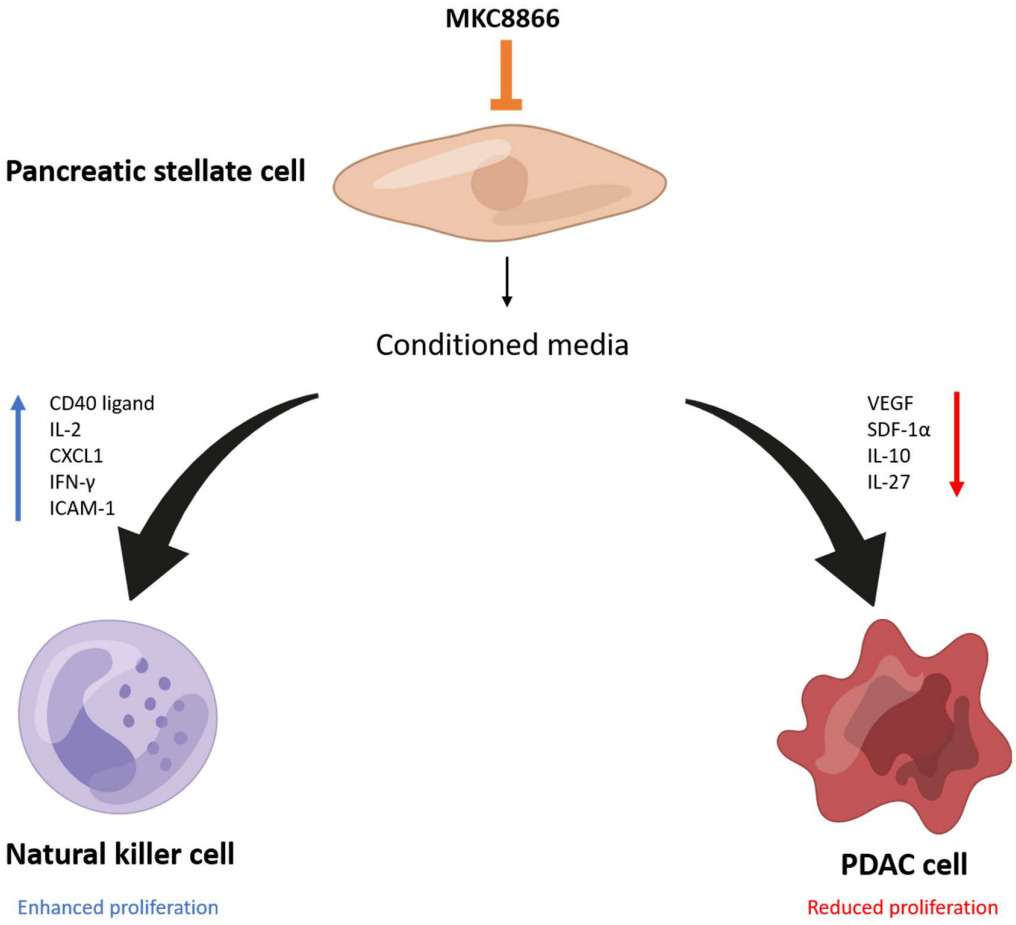

Figure 4.16. Pancreatic cancer cells and natural killer cells exhibit divergent responses to MKC8866 conditioned pancreatic stellate cell media. Treatment of PSC with MKC8866 and subsequent indirect co-cultures of PDAC and NK cell lines with the conditioned media generated, led to a differential response in terms of cell proliferation. When examining the cytokines present in this conditioned media, important regulators of PDAC and NK proliferation were found to be altered in a manner that supports this physiological response. Factors associated with each cell types proliferation that were found to be altered upon MKC8866 in PSC, are highlighted above.

4.17 Future directions

Our work examining the role of IRE1 in PDAC signalling has revealed multiple potential avenues to be pursued in the future. How does IRE1 mediated cytokine signalling in PSC impact PDAC tumorigenesis? How does IRE1 mediated cytokine signalling in PDAC impact PSC activation in PDAC patients? How does IRE1 impact NK cell activity and their role in the tumour microenvironment? The answers will likely be massively complex and context dependent. The use of primary samples in future will likely bring us closer to the reality of what role IRE1 plays in PDAC tumours but elucidating the mechanisms *in vitro* and highlighting potential targets to pursue in the future are also very valuable to this understanding.

4.18 IRE1-regulated cytokines in PDAC and PSC

Numerous cytokines of interest were observed to be regulated in response to MKC8866 treatment in both PANC1 and PSC cell lines (Fig. 4.7, 4.8). In respect to our PANC1 secretome analysis, several factors that we observed to be downregulated upon IRE1 RNase inhibition can be linked to PDAC tumorigenesis and stromal cell interactions. For example, ENA-78 (also known as CXCL5) is a chemokine that regulates tumour angiogenesis, growth and metastasis. In PDAC, ENA-78 has been identified to be overexpressed in tumour tissues and correlate with reduced patient survivability[304]. The authors have shown that ENA-78 is capable of enhancing PDAC angiogenesis through the activation of multiple downstream signalling pathways including protein kinase B (PKB) and signal transducer and activator of transcription (STAT)[305]. FGF (Fibroblast growth factor) is a signalling factor named after its role in the enhancement of stromal cell proliferation that we found downregulated under the same conditions. In PDAC, FGF is overexpressed and associated with advanced tumour stage and reduced survivability[306]. In addition to this, given the high abundance of the fibroblast-like pancreatic stellate cells that are present in PDAC tumours, FGF plays an important role in the regulation of the pancreatic cancer desmoplasia[307]. Given the high abundance of FGF in PDAC tumours and its importance in PSC's, it could represent an interesting target in the future when targeting the stromal microenvironment. Another downregulated factor in PDAC that could represent an interesting target is IL-10. IL-10 is an anti-inflammatory cytokine that inhibits immune cell functionality. This role means IL-10 can induce conditions of reduced pathogen clearance and the associated inflammatory responses but also can prevent over-activation or autoimmune conditions[308]. Data on IL-10 in PDAC patients is currently limited and therefore not conclusive. There is some limited

data also suggesting that IL-10 regulates PSC activation status and ECM production[309], given that we observe IRE1 reduces its release from PDAC tumour cells this could be worth investigating in future.

When analysing cytokine regulation in response to MKC8866 treatment in a pancreatic stellate cell line (Fig. 4.8), conversely to our PDAC cell line analysis (Fig. 4.7), we observed proteins that were upregulated and downregulated. An interesting factor that is strongly upregulated in response to MKC8866 in PSC is IL-24. IL-24 has gained traction as a target of interest due to its known anti-cancer effects including inhibition of angiogenesis, chemotherapy sensitising and induction of apoptosis in tumour cells. This apoptosis is of particular interest as it has been demonstrated to occur specifically in tumour cells and not in the neighbouring "normal" cells[310]. This is believed to occur via the IL-24 receptor, IL-20, and through downstream activation of JAK/STAT and MAPK signalling pathways[311]. Expression of IL-24 in PDAC patients has been linked to patient prognosis and tumour stage[312] and has been demonstrated to kill pancreatic cancer cells via apoptosis [313]. The upregulation of IL-24 in PSC could represent an important mechanism behind the regulation of a pro-apoptotic cytokine against PDAC tumour cells, although further elucidation is absolutely required.

4.19 SDF-1α

Stromal derived factor-1α (SDF-1α), also termed CXCL12, has associated roles in both pathological and physiological conditions. Physiologically it is known to regulate embryogenesis, cardiovascular and nervous system development, cell proliferation, cell differentiation and survival. In terms of pathology it has been proven to be involved in multiple disease types but a particular emphasis has been placed on its role in cancer[288]. SDF-1α signalling is capable of regulating tumour cell migration, proliferation, angiogenesis, EMT status and metastasis. SDF-1α interacts with two receptors, CXCR4 and CXCR7. These receptors can exist in homo or hetero dimers or as monomers alone, the precise combination determining the downstream outputs induced from SDF-1α binding. SDF-1α induces a myriad of cellular pathways linked to multiple cellular processes such as MAPK/PI3K/Akt signalling, JAK/STAT pathways and ERK signalling[314]. Both SDF-1α receptors are known to be over expressed in pancreatic cancer and multiple studies have shown that SDF-1α regulates the proliferation, invasion, migration and metastasis of PDAC cells[303, 315]. In

particular, SDF-1α is known to be heavily secreted from PSC cells and is capable of modulating PDAC tumorigenesis. Conditioned media isolated from PSC enhances PDAC cell line invasion[316], migration[317], proliferation[318] and EMT[319]. SDF-1α also enhances PDAC chemoresistance to gemcitabine[320]. We have identified SDF-1α regulation by IRE1 RNase in PSC at both mRNA and protein levels and predictive promotor analysis suggests XBP1 may be able to transcriptionally regulate it. We also showed that MKC8866-conditioned PSC media reduced PDAC cell line proliferation compared to control media. This suggests to us that IRE1 through conditioned pancreatic stellate cell media could regulate multiple facets of PDAC tumorigenesis. Based on the known roles of SDF-1α in other aspects of PDAC tumorigenesis, it will be interesting to examine IRE1's role in the migration, invasion and EMT status of PDAC cells.

4.20 Transmissible ER stress (TERS)

The concept of transmissible ER stress (TERS) is a recent one that is quickly gaining traction in the UPR field. It is believed that cells experiencing ER stress secrete unknown factors to nearby cells capable of inducing a subsequent ER-stress response in the recipient cell. Originally identified in myeloid cells by *Zanetti et al* in 2011[321], TERS has also been reported in tumour cells[322] and cells of the central nervous system (CNS)[323]. The idea of TERS contributing to tumorigenesis is an intriguing one as it could suggest that cells experiencing ER stress stimulate a sort of cascade enhancing the UPR signalling of neighbour cells. Intracellular cross talk between PSC and PDAC is well recognized and can occur via aforementioned cytokine signalling but also through metabolic component signals. A fascinating article by *Sousa et al[324]* demonstrated that PDAC cells induce alanine catabolism via autophagy in PSC which is then released and regulates tumour metabolism. The factor released from PDAC cells to initiate PSC autophagy is unknown but could it represent a form of TERS considering PSC highly secretory nature and basal ER stress levels we have observed? What signals make up TERS remains to be seen but given the evidence that IRE1 regulates cytokine signalling and metabolic pathways[325, 326], it represents a strong candidate for further investigation into this area.

Chapter 5: General discussion and future directions

5.1 Chapter V: General discussion

As evidenced in this thesis and in the expanding literature, IRE1 can no longer be considered a protein with a singular function. Novel roles for it have been identified in multiple areas outside of its traditional ER stress and protein folding niche. Whilst many of these novel roles for IRE1 can be linked to ER stress associated responses due to increased protein folding demands such as in B-cell differentiation[242], MYC-driven proliferation in breast[188] or prostate cancers[253] and pancreatic β-cell oxidative pathways[16], others seem to be less closely linked to protein folding. These include IRE1's role in Filamin A (FLNA) scaffold regulation[327] and its role in memory formation via XBP1[328], for example. In this thesis, I have identified a role for IRE1 in two distinct circumstances with the regulation of cytokines being the unifying element between both. Firstly, while IRE1's role in NLRP3 activity has been established, it remains ambiguous to some extent. Here, we identified a role for IRE1 in the activation step of this process and showed that inhibition of IRE1's RNase domain prevents efficient NLRP3 inflammasome assembly, although this is not essential for NLRP3 functionality (Fig 3.5, 3.11). Given the importance of NLRP3-mediated IL-1β release to a myriad of inflammatory diseases, IRE1 represents a potential therapeutic target, albeit more functional studies are essential to fully understand its role.

Secondly, we analysed IRE1 in the context of pancreatic cancer (PDAC). We found basal IRE1 and PERK levels to varying extents in PDAC cell lines (Fig. 4.1). The use of IRE1 and PERK inhibitors also reduced PDAC cell line proliferation and viability suggesting the UPR plays an important role in the biology of these cells (Fig 4.2, 4.3). Given recent evidences by *Logue et al* in breast cancer that IRE1 regulates the levels of cytokines associated with disease relapse and cell proliferation, we sought to identify a similar pathway in the PDAC model. As explained earlier, PDAC has long been associated with an extremely poor prognosis due to a dense stromal layer that develops around the tumour site and enhances tumour growth[283]. This stroma consists of multiple key cell types, largely fibroblastic or immune type cells. We chose to expand our analysis to these cell types by analysing the effects of UPR inhibition in natural killer (NK) and pancreatic stellate cells (PSC), with a focus on IRE1's ability

to regulate cytokines. We found that IRE1 regulates a large array of cytokines secreted from PSC that are known to influence both PDAC cells and NK cells (Fig. 4.8). This result indicates a potentially crucial role for IRE1 in mediating interactions between PDAC stromal components that are known orchestrators of PDAC tumour proliferation, migration, invasion and EMT. Conditioned media harvested from PSC treated with MKC8866 was co-cultured with PDAC and NK cells leading to reduced and enhanced proliferation, respectively (Fig 4.13, 4.15). This suggests that IRE1 can potentially mediate signalling factors between different cell types commonly found in the PDAC TME.

5.2 What role does IRE1 play in inflammation?

An important and interesting question asked often is why and how IRE1(or the UPR as a whole) actually regulates cytokine levels. In reality, ER stress and inflammatory interactions operate in a "two-way street". This is to say that ER stress is capable of arising from inflammatory signals (PAMP's, DAMP's, MAMP's) but at the same time, ER stress can also induce an inflammatory response[87]. This suggests a that ER stress acts in a sort of positive feedback loop with inflammatory signals. In fact, chemical inducers of ER stress have actually been shown to induce low levels of inflammatory cytokine production under what can be considered sterile conditions[245, 256]. These ER-stress induced cytokine levels are low when compared to the levels observed under PRR activation, for example, but it was found that ER stress induction was capable of "sensitizing" the cell to enhanced cytokine production[91, 329]. PRR stimuli were applied to cells after ER stress induction and cytokine levels were increased suggesting that synergy exists between the two stress types. Naturally, this means that IRE1 activation and downstream cytokine signalling are heavily linked and upregulated during a range of inflammatory and ER-stress associated disease conditions. All three UPR sensors are capable of activating downstream transcription factors that regulate classical pro-inflammatory cytokines. These include NF-κB, activator protein 1 (AP-1), ERK, JNK, p38 transcription factors[82]. Furthermore, UPR-associated transcription factors can directly regulate cytokine production via binding to their promotor regions. Both XBP1s and ATF4 are known to bind to *IL6* promotors, for example[245, 330, 331]. The close relationship of ER stress and inflammatory

cytokine production gives rise to the possibility of IRE1 signalling having relevance in bacterial, viral and autoimmune signalling and roles in a broad spectrum of diseases ranging from inflammatory bowel disease (IBS), to TRAPS and type 1 diabetes.

The importance of ER stress attenuation and the reliance a cell has on correct protein folding leaves the ER in a position of vital importance. The ER acts as a cellular crossroads that interacts with a multitude of other cellular stressors such as oxidative stress, mitochondrial stress and inflammatory/immunogenic stress. It has been suggested that ER stress itself may act as a DAMP[332] considering the UPR arose in an evolutionary perspective from proto-anti-viral protein pathways (PERK from PKR, IRE1 from RNaseL). The close relationship of UPR signalling and that of inflammatory processes may suggest the UPR acts as a support role by furthering the immune system's ability to detect threat vs non-threat, self vs non-self and increase the cell's pathogen detection abilities in the absence of PRR stimulation.

5.3 Targeting the NLRP3 inflammasome

Multiple diseases that are commonly associated with ageing and decaying bodily functions are associated with hyperactivated immune responses due to a build-up of immunogenic "debris". These diseases range from autoimmune disease to neurodegenerative diseases to heart diseases. NLRP3 represents a central node in the immune signalling that has become attributed to the development of these diseases in recent years, highlighting its importance as a therapeutic target. Given the broad range of stimuli capable of inducing NLRP3 activation it has been hypothesized that the benefits of this response outstay their welcome in the ageing populations of the modern day. Rare, inherited, autosomal dominant NLRP3 mutations that cause persistent activation of the complex develop auto-inflammatory conditions known as cryopyrin-associated periodic syndromes (CAPS). CAPS is a broad term for a collection of autoimmune diseases caused by activating mutations in NLRP3 of which there are multiple. To date, over 200 known mutations in NLRP3 are implicated in associated autoimmunity diseases[333]. NLRP3 also contributes to diseases that involve dysregulated metabolic processes, aggregation and fibrosis following chronic inflammation[334]. NLRP3 agonists represent an opportunity to enhance immune activity under conditions in which

immunosuppressive signalling prevails, such as in cancers. NLRP3 activity leads to the release of potent pro-inflammatory cytokines (IL-1β, IL-18) and downstream pyroptosis. Targeting NLRP3 in conjunction with T-cell check point inhibitors could be a potent anti-tumour strategy[335, 336]. This idea comes with the caveat that inflammation can paradoxically nurture tumorigenesis, rather than antagonise it. The use of short, acute inflammatory inductions in the tumour may be the key in avoiding long-term chronic inflammation capable of having inverse effects. There are multiple avenues of intervention considering the complex nature of NLRP3's activation. The regulation of NLRP3 transcription by modulating the TLR4 associated interleukin-1 receptor associated kinase 4 (IRAK4) has been considered but considering the wide-reaching effects of TLR4-mediated transcription the potential for off-target effects is troublesome[337]. NLRP3 activity is heavily mediated by post-translational modifications such as phosphorylation and deubiquitylation[140]. Similar to TLR4 targeting, the kinases and deubiquitylases responsible for NLRP3 regulation could have specificity issues. IL-1β is the most potent inflammatory cytokine released upon NLRP3 activation and is linked to multiple NLRP3-associated diseases. Therefore, it is no surprise that it has been selected as a target against NLRP3. The issue with IL-1β antagonism is that if you target the IL-1 receptor (IL-1R) you may inadvertently affect other IL-1 family members, conversely, the direct targeting of IL-1β itself may only dampen NLRP3 associated inflammatory signalling and other effectors (IL-18, prostaglandins) remain unaffected[334].

Given the data we presented in this thesis regarding IRE1 and its role in NLRP3 inflammasome activity, IRE1 could represent an effective target against NLRP3 inflammasome activity. We have shown that IRE1 RNase ablation has no effect on the transcript or protein levels of key NLRP3 inflammasome complex members (NLRP3, ASC, Caspase-1) but reduces the levels of its key effector molecule, IL-1β (Fig 3.8). This suggests that IRE1 regulates the efficiency of NLRP3 assembly. The precise mechanism remains unclear but we have ruled out one commonly cited link between IRE1 and NLRP3 in the form of TXNIP, which has been reported to upregulate NLRP3 activity in response to enhanced IRE1 activity (Fig. 3.10). In our system, we did not observe this relationship, as discussed in chapter 3. IRE1 RNase represents a valuable

therapeutic target against NLRP3 activation and the subsequent release of IL-1β when combined with the evidences we have generated that IRE1 RNase ablation also reduced other TLR4-mediated inflammatory cytokines such as IL-6, TNFα and CXCL1 (Fig. 3.4). However, the precise mechanism through which IRE1 regulates NLRP3 assembly remains to be fully elucidated.

5.3.1 The roles of IL-6, IL-8 and CXCL1 in IL-1β regulation

CXCL1 upregulates NLRP3 activity and is downregulated upon IRE1 inhibition in THP-1 cells after TLR4 stimulation[259]. CXCL1 is also a confirmed transcriptional target of XBP1 in breast cancer cells[86]. CXCL1 blocking antibody slightly reduced IL-1β levels after TLR4 stimulation in our hands (Fig. 3.12). Interestingly, IL-6 blocking antibodies also reduced IL-1β levels under these conditions (Fig. 3.12). Previous reports found that IL-6 transcriptionally regulates CXCL1 in cerebral endothelial cells, although we did not observe this in our model[338]. While these reports used different cell types and did not analyse TLR4-mediated cytokine pathways, it was an interesting prospect that IL-6 and CXCL1 could reduce IL-1β levels upon IRE1 RNase inhibition. Another interesting result we obtained from our analysis using blocking antibodies after LPS-mediated TLR4 stimulation was that IL-8 blocking antibodies led to an increase in IL-1β levels (Fig. 3.12). This has not been previously observed and could indicate a novel function of IL-8. Interestingly, both CXCL1 and IL-8 are known ligands for the receptor CXCR2[339]. CXCR2 is a G-protein-coupled receptor that primarily functions in neutrophil migration control to sites of inflammation[340]. Multiple signalling pathways are activated downstream of CXCR2 including phospholipase C (PLC), protein kinase C (PKC), phosphatidylinositol-3 kinase (PI3K), mitogen-activated protein kinase (MAPK), janus kinase/signal transducer and activator of transcription (STAT3) signalling pathway[341]. Given the diverse response observed in IL-1β levels after IL-8 and CXCL1 blocking antibodies and their shared downstream outputs, it is difficult to hypothesize what is happening here. Additionally, it is worth noting that IL-6 also regulates STAT3 signalling via the IL-6R[342]. IL-6 activation via the IL-6R pathway has been shown to synergise with TLR4 mediated IL-6 release upon LPS treatment via STAT3 signalling [343]. Importantly, blockage of the STAT3 pathway under LPS stimulation also leads to reduced IL-6 and

IL-1β levels suggesting there is some feedback in play similar to what we have observed [344]. Is it possible that the reduction of IL-6 or CXCL1 in the priming stage of NLRP3 activation is responsible for the IL-1β reduction we observe after IRE1 has been inhibited? Further experimentation is required but it presents a very interesting prospect for the future.

5.4 What role does IRE1 play in PDAC?

Our data provides new insights into the role of IRE1 in PDAC progression. Firstly, the basal UPR signals we observed could contribute to the basal cytokine secretion of PDAC cells (Fig. 4.1) [345]. The dense stroma in PDAC tumours largely consists of fibroblasts and immune cells that both secrete and are activated by cytokines. Perhaps the onset of chronic ER stress due to increasing protein demands to support tumour growth leads to a constitutively activated IRE1 response. This could be considered by the cell to be pathological as IRE1 is believed to be activated early and transiently under normal conditions[346]. The basal UPR present as a result of the tumour microenvironment coupled with the high volumes of circulating cytokines results in a highly inflammatory environment. Perhaps IRE1 signalling aims to relieve this inflammatory stress by activating an immune response to target the tumour. However, it could be that IRE1 signalling only further exacerbates the inflammatory profile by increasing cytokine secretion. Potentially this could lead to enhanced fibrosis by PSC's through prolonged activation[284], a dampening of the anti-inflammatory response due to unbalanced pro- vs anti-inflammatory cytokine levels[347] and immune cell exhaustion. While this is mostly speculation, the association of inflammatory cytokines with poor PDAC disease prognosis, the knowledge of the interlinked pathways of the UPR and cytokine production and the uniquely dense, inflammatory environment caused by a PDAC tumour stroma make it a plausible hypothesis that IRE1 signalling could be important in PDAC tumorigenesis at multiple levels. Taking all our data together it seems that IRE1 is capable of not only regulating PDAC cell line cytokine production but also the secretomes of associated stromal cells, like PSC. Given the importance of cytokine signalling in proliferative autocrine signalling in PDAC cells and paracrine interactions within the stromal niche, it is fair to say that IRE1 represents an interesting prospect

for future studies. PSC signalling has been established as a key aspect of PDAC development, progression and prognosis. We have identified several factors that are essential for PSC-PDAC interactions to be IRE1 regulated (e.g. SDF-1α) (Fig. 4.10). This provides interesting groundwork for future studies that may elucidate IRE1 signalling from a basic research point of view but also help us understand if it could be an effective target in PDAC.

5.4.1 What about PERK and ATF6?

Since ER stress induces cytokine secretion, it remains unclear whether all three UPR arms responsible or just IRE1. While PERK inhibition and its role in PDAC and PSC proliferation and viability were analysed in this thesis (Fig. 4.2, 4.3, 4.4), the decision to focus on IRE1 was taken because IRE1 is the most conserved and well-studied of the UPR sensors and PERK inhibition can induce pancreatic toxicity[281] making it a less viable therapeutic target. Regarding chapter 3, LPS-induced TLR4 activation selectively upregulated the IRE1 arm of the UPR and therefore IRE1 was the only arm investigated. However, since PDAC cell lines have basal PERK activity and many papers report a role for PERK in PDAC[348], it is something for future investigation. PERK-mediated, eIF2α-dependent cytokine regulation has been observed in astrocytes, suggesting PERK mediated cytokine regulation occurs in some systems[349]. Additionally, PERK activity is upregulated by gemcitabine and may contribute to gemcitabine resistance commonly observed in PDAC patients[216]. Pumilio RNA-binding family member 1 (PUM1), an oncogene found to be upregulated in PDAC tissues that correlates with poor survival, negatively regulates PERK activity. Interestingly, PERK overexpression led to reduced proliferation, migration, invasion and EMT which could be reversed by PERK inhibition. In this scenario, PERK is suppressed by PUM1 in healthy cells but enhanced in tumour conditions due to reduced PUM1 levels[350]. To date no studies have linked ATF6 signalling to PDAC. ATF6, is largely understudied compared to IRE1 and PERK which could be due to a lack of effective, specific inhibitors and good antibodies for western blot. Importantly, even though no research has focused on ATF6 we cannot rule out its importance as it is well established that the ATF6 and XBP1 pathways are interlinked. ATF6 may affect PDAC indirectly through XBP1 upregulation[46].

5.5 Targeting the IRE1 RNase in PDAC

PDAC, despite a relatively low incidence rate, remains one of the most aggressive tumour types in humans and is the fourth leading cause of cancer-associated death[212]. While significant progress in the understanding of PDAC on a molecular scale has occurred and has led to the discovery of the importance of factors like KRAS signalling, survival rates remain dismal[351]. In this thesis we have identified that IRE1 regulates the levels of key cytokines known to play important roles in PDAC, particularly within the stromal interactions (Fig. 4.7, 4.8). IRE1 RNase ablation led to the reduction of certain cytokines in PANC1 cells, some of which have been previously identified by *Logue et al* and others as being IRE1 RNase regulated[86, 245]. We have also discovered novel IRE1 regulated cytokines in PDAC cells for the first time (Fig. 4.12). Three interesting factors downregulated upon MKC8866 treatment are (1)CXCL1 which is overexpressed in PDAC tissue compared to surrounding tissues and can influence T-cell infiltration and subsequent treatment efficacy[352, 353] (2) ICAM-1, an adhesion molecule, also upregulated in PDAC[354] and contributes to metastasis and (3) Macrophage inhibitory factor (MIF), which is upregulated in multiple tumour types, promotes metastasis and proliferation, and is associated with poor PDAC prognosis[355]. A similar analysis into PSC cytokines led to us identifying a divergent response to IRE1 RNase inhibition in which different cytokines were upregulated and downregulated simultaneously (Fig. 4.8). This represents a novel discovery into the regulation of cytokines in PSC by IRE1 RNase and contrasts PANC1 data which only presented downregulated targets. The exact mechanism of regulation by IRE1 is not confirmed but it could represent a situation in which both functions of the RNase domain, XBP1s signalling and RIDD, are acting simultaneously to regulate cytokines. Additional experiments are required to confirm RIDD regulation. It could also be that RIDD is targeting negative regulators of cytokine transcription and therefore indirectly regulating their levels. An interesting observation was that the downregulated group could largely be linked to processes or pathways that have been shown to enhance various aspects of PDAC progression (Fig. 4.9). The most interesting of these is undoubtedly SDF-1α (discussed in chapter 4), a chemokine that is heavily secreted from PSCs and has been proven to induce PDAC proliferation, migration, invasion and EMT. Given that we have confirmed

reduced levels of SDF-1α by ELISA analysis and also identified reduced transcript levels by qPCR upon MKC8866 treatment, SDF-1α represents a novel XBP1s target in PSCs. Importantly, SDF-1α could be responsible for the reduction in PSC-induced PDAC proliferation in response to MKC8866.SDF-1α represents "low-hanging fruit" and should be pursued further to confirm that it is an IRE1-regulated cytokine that regulates inter-cellular signalling between PSCs and PDAC cells.

5.6 Targeting IRE1 in the interactions between PSC and NK cells

As mentioned, the cytokine array analysis in PSC identified differentially regulated cytokines upon MKC8866 treatment. While the downregulated factors often correlated to roles in enhancing PDAC tumorigenesis, the upregulated factors were associated with immune cell regulation (Fig. 4.14). Closer analysis of these factors revealed multiple that were associated with NK cell proliferation and activity. Given that NK cells are deemed to be generally repressed by the immunosuppressive nature of a PDAC tumour microenvironment or often exhibit signs of "exhaustion" seen in tumour associated immune cells, it was of great interest to us to determine IRE1 could be involved in regulating NK cells interactions with PSC. One of the most interesting factors we found was CD40 ligand (CD40L). CD40L is normally secreted from immune cells but can be expressed in cancer cells, fibroblasts and other epithelial cell types meaning its presence in pancreatic stellate cells is not surprising. CD40L activates the CD40 receptor which enhances surface expression of costimulatory molecules, induces inflammatory cytokine release and enhances T cell and NK cell-mediated killing[356]. Antigen presenting cells (APC) activated by CD40 ligation lead to the induction of NK cell cytotoxicity. Given that NK cells exhibit a defective cytotoxic response in PDAC, it could be interesting to determine if IRE1 RNase activity can regulate CD40L secretion in PSCs. ICAM-1, which we found to be downregulated in PANC1 cells, was upregulated in PSC and plays important roles in the migration of immune cells to sites of inflammation and mediates APC and T cell/NK cell interactions. ICAM-1 is known to enhance NK-mediated cytotoxicity[357]. Another upregulated factor upon MKC8866 treatment in PSC was IFN-γ, a vital immunoregulatory molecule with wide ranging effects including T-cell differentiation, leukocyte migration and major histocompatibility complex (MHC)

expression enhancement on T cells[358]. One of the known transcriptional regulators of IFN-γ, AP-1, has previously been associated with IRE1 activity[359]. IL-2 is a vital cytokine with many functions within immunomodulatory signalling and has been heavily studied specifically in relation to NK cells. It has been shown that the addition of IL-2 to NK cells enhances their proliferation and also increases their cytotoxic functions[298]. IL-2 shares its receptor (IL-2R) with IL-15, another well-studied cytokine associated with NK cell activity. It shares similar functional roles with IL-2 and both have been linked downstream to JAK/STAT signalling, the PI3K pathway, and NF-κB regulation[299]. In fact, both IL-2 and IL-15 are capable of enhancing NK cell killing of PSC and PDAC cell lines[360]. Since MKC8866 enhances IL-2 and IL-15 levels in PSC and this conditioned media subsequently enhances NK proliferation, both represent interesting targets for the future. This is boosted by a report that showed IL-15 supplementation in NK cells enhanced XBP1s expression which with increased cytotoxic functionality[361].

References

1. Porter, K.R., A. Claude, and E.F. Fullam, *A Study of Tissue Culture Cells by Electron Microscopy : Methods and Preliminary Observations.* J Exp Med, 1945. **81**(3): p. 233-46.
2. Schwarz, D.S. and M.D. Blower, *The endoplasmic reticulum: structure, function and response to cellular signaling.* Cell Mol Life Sci, 2016. **73**(1): p. 79-94.
3. Nyathi, Y., B.M. Wilkinson, and M.R. Pool, *Co-translational targeting and translocation of proteins to the endoplasmic reticulum.* Biochim Biophys Acta, 2013. **1833**(11): p. 2392-402.
4. Gorlich, D., et al., *A mammalian homolog of SEC61p and SECYp is associated with ribosomes and nascent polypeptides during translocation.* Cell, 1992. **71**(3): p. 489-503.
5. Agostinis, P.S., A., *Endoplasmic reticulum stress in health and disease*. 2012: Springer.
6. Feige, M.J. and L.M. Hendershot, *Disulfide bonds in ER protein folding and homeostasis.* Curr Opin Cell Biol, 2011. **23**(2): p. 167-75.
7. Saibil, H., *Chaperone machines for protein folding, unfolding and disaggregation.* Nat Rev Mol Cell Biol, 2013. **14**(10): p. 630-42.
8. Qi, L., B. Tsai, and P. Arvan, *New Insights into the Physiological Role of Endoplasmic Reticulum-Associated Degradation.* Trends Cell Biol, 2017. **27**(6): p. 430-440.
9. Dikic, I. and Z. Elazar, *Mechanism and medical implications of mammalian autophagy.* Nat Rev Mol Cell Biol, 2018. **19**(6): p. 349-364.
10. Bento, C.F., et al., *Mammalian Autophagy: How Does It Work?* Annu Rev Biochem, 2016. **85**: p. 685-713.
11. Fagone, P. and S. Jackowski, *Membrane phospholipid synthesis and endoplasmic reticulum function.* J Lipid Res, 2009. **50 Suppl**: p. S311-6.
12. Koch, G.L., *The endoplasmic reticulum and calcium storage.* Bioessays, 1990. **12**(11): p. 527-31.
13. Cribb, A.E., et al., *The endoplasmic reticulum in xenobiotic toxicity.* Drug Metab Rev, 2005. **37**(3): p. 405-42.
14. Almanza, A., et al., *Endoplasmic reticulum stress signalling - from basic mechanisms to clinical applications.* FEBS J, 2019. **286**(2): p. 241-278.
15. Xiang, C., et al., *The role of endoplasmic reticulum stress in neurodegenerative disease.* Apoptosis, 2017. **22**(1): p. 1-26.
16. Fonseca, S.G., J. Gromada, and F. Urano, *Endoplasmic reticulum stress and pancreatic beta-cell death.* Trends Endocrinol Metab, 2011. **22**(7): p. 266-74.
17. Tameire, F., Verginadis, II, and C. Koumenis, *Cell intrinsic and extrinsic activators of the unfolded protein response in cancer: Mechanisms and targets for therapy.* Semin Cancer Biol, 2015. **33**: p. 3-15.
18. Richter, K., M. Haslbeck, and J. Buchner, *The heat shock response: life on the verge of death.* Mol Cell, 2010. **40**(2): p. 253-66.
19. Oslowski, C.M. and F. Urano, *Measuring ER stress and the unfolded protein response using mammalian tissue culture system.* Methods Enzymol, 2011. **490**: p. 71-92.
20. Ron, D. and P. Walter, *Signal integration in the endoplasmic reticulum unfolded protein response.* Nat Rev Mol Cell Biol, 2007. **8**(7): p. 519-29.
21. Xu, C., B. Bailly-Maitre, and J.C. Reed, *Endoplasmic reticulum stress: cell life and death decisions.* J Clin Invest, 2005. **115**(10): p. 2656-64.

22. Shiu, R.P., J. Pouyssegur, and I. Pastan, *Glucose depletion accounts for the induction of two transformation-sensitive membrane proteinsin Rous sarcoma virus-transformed chick embryo fibroblasts.* Proc Natl Acad Sci U S A, 1977. **74**(9): p. 3840-4.
23. Kozutsumi, Y., et al., *The presence of malfolded proteins in the endoplasmic reticulum signals the induction of glucose-regulated proteins.* Nature, 1988. **332**(6163): p. 462-4.
24. Mori, K., et al., *A transmembrane protein with a cdc2+/CDC28-related kinase activity is required for signaling from the ER to the nucleus.* Cell, 1993. **74**(4): p. 743-56.
25. Cox, J.S., C.E. Shamu, and P. Walter, *Transcriptional induction of genes encoding endoplasmic reticulum resident proteins requires a transmembrane protein kinase.* Cell, 1993. **73**(6): p. 1197-206.
26. Cox, J.S. and P. Walter, *A novel mechanism for regulating activity of a transcription factor that controls the unfolded protein response.* Cell, 1996. **87**(3): p. 391-404.
27. Mori, K., et al., *Signalling from endoplasmic reticulum to nucleus: transcription factor with a basic-leucine zipper motif is required for the unfolded protein-response pathway.* Genes Cells, 1996. **1**(9): p. 803-17.
28. Tirasophon, W., A.A. Welihinda, and R.J. Kaufman, *A stress response pathway from the endoplasmic reticulum to the nucleus requires a novel bifunctional protein kinase/endoribonuclease (Ire1p) in mammalian cells.* Genes Dev, 1998. **12**(12): p. 1812-24.
29. Harding, H.P., Y.H. Zhang, and D. Ron, *Protein translation and folding are coupled by an endoplasmic-reticulum-resident kinase.* Nature, 1999. **397**(6716): p. 271-274.
30. Haze, K., et al., *Mammalian transcription factor ATF6 is synthesized as a transmembrane protein and activated by proteolysis in response to endoplasmic reticulum stress.* Mol Biol Cell, 1999. **10**(11): p. 3787-99.
31. Bertolotti, A., et al., *Dynamic interaction of BiP and ER stress transducers in the unfolded-protein response.* Nature Cell Biology, 2000. **2**(6): p. 326-332.
32. Woehlbier, U. and C. Hetz, *Modulating stress responses by the UPRosome: a matter of life and death.* Trends Biochem Sci, 2011. **36**(6): p. 329-37.
33. Shi, Y.G., et al., *Identification and characterization of pancreatic eukaryotic initiation factor 2 alpha-subunit kinase, PEK, involved in translational control.* Molecular and Cellular Biology, 1998. **18**(12): p. 7499-7509.
34. Harding, H.P., et al., *An integrated stress response regulates amino acid metabolism and resistance to oxidative stress.* Molecular Cell, 2003. **11**(3): p. 619-633.
35. Donnelly, N., et al., *The eIF2 alpha kinases: their structures and functions.* Cellular and Molecular Life Sciences, 2013. **70**(19): p. 3493-3511.
36. Pakos-Zebrucka, K., et al., *The integrated stress response.* EMBO Rep, 2016. **17**(10): p. 1374-1395.
37. Harding, H.P., et al., *Regulated translation initiation controls stress-induced gene expression in mammalian cells.* Molecular Cell, 2000. **6**(5): p. 1099-1108.
38. Jackson, R.J., C.U.T. Hellen, and T.V. Pestova, *The mechanism of eukaryotic translation initiation and principles of its regulation.* Nature Reviews Molecular Cell Biology, 2010. **11**(2): p. 113-127.
39. Novoa, I., et al., *Stress-induced gene expression requires programmed recovery from translational repression.* Embo Journal, 2003. **22**(5): p. 1180-1187.
40. Puthalakath, H., et al., *ER stress triggers apoptosis by activating BH3-only protein Bim.* Cell, 2007. **129**(7): p. 1337-1349.
41. Ye, J., et al., *ER stress induces cleavage of membrane-bound ATF6 by the same proteases that process SREBPs.* Molecular Cell, 2000. **6**(6): p. 1355-1364.

42. Nadanaka, S., et al., *Activation of mammalian unfolded protein response is compatible with the quality control system operating in the endoplasmic reticulum.* Mol Biol Cell, 2004. **15**(6): p. 2537-48.
43. Schindler, A.J. and R. Schekman, *In vitro reconstitution of ER-stress induced ATF6 transport in COPII vesicles.* Proc Natl Acad Sci U S A, 2009. **106**(42): p. 17775-80.
44. Yoshida, H., et al., *ATF6 activated by proteolysis binds in the presence of NF-Y (CBF) directly to the cis-acting element responsible for the mammalian unfolded protein response.* Molecular and Cellular Biology, 2000. **20**(18): p. 6755-6767.
45. Shoulders, M.D., et al., *Stress-Independent Activation of XBP1s and/or ATF6 Reveals Three Functionally Diverse ER Proteostasis Environments.* Cell Reports, 2013. **3**(4): p. 1279-1292.
46. Yoshida, H., et al., *XBP1 mRNA is induced by ATF6 and spliced by IRE1 in response to ER stress to produce a highly active transcription factor.* Cell, 2001. **107**(7): p. 881-91.
47. Wang, X.Z., et al., *Cloning of mammalian Ire1 reveals diversity in the ER stress responses.* Embo Journal, 1998. **17**(19): p. 5708-5717.
48. Bertolotti, A., et al., *Increased sensitivity to dextran sodium sulfate colitis in IRE1 beta-deficient mice.* Journal of Clinical Investigation, 2001. **107**(5): p. 585-593.
49. Martino, M.B., et al., *The ER stress transducer IRE1 beta is required for airway epithelial mucin production.* Mucosal Immunology, 2013. **6**(3): p. 639-654.
50. Imagawa, Y., et al., *RNase domains determine the functional difference between IRE1alpha and IRE1beta.* FEBS Lett, 2008. **582**(5): p. 656-60.
51. Nikawa, J.I. and S. Yamashita, *Ire1 Encodes a Putative Protein-Kinase Containing a Membrane-Spanning Domain and Is Required for Inositol Phototrophy in Saccharomyces-Cerevisiae.* Molecular Microbiology, 1992. **6**(11): p. 1441-1446.
52. Credle, J.J., et al., *On the mechanism of sensing unfolded protein in the endoplasmic reticulum.* Proceedings of the National Academy of Sciences of the United States of America, 2005. **102**(52): p. 18773-18784.
53. Gardner, B.M. and P. Walter, *Unfolded Proteins Are Ire1-Activating Ligands That Directly Induce the Unfolded Protein Response.* Science, 2011. **333**(6051): p. 1891-1894.
54. Korennykh, A.V., et al., *The unfolded protein response signals through high-order assembly of Ire1.* Nature, 2009. **457**(7230): p. 687-U2.
55. Urano, F., et al., *Coupling of stress in the ER to activation of JNK protein kinases by transmembrane protein kinase IRE1.* Science, 2000. **287**(5453): p. 664-666.
56. Calfon, M., et al., *IRE1 couples endoplasmic reticulum load to secretory capacity by processing the XBP-1 mRNA (vol 415, pg 92, 2002).* Nature, 2002. **420**(6912): p. 202-202.
57. Hollien, J. and J.S. Weissman, *Decay of endoplasmic reticulum-localized mRNAs during the unfolded protein response.* Science, 2006. **313**(5783): p. 104-107.
58. Hollien, J. and J.S. Weissman, *Decay of endoplasmic reticulum-localized mRNAs during the unfolded protein response.* Science, 2006. **313**(5783): p. 104-7.
59. Ghosh, R., et al., *Allosteric inhibition of the IRE1alpha RNase preserves cell viability and function during endoplasmic reticulum stress.* Cell, 2014. **158**(3): p. 534-48.
60. Tam, A.B., A.C. Koong, and M. Niwa, *Ire1 has distinct catalytic mechanisms for XBP1/HAC1 splicing and RIDD.* Cell Rep, 2014. **9**(3): p. 850-8.
61. Lu, Y.Y., F.X. Liang, and X.Z. Wang, *A Synthetic Biology Approach Identifies the Mammalian UPR RNA Ligase RtcB.* Molecular Cell, 2014. **55**(5): p. 758-770.
62. Lee, A.H., N.N. Iwakoshi, and L.H. Glimcher, *XBP-1 regulates a subset of endoplasmic reticulum resident chaperone genes in the unfolded protein response.* Mol Cell Biol, 2003. **23**(21): p. 7448-59.

63. Schuck, S., et al., *Membrane expansion alleviates endoplasmic reticulum stress independently of the unfolded protein response.* J Cell Biol, 2009. **187**(4): p. 525-36.
64. Sriburi, R., et al., *XBP1: a link between the unfolded protein response, lipid biosynthesis, and biogenesis of the endoplasmic reticulum.* J Cell Biol, 2004. **167**(1): p. 35-41.
65. Yoshida, H., et al., *pXBP1(U) encoded in XBP1 pre-mRNA negatively regulates unfolded protein response activator pXBP1(S) in mammalian ER stress response.* J Cell Biol, 2006. **172**(4): p. 565-75.
66. Yoshida, H., A. Uemura, and K. Mori, *pXBP1(U), a negative regulator of the unfolded protein response activator pXBP1(S), targets ATF6 but not ATF4 in proteasome-mediated degradation.* Cell Struct Funct, 2009. **34**(1): p. 1-10.
67. Yanagitani, K., et al., *Translational pausing ensures membrane targeting and cytoplasmic splicing of XBP1u mRNA.* Science, 2011. **331**(6017): p. 586-9.
68. Oikawa, D., et al., *Identification of a consensus element recognized and cleaved by IRE1 alpha.* Nucleic Acids Research, 2010. **38**(18): p. 6265-6273.
69. Maurel, M., et al., *Getting RIDD of RNA: IRE1 in cell fate regulation.* Trends Biochem Sci, 2014. **39**(5): p. 245-54.
70. Upton, J.P., et al., *IRE1alpha cleaves select microRNAs during ER stress to derepress translation of proapoptotic Caspase-2.* Science, 2012. **338**(6108): p. 818-22.
71. Lipson, K.L., et al., *Regulation of insulin biosynthesis in pancreatic beta cells by an endoplasmic reticulum-resident protein kinase IRE1.* Cell Metab, 2006. **4**(3): p. 245-54.
72. Hassler, J.R., et al., *The IRE1alpha/XBP1s Pathway Is Essential for the Glucose Response and Protection of beta Cells.* PLoS Biol, 2015. **13**(10): p. e1002277.
73. Chen, D., et al., *IRE1alpha inhibition decreased TXNIP/NLRP3 inflammasome activation through miR-17-5p after neonatal hypoxic-ischemic brain injury in rats.* J Neuroinflammation, 2018. **15**(1): p. 32.
74. Benhamron, S., et al., *Regulated IRE1-dependent decay participates in curtailing immunoglobulin secretion from plasma cells.* Eur J Immunol, 2014. **44**(3): p. 867-76.
75. Hetz, C. and L.H. Glimcher, *Fine-tuning of the unfolded protein response: Assembling the IRE1alpha interactome.* Mol Cell, 2009. **35**(5): p. 551-61.
76. Yoneda, T., et al., *Activation of caspase-12, an endoplastic reticulum (ER) resident caspase, through tumor necrosis factor receptor-associated factor 2-dependent mechanism in response to the ER stress.* Journal of Biological Chemistry, 2001. **276**(17): p. 13935-13940.
77. Yoneda, T., et al., *Activation of caspase-12, an endoplastic reticulum (ER) resident caspase, through tumor necrosis factor receptor-associated factor 2-dependent mechanism in response to the ER stress.* J Biol Chem, 2001. **276**(17): p. 13935-40.
78. Tam, A.B., et al., *ER stress activates NF-kappaB by integrating functions of basal IKK activity, IRE1 and PERK.* PLoS One, 2012. **7**(10): p. e45078.
79. Sowers, C.R., et al., *The protein kinase PERK/EIF2AK3 regulates proinsulin processing not via protein synthesis but by controlling endoplasmic reticulum chaperones.* J Biol Chem, 2018. **293**(14): p. 5134-5149.
80. Glimcher, L.H. and A.H. Lee, *From sugar to fat: How the transcription factor XBP1 regulates hepatic lipogenesis.* Ann N Y Acad Sci, 2009. **1173 Suppl 1**: p. E2-9.
81. Tang, C.H., et al., *Phosphorylation of IRE1 at S729 regulates RIDD in B cells and antibody production after immunization.* J Cell Biol, 2018. **217**(5): p. 1739-1755.
82. Smith, J.A., *Regulation of Cytokine Production by the Unfolded Protein Response; Implications for Infection and Autoimmunity.* Front Immunol, 2018. **9**: p. 422.
83. So, J.S., *Roles of Endoplasmic Reticulum Stress in Immune Responses.* Mol Cells, 2018. **41**(8): p. 705-716.

84. Harnoss, J.M., et al., *Disruption of IRE1alpha through its kinase domain attenuates multiple myeloma.* Proc Natl Acad Sci U S A, 2019. **116**(33): p. 16420-16429.
85. Talty, A., et al., *Inhibition of IRE1alpha RNase activity reduces NLRP3 inflammasome assembly and processing of pro-IL1beta.* Cell Death Dis, 2019. **10**(9): p. 622.
86. Logue, S.E., et al., *Inhibition of IRE1 RNase activity modulates the tumor cell secretome and enhances response to chemotherapy.* Nat Commun, 2018. **9**(1): p. 3267.
87. Zhang, K., et al., *Endoplasmic reticulum stress activates cleavage of CREBH to induce a systemic inflammatory response.* Cell, 2006. **124**(3): p. 587-99.
88. Allagnat, F., et al., *C/EBP homologous protein contributes to cytokine-induced pro-inflammatory responses and apoptosis in beta-cells.* Cell Death Differ, 2012. **19**(11): p. 1836-46.
89. Brozzi, F., et al., *Cytokines induce endoplasmic reticulum stress in human, rat and mouse beta cells via different mechanisms.* Diabetologia, 2015. **58**(10): p. 2307-16.
90. Beisel, C., et al., *TLR7-mediated activation of XBP1 correlates with the IFNalpha production in humans.* Cytokine, 2017. **94**: p. 55-58.
91. Hu, F., et al., *ER stress and its regulator X-box-binding protein-1 enhance polyIC-induced innate immune response in dendritic cells.* Eur J Immunol, 2011. **41**(4): p. 1086-97.
92. Lencer, W.I., et al., *Innate immunity at mucosal surfaces: the IRE1-RIDD-RIG-I pathway.* Trends Immunol, 2015. **36**(7): p. 401-9.
93. Chaplin, D.D., *Overview of the immune response.* J Allergy Clin Immunol, 2010. **125**(2 Suppl 2): p. S3-23.
94. Brubaker, S.W., et al., *Innate immune pattern recognition: a cell biological perspective.* Annu Rev Immunol, 2015. **33**: p. 257-90.
95. Litman, G.W., J.P. Rast, and S.D. Fugmann, *The origins of vertebrate adaptive immunity.* Nat Rev Immunol, 2010. **10**(8): p. 543-53.
96. Schatz, D.G. and Y. Ji, *Recombination centres and the orchestration of V(D)J recombination.* Nat Rev Immunol, 2011. **11**(4): p. 251-63.
97. Pradeu, T. and L. Du Pasquier, *Immunological memory: What's in a name?* Immunol Rev, 2018. **283**(1): p. 7-20.
98. Kumar, B.V., T.J. Connors, and D.L. Farber, *Human T Cell Development, Localization, and Function throughout Life.* Immunity, 2018. **48**(2): p. 202-213.
99. Luckheeram, R.V., et al., *CD4(+)T cells: differentiation and functions.* Clin Dev Immunol, 2012. **2012**: p. 925135.
100. Andersen, M.H., et al., *Cytotoxic T cells.* J Invest Dermatol, 2006. **126**(1): p. 32-41.
101. Josefowicz, S.Z., L.F. Lu, and A.Y. Rudensky, *Regulatory T cells: mechanisms of differentiation and function.* Annu Rev Immunol, 2012. **30**: p. 531-64.
102. Korn, T., et al., *IL-17 and Th17 Cells.* Annu Rev Immunol, 2009. **27**: p. 485-517.
103. Janeway, C.A., Jr., *Approaching the asymptote? Evolution and revolution in immunology.* Cold Spring Harb Symp Quant Biol, 1989. **54 Pt 1**: p. 1-13.
104. Akira, S., S. Uematsu, and O. Takeuchi, *Pathogen recognition and innate immunity.* Cell, 2006. **124**(4): p. 783-801.
105. Kawai, T. and S. Akira, *The role of pattern-recognition receptors in innate immunity: update on Toll-like receptors.* Nat Immunol, 2010. **11**(5): p. 373-84.
106. Kawasaki, T. and T. Kawai, *Toll-like receptor signaling pathways.* Front Immunol, 2014. **5**: p. 461.
107. Palsson-McDermott, E.M. and L.A. O'Neill, *Signal transduction by the lipopolysaccharide receptor, Toll-like receptor-4.* Immunology, 2004. **113**(2): p. 153-62.

108. Schumann, R.R., et al., *Structure and function of lipopolysaccharide binding protein.* Science, 1990. **249**(4975): p. 1429-31.
109. O'Neill, L.A., *The interleukin-1 receptor/Toll-like receptor superfamily: signal transduction during inflammation and host defense.* Sci STKE, 2000. **2000**(44): p. re1.
110. Dunne, A. and L.A. O'Neill, *Adaptor usage and Toll-like receptor signaling specificity.* FEBS Lett, 2005. **579**(15): p. 3330-5.
111. Lawrence, T., *The nuclear factor NF-kappaB pathway in inflammation.* Cold Spring Harb Perspect Biol, 2009. **1**(6): p. a001651.
112. Guha, M. and N. Mackman, *LPS induction of gene expression in human monocytes.* Cell Signal, 2001. **13**(2): p. 85-94.
113. Doyle, S., et al., *IRF3 mediates a TLR3/TLR4-specific antiviral gene program.* Immunity, 2002. **17**(3): p. 251-63.
114. Broz, P. and V.M. Dixit, *Inflammasomes: mechanism of assembly, regulation and signalling.* Nat Rev Immunol, 2016. **16**(7): p. 407-20.
115. Martinon, F., K. Burns, and J. Tschopp, *The inflammasome: a molecular platform triggering activation of inflammatory caspases and processing of proIL-beta.* Mol Cell, 2002. **10**(2): p. 417-26.
116. Strowig, T., et al., *Inflammasomes in health and disease.* Nature, 2012. **481**(7381): p. 278-86.
117. Church, L.D., G.P. Cook, and M.F. McDermott, *Primer: inflammasomes and interleukin 1beta in inflammatory disorders.* Nat Clin Pract Rheumatol, 2008. **4**(1): p. 34-42.
118. Hoffman, H.M., et al., *Mutation of a new gene encoding a putative pyrin-like protein causes familial cold autoinflammatory syndrome and Muckle-Wells syndrome.* Nat Genet, 2001. **29**(3): p. 301-5.
119. Poyet, J.L., et al., *Identification of Ipaf, a human caspase-1-activating protein related to Apaf-1.* J Biol Chem, 2001. **276**(30): p. 28309-13.
120. Hornung, V., et al., *AIM2 recognizes cytosolic dsDNA and forms a caspase-1-activating inflammasome with ASC.* Nature, 2009. **458**(7237): p. 514-8.
121. Fernandes-Alnemri, T., et al., *AIM2 activates the inflammasome and cell death in response to cytoplasmic DNA.* Nature, 2009. **458**(7237): p. 509-13.
122. Burckstummer, T., et al., *An orthogonal proteomic-genomic screen identifies AIM2 as a cytoplasmic DNA sensor for the inflammasome.* Nat Immunol, 2009. **10**(3): p. 266-72.
123. Roberts, T.L., et al., *HIN-200 proteins regulate caspase activation in response to foreign cytoplasmic DNA.* Science, 2009. **323**(5917): p. 1057-60.
124. Richards, N., et al., *Interaction between pyrin and the apoptotic speck protein (ASC) modulates ASC-induced apoptosis.* J Biol Chem, 2001. **276**(42): p. 39320-9.
125. Russo, A.J., et al., *Emerging Insights into Noncanonical Inflammasome Recognition of Microbes.* J Mol Biol, 2018. **430**(2): p. 207-216.
126. Pellegrini, C., et al., *Canonical and Non-Canonical Activation of NLRP3 Inflammasome at the Crossroad between Immune Tolerance and Intestinal Inflammation.* Front Immunol, 2017. **8**: p. 36.
127. Gurung, P., et al., *Toll or interleukin-1 receptor (TIR) domain-containing adaptor inducing interferon-beta (TRIF)-mediated caspase-11 protease production integrates Toll-like receptor 4 (TLR4) protein- and Nlrp3 inflammasome-mediated host defense against enteropathogens.* J Biol Chem, 2012. **287**(41): p. 34474-83.
128. Shi, J., et al., *Inflammatory caspases are innate immune receptors for intracellular LPS.* Nature, 2014. **514**(7521): p. 187-92.

129. Lim, Y. and S. Kumar, *A single cut to pyroptosis.* Oncotarget, 2015. **6**(35): p. 36926-7.
130. Aksentijevich, I., et al., *The clinical continuum of cryopyrinopathies: novel CIAS1 mutations in North American patients and a new cryopyrin model.* Arthritis Rheum, 2007. **56**(4): p. 1273-1285.
131. Lu, A. and H. Wu, *Structural mechanisms of inflammasome assembly.* FEBS J, 2015. **282**(3): p. 435-44.
132. Cai, X., et al., *Prion-like polymerization underlies signal transduction in antiviral immune defense and inflammasome activation.* Cell, 2014. **156**(6): p. 1207-1222.
133. Lu, A., et al., *Unified polymerization mechanism for the assembly of ASC-dependent inflammasomes.* Cell, 2014. **156**(6): p. 1193-1206.
134. Sborgi, L., et al., *Structure and assembly of the mouse ASC inflammasome by combined NMR spectroscopy and cryo-electron microscopy.* Proc Natl Acad Sci U S A, 2015. **112**(43): p. 13237-42.
135. Broz, P., *Inflammasome assembly: The wheels are turning.* Cell Res, 2015. **25**(12): p. 1277-8.
136. O'Connor, W., Jr., et al., *Cutting edge: CIAS1/cryopyrin/PYPAF1/NALP3/CATERPILLER 1.1 is an inducible inflammatory mediator with NF-kappa B suppressive properties.* J Immunol, 2003. **171**(12): p. 6329-33.
137. Bauernfeind, F.G., et al., *Cutting edge: NF-kappaB activating pattern recognition and cytokine receptors license NLRP3 inflammasome activation by regulating NLRP3 expression.* J Immunol, 2009. **183**(2): p. 787-91.
138. Gupta, N., et al., *Activation of NLRP3 inflammasome complex potentiates venous thrombosis in response to hypoxia.* Proc Natl Acad Sci U S A, 2017. **114**(18): p. 4763-4768.
139. Moon, J.S., et al., *mTORC1-Induced HK1-Dependent Glycolysis Regulates NLRP3 Inflammasome Activation.* Cell Rep, 2015. **12**(1): p. 102-115.
140. Shim, D.W. and K.H. Lee, *Posttranslational Regulation of the NLR Family Pyrin Domain-Containing 3 Inflammasome.* Front Immunol, 2018. **9**: p. 1054.
141. Cassel, S.L., et al., *The Nalp3 inflammasome is essential for the development of silicosis.* Proc Natl Acad Sci U S A, 2008. **105**(26): p. 9035-40.
142. Cruz, C.M., et al., *ATP activates a reactive oxygen species-dependent oxidative stress response and secretion of proinflammatory cytokines in macrophages.* J Biol Chem, 2007. **282**(5): p. 2871-9.
143. Dostert, C., et al., *Innate immune activation through Nalp3 inflammasome sensing of asbestos and silica.* Science, 2008. **320**(5876): p. 674-7.
144. Kanneganti, T.D., et al., *Bacterial RNA and small antiviral compounds activate caspase-1 through cryopyrin/Nalp3.* Nature, 2006. **440**(7081): p. 233-6.
145. Franchi, L., et al., *Differential requirement of P2X7 receptor and intracellular K+ for caspase-1 activation induced by intracellular and extracellular bacteria.* J Biol Chem, 2007. **282**(26): p. 18810-8.
146. Compan, V., et al., *Cell volume regulation modulates NLRP3 inflammasome activation.* Immunity, 2012. **37**(3): p. 487-500.
147. Halle, A., et al., *The NALP3 inflammasome is involved in the innate immune response to amyloid-beta.* Nat Immunol, 2008. **9**(8): p. 857-65.
148. Munoz-Planillo, R., et al., *K(+) efflux is the common trigger of NLRP3 inflammasome activation by bacterial toxins and particulate matter.* Immunity, 2013. **38**(6): p. 1142-53.
149. Schorn, C., et al., *Sodium overload and water influx activate the NALP3 inflammasome.* J Biol Chem, 2011. **286**(1): p. 35-41.

150. Zhou, R., et al., *A role for mitochondria in NLRP3 inflammasome activation.* Nature, 2011. **469**(7329): p. 221-5.
151. Petrilli, V., et al., *Activation of the NALP3 inflammasome is triggered by low intracellular potassium concentration.* Cell Death Differ, 2007. **14**(9): p. 1583-9.
152. Murakami, T., et al., *Critical role for calcium mobilization in activation of the NLRP3 inflammasome.* Proc Natl Acad Sci U S A, 2012. **109**(28): p. 11282-7.
153. Yaron, J.R., et al., *K(+) regulates Ca(2+) to drive inflammasome signaling: dynamic visualization of ion flux in live cells.* Cell Death Dis, 2015. **6**: p. e1954.
154. Di, A., et al., *The TWIK2 Potassium Efflux Channel in Macrophages Mediates NLRP3 Inflammasome-Induced Inflammation.* Immunity, 2018. **49**(1): p. 56-65 e4.
155. Gross, C.J., et al., *K(+) Efflux-Independent NLRP3 Inflammasome Activation by Small Molecules Targeting Mitochondria.* Immunity, 2016. **45**(4): p. 761-773.
156. Zhong, Z., et al., *New mitochondrial DNA synthesis enables NLRP3 inflammasome activation.* Nature, 2018. **560**(7717): p. 198-203.
157. Gurung, P., J.R. Lukens, and T.D. Kanneganti, *Mitochondria: diversity in the regulation of the NLRP3 inflammasome.* Trends Mol Med, 2015. **21**(3): p. 193-201.
158. Bauernfeind, F., et al., *Cutting edge: reactive oxygen species inhibitors block priming, but not activation, of the NLRP3 inflammasome.* J Immunol, 2011. **187**(2): p. 613-7.
159. Zhang, Q., et al., *Circulating mitochondrial DAMPs cause inflammatory responses to injury.* Nature, 2010. **464**(7285): p. 104-7.
160. Lemasters, J.J., et al., *Mitochondrial calcium and the permeability transition in cell death.* Biochim Biophys Acta, 2009. **1787**(11): p. 1395-401.
161. Shimada, K., et al., *Oxidized mitochondrial DNA activates the NLRP3 inflammasome during apoptosis.* Immunity, 2012. **36**(3): p. 401-14.
162. Afonina, I.S., et al., *Proteolytic Processing of Interleukin-1 Family Cytokines: Variations on a Common Theme.* Immunity, 2015. **42**(6): p. 991-1004.
163. Monteleone, M., J.L. Stow, and K. Schroder, *Mechanisms of unconventional secretion of IL-1 family cytokines.* Cytokine, 2015. **74**(2): p. 213-8.
164. Brough, D. and N.J. Rothwell, *Caspase-1-dependent processing of pro-interleukin-1beta is cytosolic and precedes cell death.* J Cell Sci, 2007. **120**(Pt 5): p. 772-81.
165. Brough, D., P. Pelegrin, and N.J. Rothwell, *Pannexin-1-dependent caspase-1 activation and secretion of IL-1beta is regulated by zinc.* Eur J Immunol, 2009. **39**(2): p. 352-8.
166. MacKenzie, A., et al., *Rapid secretion of interleukin-1beta by microvesicle shedding.* Immunity, 2001. **15**(5): p. 825-35.
167. Cullen, S.P., et al., *Diverse Activators of the NLRP3 Inflammasome Promote IL-1beta Secretion by Triggering Necrosis.* Cell Rep, 2015. **11**(10): p. 1535-48.
168. Man, S.M., R. Karki, and T.D. Kanneganti, *Molecular mechanisms and functions of pyroptosis, inflammatory caspases and inflammasomes in infectious diseases.* Immunol Rev, 2017. **277**(1): p. 61-75.
169. Galluzzi, L., et al., *Molecular mechanisms of cell death: recommendations of the Nomenclature Committee on Cell Death 2018.* Cell Death Differ, 2018. **25**(3): p. 486-541.
170. Liu, X., et al., *Inflammasome-activated gasdermin D causes pyroptosis by forming membrane pores.* Nature, 2016. **535**(7610): p. 153-8.
171. Evavold, C.L., et al., *The Pore-Forming Protein Gasdermin D Regulates Interleukin-1 Secretion from Living Macrophages.* Immunity, 2018. **48**(1): p. 35-44 e6.
172. Coussens, L.M. and Z. Werb, *Inflammation and cancer.* Nature, 2002. **420**(6917): p. 860-7.

173. Landskron, G., et al., *Chronic inflammation and cytokines in the tumor microenvironment.* J Immunol Res, 2014. **2014**: p. 149185.
174. Yang, L., Y. Pang, and H.L. Moses, *TGF-beta and immune cells: an important regulatory axis in the tumor microenvironment and progression.* Trends Immunol, 2010. **31**(6): p. 220-7.
175. Li, Y.L., H. Zhao, and X.B. Ren, *Relationship of VEGF/VEGFR with immune and cancer cells: staggering or forward?* Cancer Biol Med, 2016. **13**(2): p. 206-14.
176. Weinberg, F., N. Ramnath, and D. Nagrath, *Reactive Oxygen Species in the Tumor Microenvironment: An Overview.* Cancers (Basel), 2019. **11**(8).
177. Chen, X., et al., *Reactive Oxygen Species Regulate T Cell Immune Response in the Tumor Microenvironment.* Oxid Med Cell Longev, 2016. **2016**: p. 1580967.
178. Yadav, D. and A.B. Lowenfels, *The epidemiology of pancreatitis and pancreatic cancer.* Gastroenterology, 2013. **144**(6): p. 1252-61.
179. Keller, D.S., et al., *Colorectal cancer in inflammatory bowel disease: review of the evidence.* Tech Coloproctol, 2019. **23**(1): p. 3-13.
180. Freeman, H.J., *Colorectal cancer risk in Crohn's disease.* World J Gastroenterol, 2008. **14**(12): p. 1810-1.
181. Moossavi, M., et al., *Role of the NLRP3 inflammasome in cancer.* Mol Cancer, 2018. **17**(1): p. 158.
182. Urra, H., et al., *Endoplasmic Reticulum Stress and the Hallmarks of Cancer.* Trends Cancer, 2016. **2**(5): p. 252-262.
183. Ma, Y. and L.M. Hendershot, *The role of the unfolded protein response in tumour development: friend or foe?* Nat Rev Cancer, 2004. **4**(12): p. 966-77.
184. Chevet, E., C. Hetz, and A. Samali, *Endoplasmic reticulum stress-activated cell reprogramming in oncogenesis.* Cancer Discov, 2015. **5**(6): p. 586-97.
185. Forbes, S.A., et al., *COSMIC (the Catalogue of Somatic Mutations in Cancer): a resource to investigate acquired mutations in human cancer.* Nucleic Acids Res, 2010. **38**(Database issue): p. D652-7.
186. Maurel, M., et al., *Controlling the unfolded protein response-mediated life and death decisions in cancer.* Semin Cancer Biol, 2015. **33**: p. 57-66.
187. Madden, E., et al., *The role of the unfolded protein response in cancer progression: From oncogenesis to chemoresistance.* Biol Cell, 2019. **111**(1): p. 1-17.
188. Zhao, N., et al., *Pharmacological targeting of MYC-regulated IRE1/XBP1 pathway suppresses MYC-driven breast cancer.* J Clin Invest, 2018. **128**(4): p. 1283-1299.
189. Blazanin, N., et al., *ER stress and distinct outputs of the IRE1alpha RNase control proliferation and senescence in response to oncogenic Ras.* Proc Natl Acad Sci U S A, 2017. **114**(37): p. 9900-9905.
190. Rong, R., et al., *Oncogenic Ras-mediated downregulation of Gadd153/CHOP is required for Ras-induced cellular transformation.* Oncogene, 2005. **24**(30): p. 4867-72.
191. Hart, L.S., et al., *ER stress-mediated autophagy promotes Myc-dependent transformation and tumor growth.* J Clin Invest, 2012. **122**(12): p. 4621-34.
192. Namba, T., et al., *Loss of p53 enhances the function of the endoplasmic reticulum through activation of the IRE1alpha/XBP1 pathway.* Oncotarget, 2015. **6**(24): p. 19990-20001.
193. Greenman, C., et al., *Patterns of somatic mutation in human cancer genomes.* Nature, 2007. **446**(7132): p. 153-8.
194. Sheng, X., et al., *Divergent androgen regulation of unfolded protein response pathways drives prostate cancer.* EMBO Mol Med, 2015. **7**(6): p. 788-801.
195. Lhomond, S., et al., *Dual IRE1 RNase functions dictate glioblastoma development.* EMBO Mol Med, 2018. **10**(3).

196. Chien, W.W., et al., *Selective inhibition of unfolded protein response induces apoptosis in pancreatic cancer cells.* Oncotarget, 2014. **5**(13): p. 4881-4894.
197. Li, X.X., et al., *Knockdown of IRE1alpha inhibits colonic tumorigenesis through decreasing beta-catenin and IRE1alpha targeting suppresses colon cancer cells.* Oncogene, 2017. **36**(48): p. 6738-6746.
198. Thorpe, J.A. and S.R. Schwarze, *IRE1alpha controls cyclin A1 expression and promotes cell proliferation through XBP-1.* Cell Stress Chaperones, 2010. **15**(5): p. 497-508.
199. Harding, H.P., et al., *An integrated stress response regulates amino acid metabolism and resistance to oxidative stress.* Mol Cell, 2003. **11**(3): p. 619-33.
200. Bobrovnikova-Marjon, E., et al., *PERK promotes cancer cell proliferation and tumor growth by limiting oxidative DNA damage.* Oncogene, 2010. **29**(27): p. 3881-95.
201. Romero-Ramirez, L., et al., *XBP1 is essential for survival under hypoxic conditions and is required for tumor growth.* Cancer Res, 2004. **64**(17): p. 5943-7.
202. Chen, X., et al., *XBP1 promotes triple-negative breast cancer by controlling the HIF1alpha pathway.* Nature, 2014. **508**(7494): p. 103-107.
203. Shibuya, M., *Vascular Endothelial Growth Factor (VEGF) and Its Receptor (VEGFR) Signaling in Angiogenesis: A Crucial Target for Anti- and Pro-Angiogenic Therapies.* Genes Cancer, 2011. **2**(12): p. 1097-105.
204. Dongre, A. and R.A. Weinberg, *New insights into the mechanisms of epithelial-mesenchymal transition and implications for cancer.* Nat Rev Mol Cell Biol, 2019. **20**(2): p. 69-84.
205. Li, H., et al., *XBP1 induces snail expression to promote epithelial- to-mesenchymal transition and invasion of breast cancer cells.* Cell Signal, 2015. **27**(1): p. 82-9.
206. Dejeans, N., et al., *Autocrine control of glioma cells adhesion and migration through IRE1alpha-mediated cleavage of SPARC mRNA.* J Cell Sci, 2012. **125**(Pt 18): p. 4278-87.
207. Kleeff, J., et al., *Pancreatic cancer.* Nature Reviews Disease Primers, 2016. **2**: p. 16022.
208. Pandol, S., et al., *Desmoplasia of pancreatic ductal adenocarcinoma.* Clin Gastroenterol Hepatol, 2009. **7**(11 Suppl): p. S44-7.
209. Carr, R.M. and M.E. Fernandez-Zapico, *Pancreatic cancer microenvironment, to target or not to target?* EMBO Mol Med, 2016. **8**(2): p. 80-2.
210. Heinemann, V., et al., *Comparison of the cellular pharmacokinetics and toxicity of 2',2'-difluorodeoxycytidine and 1-beta-D-arabinofuranosylcytosine.* Cancer Res, 1988. **48**(14): p. 4024-31.
211. Heinemann, V., *Gemcitabine: progress in the treatment of pancreatic cancer.* Oncology, 2001. **60**(1): p. 8-18.
212. Kleeff, J., et al., *Pancreatic cancer.* Nat Rev Dis Primers, 2016. **2**: p. 16022.
213. Gifford, J.B., et al., *Expression of GRP78, Master Regulator of the Unfolded Protein Response, Increases Chemoresistance in Pancreatic Ductal Adenocarcinoma.* Mol Cancer Ther, 2016. **15**(5): p. 1043-52.
214. Niu, Z., et al., *Elevated GRP78 expression is associated with poor prognosis in patients with pancreatic cancer.* Sci Rep, 2015. **5**: p. 16067.
215. Moore, P.C., et al., *Parallel signaling through IRE1alpha and PERK regulates pancreatic neuroendocrine tumor growth and survival.* Cancer Res, 2019.
216. Palam, L.R., et al., *Integrated stress response is critical for gemcitabine resistance in pancreatic ductal adenocarcinoma.* Cell Death Dis, 2015. **6**: p. e1913.
217. Chien, W., et al., *Selective inhibition of unfolded protein response induces apoptosis in pancreatic cancer cells.* Oncotarget, 2014. **5**(13): p. 4881-94.

218. Dumartin, L., et al., *ER stress protein AGR2 precedes and is involved in the regulation of pancreatic cancer initiation.* Oncogene, 2017. **36**(22): p. 3094-3103.
219. Zhou, L., et al., *ATF6 regulates the development of chronic pancreatitis by inducing p53-mediated apoptosis.* Cell Death Dis, 2019. **10**(9): p. 662.
220. Jorgensen, E., et al., *Cigarette smoke induces endoplasmic reticulum stress and the unfolded protein response in normal and malignant human lung cells.* BMC Cancer, 2008. **8**: p. 229.
221. Ji, C., *Mechanisms of alcohol-induced endoplasmic reticulum stress and organ injuries.* Biochem Res Int, 2012. **2012**: p. 216450.
222. Procacci, P., et al., *Tumor(-)Stroma Cross-Talk in Human Pancreatic Ductal Adenocarcinoma: A Focus on the Effect of the Extracellular Matrix on Tumor Cell Phenotype and Invasive Potential.* Cells, 2018. **7**(10).
223. Yamamoto, G., et al., *Pancreatic Stellate Cells Have Distinct Characteristics From Hepatic Stellate Cells and Are Not the Unique Origin of Collagen-Producing Cells in the Pancreas.* Pancreas, 2017. **46**(9): p. 1141-1151.
224. Nielsen, M.F.B., M.B. Mortensen, and S. Detlefsen, *Identification of markers for quiescent pancreatic stellate cells in the normal human pancreas.* Histochem Cell Biol, 2017. **148**(4): p. 359-380.
225. Bynigeri, R.R., et al., *Pancreatic stellate cell: Pandora's box for pancreatic disease biology.* World J Gastroenterol, 2017. **23**(3): p. 382-405.
226. Fu, Y., et al., *The critical roles of activated stellate cells-mediated paracrine signaling, metabolism and onco-immunology in pancreatic ductal adenocarcinoma.* Mol Cancer, 2018. **17**(1): p. 62.
227. Schnittert, J., R. Bansal, and J. Prakash, *Targeting Pancreatic Stellate Cells in Cancer.* Trends Cancer, 2019. **5**(2): p. 128-142.
228. Wang, D. and R.N. DuBois, *Immunosuppression associated with chronic inflammation in the tumor microenvironment.* Carcinogenesis, 2015. **36**(10): p. 1085-93.
229. Gentles, A.J., et al., *The prognostic landscape of genes and infiltrating immune cells across human cancers.* Nat Med, 2015. **21**(8): p. 938-945.
230. Karamitopoulou, E., *Tumour microenvironment of pancreatic cancer: immune landscape is dictated by molecular and histopathological features.* Br J Cancer, 2019. **121**(1): p. 5-14.
231. Bates, S.E., *Pancreatic Cancer: Challenge and Inspiration.* Clin Cancer Res, 2017. **23**(7): p. 1628.
232. Young, K., et al., *Immunotherapy and pancreatic cancer: unique challenges and potential opportunities.* Ther Adv Med Oncol, 2018. **10**: p. 1758835918816281.
233. Ljunggren, H.G. and K. Karre, *In search of the 'missing self': MHC molecules and NK cell recognition.* Immunol Today, 1990. **11**(7): p. 237-44.
234. Chiossone, L., et al., *Natural killer cell immunotherapies against cancer: checkpoint inhibitors and more.* Semin Immunol, 2017. **31**: p. 55-63.
235. Paul, S. and G. Lal, *The Molecular Mechanism of Natural Killer Cells Function and Its Importance in Cancer Immunotherapy.* Front Immunol, 2017. **8**: p. 1124.
236. Van Audenaerde, J.R.M., et al., *Natural killer cells and their therapeutic role in pancreatic cancer: A systematic review.* Pharmacol Ther, 2018. **189**: p. 31-44.
237. Lim, S.A., et al., *Defective Localization With Impaired Tumor Cytotoxicity Contributes to the Immune Escape of NK Cells in Pancreatic Cancer Patients.* Front Immunol, 2019. **10**: p. 496.
238. Peng, Y.P., et al., *Comprehensive analysis of the percentage of surface receptors and cytotoxic granules positive natural killer cells in patients with pancreatic cancer, gastric cancer, and colorectal cancer.* J Transl Med, 2013. **11**: p. 262.

239. Peng, Y.P., et al., *Elevation of MMP-9 and IDO induced by pancreatic cancer cells mediates natural killer cell dysfunction.* BMC Cancer, 2014. **14**: p. 738.
240. Sousa, C.M., et al., *Erratum: Pancreatic stellate cells support tumour metabolism through autophagic alanine secretion.* Nature, 2016. **540**(7631): p. 150.
241. Maess, M.B., B. Wittig, and S. Lorkowski, *Highly efficient transfection of human THP-1 macrophages by nucleofection.* J Vis Exp, 2014(91): p. e51960.
242. Reimold, A.M., et al., *Plasma cell differentiation requires the transcription factor XBP-1.* Nature, 2001. **412**(6844): p. 300-7.
243. Osorio, F., et al., *The unfolded-protein-response sensor IRE-1α regulates the function of CD8α+ dendritic cells.* Nat Immunol, 2014. **15**(3): p. 248-57.
244. Shan, B., et al., *The metabolic ER stress sensor IRE1alpha suppresses alternative activation of macrophages and impairs energy expenditure in obesity.* Nat Immunol, 2017. **18**(5): p. 519-529.
245. Martinon, F., et al., *TLR activation of the transcription factor XBP1 regulates innate immune responses in macrophages.* Nat Immunol, 2010. **11**(5): p. 411-8.
246. Bronner, D.N., et al., *Endoplasmic Reticulum Stress Activates the Inflammasome via NLRP3- and Caspase-2-Driven Mitochondrial Damage.* Immunity, 2015. **43**(3): p. 451-62.
247. Abuaita, B.H., et al., *The Endoplasmic Reticulum Stress Sensor Inositol-Requiring Enzyme 1alpha Augments Bacterial Killing through Sustained Oxidant Production.* MBio, 2015. **6**(4): p. e00705.
248. Qiu, Q., et al., *Toll-like receptor-mediated IRE1alpha activation as a therapeutic target for inflammatory arthritis.* EMBO J, 2013. **32**(18): p. 2477-90.
249. Tsuchiya, S., et al., *Establishment and characterization of a human acute monocytic leukemia cell line (THP-1).* Int J Cancer, 1980. **26**(2): p. 171-6.
250. Lu, Y.C., W.C. Yeh, and P.S. Ohashi, *LPS/TLR4 signal transduction pathway.* Cytokine, 2008. **42**(2): p. 145-151.
251. Volkmann, K., et al., *Potent and selective inhibitors of the inositol-requiring enzyme 1 endoribonuclease.* J Biol Chem, 2011. **286**(14): p. 12743-55.
252. Sanches, M., et al., *Structure and mechanism of action of the hydroxy-aryl-aldehyde class of IRE1 endoribonuclease inhibitors.* Nat Commun, 2014. **5**: p. 4202.
253. Sheng, X., et al., *IRE1alpha-XBP1s pathway promotes prostate cancer by activating c-MYC signaling.* Nat Commun, 2019. **10**(1): p. 323.
254. Lopez-Castejon, G. and D. Brough, *Understanding the mechanism of IL-1beta secretion.* Cytokine Growth Factor Rev, 2011. **22**(4): p. 189-95.
255. Yang, Y., et al., *Recent advances in the mechanisms of NLRP3 inflammasome activation and its inhibitors.* Cell Death Dis, 2019. **10**(2): p. 128.
256. Lerner, A.G., et al., *IRE1alpha induces thioredoxin-interacting protein to activate the NLRP3 inflammasome and promote programmed cell death under irremediable ER stress.* Cell Metab, 2012. **16**(2): p. 250-64.
257. Oslowski, C.M., et al., *Thioredoxin-interacting protein mediates ER stress-induced beta cell death through initiation of the inflammasome.* Cell Metab, 2012. **16**(2): p. 265-73.
258. Zha, Q.B., et al., *ATP-Induced Inflammasome Activation and Pyroptosis Is Regulated by AMP-Activated Protein Kinase in Macrophages.* Front Immunol, 2016. **7**: p. 597.
259. Boro, M. and K.N. Balaji, *CXCL1 and CXCL2 Regulate NLRP3 Inflammasome Activation via G-Protein-Coupled Receptor CXCR2.* J Immunol, 2017. **199**(5): p. 1660-1671.
260. Sanders, R., et al., *Considerations for accurate gene expression measurement by reverse transcription quantitative PCR when analysing clinical samples.* Anal Bioanal Chem, 2014. **406**(26): p. 6471-83.

261. Tufanli, O., et al., *Targeting IRE1 with small molecules counteracts progression of atherosclerosis.* Proc Natl Acad Sci U S A, 2017. **114**(8): p. E1395-E1404.
262. He, Y., H. Hara, and G. Nunez, *Mechanism and Regulation of NLRP3 Inflammasome Activation.* Trends Biochem Sci, 2016. **41**(12): p. 1012-1021.
263. Savic, S., et al., *TLR dependent XBP-1 activation induces an autocrine loop in rheumatoid arthritis synoviocytes.* J Autoimmun, 2014. **50**: p. 59-66.
264. Dickie, L.J., et al., *Involvement of X-box binding protein 1 and reactive oxygen species pathways in the pathogenesis of tumour necrosis factor receptor-associated periodic syndrome.* Ann Rheum Dis, 2012. **71**(12): p. 2035-43.
265. Wang, W., et al., *Inhibition of NLRP1 inflammasome might be a novel therapeutic target in the treatment of peripheral arterial disease.* Int J Cardiol, 2018. **256**: p. 29.
266. D'Osualdo, A., et al., *Transcription Factor ATF4 Induces NLRP1 Inflammasome Expression during Endoplasmic Reticulum Stress.* PLoS One, 2015. **10**(6): p. e0130635.
267. Kim, Y.H., H.S. Joo, and D.S. Kim, *Nitric oxide induction of IRE1-alpha-dependent CREB phosphorylation in human glioma cells.* Nitric Oxide, 2010. **23**(2): p. 112-20.
268. Xu, Z., et al., *Inhibition of ER stress-related IRE1alpha/CREB/NLRP1 pathway promotes the apoptosis of human chronic myelogenous leukemia cell.* Mol Immunol, 2018. **101**: p. 377-385.
269. He, Y., et al., *NEK7 is an essential mediator of NLRP3 activation downstream of potassium efflux.* Nature, 2016. **530**(7590): p. 354-7.
270. Zhang, P., et al., *A novel indication of thioredoxin-interacting protein as a tumor suppressor gene in malignant glioma.* Oncol Lett, 2017. **14**(2): p. 2053-2058.
271. Park, Y.J., et al., *TXNIP deficiency exacerbates endotoxic shock via the induction of excessive nitric oxide synthesis.* PLoS Pathog, 2013. **9**(10): p. e1003646.
272. Hernandez-Cuellar, E., et al., *Cutting edge: nitric oxide inhibits the NLRP3 inflammasome.* J Immunol, 2012. **189**(11): p. 5113-7.
273. Oberstein, P.E. and K.P. Olive, *Pancreatic cancer: why is it so hard to treat?* Therap Adv Gastroenterol, 2013. **6**(4): p. 321-37.
274. Cannon, A., et al., *Desmoplasia in pancreatic ductal adenocarcinoma: insight into pathological function and therapeutic potential.* Genes Cancer, 2018. **9**(3-4): p. 78-86.
275. Watari, N., Y. Hotta, and Y. Mabuchi, *Morphological studies on a vitamin A-storing cell and its complex with macrophage observed in mouse pancreatic tissues following excess vitamin A administration.* Okajimas Folia Anat Jpn, 1982. **58**(4-6): p. 837-58.
276. Apte, M.V., R.C. Pirola, and J.S. Wilson, *Pancreatic stellate cells: a starring role in normal and diseased pancreas.* Front Physiol, 2012. **3**: p. 344.
277. Steele, C.W., et al., *Exploiting inflammation for therapeutic gain in pancreatic cancer.* Br J Cancer, 2013. **108**(5): p. 997-1003.
278. Lieber, M., et al., *Establishment of a continuous tumor-cell line (panc-1) from a human carcinoma of the exocrine pancreas.* Int J Cancer, 1975. **15**(5): p. 741-7.
279. Tan, M.H., et al., *Characterization of a new primary human pancreatic tumor line.* Cancer Invest, 1986. **4**(1): p. 15-23.
280. Kyriazis, A.P., et al., *Establishment and characterization of human pancreatic adenocarcinoma cell line SW-1990 in tissue culture and the nude mouse.* Cancer Res, 1983. **43**(9): p. 4393-401.
281. Yu, Q., et al., *Type I interferons mediate pancreatic toxicities of PERK inhibition.* Proc Natl Acad Sci U S A, 2015. **112**(50): p. 15420-5.
282. Apte, M.V., et al., *Pancreatic stellate cells are activated by proinflammatory cytokines: implications for pancreatic fibrogenesis.* Gut, 1999. **44**(4): p. 534-41.

283. Fujita, H., et al., *alpha-Smooth Muscle Actin Expressing Stroma Promotes an Aggressive Tumor Biology in Pancreatic Ductal Adenocarcinoma.* Pancreas, 2010. **39**(8): p. 1254-1262.
284. Thomas, D. and P. Radhakrishnan, *Tumor-stromal crosstalk in pancreatic cancer and tissue fibrosis.* Mol Cancer, 2019. **18**(1): p. 14.
285. Yang, B., et al., *The role of interleukin 17 in tumour proliferation, angiogenesis, and metastasis.* Mediators Inflamm, 2014. **2014**: p. 623759.
286. Xie, S., et al., *IL-17 activates the canonical NF-kappaB signaling pathway in autoimmune B cells of BXD2 mice to upregulate the expression of regulators of G-protein signaling 16.* J Immunol, 2010. **184**(5): p. 2289-96.
287. Zhang, Y., et al., *Immune Cell Production of Interleukin 17 Induces Stem Cell Features of Pancreatic Intraepithelial Neoplasia Cells.* Gastroenterology, 2018. **155**(1): p. 210-223 e3.
288. Teicher, B.A. and S.P. Fricker, *CXCL12 (SDF-1)/CXCR4 pathway in cancer.* Clin Cancer Res, 2010. **16**(11): p. 2927-31.
289. Longo, V., et al., *Angiogenesis in pancreatic ductal adenocarcinoma: A controversial issue.* Oncotarget, 2016. **7**(36): p. 58649-58658.
290. Craven, K.E., J. Gore, and M. Korc, *Overview of pre-clinical and clinical studies targeting angiogenesis in pancreatic ductal adenocarcinoma.* Cancer Lett, 2016. **381**(1): p. 201-10.
291. Kim, H.W., et al., *Serum interleukin-6 is associated with pancreatic ductal adenocarcinoma progression pattern.* Medicine (Baltimore), 2017. **96**(5): p. e5926.
292. Shek, F.W., et al., *Expression of transforming growth factor-beta 1 by pancreatic stellate cells and its implications for matrix secretion and turnover in chronic pancreatitis.* Am J Pathol, 2002. **160**(5): p. 1787-98.
293. Principe, D.R., et al., *TGFbeta Signaling in the Pancreatic Tumor Microenvironment Promotes Fibrosis and Immune Evasion to Facilitate Tumorigenesis.* Cancer Res, 2016. **76**(9): p. 2525-39.
294. Meng, Z. and M. Lu, *RNA Interference-Induced Innate Immunity, Off-Target Effect, or Immune Adjuvant?* Front Immunol, 2017. **8**: p. 331.
295. Cullinan, S.B., et al., *Nrf2 is a direct PERK substrate and effector of PERK-dependent cell survival.* Mol Cell Biol, 2003. **23**(20): p. 7198-209.
296. Xie, H., et al., *IRE1alpha RNase-dependent lipid homeostasis promotes survival in Myc-transformed cancers.* J Clin Invest, 2018. **128**(4): p. 1300-1316.
297. Haqq, J., et al., *Pancreatic stellate cells and pancreas cancer: current perspectives and future strategies.* Eur J Cancer, 2014. **50**(15): p. 2570-82.
298. Lehmann, C., M. Zeis, and L. Uharek, *Activation of natural killer cells with interleukin 2 (IL-2) and IL-12 increases perforin binding and subsequent lysis of tumour cells.* Br J Haematol, 2001. **114**(3): p. 660-5.
299. Ikemizu, S., M. Chirifu, and S.J. Davis, *IL-2 and IL-15 signaling complexes: different but the same.* Nat Immunol, 2012. **13**(12): p. 1141-2.
300. Paolini, R., et al., *NK cells and interferons.* Cytokine Growth Factor Rev, 2015. **26**(2): p. 113-20.
301. Yagita, M., et al., *A novel natural killer cell line (KHYG-1) from a patient with aggressive natural killer cell leukemia carrying a p53 point mutation.* Leukemia, 2000. **14**(5): p. 922-30.
302. Garcia-Carbonero, N., et al., *New Hope for Pancreatic Ductal Adenocarcinoma Treatment Targeting Endoplasmic Reticulum Stress Response: A Systematic Review.* Int J Mol Sci, 2018. **19**(9).

303. Ding, Y. and Y. Du, *Clinicopathological significance and prognostic role of chemokine receptor CXCR4 expression in pancreatic ductal adenocarcinoma, a meta-analysis and literature review.* Int J Surg, 2019. **65**: p. 32-38.
304. Hu, B., et al., *Prognostic significance of CXCL5 expression in cancer patients: a meta-analysis.* Cancer Cell Int, 2018. **18**: p. 68.
305. Li, A., et al., *Overexpression of CXCL5 is associated with poor survival in patients with pancreatic cancer.* Am J Pathol, 2011. **178**(3): p. 1340-9.
306. Yamanaka, Y., et al., *Overexpression of acidic and basic fibroblast growth factors in human pancreatic cancer correlates with advanced tumor stage.* Cancer Res, 1993. **53**(21): p. 5289-96.
307. Coleman, S.J., et al., *Nuclear translocation of FGFR1 and FGF2 in pancreatic stellate cells facilitates pancreatic cancer cell invasion.* EMBO Mol Med, 2014. **6**(4): p. 467-81.
308. Couper, K.N., D.G. Blount, and E.M. Riley, *IL-10: the master regulator of immunity to infection.* J Immunol, 2008. **180**(9): p. 5771-7.
309. Mews, P., et al., *Pancreatic stellate cells respond to inflammatory cytokines: potential role in chronic pancreatitis.* Gut, 2002. **50**(4): p. 535-41.
310. Persaud, L., et al., *Mechanism of Action and Applications of Interleukin 24 in Immunotherapy.* Int J Mol Sci, 2016. **17**(6).
311. Sauane, M., et al., *Mda-7/IL-24 induces apoptosis of diverse cancer cell lines through JAK/STAT-independent pathways.* J Cell Physiol, 2003. **196**(2): p. 334-45.
312. Jia, Y., et al., *IL24 and its Receptors Regulate Growth and Migration of Pancreatic Cancer Cells and Are Potential Biomarkers for IL24 Molecular Therapy.* Anticancer Res, 2016. **36**(3): p. 1153-63.
313. Chada, S., et al., *mda-7/IL24 kills pancreatic cancer cells by inhibition of the Wnt/PI3K signaling pathways: identification of IL-20 receptor-mediated bystander activity against pancreatic cancer.* Mol Ther, 2005. **11**(5): p. 724-33.
314. Petit, I., D. Jin, and S. Rafii, *The SDF-1-CXCR4 signaling pathway: a molecular hub modulating neo-angiogenesis.* Trends Immunol, 2007. **28**(7): p. 299-307.
315. Krieg, A., et al., *CXCR4--A Prognostic and Clinicopathological Biomarker for Pancreatic Ductal Adenocarcinoma: A Meta-Analysis.* PLoS One, 2015. **10**(6): p. e0130192.
316. Gao, Z., et al., *Pancreatic stellate cells increase the invasion of human pancreatic cancer cells through the stromal cell-derived factor-1/CXCR4 axis.* Pancreatology, 2010. **10**(2-3): p. 186-93.
317. Mori, T., et al., *CXCR4 antagonist inhibits stromal cell-derived factor 1-induced migration and invasion of human pancreatic cancer.* Mol Cancer Ther, 2004. **3**(1): p. 29-37.
318. Wu, Y.S., et al., *Soluble factors from stellate cells induce pancreatic cancer cell proliferation via Nrf2-activated metabolic reprogramming and ROS detoxification.* Oncotarget, 2016. **7**(24): p. 36719-36732.
319. Kikuta, K., et al., *Pancreatic stellate cells promote epithelial-mesenchymal transition in pancreatic cancer cells.* Biochem Biophys Res Commun, 2010. **403**(3-4): p. 380-4.
320. Liu, Y., et al., *Blockade of SDF-1/CXCR4 reduces adhesion-mediated chemoresistance of multiple myeloma cells via interacting with interleukin-6.* J Cell Physiol, 2019. **234**(11): p. 19702-19714.
321. Mahadevan, N.R., et al., *Transmission of endoplasmic reticulum stress and pro-inflammation from tumor cells to myeloid cells.* Proc Natl Acad Sci U S A, 2011. **108**(16): p. 6561-6.
322. Rodvold, J.J., et al., *Intercellular transmission of the unfolded protein response promotes survival and drug resistance in cancer cells.* Sci Signal, 2017. **10**(482).

323. Sprenkle, N.T., et al., *Endoplasmic reticulum stress is transmissible in vitro between cells of the central nervous system.* J Neurochem, 2019. **148**(4): p. 516-530.
324. Sousa, C.M., et al., *Pancreatic stellate cells support tumour metabolism through autophagic alanine secretion.* Nature, 2016. **536**(7617): p. 479-83.
325. van der Harg, J.M., et al., *The UPR reduces glucose metabolism via IRE1 signaling.* Biochim Biophys Acta Mol Cell Res, 2017. **1864**(4): p. 655-665.
326. Cheng, X., et al., *Connecting endoplasmic reticulum stress to autophagy through IRE1/JNK/beclin-1 in breast cancer cells.* Int J Mol Med, 2014. **34**(3): p. 772-81.
327. Urra, H., et al., *IRE1alpha governs cytoskeleton remodelling and cell migration through a direct interaction with filamin A.* Nat Cell Biol, 2018. **20**(8): p. 942-953.
328. Martinez, G., et al., *Regulation of Memory Formation by the Transcription Factor XBP1.* Cell Rep, 2016. **14**(6): p. 1382-1394.
329. Smith, J.A., et al., *Endoplasmic reticulum stress and the unfolded protein response are linked to synergistic IFN-beta induction via X-box binding protein 1.* Eur J Immunol, 2008. **38**(5): p. 1194-203.
330. Iwasaki, Y., et al., *Activating transcription factor 4 links metabolic stress to interleukin-6 expression in macrophages.* Diabetes, 2014. **63**(1): p. 152-61.
331. Zeng, L., et al., *XBP-1 couples endoplasmic reticulum stress to augmented IFN-beta induction via a cis-acting enhancer in macrophages.* J Immunol, 2010. **185**(4): p. 2324-30.
332. Land, W.G., et al., *Transplantation and Damage-Associated Molecular Patterns (DAMPs).* Am J Transplant, 2016. **16**(12): p. 3338-3361.
333. Touitou, I., et al., *Infevers: an evolving mutation database for auto-inflammatory syndromes.* Hum Mutat, 2004. **24**(3): p. 194-8.
334. Mangan, M.S.J., et al., *Targeting the NLRP3 inflammasome in inflammatory diseases.* Nat Rev Drug Discov, 2018. **17**(9): p. 688.
335. Segovia, M., et al., *Targeting TMEM176B Enhances Antitumor Immunity and Augments the Efficacy of Immune Checkpoint Blockers by Unleashing Inflammasome Activation.* Cancer Cell, 2019. **35**(5): p. 767-781 e6.
336. Dietsch, G.N., et al., *Coordinated Activation of Toll-Like Receptor8 (TLR8) and NLRP3 by the TLR8 Agonist, VTX-2337, Ignites Tumoricidal Natural Killer Cell Activity.* PLoS One, 2016. **11**(2): p. e0148764.
337. Nunes, J., et al., *Targeting IRAK4 for Degradation with PROTACs.* ACS Med Chem Lett, 2019. **10**(7): p. 1081-1085.
338. Roy, M., et al., *CXCL1 can be regulated by IL-6 and promotes granulocyte adhesion to brain capillaries during bacterial toxin exposure and encephalomyelitis.* J Neuroinflammation, 2012. **9**: p. 18.
339. Stadtmann, A. and A. Zarbock, *CXCR2: From Bench to Bedside.* Front Immunol, 2012. **3**: p. 263.
340. Cacalano, G., et al., *Neutrophil and B cell expansion in mice that lack the murine IL-8 receptor homolog.* Science, 1994. **265**(5172): p. 682-4.
341. Cheng, Y., et al., *Potential roles and targeted therapy of the CXCLs/CXCR2 axis in cancer and inflammatory diseases.* Biochim Biophys Acta Rev Cancer, 2019. **1871**(2): p. 289-312.
342. Johnson, D.E., R.A. O'Keefe, and J.R. Grandis, *Targeting the IL-6/JAK/STAT3 signalling axis in cancer.* Nat Rev Clin Oncol, 2018. **15**(4): p. 234-248.
343. Greenhill, C.J., et al., *IL-6 trans-signaling modulates TLR4-dependent inflammatory responses via STAT3.* J Immunol, 2011. **186**(2): p. 1199-208.
344. Samavati, L., et al., *STAT3 tyrosine phosphorylation is critical for interleukin 1 beta and interleukin-6 production in response to lipopolysaccharide and live bacteria.* Mol Immunol, 2009. **46**(8-9): p. 1867-77.

345. Yako, Y.Y., et al., *Cytokines as Biomarkers of Pancreatic Ductal Adenocarcinoma: A Systematic Review.* PLoS One, 2016. **11**(5): p. e0154016.
346. Walter, F., et al., *Imaging of single cell responses to ER stress indicates that the relative dynamics of IRE1/XBP1 and PERK/ATF4 signalling rather than a switch between signalling branches determine cell survival.* Cell Death Differ, 2015. **22**(9): p. 1502-16.
347. Padoan, A., M. Plebani, and D. Basso, *Inflammation and Pancreatic Cancer: Focus on Metabolism, Cytokines, and Immunity.* Int J Mol Sci, 2019. **20**(3).
348. Wang, E.M., et al., *Expression and Clinical Significance of Protein Kinase RNA-Like Endoplasmic Reticulum Kinase and Phosphorylated Eukaryotic Initiation Factor 2alpha in Pancreatic Ductal Adenocarcinoma.* Pancreas, 2019. **48**(3): p. 323-328.
349. Meares, G.P., et al., *PERK-dependent activation of JAK1 and STAT3 contributes to endoplasmic reticulum stress-induced inflammation.* Mol Cell Biol, 2014. **34**(20): p. 3911-25.
350. Dai, H., et al., *PUM1 knockdown prevents tumor progression by activating the PERK/eIF2/ATF4 signaling pathway in pancreatic adenocarcinoma cells.* Cell Death Dis, 2019. **10**(8): p. 595.
351. Waters, A.M. and C.J. Der, *KRAS: The Critical Driver and Therapeutic Target for Pancreatic Cancer.* Cold Spring Harb Perspect Med, 2018. **8**(9).
352. Lian, S., et al., *Elevated expression of growth-regulated oncogene-alpha in tumor and stromal cells predicts unfavorable prognosis in pancreatic cancer.* Medicine (Baltimore), 2016. **95**(30): p. e4328.
353. Li, J., et al., *Tumor Cell-Intrinsic Factors Underlie Heterogeneity of Immune Cell Infiltration and Response to Immunotherapy.* Immunity, 2018. **49**(1): p. 178-193 e7.
354. Liou, G.Y., et al., *Mutant KRAS-induced expression of ICAM-1 in pancreatic acinar cells causes attraction of macrophages to expedite the formation of precancerous lesions.* Cancer Discov, 2015. **5**(1): p. 52-63.
355. Wang, D., et al., *Upregulation of macrophage migration inhibitory factor promotes tumor metastasis and correlates with poor prognosis of pancreatic ductal adenocarcinoma.* Oncol Rep, 2018. **40**(5): p. 2628-2636.
356. Elgueta, R., et al., *Molecular mechanism and function of CD40/CD40L engagement in the immune system.* Immunol Rev, 2009. **229**(1): p. 152-72.
357. Chong, A.S., et al., *CD54/ICAM-1 is a costimulator of NK cell-mediated cytotoxicity.* Cell Immunol, 1994. **157**(1): p. 92-105.
358. Schroder, K., et al., *Interferon-gamma: an overview of signals, mechanisms and functions.* J Leukoc Biol, 2004. **75**(2): p. 163-89.
359. Kaneko, M., et al., *Manganese superoxide dismutase is induced by endoplasmic reticulum stress through IRE1-mediated nuclear factor (NF)-kappaB and AP-1 activation.* Biol Pharm Bull, 2004. **27**(8): p. 1202-6.
360. Van Audenaerde, J.R.M., et al., *Interleukin-15 stimulates natural killer cell-mediated killing of both human pancreatic cancer and stellate cells.* Oncotarget, 2017. **8**(34): p. 56968-56979.
361. Wang, Y., et al., *The IL-15-AKT-XBP1s signaling pathway contributes to effector functions and survival in human NK cells.* Nat Immunol, 2019. **20**(1): p. 10-17.